Imperial College London
Department of Chemistry

# INVESTIGATION OF THE ACIDITY OF BRØNSTED ACIDS IN IONIC LIQUIDS

Hanim Salami Binti Mohd Saupi

Thesis submitted as partial fulfilment of the requirements for the degree of
Doctor of Philosophy, Imperial College London, 2014-2018

# Declaration of Originality

The work described in this thesis was carried out at Imperial College London between January 2014 and January 2018. The entire body of work is my own unless expressly stated to the contrary and has not been submitted previously for a degree at this or any other university.

# Copyright Declaration

The copyright of this thesis rests with the author and is made available under a Creative Commons Attribution Non-Commercial No Derivatives licence. Researchers are free to copy, distribute or transmit the thesis on the condition that they attribute it, that they do not use it for commercial purposes and that they do not alter, transform or build upon it. For any reuse or redistribution, researchers must make clear to others the licence terms of this work.

# Abstract

The Hammett acidity functions ($H_0$) of mixtures of Brønsted acids-ionic liquids were measured using a $^{13}C$ NMR probe and several UV-Vis probes. Successful measurements for all of the systems were demonstrated using the UV-Vis probes. A suitable probe was chosen and used to measure each mixture with the estimation of $H_0$ values from the $^{13}C$ NMR probe. The $^{13}C$ NMR probe can be used to calculate the acidity of the mixtures approximately while the UV-Vis probe gave more precise results. The $H_0$ of Brønsted acids-ionic liquids systems with different acids were successfully measured using the $^{13}C$ NMR probe. Additional measurements were done using the UV-Vis probe to get a full acidity measurements for each system that cannot be measured using the $^{13}C$ NMR probe. Finally, the effect on acidity of the cation of the ionic liquid was found to depend on the strength of the acid mixed with ionic liquids. There is no difference in the acidity of mixtures with a weak acid.

# Acknowledgements

*'In the name of Allah, the Most Gracious, the Most Merciful'*

I would like to dedicate this thesis to everyone who has helped me survived throughout my PhD journey.

Firstly, I would like to express my highest appreciation to my supervisor, Professor Tom Welton. My PhD has been a fantastic experience, and I thank Tom wholeheartedly for his tremendous academic support and also for giving me so many wonderful advice and opportunities for the past four years.

In regards to the world of acidity, I thank John Gräsvik for being patient with me throughout my first year and keep on supporting me and my research even after he left Imperial College. Similar, profound gratitude goes to Pete Haycock, who has been patiently helping and cooperating with me and ton of my NMR samples.

My PhD journey will be less exciting without the Welton Research Group members, past and present; Gilly, Cameron, Raquel, Alastair, Olga, Ryan, Jay and the numerous summer and visiting students who have come through the lab. The group has been a source of friendships, as well as good advice and collaborations. I can't thank you enough for Friday doughnuts session, helps, gossips and laughed that we shared for the past four years. Thank you for always cheering me up for my love-hate relationship with the Grandma Glovebox. A special shoutout to Eduards, the babysitter / the best deskmate ever, who has been taking care of me especially in the lab. I am grateful and appreciate his enthusiasm and willingness to solve every single problem that I came across during my research journey. I would like to express my gratitude to my acidity partner; Mikkaila for working together with me during the summer and for all the tea sessions and laughs that we shared together. My time in the Welton Group was more enjoyable due to the Malaysian members; Rafiq, Nik, Azizi and Shahrul that always made me feel miserable with their antics but ready to help me whenever I need their help. I am

especially grateful to Liyana who is always worrying about me like a real sister and for taking care of me from day zero of my PhD journey until now.

A special mention goes to Kak Norle, Aishah and Kak Lin who has been feeding this glutton girl with non-existent cooking skills with so much good food and making me feel less homesick with their presence. To Hajah Firazalia, my dear friend in Malaysia for her unwavering loyalty in our friendship, encouragements and critiques for the past ten years. I also would like to thank Cik Puan Intan and Mek Zati Bayani for the beautiful friendships that we made here in London. I am also very grateful for my friendships with my madu-madu; Zawa, Asyura and Ainaa, for all the beautiful memories that we made, misfortunes that we came across while travelling, all the good and bad foods that we ate and for all nonsensical matters that we shared together. Not to forget to all kind souls in Vellacott House and Ducane Housing Association that made my daily life more meaningful and blessed. My time in London was made enjoyable in large part due to the many friends that became a part of my life.

I gratefully acknowledge my funder, Majlis Amanah Rakyat Malaysia (MARA) that made my PhD journey possible.

My final display of gratitude and the overall dedication of this thesis goes to my family and extended family for their love and encouragement. For my siblings, Hanif and Atiqah for patiently listening to my daily emotional outbursts and for always being there whenever I need someone to talk. To Hanis and Azhari, thank you for taking care of our parents while I'm away. Last but not least, I would like to thank my parents, Noridah Atan and Mohd Saupi Mat Deris for all of the love, encouragement, du'a and for willing to spend time, money and energy to visit me whenever I need them here. The abundance of support you have provided me throughout the past thirty years is insurmountable, and I can never repay for everything they have sacrificed for me.

*'Verily, with every hardship comes ease - 94:5'*

# Contents


**1 Introductions** **23**

1.1 Ionic Liquids . . . . . 23

1.1.1 A brief history of ionic liquids . . . . . 23

1.1.2 Ionic Liquids Nomenclature . . . . . 27

1.1.3 Applications and Properties of ionic liquids . . . . . 28

1.1.4 Preparation of Ionic Liquids . . . . . 31

1.1.4.1 Preparation of ionic liquids via halide intermediates 32

1.1.4.2 Acid-base neutralisation . . . . . 34

1.1.4.3 Direct alkylation . . . . . 35

1.1.4.4 Purification of ionic liquids . . . . . 36

1.1.4.5 Other synthesis routes . . . . . 38

1.2 The theory of acidity . . . . . 38

1.2.1 Brønsted-Lowry Theory . . . . . 40

1.2.2 Lewis Theory . . . . . 43

1.2.3 Levelling effect . . . . . 45

1.2.4 Mesuring acidity, the pH scale . . . . . 46

1.2.4.1 Measuring pH in water . . . . . 47

1.2.4.2 Measurement of pH . . . . . 47

1.3 Brønsted Acids in Ionic Liquids . . . . . 49

1.3.1 Applications of Brønsted Acidic Ionic Liquids . . . . . 52

1.3.2 Acidity measurements of ionic liquids . . . . . 59

1.4 Scope of thesis . . . . . 66

**2 The Acidity Measurements of Brønsted Acids in Ionic Liquids** **69**

2.1 Measuring the acidity of ionic liquids - . . . . . 69

2.2 Hammett acidity function ($H_0$ function) - The UV-Vis Probe . . . . 70
2.2.1 Determination of $H_0$ values . . . . . 72
2.2.1.1 Step 1: Measurement of $\frac{[BH^+]}{[B]}$ . . . . . 73
2.2.1.2 Step 2: Measurement of $pK_{BH^+}$ . . . . . 76
2.3 Acidity functions from $^{13}C$ NMR Spectroscopy - The $^{13}C$ NMR Probe 80
2.3.1 Principle and development of the method . . . . . 81
2.3.1.1 Determination of the $\Delta\delta^0$ value . . . . . 81
2.3.1.2 Determination of the $pK_a$ of the mesityl oxide . . 85
2.3.2 Applying the $^{13}C$ Probe into Brønsted acid-ionic liquid systems . . . . . 87
2.4 Results: The acidity measurements of Brønsted acids-ionic liquids system with the same conjugate anion using the $^{13}C$ NMR Probe . . 91
2.4.1 The acidity measurements of $[C_4C_1im][NTf_2]$-H$[NTf_2]$ system 92
2.4.2 The acidity measurements of $[C_4C_1im][OTf]$-H[OTf] system 99
2.4.3 The acidity measurements of $[C_4C_1im][Me_2PO_4]$-$H_3PO_4$ system . . . . . 107
2.4.4 Discussion and Conclusions for $^{13}C$ NMR Probe . . . . . 112
2.5 The acidity measurements using the UV-Vis Probe . . . . . 113
2.5.1 Experimental procedures . . . . . 114
2.5.1.1 Measurement of $\epsilon_0$ in non-acidic reference solution . . . . . 114
2.5.1.2 Measurement of $\epsilon$ in Brønsted acid-ionic liquids mixtures . . . . . 114
2.5.2 Measurement of $\epsilon_0$ of Hammett bases in dichloromethane . 114
2.5.3 The acidity measurements of $[C_4C_1im][NTf_2]$-H$[NTf_2]$ system 115
2.5.4 The acidity measurements of $[C_4C_1im][OTf]$-H[OTf] system 121
2.5.5 The acidity measurements of $[C_4C_1im][Me_2PO_4]$-$H_3PO_4$ system . . . . . 124
2.5.6 Discussion . . . . . 127
2.6 Conclusions . . . . . 130

**3 Acidity Measurements of Brønsted acids in ionic liquids with different conjugate bases 131**

3.1 Aims and Objectives . . . . . 131
3.2 Acidity measurements of [$C_4C_1$im][$NTf_2$] with different acids . . . . 132
3.2.1 [$C_4C_1$im][$NTf_2$]-H[OTf] system . . . . . 133
3.2.2 [$C_4C_1$im][$NTf_2$]-$H_2SO_4$ system . . . . . 134
3.3 Acidity measurements of [$C_4C_1$im][OTf] with different acids . . . . . 137
3.3.1 [$C_4C_1$im][OTf]-H[$NTf_2$] system] . . . . . 137
3.3.2 [$C_4C_1$im][OTf]-$H_2SO_4$ system . . . . . 140
3.3.3 [$C_4C_1$im][OTf]-$H_3PO_4$ system . . . . . 143
3.4 The acidity measurements of [$C_4C_1$im][$HSO_4$] with different acids . . 145
3.4.1 [$C_4C_1$im][$HSO_4$]-H[$NTf_2$] system . . . . . 145
3.4.2 [$C_4C_1$im][$HSO_4$]-H[OTf] system . . . . . 148
3.4.3 [$C_4C_1$im][$HSO_4$]-$H_3PO_4$ system . . . . . 149
3.5 Acidity measurements of [$C_4C_1$im][$Me_2PO_4$] with different acids . . . 153
3.5.1 [$C_4C_1$im][$Me_2PO_4$]-H[$NTf_2$] system . . . . . 153
3.5.2 [$C_4C_1$im][$Me_2PO_4$]-H[OTf] system . . . . . 156
3.5.3 [$C_4C_1$im][$Me_2PO_4$]-$H_2SO_4$ system . . . . . 159
3.6 Discussion . . . . . 164
3.6.1 Ionic liquids with different Brønsted acids . . . . . 164
3.6.2 Brønsted acids behaviour in different ionic liquids . . . . . 171
3.7 Conclusion . . . . . 174

**4 Acidity Measurements of Brønsted acid in ionic liquids with different cations 177**
4.1 Acidity measurements of [$HC_4$im][$HSO_4$] with different acids . . . . . 177
4.1.1 [$HC_4$im][$HSO_4$]-H[$NTf_2$] system . . . . . 178
4.1.2 [$HC_4$im][$HSO_4$]-H[OTf] system . . . . . 179
4.1.3 [$HC_4$im][$HSO_4$]-$H_3PO_4$ system . . . . . 181
4.2 Discussions and conclusions . . . . . 183

**5 Synthesis and Experimental 189**
5.1 General Laboratory Procedures . . . . . 189
5.2 Synthesis of Ionic Liquids . . . . . 189
5.2.1 1-Butyl-3-methylimidazolium chloride . . . . . 189

5.2.2 1-Butyl-3-methylimidazolium trifluoromethanesulfonate . . 190
5.2.3 1-Butyl-3-methylimidazolium bis(trifluoromethylsulfonyl)imide191
5.2.4 1-Butylimidazolium hydrogen sulphate . . . . . 192
5.2.5 1-Butyl-3-methylimidazolium methyl sulphate . . . . . 192
5.2.6 1-Butyl-3-methylimidazolium hydrogen sulphate . . . . . 193
5.2.7 1-Butyl-3-methylimidazolium dimethyl phosphate . . . . . 194
5.3 Acidity Measurements of Brønsted Acids-Ionic Liquids . . . . . 194
5.3.1 $^{13}$C NMR Probe[147] . . . . . 194
5.3.2 UV-Vis probe[147] . . . . . 195
5.3.2.1 Obtaining extinction coefficients, $\epsilon_0$ of Hammett probe . . . . . 195
5.3.2.2 Preparation of solutions of Hammett dye mixtures of ionic liquids with their related Brønsted acids . . . . . 200

**6 Overall Conclusions and Outlook** **201**
6.1 Conclusions . . . . . 201

**Bibliography** **203**

**A Appendix** **219**
A.1 Maths : From equation 16 to equation 17 (Chapter 2) . . . . . 219
A.2 Data for the acidity measurements of $[C_4C_1im][HSO_4]$-$H_2SO_4$ system 220

# List of Figures


1.1.1 Structures of early ionic liquid compounds : ethylammonium nitrate, [$EtNH_3$][$NO_3$] and the 'melt' [Etpy]Br.$AlCl_3$ (examples of observed anion structures) . . . . . 25

1.1.2 Structures of common ionic liquids cations and anions. The $R$ groups are usually H, -$CH_3$ or other short chain aliphatic substituents . . . . . 26

1.1.3 The BASIL$^{TM}$process . . . . . 31

1.1.4 Typical synthesis steps for preparing ionic liquids, ($NR_3$ stands for an initial amine substrate) . . . . . 32

1.1.5 Reaction scheme for synthesis of [$C_4C_1$im]Cl using the direct alkylation step . . . . . 33

1.1.6 Methathesis reaction of [$C_4C_1$im]Cl with Li[$NTf_2$] to produce [$C_4C_1$im][$NTf_2$] . . . . . 34

1.1.7 Acid-base reaction of reaction of 1-butylimidazole with sulphuric acid to produce [$HC_4$im][$HSO_4$] . . . . . 35

1.1.8 Synthesis of ionic liquids by direct alkylation . . . . . 36

1.2.1 The formation of carbonic acid . . . . . 44

1.2.2 Schematics of a glass electrode[81] . . . . . 49

1.3.1 Possible cations and anions of BAILs . . . . . 51

1.3.2 $^t$-butylation of phenol with $^t$-butanol using different acidic ionic liquids catalysts: [$(HSO_3)C_4C_1$im][$HSO_4$], [$(HSO_3)^4C_4(C_2)$N][$HSO_4$] and [$(HSO_3)^4C_4$pyr][$HSO_4$] . . . . . 54

1.3.3 Lignocellulosic pathways. A scheme for a chemo-catalytic biorefinery[110] . . . . . 56

1.3.4 Substituted dinitroanilines indicator . . . . . 62

1.3.5 Mesityl oxide protonation . . . . . 65

1.3.6 Interactions of the spectroscopic probem triethylphosphine oxide with a Lewis acid (LA) and a Brønsted acid (BA) . . . . . 66

2.2.1 UV spectrum of 3-nitroaniline in DCM (example of UV spectrum with ($\lambda_{max}$) . . . . . 74
2.2.2 UV spectrum of 4-nitrotoluene in neat $H_2SO_4$ . . . . . 75
2.2.3 Plot for determination of p$K_{BH^+}$ of 4-nitroaniline in hydrochloric acid solutions. ∘ Braude[159] and □ Paul[158]. Image taken from the paper by Paul and Long.[154] . . . . . 77
2.2.4 Logarithm of ionisation ratios of Hammett bases in sulphuric acid-water solutions. Dye: (1) 4-nitroaniline, (2) 2-nitroaniline, (3) 4-chloro-2-nitroaniline, (4) p-nitrodiphenylamine, (5) 2,4-dichloro-6-nitroaniline, (6) p-nitroazobenzene, (7) 2,6-dinitro-4-methylaniline. (8) 2,4-dinitroaniline, (9) *N,N*-dimethyl-2,4,6-trinitroaniline, (10) benzalacetophenone, (11) $\beta$-benzoylnaphthalene, (12) p-benzoylbiphenyl, (13) 6-bromo-2,4-dinitroaniline, (14) anthraquinone, (15) 2,4,6-trinitroaniline. Image taken from Hammett's paper. . . . . 79
2.3.1 Conjugation mode of mesityl oxide . . . . . 83
2.3.2 $\Delta\delta$ vs. concentration of 4-hexen-3-one in 75% $H_2SO_4$ where $\Delta\delta^0$= 46.7 ppm.[169] . . . . . 84
2.3.3 Plot of (a) mol % $H_2SO_4$ in $H_2O$-$H_2SO_4$ system vs. $\Delta\delta^0$ , and (b) $\Delta\delta^0$ vs. $H_0$ values. . . . . 85
2.3.4 Plot of *s,* slopes of the linear correlations between $\Delta\delta$ vs. total concentration of mesityl oxide against $H_0$ values obtained using UV-Vis spectroscopy. Image taken from Fărcaşiu and Ghenciu's paper.[169] . . . . . 86
2.3.5 Second protonation of Mesityl oxide . . . . . 87
2.3.6 $\Delta\delta^0$ vs. $H_0$ for [$C_4C_1$im][$HSO_4$ ]-$H_2SO_4$ (new IL points), $H_2O$-$H_2SO_4$ system (Farcasio) and Hammett prediction of [$C_4C_1$im][$HSO_4$ ]-$H_2SO_4$using eqn. 2.3.7.[147] . . . . . 90
2.3.7 $\Delta\delta^0$ vs. $H_0$ for [$C_4C_1$im][$HSO_4$ ]-$H_2SO_4$, [$HC_4$im][$HSO_4$ ]-$H_2SO_4$ and $H_2O$-$H_2SO_4$ system.[147] . . . . . 90

2.4.1 $^{13}$C NMR spectrum of mesityl oxide in [$C_4C_1$im][$NTf_2$] + 0.69 $\chi_{H[NTf_2]}$ . . . . . 93
2.4.2 Determination of $\Delta\delta^0$ mesityl oxide in extrapolation [$C_4C_1$im][$NTf_2$] + 0.67 $\chi_{H[NTf_2]}$ . . . . . 95
2.4.3 The $H_0$ values against the molar ratio $\chi_{H[NTf_2]}$ for the [$C_4C_1$im][$NTf_2$]-H[$NTf_2$] system . . . . . 96
2.4.4 The $H_0$ values against the molar ratio $\chi_{H[OTf]}$ for the [$C_4C_1$im][OTf]-H[OTf] system . . . . . 100
2.4.5 $^{13}$C NMR spectrum for [$C_4C_1$im][OTf] + $\chi_{H[OTf]}$ = 0.0303 + mesityl oxide . . . . . 101
2.4.6 $^{13}$C NMR spectrum for [$C_4C_1$im][OTf] + $\chi_{H[OTf]}$ = 0.300 + mesityl oxide . . . . . 102
2.4.7 $^{13}$C NMR spectrum for [$C_4C_1$im][OTf] + $\chi_{H[OTf]}$= 0.732 + mesityl oxide . . . . . 103
2.4.8 Decomposition of mesityl oxide in presence of $[OTf]^-$ . . . . . 105
2.4.9 $H_0$ values vs. $\chi_{H_3PO_4}$ in the [$C_4C_1$im][$Me_2PO_4$]-$H_3PO_4$ mixtures . 109
2.5.1 The $H_0$ values against the molar ratio $\chi_{H[NTf_2]}$ for the [$C_4C_1$im][$NTf_2$]-H[$NTf_2$] system . . . . . 116
2.5.2 The $H_0$ values against the molar ratio $\chi_{H[NTf_2]}$ for the [$C_4C_1$im][$NTf_2$]-H[$NTf_2$] system using the $^{13}$C NMR Probe and UV-Vis Probe . . 118
2.5.3 Comparison of data from Thomazeau *et al.*[58] and my results for [$C_4C_1$im][$NTf_2$]-H[$NTf_2$] mixtures using the UV-Vis probe . . . . 120
2.5.4 The $H_0$ values against the molar ratio $\chi_{H[OTf]}$ for the [$C_4C_1$im][OTf]-H[OTf] system . . . . . 122
2.5.5 The $H_0$ values against the molar ratio $\chi_{H[NTf_2]}$ for the [$C_4C_1$im][OTf]-H[OTf] system using the $^{13}$C NMR Probe and UV-Vis Probe . . 124
2.5.6 The $H_0$ values against the molar ratio $\chi_{H_3PO_4}$ for the [$C_4C_1$im][$Me_2PO_4$]-$H_3PO_4$ system . . . . . 125
2.5.7 The $H_0$ values against the molar ratio $\chi_{H_3PO_4}$ for the [$C_4C_1$im] [$C_4C_1$im][$Me_2PO_4$]-$H_3PO_4$ system using the $^{13}$C NMR Probe and UV-Vis Probe . . . . . 127

3.2.1 The $H_0$ values against the $\chi_{H[OTf]}$ for the $[C_4C_1im][NTf_2]$-H[OTf] system . . . 133
3.2.2 The $H_0$ values against the $\chi_{H_2SO_4}$ for the $[C_4C_1im][NTf_2]$-$H_2SO_4$ system . . . 135
3.2.3 The $H_0$ values against the $\chi_{acid}$ mixed with $[C_4C_1im][NTf_2]$ . . . 137
3.3.1 The $H_0$ values against the $\chi_{H[NTf_2]}$ for the $[C_4C_1im][OTf]$-$H[NTf_2]$ system . . . 138
3.3.2 The $H_0$ values against the $\chi_{H[NTf_2]}$ for the $[C_4C_1im][OTf]$-$H[NTf_2]$ system (results combined from the $^{13}C$ NMR probe and UV-Vis probe) . . . 139
3.3.3 The $H_0$ values against the $\chi_{H_2SO_4}$ for the $[C_4C_1im][OTf]$-$H_2SO_4$ system . . . 141
3.3.4 The $H_0$ values against the $\chi_{H_2SO_4}$ for the $[C_4C_1im][OTf]$-$H_2SO_4$ system (results combined from the $^{13}C$ NMR probe and UV-Vis probe) . . . 142
3.3.5 The $H_0$ values against the $\chi_{H_3PO_4}$ for the $[C_4C_1im][OTf]$-$H_3PO_4$ system . . . 144
3.4.1 The $H_0$ values against the $\chi_{H[NTf_2]}$ for the $[C_4C_1im][HSO_4]$-$H[NTf_2]$ system . . . 146
3.4.2 The $H_0$ values against the $\chi_{H[OTf]}$ for the $[C_4C_1im][HSO_4]$-H[OTf] system . . . 148
3.4.3 The $H_0$ values against the $\chi_{H_3PO_4}$ for the $[C_4C_1im][HSO_4]$-$H_3PO_4$ system . . . 149
3.4.4 The $H_0$ values against the $\chi_{H_3PO_4}$ for the $[C_4C_1im][HSO_4]$-$H_3PO_4$ system . . . 150
3.4.5 The $H_0$ values against the $\chi_{acid}$ with $[C_4C_1im][HSO_4]$ . . . 153
3.5.1 The $H_0$ values against the molar ratio $\chi_{H[NTf_2]}$ for the $[C_4C_1im][Me_2PO_4]$-$H[NTf_2]$ system . . . 154
3.5.2 The $H_0$ values against the molar ratio $\chi_{H[NTf_2]}$ for the $[C_4C_1im][Me_2PO_4]$-$H[NTf_2]$ system . . . 155
3.5.3 The $H_0$ values against the $\chi_{H[OTf]}$ for the $[C_4C_1im][Me_2PO_4]$-H[OTf] system . . . 157

3.5.4 The $H_0$ values against the $\chi_{H[OTf]}$ for the $[C_4C_1im][Me_2PO_4]$-H[OTf] system . . . . . 158
3.5.5 The $H_0$ values against the $\chi_{H_2SO_4}$ for the $[C_4C_1im][Me_2PO_4]$-$H_2SO_4$ system . . . . . 160
3.5.6 The $H_0$ values against the $\chi_{H_2SO_4}$ for the $[C_4C_1im][Me_2PO_4]$-$H_2SO_4$ system . . . . . 161
3.5.7 The $H_0$ values against the $\chi_{acid}$ mixed with $[C_4C_1im][Me_2PO_4]$ . 163
3.6.1 The $H_0$ values against the $\chi_{acid}$ mixed with $[C_4C_1im][NTf_2]$ . . . 164
3.6.2 The $H_0$ values against the $\chi_{acid}$ mixed with $[C_4C_1im][OTf]$ . . . 166
3.6.3 The $H_0$ values against the $\chi_{acid}$ mixed with $[C_4C_1im][OTf]$ ($^{13}C$ NMR Probe results) . . . . . 167
3.6.4 The $H_0$ values against the $\chi_{acid}$ with $[C_4C_1im][HSO_4]$ . . . . . 168
3.6.5 The $H_0$ values against the $\chi_{acid}$ mixed with $[C_4C_1im][Me_2PO_4]$ . 170
3.6.6 The $H_0$ values against the $\chi_{H[NTf_2]}$ for the $H[NTf_2]$-ionic liquids system . . . . . 171
3.6.7 The $H_0$ values against the $\chi_{H_2SO_4}$ for the H[OTf]-ionic liquids system . . . . . 172
3.6.8 The $H_0$ values against the $\chi_{H_2SO_4}$ for the $H_2SO_4$-ionic liquids system . . . . . 173
3.6.9 The $H_0$ values against the $\chi_{H_3PO_4}$ for the ionic liquids-$H_3PO_4$ system . . . . . 174

4.1.1 The $H_0$ values against the molar ratio $\chi_{H[NTf_2]}$ for the $[HC_4im][HSO_4]$-$H[NTf_2]$ system . . . . . 178
4.1.2 The $H_0$ values against the molar ratio $\chi_{H_2SO_4}$ for the $[HC_4im][HSO_4]$-H[OTf] system . . . . . 180
4.1.3 The $H_0$ values against the molar ratio $\chi_{H_3PO_4}$ for the $[HC_4im][HSO_4]$-$H_3PO_4$ system . . . . . 182
4.2.1 The comparison for $H[NTf_2]$ mixed with $[HSO_4]^-$ based ILs . . . 184
4.2.2 The comparison for H[OTf] mixed with $[HSO_4]^-$ based ILs . . . . 185
4.2.3 The comparison for $H_3PO_4$ mixed with $[HSO_4]^-$ based ILs . . . . 186

5.3.1 Plot of absorbance against concentration of 3-nitroaniline in DCM195
5.3.2 Plot of absorbance against concentration of 4-nitroaniline in DCM196

5.3.3 Plot of absorbance against concentration of 2-nitroaniline in DCM196
5.3.4 Plot of absorbance against concentration of 4-chloro-2-nitroaniline in DCM . . . . . 197
5.3.5 Plot of absorbance against concentration of 2,4-dichloro-6-nitroaniline in DCM . . . . . 197
5.3.6 Plot of absorbance against concentration of 2,6-dichloro-4-nitroaniline in DCM . . . . . 198
5.3.7 Plot of absorbance against concentration of 2,4-dinitroaniline in DCM . . . . . 198
5.3.8 Plot of absorbance against concentration of 2,6-dinitroaniline in DCM . . . . . 199
5.3.9 Plot of absorbance against concentration of 2-bromo-4,6-dinitroaniline in DCM . . . . . 199
5.3.10 Plot of absorbance against concentration of 4-nitrotoluene in DCM200

A.2.1 $^{13}$C NMR spectra of mesityl oxide in $[C_4C_1im][HSO_4]$ + 0.066 $\chi_{H_2SO_4}$ . . . . . 221
A.2.2 $H_0$ values vs. $\chi_{H_2SO_4}$ in the $[C_4C_1im][HSO_4]$-$H_2SO_4$ mixture . . . 222

# List of Tables


2.2.1 Selected p$K_{\mathrm{BH^+}}$ values for extended Hammett Bases[154] . . . . . 72
2.4.1 $\Delta\delta$ values for each different [mesityl oxide] for several $\chi_{H[NTf_2]}$ in the [$C_4C_1$im][$NTf_2$]-H[$NTf_2$] system. . . . . 94
2.4.2 The positive mass spectra of [$C_4C_1$im][$NTf_2$]-H[$NTf_2$] : Detected ion fragments and their relative abundances . . . . . 98
2.4.3 The negative mass spectra of [$C_4C_1$im][$NTf_2$]-H[$NTf_2$] : Detected ion fragments and their relative abundances . . . . . 98
2.4.4 $0.030 \leq \chi_{H[OTf]} \geq 0.093$ . . . . . 105
2.4.5 The positive mass spectra of [$C_4C_1$im][OTf]-H[OTf] : Detected ion fragments and their relative abundances . . . . . 106
2.4.6 The negative mass spectra of [$C_4C_1$im][OTf]-H[OTf] : Detected ion fragments and their relative abundances . . . . . 107
2.4.7 The positive mass spectra of [$C_4C_1$im][$Me_2PO_4$]-$H_3PO_4$ system : Detected ion fragments and their relative abundances . . . . . 111
2.4.8 The negative mass spectra of [$C_4C_1$im][$Me_2PO_4$]-$H_3PO_4$ system : Detected ion fragments and their relative abundances . . . . . 111
2.5.1 Extinction coefficients for Hammett bases in DCM . . . . . 115
2.5.2 List of dye used . . . . . 117
2.5.3 Calculation of the $H_0$ values for various concentrations of H[$NTf_2$] in [$C_4C_1$im][$NTf_2$][58] . . . . . 119
2.5.4 List of dye used . . . . . 123
2.5.5 List of dye used . . . . . 126

3.2.1 The negative mass spectra of [$C_4C_1$im][$NTf_2$]-H[OTf] : Detected ion fragments and their relative abundance . . . . . 134

3.3.1 The negative mass spectra of [$C_4C_1$im][OTf]-H[$NTf_2$] : Detected ion fragments and their relative abundance . . . . . 140
3.3.2 The negative mass spectra of [$C_4C_1$im][OTf]-$H_2SO_4$ : Detected ion fragments and their relative abundance . . . . . 143
3.3.3 The negative mass spectra of [[$C_4C_1$im][OTf]-$H_3PO_4$ : Detected ion fragments and their relative abundance . . . . . 145
3.4.1 The positive mass spectra of [$C_4C_1$im][$HSO_4$]-H[$NTf_2$] : Detected ion fragments and their relative abundances . . . . . 146
3.4.2 The negative mass spectra of [$C_4C_1$im][$HSO_4$]-H[$NTf_2$] : Detected ion fragments and their relative abundance . . . . . 147
3.4.3 The negative mass spectra of [$C_4C_1$im][$HSO_4$]-H[$NTf_2$] : Detected ion fragments and their relative abundances . . . . . 147
3.4.4 The $H_0$ values and Hammett probe used in the UV-Vis measurements of [$C_4C_1$im][$HSO_4$]-$H_3PO_4$ system at $\chi_{H_3PO_4} < 0.370$ . . . 151
3.4.5 The positive mass spectra of [$C_4C_1$im][$HSO_4$]-$H_3PO_4$ system : Detected ion fragments and their relative abundances . . . . . 151
3.4.6 The negative mass spectra of [$C_4C_1$im][$HSO_4$]-$H_3PO_4$ system : Detected ion fragments and their relative abundances . . . . . 152
3.5.1 The negative mass spectra of [$C_4C_1$im][$Me_2PO_4$]-H[$NTf_2$] system: Detected ion fragments and their relative abundances . . . . . 156
3.5.2 The negative mass spectra of [$C_4C_1$im][$Me_2PO_4$]-H[OTf] system: Detected ion fragments and their relative abundances . . . . . 159
3.5.3 The negative mass spectra of [$C_4C_1$im][$Me_2PO_4$]-$H_2SO_4$ system: Detected ion fragments and their relative abundances . . . . . 162

4.1.1 The positive mass spectra of [$HC_4$im][$HSO_4$]-H[$NTf_2$] system: Detected ion fragments and their relative abundances . . . . . 179
4.1.2 The positive mass spectra of [$HC_4$im][$HSO_4$]-H[OTf] system: Detected ion fragments and their relative abundances . . . . . 180
4.1.3 The negative mass spectra of [$HC_4$im][$HSO_4$]-H[OTf] system: Detected ion fragments and their relative abundances . . . . . 181
4.1.4 The positive mass spectra of [$HC_4$im][$HSO_4$]-$H_3PO_4$ system: Detected ion fragments and their relative abundances . . . . . 183

4.1.5 The negative mass spectra of $[HC_4im][HSO_4]$-$H_3PO_4$ system: Detected ion fragments and their relative abundances . . . . . 183

# Abbreviations

| | |
|---|---|
| $[C_4C_1im][HSO_4]$ | 1-Butyl-3-methyimidazolium hydrogensulphate |
| $[C_4C_1im][Me_2PO_4]$ | 1-Butyl-3-methyimidazolium dimethylphosphate |
| $[C_4C_1im][NTf_2]$ | 1-Butyl-3-methyimidazolium bis(trifluoromethanesulfonyl)imide |
| $[C_4C_1im][OAc]$ | 1-Butyl-3-methyimidazolium acetate |
| $[C_4C_1im][OTf]$ | 1-Butyl-3-methyimidazolium trifluoromethanesulfonate |
| $[C_1Him][Cl]$ | 1-Methyl-imidazolium chloride |
| $[HC_4im][HSO_4]$ | 1-Butylimidazolium hydrogensulphate |
| $[C_4C_1C_1{}^2im]^+$ | 1-Butyl-2,3-dimethylimidazolium |
| $[C_4pyr]^+$ | 1-Butylpyridinium cation |
| $[N_{4448}]^+$ | Tributyloctylammonium cation |
| EDA | Electron donor acceptor |
| $EtNO_3$ | Ammonium nitrate |
| FFA | Free fatty acids |
| $H[NTF_2]$ | Bis(trifluoromethanesulfonyl)imide |
| H[OTf] | Triflic acid |
| $H_0$ | Hammett acidity function |
| $H_2SO_4$ | Sulphuric acid |
| $H_3PO_4$ | Phosphoric acid |
| HOAc | Acetic acid |
| MEK | Michler's ketone |
| Mesityl oxide | 4-methylpent-3-en-2-one |
| NMR | Nuclear Magnetic Resonance |
| PILs | Protic ionic liquids |
| $R^0(H^+)$ | Strehlow function |
| RTILs | Room temperature ionic liquids |
| TBA | $^{t\text{-}}$Butanol |
| TCNE | Tetracyanoethylene |
| TFSI | Trifluoromethanesulfonyl imide |
| UV-Vis | Ultraviolet-visible |
| $\chi_{acid}$ | molar ratio of acid to ionic liquid |

# Chapter 1

# Introductions

.

## 1.1 Ionic Liquids

Ionic liquids may be defined as salts that melt at or below 100 °C to afford materials composed of cations and anions. The melting temperature (100 °C) is very often cited as the cut-off point to distinguish ionic liquids from the related topic of molten salts,[1] which are generally regarded as high temperature systems. In some cases, ionic liquids are free-flowing liquids at room temperature where they are called room-temperature ionic liquids (RTILs). These ionic liquids have real advantages in applications over higher melting salts due to the practicality of handling these ionic liquids.

### 1.1.1 A brief history of ionic liquids

Ionic liquids (ILs) have always been in a parallel interest in academic research and industrial chemistry.[2, 3, 4] The search for alternatives to replace volatile organic compounds have become a prime concern because cleaner technologies have become a crucial concern in academic and industrial research. Solvents are considered as damaging chemicals because of their volatility, which makes these difficult to contain, and that they are being used in huge quantity. Ionic liquids were found to be suitable as solvents for synthetic processes and are potentially

to be used as replacements for volatile organic compounds.[2, 5, 6] Applications of ionic liquids are diverse in both academia and industry, including their use as electrolytes in batteries,[7, 8] in the textile processes,[9, 10, 11] in the capture and storage of $CO_2$[12, 13] and in the pre-treatment and dissolution of lignocellulosic biomass.[14, 15, 16]

In 1914, Paul Walden reported one of the first publications on ILs about the physical properties of ethylammonium nitrate ($[EtNH_3][NO_3]$, Figure 1.2.1).[17] The $[EtNH_3][NO_3]$ (mp 13-14 °C) was formed by the neutralisation of ethylamine with concentrated nitric acid. Walden investigated the electric conductivity and the molecular size of some organic ammonium salts which he derived from the capillary constant. These salts melt at relatively low temperatures (approximately 100 °C). The low melting points limit the degree of thermolysis of these salts and make the experiments possible, which was not possible at the high temperatures required to melt anhydrous mineral salts. Thus, it is possible to perform all measurements using the methods and apparatus at usual temperatures. The conditions of the low-melting salts are close to the actual experimental conditions used to measure the conventional aqueous and non-aqueous solvents. The results were predicted using the theory of electrolytic dissociation of Arrhenius and the theory of van't Hoff.[17, 18] The general results for the organic salts at low temperatures (below, or around 100 °C) have a close similarity to the experiments made with inorganic (single, non-complexing) molten salts at higher temperatures (between 300 - 600 °C).[17, 18] Walden's discovery of a new class of liquids did not gain any noteworthy interest during that time despite his comprehensive description in the paper. However, it is acknowledged nowadays that Walden's findings have left a remarkable legacy and he is known as the pioneer of the field of ionic liquids.

The research into ionic liquids remained inactive until 1948 when the application of mixtures of aluminium (III) chloride ($AlCl_3$) and 1-ethypyridinium bromide ($[C_2py]Br$) to the electrodeposition of aluminium was reported.[19, 20] The report discovered that $[C_2py]Br$ is liquid at or below room temperature with 67 mol % of $AlCl_3$. Unfortunately, it is difficult to investigate the selected system as it was based on mixed chloride and bromide salts which mean that the solvent was chemically complicated. The issue was then solved in the 1970s and 1980s when there were reports on so-called 'organic chloroaluminate' ionic liquids.[21, 22] Both papers

reported the of use Lewis acid molten salt systems to study the electrochemistry of organometallics. The 'melts' were formed from the pairing of *N*-alkylpyridinium halide salts with the strongly Lewis-acidic $AlCl_3$ (Figure 1.1.1). The molten salt systems used were found to provide a new selection of media in which to study the electrochemical and chemical properties of different compounds as these melts can easily be maintained free of water, oxygen and proton.[21]

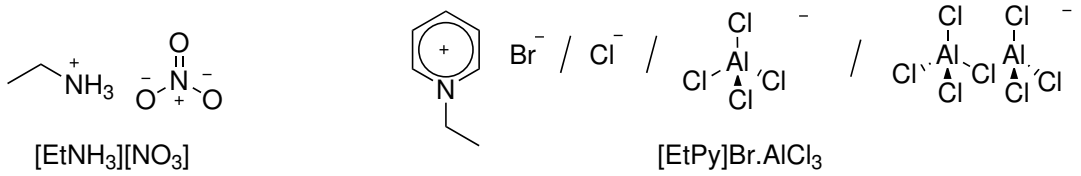
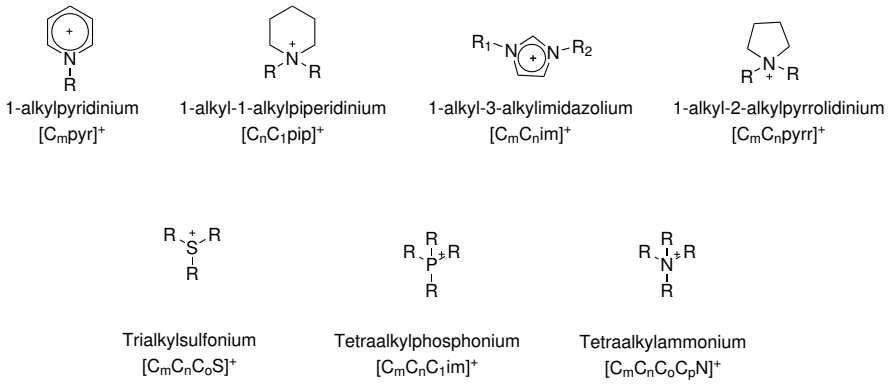



**Figure 1.1.1** – Structures of early ionic liquid compounds : ethylammonium nitrate, $[EtNH_3][NO_3]$ and the 'melt' $[Etpy]Br.AlCl_3$ (examples of observed anion structures)

The $[C_2py]Br.AlCl_3$ system developed by Osteryoung's group had a significant problem where the melt is liquid at room temperature but only with a very narrow compositional range. Also, the cation was easily reduced, which cause limitations to expand the applications in battery and electrodeposition.[21]

Tremendous effort was made to develop and improve the synthesis of a new generation of ionic liquids with better properties. Second generation ionic liquids were reported back in 1992, when 1-ethyl-3-methylimidazolium tetrafluoroborate ($[C_2C_1im][BF_4]$), mp. 12 °C) was prepared using the salt metathesis route of 1-ethyl-3-methylimidazolium iodide ($[C_2C_1im]I$) with $Ag[BF_4]$ in methanol.[23] The tetrafluoroborate ($[BF_4]^-$) was used to substitute the moisture sensitive anion used in first generation ILs to produce 'air and water stable ionic liquids'. Other new ionic liquids using the salt metathesis route then followed with different cations and anions (Figure 1.1.2).[24, 25, 26] Quarternary nitrogen centre cations are the most often used, followed by sulfonium- and phosphonium- derived ionic liquids. The anions structures are more varied compared to cations from simple halide liquids towards the complex, polyatomic anions such as the bis(trifluromethylsulfonyl)imide anion $[NTf_2]^-$. These second-generation ionic liquids have since found increased applications as reaction media for diverse types of organic reactions.[27, 28, 29]

Cations:




Anions:

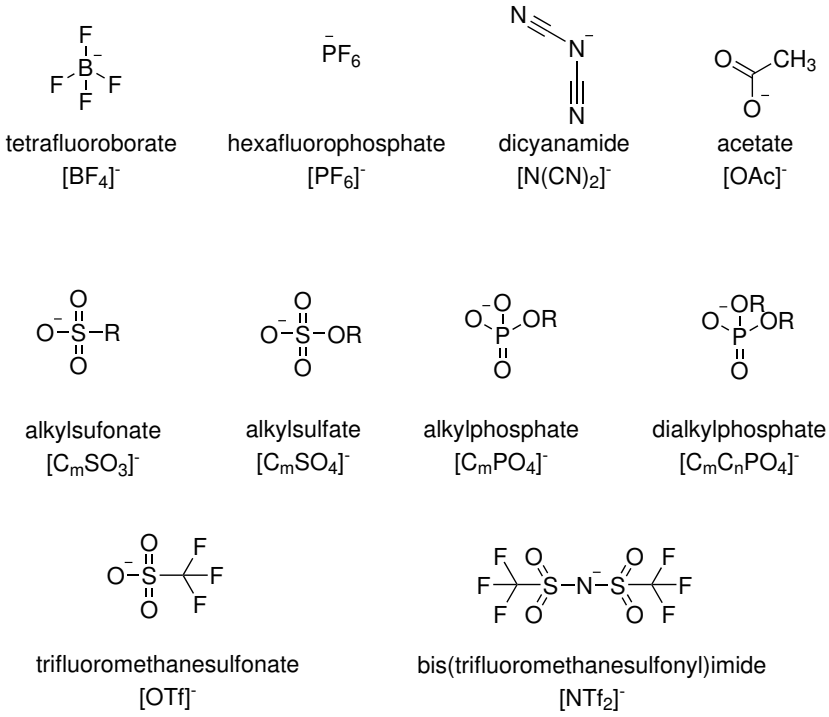



**Figure 1.1.2** – Structures of common ionic liquids cations and anions. The $R$ groups are usually H, -$CH_3$ or other short chain aliphatic substituents

### 1.1.2 Ionic Liquids Nomenclature

The high number of different abbreviations and naming schemes for ionic liquids is growing significantly, together with the number of ionic liquids synthesised and many research groups working in ionic liquids. These different abbreviations are especially evident for ionic liquids cations. Thus, it is essential to use a standard nomenclature system in naming the ionic liquids to avoid confusion.

Most abbreviations used in the literature were derived from the ion's name and often written either in upper- or lower-case letter short form for example: $[bmim]^+$ and $[BMIM]^+$ where both refer to the 1-butyl-3-methylimidazolium cation.[30, 31] Nevertheless, complications arise with the naming system as ambiguities are detected especially when the same letter is being used to represent alkyl chains with different lengths, such as for $[pmim]^+$. Should the $[pmim]^+$ acronym be used for 1-propyl–3-methylimidazolium or 1-pentyl–3-methylimidazolium cations? Or h in the $[hmim]^+$ refer to hexyl or hydrogen?

To avoid the above-mentioned complications, an alphanumeric system is used to describe the alkyl chains, with an alphabetic abbreviation for the charged centre. Examples are listed below to show how the alphanumeric system has been applied in naming the cation of ionic liquids:[3, 32]

1. 1-butyl-3-methylimidazolium cation becomes $[C_4C_1im]$ and if it is a non-linear alkyl chain (e.g. 1-*tert*-butyl-3-methylimidazolium cation can be abbreviated as $[^tC_4C_1im]$).

2. In a case of the di-/tri-alkylimidazolium cation type (e.g. $[C_mC_nim]$ in Figure 1.1.2), a combination of letters and numbers can be used. The letter $m$ and $n$ belong to the number of carbon atoms in the alkyl side chains. These side chains are assumed to be connected to the nitrogen atoms of the imidazolium ring, except when it is labelled with a superscript number which to the position of the ring.

3. This nomenclature also can be used to name a non-carbon atom as substitutions in the chain, for example, $[C_1OC_2im]$ cation.

4. When the type and position of the side chain are functionalized, the functional group are noted as (e.g. $[(OH)^4C_4C_1im]$); which means that there is

an alcohol group on the terminal carbon of the butyl chain.

5. Alkyl chains are assumed to be saturated except if mentioned otherwise.

6. Alkylation is assumed to be on the heteroatom(s) in the cyclic cations unless if not indicated by giving the numerical position of alkylation on the ring, for example; $[C_4C_1C_1{}^2im]^+$ is an abbreviation for 1-butyl-2,3-dimethylimidazolium.

The naming of ionic liquids anions is simpler than the cation due to their chemical structures. The naming of the anion is based on the nomenclature of the anion is being used throughout this thesis. For example, the standard abbreviation 'Tf' to refer the 'trifluoromethylsulfonyl' is used instead of '$[TFSI]^-$' and other alternatives that appear in different literatures.[33, 34]

### 1.1.3 Applications and Properties of ionic liquids

The unique properties of ionic liquids have sparked major interest from academia as well as in industry due to their large number of potential applications. Ionic liquids properties are determined by the interaction of ions in the melt and their structure.[35] Ionic liquids are normally composed of large asymmetric organic cations and inorganic or organic cations.[36] The properties of ionic liquids can be modified by tuning the cations and anions, and this makes ionic liquids to be called as 'designer solvents'. For example, the properties of the ionic liquids can change by varying the length and branching of the alkyl groups in the cation. Hart *et al.* reported that changing the ionic liquid cations affects the solubility of lignin.[37] In the report, the solvent-solute interactions of solutions of lignin in $[C_4C_1im]^+$, $[C_4C_2im]^+$, and $[C_4pyr]^+$,and $[N_{4448}]^+$ -based ionic liquids was measured using $^1H$ and $^{13}C$ NMR spectra. The report concluded that the planar cations have a subtle effect on the lignin solubility. There is about 30 wt% difference in lignin solubility between $[C_4C_1im]^+$and $[N_{4448}]^+$-based ionic liquids. It also mentioned that there is no difference in solubility of lignin between ionic liquids with different anions.

The melting points of ionic liquids can be influenced by the H-bonding ability, the charge distribution on the ions, the van der Waals interactions and the symmetry of the ions. For comparison, the inorganic salt NaCl has a melting point of 801 °C[38] while 1-propyl-3-methylimidazolium chloride's melting point is 77-79 °C.[35]

The change of the small inorganic cations to large asymmetric organic cations has decreased the melting points.

Ionic liquids have a wide range of polarities which offer many advantages in the properties of the ionic liquids. Polarity can be defined quantitatively as a polar solvent is one that will dissolve and stabilise charged or dipolar solutes.[2] This definition causes ionic liquids to be considered as polar solvents. The polarity of a solvent is critical as it directly influences the electronic environment of the solute. Ionic liquids have the potential to be highly polar, yet noncoordinating solvents since ionic liquids are usually composed of poorly coordinating ions.[17, 39] The reactivity of ionic liquids in organic reactions can be modified by enhancing stabilisation of transition states or starting materials.[2] Also, ionic liquids can provide a nonaqueous, polar alternative for two-phase systems because hydrophobic ionic liquids are miscible with a number of organic solvents. Ionic liquids can also be used as immiscible polar phases with water.[40]

One of the properties that makes ionic liquids attractive especially from an industrial and processing perspective is their extremely low volatility.[41] The low volatility makes ionic liquids non-flammable and have high thermal stability gives wide liquidus temperatures. Moreover, it also makes ionic liquids an attractive option to electrochemists as a conductive media. Ionic liquids will not suffer diffusive losses or long-term evaporation, and they are easy to confine. With traditional electrolytes, diffusive losses can reduce device lifetimes by causing salt deposits on electrode surfaces.

In the last two decades, lots of literature reported on several applications of ionic liquids in industry. They have been used as catalysts for different synthetic transformations[42] and as alternatives to traditional organic solvents[2]. Ionic liquids, in addition, have been used as acid catalysts in many organic reactions as well as in industry. In this subchapter, two examples that demonstrate the capability of ionic liquid technology as acid catalysts in the chemical industry will be briefly discussed.

On 22$^{nd}$ September 2016, Honeywell UOP released a press release on a new application of ionic liquids in the refining industry.[43] Honeywell UOP announced that Chevron U.S.A. Inc. had developed a new alkylation technology which uses ionic liquids as a catalyst to produce high-octane motor fuels, called ISOALKY$^{TM}$.

Quoting from the press release, Mike Millard (vice president and general manager of Honeywell UOP's Process and Technology and Equipment business) said that, "Ionic liquids alkylation offers a compelling economic solution compared to conventional liquid acid technologies while delivering the same yields and high levels of octane". He also added that "This is a revolutionary new technology for refiners to produce alkylate and improve the quality of their gasoline pool". Alkylation technologies are usually being used in the refining industry to produce high-octane gasoline blending components to produce clean-burning fuels. It is the first new successful liquid alkylation technology to be introduced in 75 years. At present, most of the alkylation processes use a traditional technology that was developed in between 1938-1942 by or in concert with UOP. ISOALKY$^{TM}$ technology is an alternative to traditional technology that use sulphuric or hydrofluoric acid as a liquid alkylation catalyst. Ionic liquids that have strong acid properties are used as the acid catalyst to convert a typical stream from a fluid catalytic cracker into a valuable high octane blending component. One of the many advantages of this new technology is that a lower volume of catalyst is used to produce an alkylate using a more extensive range of feedstocks. This technology also can be used in both new refineries and existing facilities. Moreover, the ionic liquids can be regenerated onsite, giving it a lower environmental footprint compared to other technologies.[43]

Publicly, BASF$^{TM}$ is one of the industrial giants that has implemented the ionic liquids technology. They have the broadest range of applications, the largest patent portfolio and work openly with leading academics. BASIL$^{TM}$ (Biphasic Acid Scavenging utilising Ionic Liquids) is one of the most successful examples of using ionic liquids technology in an industrial process.[44, 45, 46, 47] This process is used to produce a generic photoinitiator precursor, alkoxyphenylphosphines. Triethylamine was used to scavenge the acid that was formed in the course of the reaction in the original process. However, it is difficult to handle the reaction as triethylammonium chloride (waste by-product) formed a dense insoluble paste. 1-methylimidazole replaced the triethylamine, which results in the formation of 1-methylimidazolium chloride, which then separates out from the reaction mixture (Figure 1.1.3). This reaction has proved that it is possible and practical to handle large quantities of ionic liquids in the industry as the reaction is now being carried

out on a multi-ton scale. The process was immediately acknowledged in 2004 as the process won the ECN Innovation Award.[48]

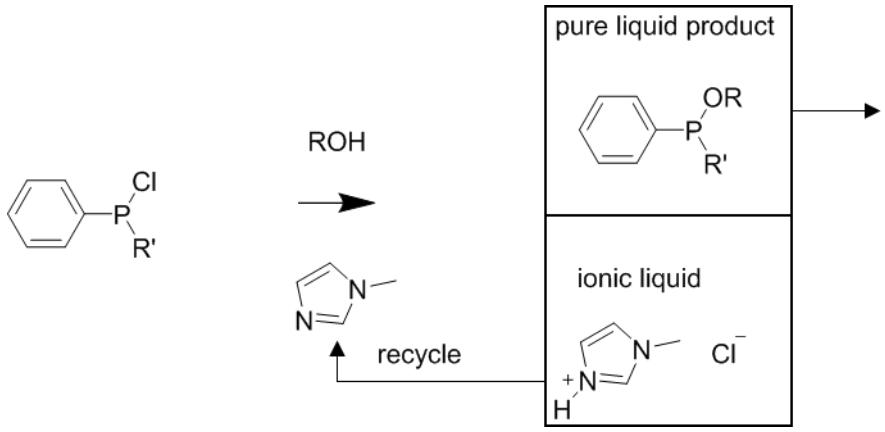



**Figure 1.1.3 –** The BASIL$^{TM}$process

### 1.1.4 Preparation of Ionic Liquids

There has been a rapid increase in the number of ionic liquids that have been prepared during the past 20 years using a variety of methods. As a result, there is a common two step route that is being used in the synthesis of ILs, although the details may vary; step 1) alkylation of an amine/sulphide/phosphine to give an intermediate salt and step 2) an anion exchange from the intermediate salt to give the ionic liquid. Figure 1.1.4 summarises the steps used to synthesis ionic liquids as illustrated by Welton and Wassercheid.[4] It is important to follow a synthesis route that can produce high-purity ionic liquids as it is not possible to distil most ionic liquids in large quantities.

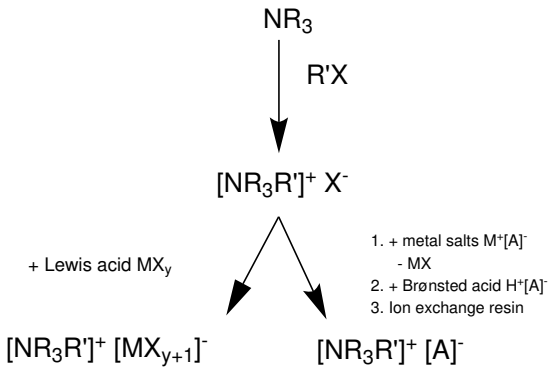



**Figure 1.1.4 –** Typical synthesis steps for preparing ionic liquids, ($NR_3$ stands for an initial amine substrate)

The preparation of ionic liquids is still an expensive process compared to molecular solvents; which can be synthesised cheaply (e.g. acetone) or extracted directly from nature (e.g. petroleum spirit, methanol or ethanol). The starting materials used to prepare ionic liquids are expensive due to the complex structure of the ions in ionic liquids.

The general preparations of ionic liquids listed below have been used to produce ionic liquids in this work. There are a lot of other standard and optimised methods described in the literature, and the details may vary between ionic liquids and research group with a possibility of not being reported in detail.

#### 1.1.4.1 Preparation of ionic liquids via halide intermediates

Aprotic ionic liquids can be synthesized using two-step procedure using alkylated cations and all other anions.[3]

**Step 1: Making the halide salts** The alkylation of tertiary amine or phosphine can be used to form the cation after purifying the starting materials. It is important to exclude any moisture and air while performing this step. Haloalkanes are the most common alkylating agents as they are inexpensive and it is easy to replace the halide salts formed during post reaction by other anions. Chloro-, bromo- and iodoalkanes (ease of alkylation, I > Br > Cl) are used as alkylating agents, where the nucleophilic substitution reactions occur.[4] The nucleophilic substitution reactions are highly exothermic and can lead to runway reactions.[49, 50]

Synthesis of $[C_4C_1im]Cl$ shown is an example to prepare the halide intermediates (Figure 1.1.5).

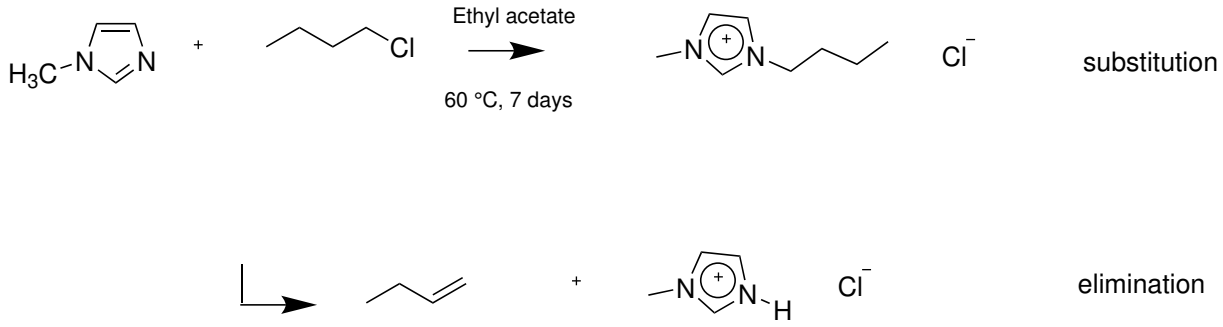



**Figure 1.1.5 –** Reaction scheme for synthesis of $[C_4C_1im]Cl$ using the direct alkylation step

There is a possibility of formation of elimination products from the competing reactions if the solution is overheated (Figure 1.1.5). Thus, the reactions are usually conducted in a solution (with the addition of solvent) followed by adding reactants drop-wise to avoid hotspots. The crude ILs obtained once the reaction has completed are usually salts at room temperature. A recrystallization process is necessary to purify the halide salts with the addition of solvents such as acetonitrile and ethyl acetate to help the precipitation of the salt and removal of unreacted starting materials. It is important to make sure that the alkylation is complete as it is nearly impossible to remove the remaining tertiary amine or phosphine. There has been a trend of practice in academic laboratories to leave the reaction longer and reduce the temperature to make sure the reaction is fully completed and to avoid coloured ionic liquids.

The alkylation synthesis of ionic liquids can also be done quickly with the assistance of microwave heating.[51] The report claimed that the reaction time was substantially reduced compared to the conventional methods with good yields. However, there also has been a report mentioned that it is difficult to control the reactions conditions where hot spots are possible which produce low-quality products.[52]

**Step 2: Metathesis - exchange of anions** Metathesis of the halide salts with a metal or ammonium salt or the conjugate acid of the required anion is then

performed using the halide salts formed from Step 1. The standard procedure of this method is by mixing the IL precursor (Figure 1.1.5) with metal a salt of the required anion in a dry, water immiscible solvent (e.g. dichloromethane) to prepare hydrophilic ionic liquids or water for the hydrophobic ionic liquid. The addition of water will lead to separation of hydrophobic ionic liquids during the reaction.[23] Preparation of $[C_4C_1im][NTf_2]$ will be used as an example for salt metathesis reaction (Figure 1.1.6).

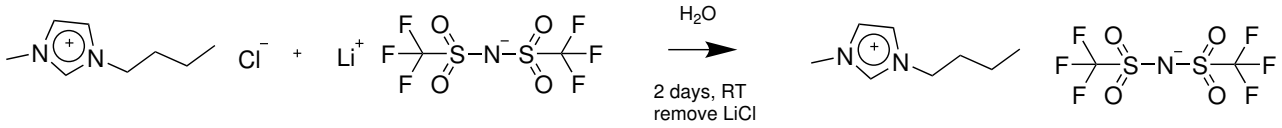



**Figure 1.1.6** – Methathesis reaction of $[C_4C_1im]Cl$ with $Li[NTf_2]$ to produce $[C_4C_1im][NTf_2]$

The formed lithium chloride salts will be precipitated from the solution during anion exchange which will assist the reaction to completion. The aqueous solution is then repeatedly washed with dichloromethane, and further isolation of the ionic liquid from the dichloromethane solution will increase overall yield. Any remaining water is then removed in *vacuo* to obtain a dry ionic liquid ($<$ 20 ppm $H_2O$). For hydrophilic ionic liquids, the resulting mixture (solvent + IL + halide salts) is then filtered and the organic phase is then is washed with water to remove any remaining halide salt. It is difficult to obtain a high yield as the miscibility of IL in water increases.[5]

### 1.1.4.2 Acid-base neutralisation

Acid-base neutralisation reactions are limited to the preparation of only one type of ionic liquids called protic ionic liquids. However, it is the cheapest and the quickest way to prepare protic ionic liquids. The heteroatom (N, P or S) of the protic ionic liquid's cation is charged by protonation. An acid-base reaction is involved during the formation of the ionic liquid where a base reacts with an acid (eqn. 1.1.1). The base becomes positively charged as the proton, $H^+$ from acid is transferred, and the acid anion becomes the anion of the ionic liquid.

$$B + AH \rightarrow BH^+ + A^- \tag{1.1.1}$$

The acid-base neutralisation reaction is a fast reaction compared to other methods. The reactions can be carried out in a neat condition and the synthesis of 1-butylimidazolium hydrogensulfate ([$HC_4$im][$HSO_4$]) is used as an example to describe the acid-base preparation of ionic liquid by reacting 1-butylimidazole with 97% sulfuric acid (Figure 1.1.7).

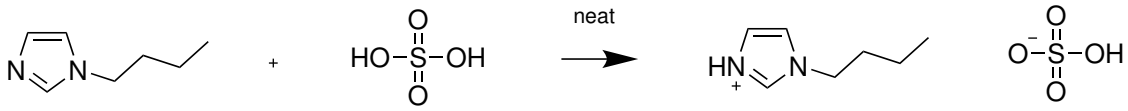



**Figure 1.1.7** – Acid-base reaction of reaction of 1-butylimidazole with sulphuric acid to produce [$HC_4$im][$HSO_4$]

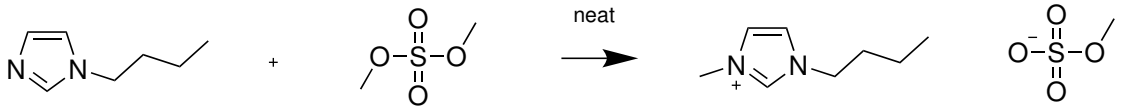
The reactions are often carried out in water, even though it can be done in a neat condition, as the reaction is exothermic. Both the acid and base are well miscible with water and the water helps to control the reaction as heat is produced during the reaction. Coloured products will be obtained if the reaction is too exothermic, thus it is important to add the diluted sulfuric acid in the base in a slow manner. It was followed by purification and water removal steps after the reaction is completed. The prepared ionic liquids must be further dried in vacuo to remove water (<100 ppm $H_2O$). This technique has been commercialised and was used by BASF in the BASIL (biphasic acid scavenging utilising ionic liquids) process.[47] In this process the protic ionic liquid, 1-methyl-imidazolium chloride 1-methylimidazole ([$C_1$Him][Cl]) is produced during a proton transfer reaction between 1-methylimidazole and HCl. 1-methylimidazole acts as an acid scavenger to remove HCl.

### 1.1.4.3 Direct alkylation

Alkyl sulfate and dialkyl phosphate salts can prepared using dialkyl sulfates or trialkyl phosphates as an alkylating agent respectively via the direct alkylation route.[53, 54] The direct alkylation route is a cheap and halide free method to prepare alkyl sulfate and dialkyl phosphate aprotic ionic liquids. There was a report in the

literature where the first alkyl sulfate ionic liquid $[C_4C_1im][C_8OSO_3]$, was prepared using the halide intermediates route using $[C_4C_1im]Cl$ and $Na[C_8OSO_3]$.[30] The most common alkylating agents used are dimethyl sulfate, $Me_2SO_4$ and trimethyl phosphate, $Me_3PO_4$. Figure 1.1.8 is used as an example for the direct alkylation route.

(a) Alkylsulfates




(b) Alkylphosphates

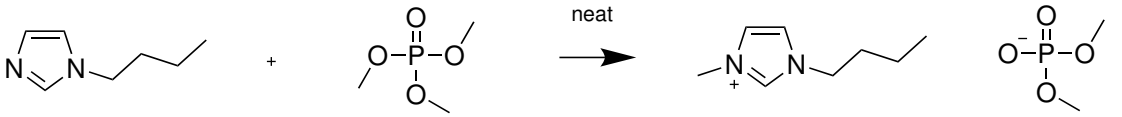



**Figure 1.1.8** – Synthesis of ionic liquids by direct alkylation

The direct alkylation is also an exothermic reaction and care is required to avoid overheating that can produce low-quality ionic liquids. It is also possible to convert the ionic liquids prepared from the direct alkylation method into other ionic liquids (e.g. $[C_4C_1im][HSO_4]$).[55] $[C_4C_1im][HSO_4]$ can be produced by the hydrolysis of the anion of $[C_4C_1im][MeSO_4]$ with methanol as a side-product that can be easily removed by evaporation.

#### 1.1.4.4 Purification of ionic liquids

Most ionic liquids prepared in the academic laboratory and commercially produced are bound to have colour which indicates reduced purity and quality of the ionic liquids. Commercial ionic liquids available nowadays usually have a purity claimed between 90% - 99% which is relatively poor compared to other commercially available solvents. Even though the colour of the ionic liquids did

not obstruct the ability of ionic liquids in industrial processes,[56, 57] it is essential to acknowledge that it can cause a significant limitation for analytical measurements (e.g. UV-Vis techniques).[58] In addition, there were reports mentioned that the physico-chemical properties of the ionic liquids can be affected even with small amounts of impurities.[59, 60] The impurities in the ionic liquids can come from various factors, from the starting material used to the temperature applied while preparing the ionic liquid. It is important to remove the impurities to produce a high-quality ionic liquids. The list below represents common impurities and their removal methods.

1. Impurities from the starting materials: The starting materials must be purified prior use. The most typical purification step is distillation from a suitable drying agent in an inert atmosphere. Prewashing of the starting materials is used as an additional step whenever preparing a very pure "spectroscopic grade" ionic liquids.[61, 62]

2. Excess starting materials: In the direct alkylation route, there is a possibility of leftover base such as imidazole or pyrrolidine in this reaction. Small excess amount alkylating agent can be added to maximize the alkylation of base with the alkylating agents. The removal of solvent used in the reaction helps to remove any remaining excess starting materials. The ionic liquids prepared can be recrystallised with an anti-solvent for extra purity purposes.[3]

3. Colour contaminants: The presence of trace molecular solvents or halogens or the decomposition of the ionic liquid could be the reason of coloured ionic liquids. Stirring the ionic liquid mixed with charcoal overnight can remove the colour of the ionic liquid, followed by filtration step. Diluting the ionic liquid with solvent is also possible if the ionic liquid is too viscous. The solvent is further removed in vacuo.[57]

4. Acid or base contaminants: Ionic liquid with excess acid or base can be removed by passing the ionic liquids through alumina powder. Excess base is removed by acidic alumina while excess acid is removed by basic alumina.[57]

The most persistent and major impurities found from today's ionic liquids are thought to be water and halides. Impurities can be detected by NMR spectroscopy

if it is coming from the unreacted starting materials. Karl-Fisher titration is a desirable method to determine the water content of the ionic liquids down to ppm levels. Few samples and fast measurements are one of the advantages of this titration method.[56]

#### 1.1.4.5 Other synthesis routes

There are lots of other synthesis routes available to prepare ionic liquids with some are innovative ideas towards greener solutions (e.g. less solvent, halide-free or faster reaction). It is worth to mention their names although it will not be discussed here in detail. Some of them are: methyl carbonate route [63, 64], ion exchange with silver salts [23] and ion metathesis with ion exchange resins [65].

## 1.2 The theory of acidity

The hydrogen nucleus, *i.e.*, the proton $H^+$, is a chemical species that plays a privileged and unique role in acidity. The proton by itself has a powerful polarising effect and is not prone to electronic repulsion since its $1s$ orbital is empty. It is impossible for the proton to be in a free "naked" species in the condensed state because of its strong electron affinity. The strong electron affinity of the proton causes the proton to be always associated with one or more molecules of the solvent or the acid itself. Free protons only exist in the gas phase (for example, in mass spectrometry studies).[66] Proton transfer is a straightforward chemical reaction because of its very small size ($10^5$ times lower than any other cation), and only the $1s$ orbital is used in the bonding by hydrogen. It is important to understand the nature of the proton while studying the acidity measurements.

Between 1880 and 1890, Arrhenius explained the variation in the strength of different acids using the theory of ionic dissociation in water.[67] Arrhenius defines an acid as a hydrogen-containing substance that dissociates into hydrogen ions and anions when dissolved in water whereas bases dissociate to yield the hydroxide ion. Equation 1.2.1 gives an example of an Arrhenius type of acid:

$$HCl \rightarrow H^+ + Cl^- \tag{1.2.1}$$

The Arrhenius definition of acid is based on electrolytic experiments such as conductance measurements.[68] Acid strengths can be quantitatively compared by measuring the conductivities of their aqueous solutions at equal analytical concentrations since conductivity increases with increasing acid dissociation. For example, HCl (eqn. 1.2.1) is regarded as a strong acid since it exhibits high conductivities in aqueous solutions. The low conductivities of solutions of incompletely dissociated acids is attributed to their weakness. Acid dissociation is described as a dynamic equilibrium process where the rate of dissociation of electrically neutral molecules is equal to the recombination rate of their ions (eqn. 1.2.2):

$$HA \rightleftharpoons H^+ + A^- \tag{1.2.2}$$

The ionization or dissociation constant for acids ($K_a$) can be derived by applying the mass-action law to equation 1.2.2 :

$$K_a = \frac{[H^+][A^-]}{[HA]} \tag{1.2.3}$$

where the brackets represent the concentrations of bracketed species. The acid dissociation constants derived by relating conductivity to the degree of ionisation provide a means of quantifying the acid strength in aqueous solution. The dissociation constants are useful in acidity measurements, the preparation of buffers (solutions of weak acids and their salts) and titrations. Moreover, it is also correlated well with estimations of relative acid strength from catalytic and indication method.[68]

Although the Arrhenius concept of acids was able to explain several phenomena such as salt hydrolysis and strength of acids, it has many shortcomings and is known to be the most limited theory or concept to define acidity[66]:

1. Acid was defined in terms of aqueous of solutions of pure substances rather than as pure substances. The presence of water is necessary. For example, aqueous HCl is considered as an acid. Pure anhydrous hydrogen chloride was not an acid and manifested no acidic properties.

2. Acid behaviour was not acknowledged in non-aqueous solutions.

3. As a consequence of the general electrolytic dissociation theory of reactions in solution, ionisation is required to be a necessary characteristic of an acid. This characteristic caused a confusion when the acidity in nonionizing solvents was involved. For example, HCl remained practically undissociated in anhydrous sulfuric acid, toluene, benzene and in the pure liquid state although it is completely ionized in water. This has led to an unclear situation of whether HCl was an acid or not in other than aqueous solution using the Arrhenius theory, from both of the aqueous solution and ionization limitations.

4. The theory only applied to hydrogen-containing compounds with substances with pronounced and obvious acidic properties with no hydrogen being excluded (for example, $CO_2$, $SO_3$, and $SnCl_4$).

5. The free proton $H^+$ cannot exist for a long time in a water solution. The $H^+$is bound to added water and exists as the hydronium (or oxonium or hydroxonium) ion, $H_3O^+$ . The catalytic and acid properties of the hydronium ion were weak compared to that of free hydrogen ion.

Despite its shortcomings, the Arrhenius theory was the most prominent of the acidity theories during the latter part of the $19^{th}$ and early part of the $20^{th}$ century. However, a further general acid-base concept was required to overcome the shortcomings of the Arrhenius theory. It was important that the theory did not deviate from the belief in the unique nature of the hydrogen ion relative to acids and bases in particular and chemical species in general.

### 1.2.1 Brønsted-Lowry Theory

Johannes Nicolaus Brønsted generalised the Arrhenius concept to other solvents in 1923. An acid is defined as a substance that is capable of giving up a proton, and a base is defined as a substance that can accept it.[69] The definition of an acid did not have too much difference from the Arrhenius theory except where he omitted water as a requisitive solvent. Brønsted, however, rejected the definition of bases from the Arrhenius theory as being too narrow. Equation 1.2.4 summarise the theoretical relationship between acids and bases:

$$Acid \rightleftharpoons Base + H^+ \tag{1.2.4}$$

Thomas Martin Lowry on his observation of the "uniqueness of hydrogen" in 1923 independently came to the same conclusion as Brønsted on the definition of acid and base.[70] As protons were already accepted as not capable of independent existence, Lowry stated that a species that is capable of accepting a proton must present for an acid to exhibit its acidity properties (to give up a proton). He then defined bases as proton acceptors. The definition of acid and base from both Brønsted and Lowry is known as the Brønsted-Lowry theory, and it is the most used and well-known acid-base theory.

In the Brønsted-Lowry theory, a double conjugate acid-base pair reaction represents an acid-base reaction as it involves the transfer of a proton from the acid to the base. The dissociation of an acid to a base can be written as an acid-base equilibrium:

$$acid + base \rightleftharpoons conjugate\,base + conjugate\,acid \tag{1.2.5}$$

The products of an acid-base reaction are a new acid-base pair that differs only by a proton. This product comprises conjugates of the original acid, and base and it is called the conjugate acid-base pair. The acid-base equilibrium above is used to drscribe the dissociation of an acid, HA in a solvent, S:

$$HA + S \rightleftharpoons A^- + HS^+ \tag{1.2.6}$$

The ionisation of the acid (HA) in a solvent (S) produces a conjugate acid, ($HS^+$) and a conjugate base ($A^-$). Brønsted defined that the acids and bases involved in equations 1.2.5 and 1.2.6 are referred to as protolytes while the whole equation is called protolysis.[71] The advantages of equations 1.2.5 and 1.2.6 are they can be applied to neutral, positively and negatively charged acid systems and no free proton is required for proton transfer. The protolysis concept allows extension of acid-base dissociation into nonaqueous solvents. As well as the concept of acids and bases working for reactions taking place in solution, protolysis expands these concepts towards proton-transfer processes in the gas phase and in melts.[72]

Brønsted also described an acidity constant, $K_a$ in terms of the concentration ratio of the participating conjugate acid-base pair and the hydrogen ion activity[69]:

$$K_a = \frac{[A^-][HS^+]}{[HA]} \tag{1.2.7}$$

Equation 1.2.7 was derived from the application of the law of mass action and has been used in the quantitative aspects of the protonic theory. Brønsted used (eqn. 1.2.7) to measure the acid strength, in principle independent of the solvent's nature. The dissociation constant, $pK_a$ is further derived from (eqn. 1.2.7) for quantitative measurement of the strength of acids:

$$pK_a = -log(K_a) \tag{1.2.8}$$

More negative $pK_a$ values suggest the acid is stronger and this led to a conclusion that when AH is a strong acid, $A^-$ will be a weak base. It is commonly found in the literature where $pK_a$ values of their conjugate acids are used to express the strength of bases. A higher (more positive) $pK_a$ is equal to a strong base and it would have a weak conjugate acid. The Brønsted-Lowry theory has apparently overcome the shortcomings of Arrhenius theory in defining acid and base concept. However, it is difficult to establish an absolute acidity scale using the protolysis concept. The consequence of the protolysis concept is that the extent of ionisation of an acid will depend on the basicity of the solvent in which of the ionisation occurs. As acidity scales are energy scales, they are unpredictable and depend on the reference point and to the magnitude of units chosen.

Fortunately, lots of common solvents are amphiprotic or amphoteric solvents where they are capable of acting as Brønsted acids, and Brønsted bases and they can undergo self-ionisation. Self-ionisation or autopyrolysis can occur only in amphiprotic solvents because they possess both proton-accepting and donating abilities. Equation 1.2.9 is an example of solvent self-ionization:

$$2H_2O \rightleftharpoons H_3O^+ + OH^- \tag{1.2.9}$$

The equation is then re-written in general way as;

$$2HA \rightleftharpoons H_2A^+ + A^- \tag{1.2.10}$$

The equilibrium of autopyrolysis is quantitatively characterized by an autopyrolysis constant, $K_{ap}$ (eqn. 1.2.11):

$$K_{ap} = \frac{[H_2A^+][A]}{[2HA]} \tag{1.2.11}$$

$K_{ap}$ of solvents are usually very small (in $H_2O$, $K_{ap} = 10^{-14}$) compared to other protolysis constants because amphiprotic solvents are weak acids as well as weak bases.

### 1.2.2 Lewis Theory

In 1923, Gilbert Newton Lewis coincidentally came out with the electron-pair donor-acceptor acid-base definitions.[73] He proposed that the transfer of a pair of electrons defines Lewis acids and Lewis bases instead of the loss and gains of protons in the Brønsted-Lowry. In the Lewis theory of acid-base reactions, acids accept pairs of electrons donated by bases. A Lewis acid is defined as any substance that can accept a pair of nonbonding electrons and thus it is regarded as an electron-pair acceptor. A Lewis base is then defined as any substance that can donate a pair of nonbonding electrons and is, therefore, an electron-pair donor. Lewis extended the theory of acids to cover systems that do not involve proton transfers and non-aqueous systems. The equations below is one example of the Lewis theory:

$$BF_3 + : O(CH_3)_2 \rightarrow BF_3 : O(CH_3)_2 \tag{1.2.12}$$

In the eqn. 1.2.12, the lone pair from the :$O(CH_3)_2$ is donated into the empty $p$-orbital of the electron deficient boron in $BF_3$. A covalent bond is formed when the $O(CH_3)_2$ molecule is donating its pair of electrons to the $BF_3$ and thus $O(CH_3)_2$ is a Lewis base. The $BF_3$ is a Lewis acid since it accepts the lone pair electrons donated by the Lewis base. There are a few advantages of Lewis theory over Arrhenius and Brønsted - Lowry theories:

- Lewis theory complements the model of oxidation-reduction reactions. In these reactions, a transfer of electrons from one atom to one another is involved, with a net change in the oxidation number of one or more atoms. The theory indicates that no change occurs in the oxidation numbers of any atoms involved when acids react with bases to share a pair of electrons.

- Lewis theory has enlarged the number of acids and consequently the number of acid-base reactions. Lewis defined an acid as any substance that can accept a pair of nonbonding valence electrons. For example in the reaction from equation 1.2.13 :

$$Al^{3+} + 6H_2O \rightleftharpoons Al(H_2O)_6^{3+} \tag{1.2.13}$$

$Al^{3+}$ form bonds to water molecules to give a complex ion. This complex ion was formed because the $Al^{3+}$ ion has empty $3s$, $3p$ and $3d$ orbitals that can be used to hold pairs of nonbonding electrons from the water (Lewis base). The $Al(H_2O)_6{}^{3+}$ acid-base complex or complex ion is then formed based on this Lewis acid-base reaction.

- Lewis theory also explains why non-metal oxides such as $CO_2$ dissolve in water to form acids, e.g. carbonic acid, $H_2CO_3$ (eqn. 1.2.14):

$$CO_2 + H_2O \rightleftharpoons H_2CO_3 \tag{1.2.14}$$

The carbon atom in $CO_2$ no longer needs to form double bonds with both of the other O atoms as it bonds with a pair of electrons from the water (Figure 1.2.1).

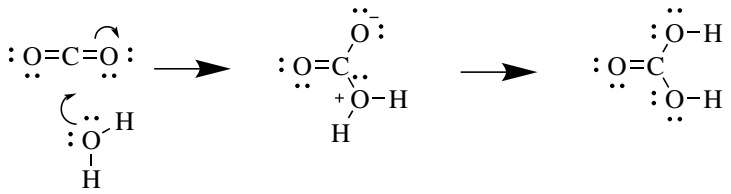


**Figure 1.2.1 –** The formation of carbonic acid

Based on the advantages listed, it can be concluded that by using Lewis theory to define acid-base reactions, many chemical reactions can be sorted out due the fact the theory works when either electrons are transferred from one atom to another, or the atoms come together to share a pair of electrons.

### 1.2.3 Levelling effect

Theoretically, the order of acid strength is constant regardless of the solvent. The constant order of acid strength happens because the ratio of the protolysis constant of any two acids in any solvent is constant to the said ratio in any other solvent and the ratio of the acidity constant of the species under consideration. However, in practice, most protolysis constants exceed the minimum value required for the basic quantitative reaction.[68] Thus, it is impossible to differentiate between acid strength in a highly basic solvent or vice versa. Hantzsch's levelling effect can be used to understand this effect qualitatively, and the Brønsted-Lowry theory provides a quantitative interpretation based on protolysis constant. Hantzsch studied various reactions of acids in different solvents and used the "levelling effect" expression to describe the influence of water in masking differences in the intrinsic strengths of acids.[74, 75, 76] A weak acid in aqueous solution, for example; acetic acid behaves like a strong acid and dissociates completely in liquid ammonia, a more basic solvent.

The levelling effect gives limits on acidity depending on the nature of the solvent.[77] The upper limits in protophilic solvents of the acidity of solutions is given by the levelling of the solute acid strengths to the strength of the conjugate acid of the solvent, called the "lyonium" ion. Acids stronger than the lyonium ion have acidity constants of a magnitude enough to produce a very large protolysis constant in combination with the solvent $K_B$ and go through quantitative protolysis. Thus, an acid that is stronger than the lyonium in a solvent does not exist.[68] The acetic acid in liquid ammonia behaviour mentioned previously is an example of such levelling.

The apparent strength of a protonic acid depends on the solvent in which the acid is dissolved. Therefore, a solution of an acid in a levelling solvent acts as if it were a solution of the lyonium ion. It is important to emphasize the difference between the Brønsted concept of acidity (the tendency to donate a proton) and the protolysis process to avoid confusion between these two processes. For example, HCl has a high acidity constant reflecting that it is a strong acid. However, aqueous HCl solutions reflect this strengths since the protolysis constant of the HCl-water reaction is high. HCl is still a strong acid even though the proton transfer may not

be completed in a less basic solvent. Thus, it is possible to differentiate between increasing true acidity in the Brønsted sense and to increase visible acidity, which stems from increasing solvent basicity. In consequence, HCl is a stronger acid in glacial acetic acid than in water, even though HCl is completely ionised in water. The situation happens because the extent of protolysis is reduced in the acidic medium, which allows the presence of the strong acid HCl in its undissociated form. On the other hand, in water, the levelling effect allows the presence of only the relatively weakly acidic hydronium ion. Moreover, what protolysis there is in acetic acid produces the formation of a stronger lyonium acid than hydronium ion.[68]

### 1.2.4 Mesuring acidity, the pH scale

The pH of a solution is a measure of its acidity or basicity.[78] The acidity or basicity of aqueous solutions relies on the concentration of hydrogen ($H^+$) ions and hydroxyl ions ($OH^-$) present in it. The pH scale is a popular method used to measure the acidity of solutions. The basic understanding of pH that is widely known; that the lower the pH value, the more acidic the solution is; and in aqueous solutions, a pH $< 7$ means acidic, while a pH $> 7$ means alkali. Sørenson defines the concept of pH as follows[78];

$$pH = log\frac{1}{H^+} = -log[H^+] \tag{1.2.15}$$

or $[H^+] = 10^{-pH}$

Thus, the pH value is the logarithm to the base ten of the reciprocal of $[H^+]$ ion in grams per litre. For example in pure water;

$[H^+] \approx 10^{-7}$g/L , $pH \approx 7$

Further development of chemical thermodynamics concludes that Sørenson's experimental values did not yield the exact $[H^+]$ ion. The definition of pH by Sørenson were functions of the apparent concentrations of the electrolytes in solution. Thus, the evident concentration is known as the activity, and the activity coefficient defines the ratio activity concentration. The pH now is defined as the hydrogen ion activity after replacing the ion concentration term. Thus, pH is defined as;

$$pH = -log\,\alpha_{H^+} \tag{1.2.16}$$

where $\alpha_{H^+}$ is the activity of the hydrogen ion.

#### 1.2.4.1 Measuring pH in water

pH is usually used to define the acidity of aqueous solutions. In an aqueous solution of acid, an acid (AH) protonate water, where;

$AH + H_2O \rightleftharpoons A^- + H_3O^+$

For strong acids, pH is equal to -log [AH], because they are completely dissociated to $H_3O^+$ and $A^-$. In weak acids, an equilibrium exists to cause the pH to depend on the dissociation constant, $K_\alpha$ (refer to the eqn. 1.2.7 and eqn. 1.2.8 for the definition of $K_\alpha$ and $pK_\alpha$) and the concentration of acids. To calculate the pH value, equation 1.2.8 can be rearranged into;

$$pH = pK_\alpha - log\left(\frac{[AH]}{[A^-]}\right) \tag{1.2.17}$$

which it is also known as the Henderson-Hasselbalch equation.[79, 80]

#### 1.2.4.2 Measurement of pH

There are two primary methods used to measure the pH of a solution, the colourimetric or indicator method and the electrometric (pH meter) method. An indicator method uses a dye where its colour is determined by the acid-base ratio of the solution to which it is added. The dye used, such as phenolphthalein or methyl orange or pH papers, behaves like a weak acid or a weak base. Both of the acid or base will give a different colour where the colour produced is dependent on the hydrogen ion concentration. The colourimetric method is a fast and low-cost way to determine pH of a solution, but it only gives an approximate value of pH.

Electrometric methods are more accurate than the colourimetric method. In the electrometric method, the electromotive force (EMF) generated by a galvanic cell determines the pH value. According to the Nernst equation, the electrode potential is proportional to pH, where;

$$E = E_0 + \frac{RT}{F} ln(\alpha_{H^+}) = E_0 - \frac{2.303RT}{F} pH \tag{1.2.18}$$

where E is the electrode potential of the measured solution, $E_0$ is the standard electrode potential, R is the gas constant, T is the temperature in Kelvin and F is the Faraday constant. The galvanic cell is consists of:

Reference electrode | standard electrode || test solution | $H_2$ | Pt

where || is a means of contact with the two electrodes and the standard electrode used is a 3M KCl solution. The $\triangle E$ is obtained when reference electrode (AgCl) is immersed in the standard solution, and both of them is connected to a $Pt/H_2$ electrode immersed in the measured solution.

A modern pH meter uses a glass electrode to detect $H^+$ is used to to replace the $Pt/H_2$ electrode used in the galvanic cell. The modern pH electrode uses a specially formulated pH sensitive glass in contact with the solution, which then develops a potential (voltage) proportional to the pH of the solution. The reference electrode is used to complete the pH measuring circuit within the solution and is designed to maintain a constant potential at any given temperature. The reference electrode supplies a known reference potential for the pH electrode. As the $\triangle E$ is directly proportional to pH according to the eqn. 1.2.17, a plot of $\triangle E$ against pH produces a straight line. The difference in the potentials of the pH and reference electrodes provides a millivolt signal proportional to pH. The electrodes must be calibrated with two standard buffer solutions with known pH prior use (usually 4 and 7, or 7 and 10).

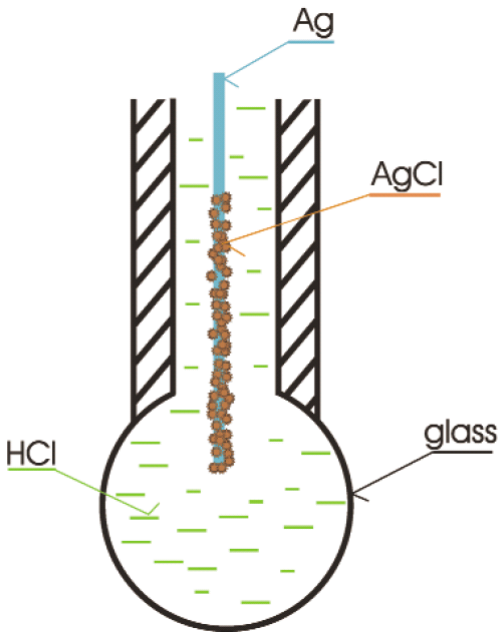



**Figure 1.2.2** – Schematics of a glass electrode[81]

## 1.3 Brønsted Acids in Ionic Liquids

. *"If Brønsted acids are involved we must remember that THE PROTON LIKES COMPANY - IT WILL NEVER WALK ALONE"* - Johnson *et al.*, 2007.[82]

Proton transfer is the most common chemical transformation in the chemical industry,[83] and it is known to be solvent dependent[84]. Acidity is one of the most crucial parameters in many industrial processes as it directly affects the selectivities, rates and yields of chemical reactions. On both industrial and laboratory scales, Brønsted acids have been used extensively in diverse chemical reactions such as esterification, alkylation, dehydration, condensation and synthesis of pharmaceutical products.[43, 85] In the Brønsted acid-catalysed reactions, proton transfer marks the reaction where it can make one reacting partner more electrophilic. Following this, acid catalysis may happen by two different routes: general acid catalysis and specific acid catalysis. General acid catalysis refers to

a system where more than one species behaves as an acid. Specific acid catalysis is a process where the reaction rates depend on the specific acid in the solution. Normally, the specific acid is the protonated form of the solvent in which the reaction is occurs.[32] Regardless of the fact that homogenous Brønsted acids are commonly used in chemical reactions, serious drawbacks have been encountered by using these chemicals. Strong homogenous acid (sulfuric acid) and even concentrated weak acids (e.g. acetic acid and formic acid) are corrosive. For example, hazardous gas is produced when sulfuric acid rapidly reacts with some of metals, which is harmful if released in the environment. Metallic wastes from a reactor may also be produced which will crack the inside of the reactor body and/or pollute the products.[86] The substitution of homogenous acid catalysts with less hazardous or even better safe compounds is necessary to address problems mentioned above. Heterogenous acid catalysts based on porous materials are a possible substitution for homogenous acid catalysts have shown a good improvements in catalyst separation and recovery.[87, 88] Unfortunately, a limitation of heterogeneous catalyst mentioned is the deactivation of the hydrophilic surface with water and weak mass transfer.[89, 90]

Ionic liquids are known as all-round chemicals in synthetic chemistry as there are lots of applications of ionic liquids in acid-catalyzed reactions and the popularity of ionic liquids as solvents has also increased.[91] Recently, Brønsted acidic ionic liquids (BAILs) have gained attention as efficient catalysts for the synthesis of valuable chemicals. Brønsted acidic ionic liquids are one of the subset of ILs or known as protic ionic liquids (PILs). They are easily produced by combining Brønsted acid and Brønsted base via proton transfer (e.g. Figure 1.1.7). They are easily produced by combining Brønsted acid and Brønsted base via proton transfer (Figure 1.3.1).[92] It is possible to improve the proton transfer process by using stronger acids and/or stronger bases, and thus cause a greater driving force for the proton transfer. The pKa values of acids and bases are usually used in aqueous solutions to indicate how strongly a proton will be transferred from the acid to base but it might not be suitable for the nonaquoeus BAILs.[93, 94]

Theoretically, Brønsted acids and Brønsted bases react completely to produce protic ionic liquids. However, in practice, neutral acid and base species are present, as the proton transfer may less than complete. Thus, it is necessary to have

standard techniques to measure the ionicity and the structure of the ionic liquids. Literature reported that the ionicity or ionic characters of the PILs were measured to assess the proton transfer in the final product.[93, 94, 95, 96] Currently, there is no "standard" method to classify which should be considered pure ILs nor to determine the ionicity PILs. MacFarlane *et al.* have recommended that any concentration of neutral species available in PILs must still lead to the mixture to be called an ionic liquid when the properties of the mixture are clearly the ionic liquid's rather than the neutral species.[93] There are a few different techniques reported in order to gain information about ionicity of PILs, for example IR spectroscopy,[97] NMR spectroscopy[97] and ionic conductivity in the form of a Walden plot[94].

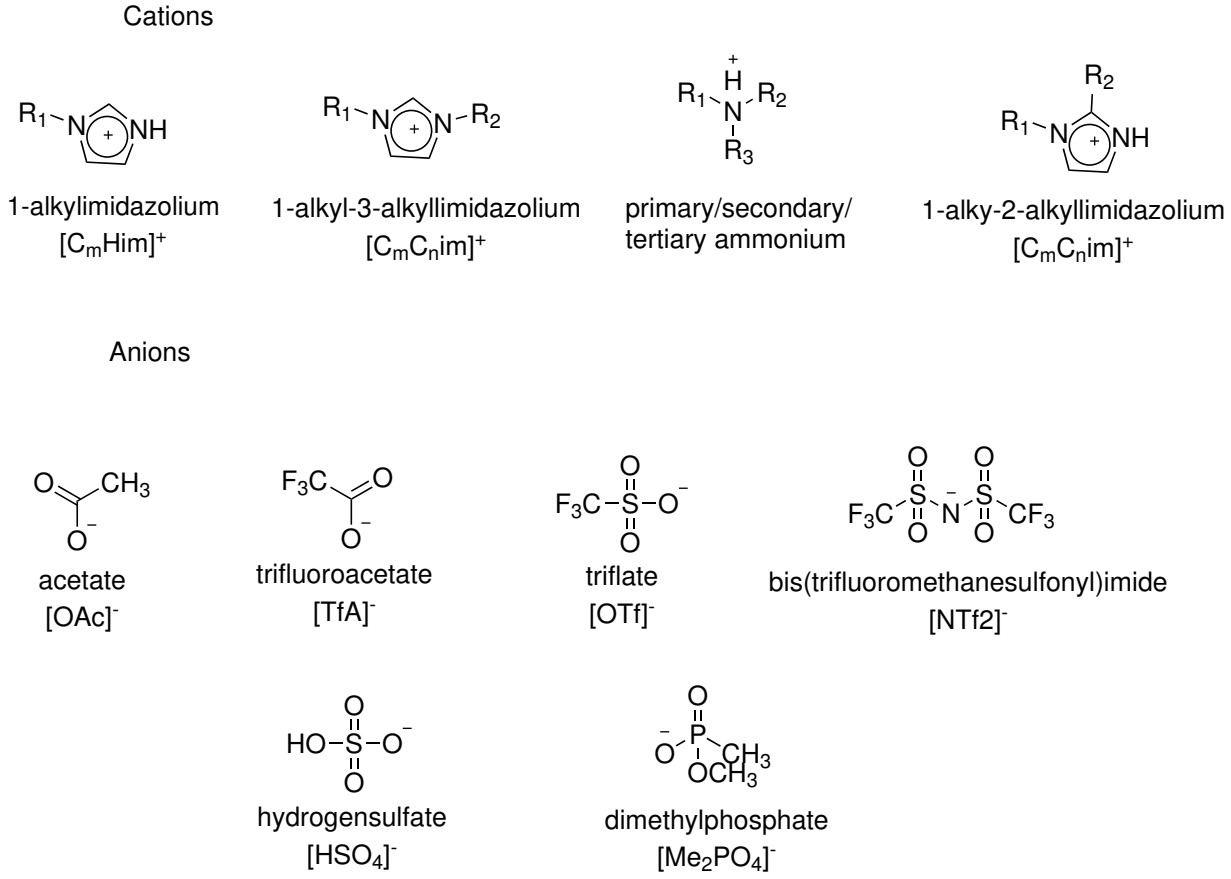



**Figure 1.3.1** – Possible cations and anions of BAILs

### 1.3.1 Applications of Brønsted Acidic Ionic Liquids

Catalysis plays a significant role in materials synthesis, environmental protection and human healthcare.[98] Thus, it is safe to say that catalysis is an important technology in the sustainability of chemistry. An extensive range of ionic liquids commonly containing imidazolium cations have been used as catalysts and solvents for many organic reactions. The main reason for using ionic liquids as catalysts or solvents is the environmental benefit of replacing solutions of strong acids in organic solvents with relatively benign ionic liquids. Most traditional methods used in organic reactions produce waste molecular solvents and large amounts of acidic waste. The catalyst is normally expensive and time-consuming catalyst-recycling procedures are usually required. Ionic liquids are usually used as catalysts for reactions that require a Brønsted or Lewis acidic catalyst. Most of these ionic liquids are cheap and easy to produce, often only produce one by-product, water, and usually only involve simple reaction processes.[92] Many papers were found reviewing the application of ionic liquids as solvents or catalysts. In 1999, Welton published an early review introducing the reactions that had been conducted in ILs as solvents.[2] Until that time, a large focus was on using chloroaluminate ionic liquids as they are able to frequently catalyze the reactions without additional catalyst. Sheldon has published a review that contains a section outlining general considerations on catalysis in ionic liquids including general properties of ionic liquids that are beneficial to this application. Potential scenarios where the ionic liquids may act as the solvent or solvent and catalyst were also included.[99] A review by Muzart in 2006 discussed the use of ionic liquids as solvents for catalyzed oxidation of organic compounds.[100] A new alkylation technology which uses an ionic liquid as a catalyst to produce high-octane motor fuels developed by Honeywell was discussed before in the subchapter 1.1.3. A few examples of catalysis applications using Brønsted acidic ionic liquids that are thought to be interesting will be discussed further in this subchapter. Alkylation or the attachment of alkyl group can be achieved through nucleophilic, electrophilic and free radical alkylation reactions. Friedel-Crafts type alkylation is one common example of electrophilic alkylation. Brønsted acidic ionic liquids can be used to generate carbocations where they are usually more effective than common Lewis and mineral

acids. A Friedel-crafts alkylation of indoles and cyclic ketones using a sulfonyl-functionalized Brønsted acid ionic liquids as catalyst was investigated by Taheri *et al.*[101] C3-cycloalkylated indole was synthesized via reductive alkylation of indole with a cyclic ketone. Both of the ionic liquids used in these reactions have the $[OTf]^-$ anion. The reaction yield obtained was 92% with the addition of 10 mol% of the ionic liquids. The results were then compared with other common strong Brønsted acids such as triflic acid and toluenesulfonic acid. Only moderate yields were obtained (51-60%) at the same reaction conditions. In the reaction, an oligomer of indole (identified as most likely a radical initiator) was formed through oxidative oligomerization with the presence of acid and oxygen. A cationic radical generated from the carbocation intermediate formed the reduced alkylation product. Water formed at the initial stage played a key role in making the reductive coupling possible. Overall, it was concluded that the C3-cycloalkylindole derivatives can be synthesized using a new and efficient method, an acid-induced reductive Friedel-Crafts alkylation. The new method was claimed to possess several properties of green organic synthesis such as easy product isolation, solvent-free conditions and high synthetic efficiency.

Tertiary alkenes or alcohols such as $^{t}$-butanol (TBA) are examples of common alkylating agents used in the acidic ionic liquid catalyzed alkylation of phenol and phenol derivatives. Elvarasan *et al.* measured the catalytic activities of Brønsted acid ionic liquids in the t-butylation of phenol with TBA (Figure 1.3.2).[102] The triethylammonium based sulfonic acid functionalized ionic liquid gave the highest phenol conversion (84.5%) after optimising the reaction conditions. The catalyst was found to retain its catalytic activity even after 5 recycles. The alkylation of $^{iso}$-butane with 1-butene is another widely studied application of acidic ionic liquids. The mentioned alkylation process is an important process in the petroleum industry as the products are usually used as premium blending stock for reformulated gasoline. The gasoline produced has a low vapor pressure, low alkenes and sulfur contents and importantly has a high octane number. Another study reported that the alkylation of $^{iso}$-butane was conducted with ammonium-based ionic liquids (with the $[HSO_4]^-$ anion) coupled with triflic acid (HOTf) as the catalyst. The addition of the ionic liquids has dramatically increased the efficiency of HOTf for the alkylation reaction.[103]

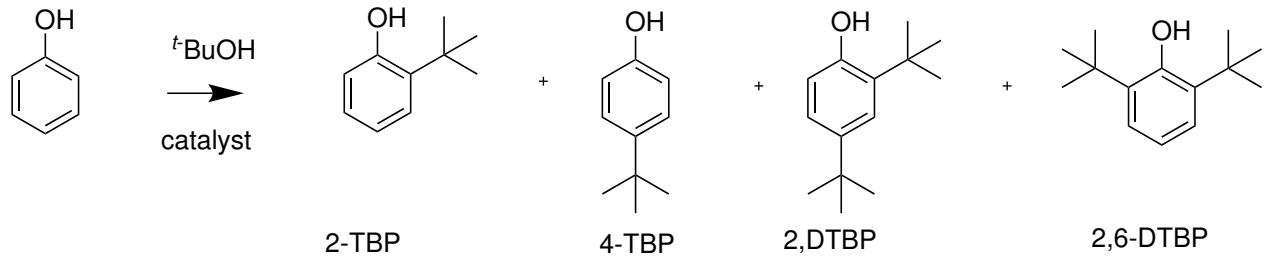



**Figure 1.3.2** – $^{t}$-butylation of phenol with $^{t}$-butanol using different acidic ionic liquids catalysts: $[(HSO_3)C_4C_1im][HSO_4]$, $[(HSO_3)^4C_4(C_2)N][HSO_4]$ and $[(HSO_3)^4C_4pyr][HSO_4]$

Esterification is another widely studied acid catalysed reaction with ionic liquids as catalyst. Esterification of $^{n}$-butyl alcohol with acetic acid was tested using $[(HSO_3)^3C_4C_1im][HSO_4]$ as a catalyst [104]. A high catalytic activity was exhibited with 98% yield of $^{n}$-butyl acetate was obtained. The catalyst showed good efficiency in the reusability as it was reused for 13 times with only 7.3 % decrease in the yield. In an esterification reaction of gallic acid with $^{n}$-propyl alcohol with the $[C_1pyrr][[HSO_4]$ ionic liquid,[105] the reaction was optimized using several parameters such as reaction temperature, molar ratio of reactants and the dosage of catalyst loaded. The optimum reaction conditions produced 89.8 % yield of propyl gallate and the synthesis was claimed as a green synthesis as no poisonous water-carrying agent involved in this reaction.

Biodiesel synthesis is another good example of an esterification process, specifically the trans-esterification reaction is involved. Biodiesel is the fatty acid methyl ester product formed by trans-esterification of animal fats or vegetable oils with methanol. Ullah *et al.* used waste palm cooking oil with an acidic ionic liquid as catalyst.[106] The synthesis of biodiesel usually uses alkaline based catalysts to catalyse the trans-esterification reaction. However, it is not possible to use direct transformation as the waste cooking oil used contains high free fatty acids (FFA). The reaction was impossible due to saponification and separation of layers. A two-step conversion was involved in this reaction; esterification and trans-esterification. The $[C_4C_1im][HSO_4]$ ionic liquid was found to be an efficient catalyst in this reaction producing 95.65% of product. The non-edible feedstock sewage sludge lipids is an example of a promising lipid source that can make biodiesel production prof-

itable. As the sewage sludge lipids contain higher FFA, acidic ionic liquids are preferred over basic catalysts.[107] Alkane sulfonic acid functional group ionic liquids (with $[OTf]^-$ anion) were found to be suitable acid catalysts in this reaction compared to other imidazolium and ammonium based ionic liquids. The Brønsted acidic ionic liquids used in this reaction possess many advantages over the conventional method that used sulfuric acid as the catalyst. The report listed advantages such as avoiding the saponification problem while converting different lipid feedstocks into biodiesel. It is also possible to reuse the catalyst to reduce the cost of the reaction. Overall, the low-cost sludge lipids can solve both environmental and economic problems associated with biodiesel production and waste management.

Lignocellulosic biomass is renewable, abundant and offers a potentially carbon-neutral alternative to petroleum.[108] The application of biomass for the global energy supply is about 12% today, but most biomass is used for low-grade heat applications.[109] Lignocellulosic biomass is the cell wall material of woody plants, with a porous micro-structure composite mainly made up of cellulose, hemicellulose and lignin. Lignocellulosic biomass can be utilized on a large scale as a source of liquid fuels to replace petroleum, as bio-based materials and bio-derived chemicals (Figure 1.3.3). One way to utilize the lignocellulosic biomass is by separating the main components of woods, followed by valorising them individually through biological and chemical processing. In the process of conversion of biomass to renewable feedstock, lots of work has been reported with ionic liquids involved in the process.[15] Some examples of the process will be discussed in this subchapter.

A number of Brønsted acidic ionic liquids have proven to be capable of achieving highly effective fractionation or pretreatment of lignocellulosic biomass. 1-H-3-methylimidazolium chloride was used for pretreatment of yellow pine wood chips under mild conditions.[111] The pretreatment caused the degradation of lignin and the hemicellulose from the cell walls of the pine wood. The wood samples were treated between 110 and 150 °C for 5 h producing a cellulose rich fraction, lignin and an aqueous fraction. The lignin was depolymerized and later on dissolved in the ionic liquid. Brandt *et al.* reported on investigating ionic liquids made up from the $[C_4C_1im]^+$ cation and $[OTf]^-$, $[MeSO_4]^-$, $[Me_2PO_4]^-$, $[DCN]^-$, $[Cl]^-$, or $[OAc]^-$ anions.[112] Small wood blocks (10 x 10 x 5 mm) of air-dried pine was treated with the ionic liquids. The ionic liquids were able to promote both

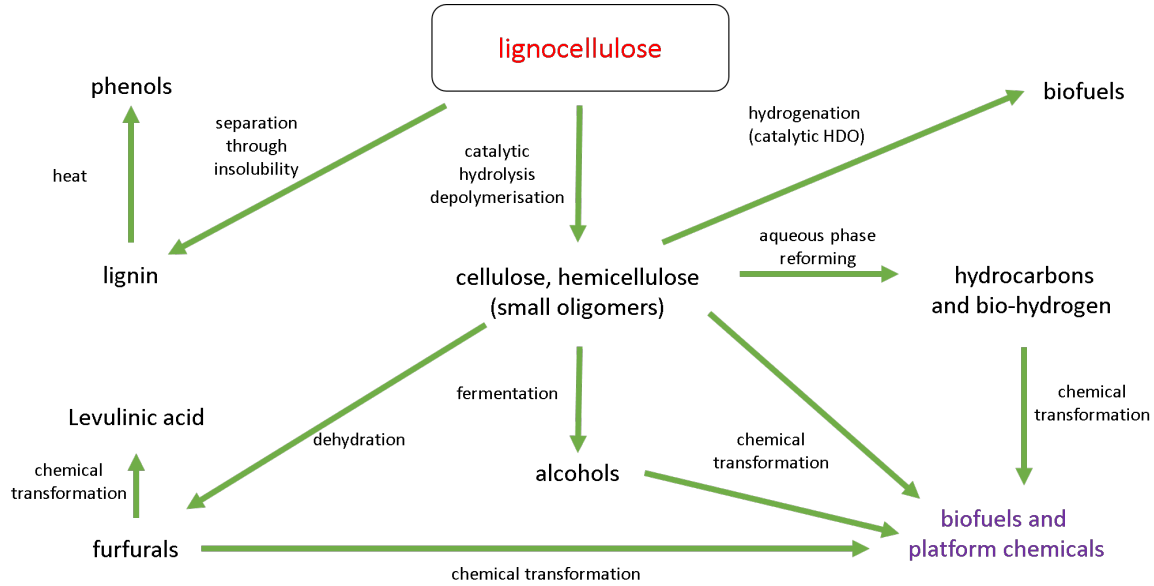



**Figure 1.3.3** – Lignocellulosic pathways. A scheme for a chemo-catalytic biorefinery[110]

dissolution and swelling of biomass except for $[C_4C_1im][DCN]$. Hydrogen sulfate $[HSO_4]^-$ based ionic liquids are one of the popular ionic liquids that are able to dissolve different types other biomass such as eucalyptus[113], hybrid aspen[114] and Norway spruce[114] ($[C_4C_1im][HSO_4]$), microalgae ($[C_mC_1im][HSO_4]$)[115], corn stover ($[C_2C_1im][HSO_4]$)[116] , grass / *Miscanthus* ($[C_4Him][HSO_4]$)[14] and willow ($[C_4C_1im][HSO_4]$)[14].

Recently, Brandt *et al.* reported on using a low cost Brønsted acidic ionic liquid $[TEA][HSO_4]$[117] with biomass using an efficient and repeated lignocellulosic fractionation process. Virgin Miscanthus x giganteus biomass was pretreated with aqueous solutions of $[TEA][HSO_4]$ was 120 °C for various lengths of time. 85 % of the lignin and up to 100% of the hemicellulose were solubilized into the ionic liquid solution. The $[TEA][HSO_4]$ solution can also be reused multiple times and showed how the reuse impacts the properties of the lignin and cellulose pulp. About 99% of the ionic liquid was recovered thanks to its non-volatility properties. The obtained cellulose rich pulps then underwent an enzymatic saccarification to produce the soluble sugar, glucose. The enzymatic saccharification was conducted for 8 h producing 77% yield. Recycling the $[TEA][HSO_4]$ solution did not have a negative

impact on saccharification yields (72 and 71% after third and fourth recycling). The lignin obtained was also recycled but unfortunately the precipitated yield after recycling was lower than the amount of lignin extracted. Quoting from the paper, "we hypothesise that the mechanism of self-cleaning involves lignin condensation reactions between freshly extracted lignin and lignin fragments left inside the ionic liquid from the previous cycle". The dissolved hemicellulose was observed to be solubilized mainly as monomers. The monomers were converted into furfural and further unidentified degradation products during processing. The furfural can be separated quantitatively from the non-volatile IL using a simple distillation method. 5-hydroxymethylfurfural (HMF) was also produced but this process was negligible as most of the glucose remained in the cellulose-rich pulp. Finally, they predicted that the capital and operating cost of this process will be lower than the bench-mark dilute acid pretreatment.

Since ionic liquids have been successfully used to separate cellulose from other components of lignocellulosic biomass, there is continuous research on acid catalysed dehydration of carbohydrates to furfural, 5-hydroxymethylfurfural and levulinic acid.[118, 119] Dehydration of fructose into 5-hydroxymethylfurfural was one of the typical dehydration reaction studied. Amarasekara and Razzaq investigated the conversion of HMF from D-glucose in DMSO with ionic liquids as catalysts.[118] A mechanism for 1-(1-propylsulfonic)-3-methylimidazolium chloride was proposed which involves an isomerization of D-glucose to D-fructose through open chain forms during the dehydration reaction. A one pot conversion of cellulose to glucose and finally to HMF can be conducted using acidic ionic catalysts.[119] The most efficient ionic liquid observed in this reaction for converting microcrystalline cellulose (MCC) to HMF was ([$(HSO_3)^4C_4C_1$im][$HSO_4$]) with 69.7% yield. $CuCl_2$ was added as co-catalyst and the $Cu^{2+}$ was thought to play an important role to achieve high yield. Another report on one pot conversion was on depolymerizing cellulose to glucose, followed by dehydration to HMF using $MnCl_2$ containing ionic liquids.[120] The highest conversion yield of glucose achieved was 91.2% and 45.7% HMF was produced from the glucose. The acidity of the solution plays an important role in this reaction as the acidic $SO_3H$-functionalized ionic liquids help to achieve higher conversion than non-functionalized ionic liquids.

Eminov *et al.* investigated a conversion of fructose to produce HMF using

the [$C_4C_1$im][$HSO_4$] ionic liquid as the reaction medium.[121] Only 38 % of conversion was obtained in the neat ionic liquid without any catalyst added. A low loading of $CrCl_3$ was added as well as chromium salt which have proved to be particularly active to catalyze this reaction. The highest conversion obtained was 80% after 24 h of reaction. Interestingly, the effect of acidity on the reaction was also discussed in this paper. Acetonitrile which acts as a catalyst (15% v/v with the IL) was added leading to equally high yields with $CrCl_3$. The acetonitrile is thought to help faster mass transport as it may act as diluent, which reduces the viscosity of the viscous [$C_4C_1$im][$HSO_4$] ionic liquid. The acidity of the neat IL and the acetonitrile-[$C_4C_1$im][$HSO_4$] was compared using the Hammett acidity method (will be discussed in the subchapter 2.3) giving $H_0$ = 1.96 and 1.12, respectively. In this acidity scale, the higher $H_0$ values means lower acidity. The $H_0$ values obtained suggested that by increasing the acidity of the solvent medium, the ability of the $[HSO_4]^-$ anion to protonate the substrate will also increase and thus help the reaction to achieve higher yields.

In fuel-cell applications, the use of acidic ionic liquids as electrolytes is an emerging field due to their thermal, chemical and electrochemical stability and their high conductivity.[122, 123] Diethylammonium trifluoromethanesulfonate ionic liquid was found to possess positive electrochemical activity and bulk properties for fuel-cell applications after screening more than 100 different protic ionic liquids.[123] Solid thin films containing the ionic liquids were fabricated using sulfonated polyimide as a matrix polymer. A non-humidifying fuel cell operated at 120 °C was used in this process. The sulfonate polyimide in ammonium form showed good compatibility and gave mechanically strong and flexible composite membranes. In different research, protic ionic liquids were applied as a component in composite proton exchange membrane (PEMs) for the next generation fuel cellsd.[124, 125, 126] PEMs are a crucial component of a proton exchange membrane fuel cell. Proton exchange membrane fuel cells are predicted to be a promising power source for automotive transportation. Alternative power sources with high efficiency energy conversion devices have attracted great interest for transportation to reduce greenhouse gas emission significantly and to preserve oil resources.[127] Examples of protic ionic liquids used in these applications are polymer electrolyte membranes based on poly(ethylene oxide)/1-butyl-3-methylimidazolium hydrogen sul-

fate [$C_4C_1$im][$HSO_4$],[126] 1-vinylimidazolium trifluoromethanesulfonate [($CH_2$ = CH) - Him][OTf][125] and [$C_1$Him][OTf][128].

### 1.3.2 Acidity measurements of ionic liquids

Brønsted acidity is one of the key properties of Brønsted acidic ionic liquids. The effect of acidity on catalysis is an interesting topic as many organic reactions can be promoted or catalyzed in an acid environment.[2, 6, 92, 129] Acidic or acidified solutions of ionic liquids have been prominently used since their introduction. Acidic chloroaluminates have received a lot of attention as they were the first ones to emerge and are able to act as dual solvent-catalyst and able to provide acidic environment.[130, 131] They can catalyze C-C bond forming reactions, such as arene alkylation with alkenes[132] or Friedel-Crafts alkylation[27] of benzene with halogenoalkanes. Despite that, chloroaluminates are very sensitive to water. The composition of the melt can change with traces of water. Thus, it is difficult to control the acidity of these ionic liquids. The interests in the development and application for acidic reactions then changed onto nonchloroaluminate ionic liquids which are air and moisture stable (e.g. [$C_nC_1$im][$NTf_2$], [$C_nC_1$im][$PF_6$] or [$C_nC_1$im][$BF_4$]).[133, 134, 135] These ionic liquids are not usually intrinsically acidic, thus were investigated first with the addition of Brønsted acids.[134] Further investigation was followed by incorporating the acid moieties into the ionic liquids themselves.[133] It was then followed by measurements of protic ionic liquids where their acidities are dependent on the strength of the acids and bases used to make these.[136]

Lots of different techniques have been used to measure the acidity of these ionic liquids to understand the correlation between their acidity and their catalytic activity in organic synthesis reactions. Measuring dissociation constants using an indicator is one of the ways to measure the acidity. The p$K_a$ values have been determined using different techniques, for example; UV-Vis, NMR, IR spectroscopies, and potentiometric, electrophoresis and conductometric measurements. However, many of these were unsuitable to determine ionic liquid p$K_a$s (p$K_a^{ILS}$). Different non-aqueous environments will produce different p$K_a^{ILS}$, as a proton's acidity is usually defined by its solvation. Thus, it will be possible to connect the acidity

of ILs with their catalytic activities in different acid-base reactions. In addition, it is possible to modify the p$K_a$ values with a careful selection of solvent since a higher chemical activity in slightly solvated protons were found. The p$K_a$ values reported are mostly in aqueous solution and it is necessary to collect p$K_a$ values for nonaqueous solutions.[137, 138] Spectrophotometric methods such as UV-Vis, NMR and IR were used instead to measure the acidity of acidic ionic liquids.[29, 58, 139, 140] UV-Vis spectroscopy is one of the most popular methods used to measure the acidity of ionic liquids. The literature regarding these measurements will be disussed in this subchapter.

Adam *et al.* reported on using Reichardt's dye as indicator of acidity by measuring the acidity constant values for protic several protic ionic liquids (p$K_a^{PILS}$) with UV-Vis spectrometry.[140] This work aimed to analyse the effect of microscopic properties of molecular solvents towards the chemical environment of the PILs' proton. Different polar molecular solvents with different abilities to donate hydrogen atoms were mixed with the PILs. The results obtained showed that the role of the solvent is dominant in the chemical equilibrium. Moreover, p$K_a^{PILS}$ values provide information about the relative ability of the PIL's proton to interact with a given solute, and the values depend on the medium. Thus, the authors predict the H-bond strength of ionic liquids, depending on the cation, anion and the type of ionic network formed. They concluded that it is possible to adjust the strength of the PILs by selecting an appropriate molecular co-solvent.

Chiappe and Pieraccini investigated the solvent properties of ionic liquids by using Michler's ketone (MK) and tetracyanoethylene (TCNE) as a UV-Vis probe.[141] MK and TCNE give an electron donor-acceptor (EDA) complex in molecular solvents. The EDA is a zwitterionic species or a radical pair depending on the ionising power and the protic or aprotic nature of the solvent. The visible absorption maxima of the charge-transfer band of the EDA complex agreed with the $\pi^*$, $\beta$ and $\alpha$ parameters of the solvents. The H-bond has a donating ability (expressed by Kamlet-Taft $\alpha$ parameter) that might be able to influence the spectral position of the charge transfer absorption band of the EDA complex. Unfortunately, the H-bond acidity of ionic liquids is not enough to measure the transformation of the EDA complex into the zwitterionic species. One advantage of this technique is that it can be used as a probe to detect the presence of water through the colour

change of the solution or by UV-Vis measurements. Traces of nucleophile (amines or chlorides) can also be detected as the formation of the EDA complex is strongly influenced by the trace of impurities.

The determination of Hammett acidity functions ($H_0$) using UV-Vis spectroscopy is another method to determine Brønsted acidity. This method evaluates the protonation extent of uncharged indicators in a solution. The substituted dinitroanilines are the chosen indicators used for this method (Figure 1.3.4). Researchers from the same research group from the Institut Francais du Petrole, France and Universite de Liege, Belgium have published several papers from 2003 to 2010 about measuring the acidity scale of Brønsted acids - ionic liquids systems. Hammett acidity measurements values were evaluated using different dyes from the substituted nitroanilines. This subchapter will discuss each of the published papers. Thomazeau *et al.* were the first to report on determining the acidic scale of RTILs using the Hammett acidity functions.[58] The behaviour observed for different Brønsted acids (e.g. H[$NTf_2$] and HOTf) in different ionic liquids ( [$C_4C_1$im][$NTf_2$] and [$C_4C_1$im][$BF_4$] ) were reported. The highest $H_0$ values obtained was -7.05 (with 105 mmol$L^{-1}$ of H[$NTf_2$] in [$C_4C_1$im][$BF_4$] ). The paper concluded that it is possible to measure the acidity of nonchloroaluminate ionic liquids with the addition of an acid with $H_0$ values ranging from -3.35 to -7.05, depending on the ionic liquid and the acid. The solvents (ionic liquids) are assumed as being totally dissociating, and thus, the known p$K_a$ values of the indicators are also thought to be valid.

The same research group published complementary studies to the previous paper in year 2007.[142] In this paper, they discuss the importance of the influence of impurities as well as measuring the acidity of Brønsted acids - ionic liquids systems. The same acid (H[$NTf_2$]) was used, but additional ionic liquids with different cations were measured. They found that the acidity of the same Brønsted acids - ionic liquids systems to be different when determined by two different indicators of different p$K_a$. The authors proposed either there is an experimental error in the values of the p$K_a$ indicators or the ionic liquids are not as dissociating as initially thought. Further experiments eliminated the first proposition The paper concluded that it is possible to measure the acidity scale of the Brønsted acids - ionic liquids system using appropriate indicators. However, the measurement

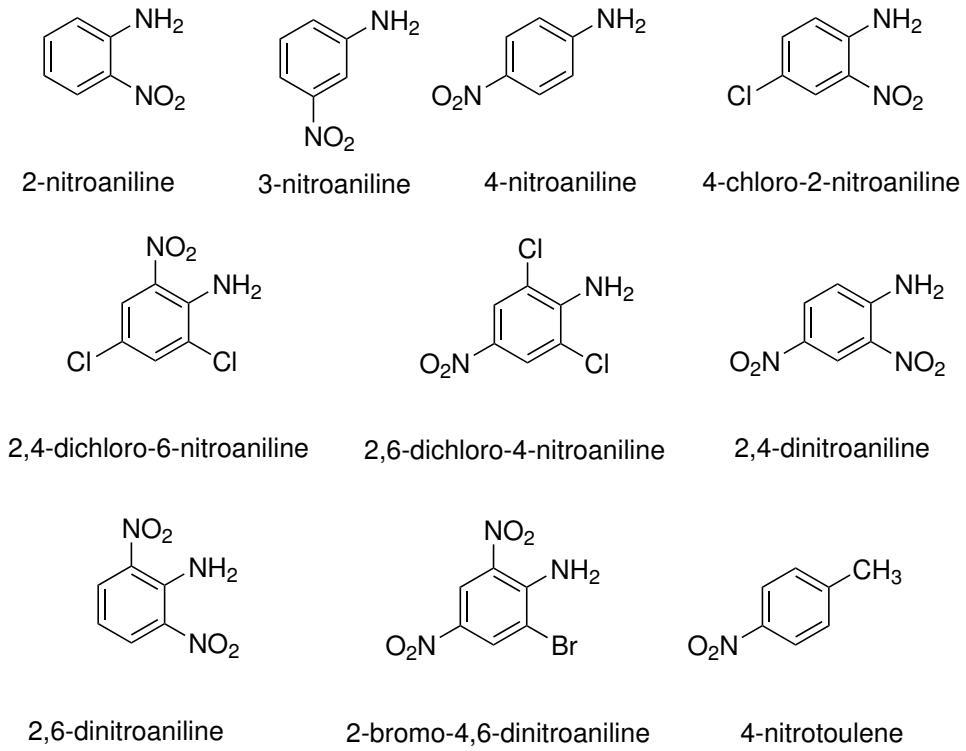



**Figure 1.3.4** – Substituted dinitroanilines indicator

gave approximate acidity values as the behaviour of two different indicators in the same solution indicates a weakly dissociating solvent. As a result, the Hammett functions must be corrected for. Another interesting finding from this paper was that the purity of the Brønsted acids - ionic liquids systems is critical to obtain meaningful results. Impurities (such as water) will act as strong bases, and all of the chemicals used in these experiments are possible candidates that will disturb the acidity measurements. All possible impurities, for examples methylimidazole, water, acetone, chloride or bromide ions should be eliminated before performing the analyses.

The research group then published another paper on measuring the Brønsted acids - ionic liquids systems with more ionic liquids (different cations and anions) but still using the same acids.[143] In this paper, two primary foci were what is the average level of acidity expected by adding a Brønsted acid into the ionic liquid system and whether the ionic liquids behave the same way; *i.e.* the same acidity

levels with different ILs. The results show an acidity range extending from -3 to -8 and ionic liquids' cations play no role in the acidity level where the added acid masks the acidity of the protons on the cationic nitrogen. In contrast, with the anion an evident variation of acidity was observed. With a similar content of acid, the order of the acidity levels are $[PF_6]^-$ > $[BF_4]^-$ > $[NTf_2]^-$ > $[OTf]^-$ and consequently it was suggested that the solvating power (or basicity) of the anions follows the reverse order. However, the acidity scales obtained were still considered as approximate values as the problem of the uncertainty of the right indicator remained unsolved.

In the same year, the research group published the final paper on these Brønsted acids - ionic liquids systems series.[144] The objective of this report was to confirm that different indicators in the same solvent does not necessarily lead to identical $H_0$ values and to evaluate another method to measure the acidity, electrochemical measurements. This method was used to avoid the uncertainty of the indicators' acidity constant. The results from the Hammett method shows that despite the acid and the ionic liquids added being the same, two different indicators gave different acidity level (difference in $H_0 = 0.6$). Although the difference is small. it is beyond the measurement error. The indicator was thought to be less dissociated than in sulphuric acid-water solutions, and hence the electrostatic interactions influenced the p$K_a$ values. Thus, to solve this problem, an electrochemical method was used as an alternative. The electrochemical method measures the $H^+/H_2$ couple potential. The results for potentiometry at zero current (an equilibrium method) was used to measure the acidity level. The ferrocenium-ferrocene ($Fc^+$-Fc) and the authors calculated the $R^0(H^+)$ Strehlow function (which is analogous to a pH function). This method has two critical problems where the quality of the hydrogen gas stabilisation strongly influences the hydrogen potential, and residual impurities were detected in the ionic liquids. Thus, the slopes of the measured potentials versus the log of the added acid amounts were not the expected ones. Nevertheless, it was concluded that the hydrogen electrode potential increases with the amount of acid added and consequently increases the acidity level, provided that all the impurities are neutralised. The acidity level range from -3 to -9 is higher than that in water ($R^0(H^+)$). Moreover, for all investigated acid solutions, higher acidity levels were approximately calculated compared to the Hammett $H_0$

function. This is in agreement with their proposition that the Hammett acidity functions give only to a minimal acidity level, because the p$K_a$ of the indicators are probably affected by ionic association.

Other literature also reports using the Hammett method using UV/Visible spectroscopy for the determination of relative Brønsted acidity in ionic liquid. Xing *et al.* determined the acidity level of ILs with pyridine cations with sulfonic acid functional groups and alkylammonium-based PILs.[145] The acidity levels of the N-propane-sulfonic acid-pyridinium cations (denoted as PSPy), were found to depend on the nature of the associated anion. It is possible for the anion to act as an available acidic site as well. The acidity order proposed ( $[BF_4]^-$ > $[HSO_4]^-$ > [p-toluenesulfonate]$^-$ > $[H_2PO_4]^-$) was consistent with the acidity observed in certain acidic reactions. A similar phenomenon was subsequently reported by Shukla et al., where the strength of a carboxylic acid in different PILs and water were assessed using Hammett acidity function ($H_0$).[146] Three carboxylic acids (formic acid, acetic acid and propionic acid) and protic ionic liquids (cations : ($[HC_1im]^+$ and ($[HC_4im]^+$) and anions : ($[OAc]^-$) and $[HCO_2]^-$) were measured. Changing cation had more effect on the strength of carboxylic acids than the anions. The relative interactions between anion and cation are different from PILs and thus complicated the work. Overall, both PILs and water have different interactions towards proton. The difference in the interactions are due to the electronic and the distinct structural differences as they behave analogously towards the carboxylic acid's strength. A simple equation can be derived further by using the linear correlation of $H_0$ values for carboxylic acids between PIL-water and PILs. This equation can be used to determine the strength of water and PIL.

Alternatively, the Hammett acidity functions ($H_0$) can be measured using NMR Spectroscopy. Welton and co-workers recently introduced mesityl oxide as a probe for measuring the acidity of Brønsted acids - ionic liquids systems using $^{13}C$ NMR Spectroscopy.[147] This technique introduces a quick, simple, robust method, and measures the acidity range from $H_0$ = -1 to -9. The range obtained is an extensive range that exceeds that of any single UV-Vis probe. The measurements were modified based on the method developed by Farcasiu for the acidity of $H_2O$ - $H_2SO_4$ system.[148] A wide range of different concentrations of $H_2SO_4$ added into the $[C_4Him][HSO_4]$ and $[C_4C_1im][HSO_4]$ ionic liquids were measured. The dif-

ference ($\triangle\delta$) between the $^{13}C$ NMR signals of $\alpha$ and $\beta$ carbons of mesityl oxide (Figure 1.3.5 ) gives the $H_0$ values. The method eliminates the need for colourless ionic liquids, which is a significant problem in UV-Vis spectroscopy. The high concentrations of mesityl oxide used in the measurements eliminate the sensitivity of the measurement to small traces of impurities. This method saves a lot of time in identifying a suitable probe because it is a single probe technique. However, the large number of Hammett probes available means that one of these can usually be used to produce a very precise acidity once the approximate acidity of the solution being measured is known. The advantages of this NMR method will permit more measurements of the acidity of acids-ionic liquids system in future

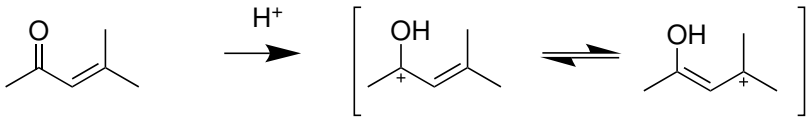



**Figure 1.3.5** – Mesityl oxide protonation

Other literature reports using NMR spectroscopy using the NH shift for the available proton which correlates with the Brønsted acidity using $^1H$ NMR. A correlation between the chemical shifts was observed where larger chemical shifts strongly suggest the higher Brønsted acidity.[149] The yield of the synthesized product (1-pyridylimidazol[1,5-a]pyridines) was compared with NH proton chemical shift from the ILs. The polarity of the measured ILs also increases as the Brønsted acidity increases. The paper also points out that ionic liquids promote the heterocyclisation reaction. A contribution by McCune *et al.* also used NMR spectroscopy to measure the acidity of Brønsted acids in ionic liquids.[150] Gutmann Acceptor Number (AN) values were used to determine the acidity of wide compositional range of Brønsted acid-ionic liquids mixtures. Four systems of general formula ($[C_2C_1im][A]$-HA with $A^- = [NTf_2]^-$, $[OTF]^-$, $[OAc]^-$, or $[OMs^-]$) were measured. AN values were determined using $^{31}P$ NMR with triethylphosphine oxide (tepo) as a probe. In the measurement, partial protonation by Brønsted acids or formation of acid-base adducts with Lewis acids induces the chemical shifts in the $^{31}P$ NMR (Figure 1.3.6). The results reported were that HOAc, HOMs and HOTf were associated with the respective anions to form hydrogen-bonded anionic clus-

ters $[A(HA)_x]^-$ when dissolved in ionic liquids. However, the authors claimed that $HNTf_2$ was solubilised as undissociated, discrete molecules. The acidity could be buffered to a certain particular AN by binding the solubilized acid in the anionic cluster form as the AN values were sensitive to the presence of anionic clusters. Generally, this is an easy way to quantify and manipulate the Brønsted acidity of an acid-ionic liquid mixture.

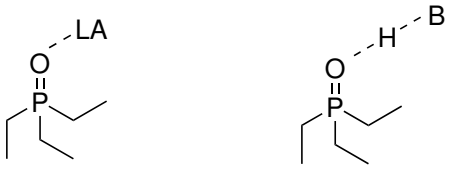



**Figure 1.3.6** – Interactions of the spectroscopic probem triethylphosphine oxide with a Lewis acid (LA) and a Brønsted acid (BA)

In the past decade, the ionic liquid field has spread into a broad subject area with acidic ionic liquids as an important section of this subject. Catalysis, lignocellulosic biomass processing and electrolyte applications are examples of the latest advancements of utilising acidic ionic liquids. The acidity and the catalytic activity shows a strong relationship in many organic reactions. Thus, it is essential to understand the effects of ionic liquids on acidity and proton transfer to realise what happens between acids, ionic liquids, acidic ionic liquids and their acidity. Improvement in the reaction conditions and yield will also be possible if enough data on the acidic properties of ionic liquids are available for reference. To date, there are several methods used to measure the acidity of these ionic liquids available but less data on the acidity of ionic liquids are available.

## 1.4 Scope of thesis

The work described in this thesis aims to collect acidity data on five different ionic liquids: 1-Butyl-3-methylimidazolium trifluoromethanesulfonate ($[C_4C_1im][OTf]$), 1-Butyl-3-methylimidazolium bis(trifluoromethanesulfonyl)imide ($[C_4C_1im][NTf_2]$), 1-Butyl-3-methylimidazolium hydrogensulfate ($[C_4C_1im][HSO_4]$), 1-Butyl-3-methylimidazolium dimethylphosphate ($[C_4C_1im][Me_2PO_4]$) and 1-Butyl-3-methylimidazolium dimethylphos-

phate ([$HC_4$im][$HSO_4$]). Since these ionic liquids are not usually intrinsically acidic, they have been investigated with the addition of the Brønsted acids, triflic acid (H[OTf]), bis(trifluoromethanesulfonyl)imide (H[$NTf_2$]), sulphuric acid ($H_2SO_4$) and phosphoric acid ($H_3PO_4$). Hammett acidity function, $H_0$ values will be determined using two different methods of acidity measurement using $^{13}$C NMR spectroscopy and UV-Vis spectroscopy. The Hammett acidity function, was chosen instead of the pH scale, because the nature of the ionic liquids themselves are non-aqueous, and thus make the pH measurements not suitable for this system. The directions of this thesis will be set out as follows, with each point representing an individual chapter:

1. Initial measurements of the acidity of Brønsted acid-ionic liquid systems. The Brønsted acid chosen will be the conjugate acid of the anion of the ionic liquid. The acidity of all systems will be measured using both $^{13}$C NMR and UV-Vis spectroscopic methods. Data obtained from both of the methods will be compared with each other. Initial conclusion for each of the method used will be made about which method will be suitable to measure the acidity of the ionic liquids.

2. A further investigation and more data collection on the Brønsted acid-ionic liquid systems using the $^{13}$C NMR specroscopic method. The effect of the anion on the acidity of the system will also be explored, but with a more complicated system. Each of ionic liquids is mixed with Brønsted acids which are different to the conjugate anions of the ionic liquids.

3. The final chapter will look into the effect on acidity of the cation of the ionic liquid. The chosen ionic liquid is mixed with each of the Brønsted acids used in the previous system. The data obtained will be compared to study the effect of the cation on the acidity values.

# Chapter 2

# The Acidity Measurements of Brønsted Acids in Ionic Liquids

## 2.1 Measuring the acidity of ionic liquids - the reason why the pH scale is not suitable

The pH measurements fit well for a highly diluted acid solution in water. However, it cannot be simply applied when the acid concentration increases and/or if nonaqueous media is used. The pH scale is limited to only aqueous solutions.[78] Although pH scales in molecular solvents are available, pH values in different solvents are non-comparable.[151] Also, the pH measurements method requires for it to be in an ideal solution. The potential at the liquid junction in the reference cell used also needs to be known. The hydrogen ion activity cannot be measured independently and thus the equality pH = -log($a_{H^+}$) cannot be established for any solution. Another limitation of pH is in the pH electrodes, the glass bubble head of the electrodes can get hydrated and break down. The counter ions of $H^+$ and $OH^-$ will become too concentrated beyond the scale of pH in water (pH scale, 0-14) and start to interact among themselves, causing the solution to not be ideal.

Autopyrolysis reactions of solvents are the reason why pH values of neutral solutions are different in different solvents.[152] Autopyrolysis of some solvent molecules in the absence of acids and bases produce protons. For example in pure water;

$H_2O \rightleftharpoons H^+ + OH^-$

Since the density of pure water is 1000g/L, the concentration of water at pure condition is equal to 55.6mmolL$^{-1}$. Thus, the $K_a$ of the reaction above is:

$K_a = \frac{[H^+][OH^-]}{H_2O} = 10^{-15.75}$

The [H$^+$] and [OH$^-$] are equal because there are no other acids or bases exists in pure water. The equation above can be rearranged to:

$[H^+] = \sqrt{K_a[H_2O]}$

$=\sqrt{10^{-15.75} \cdot 55.6}$

$= 10^{-7}$

Thus, pH of neutral water is:

$pH = -log[H^+] = 7.0$

Neutral pH values vary in different solvents. The variation is because the concentration of protons obtained by autopyrolysis is dependent on the solvent's $pK_a$ values. For example, pure ethanol is neutral at pH 9.8 because in pure ethanol, [H$^+$] is equal to 1.58 x 10$^{-10}$ molL$^{-1}$. Thus, pH values measured in different solvents are non-comparable. The pH scale cannot be employed in the measurement of the acidity of the ionic liquids as they are not aqueous. A quantitative scale is needed to express the acidity scale of nonaqueous solutions or more concentrated solutions to overcome the limited application of the pH scale.[66] It is necessary for the scale to be able to estimate the degree of transformation of a given base to its protonated form, its conjugate acid. Therefore, the Hammett acidity function, a universal acidity function is thought to be more suitable to measure the acidity of ionic liquids.

## 2.2 Hammett acidity function ($H_0$ function) - The UV-Vis Probe

In 1932, Hammett and Deyrup were the first to propose a method for measuring the degree of protonation of weakly basic indicators in acid solution.[153] Hammett suggested that the extent of protonation of a base could be used as an indicator of how acidic a solution is, since the true acidity of a solution lies in its ability to protonate a basic species. A set of indicators were carefully selected to de-

velop an acidity scale in concentrated sulphuric acid-water mixtures. The chosen indicator was a simple basic indicator that is a non-ionised or neutral substance capable of adding one hydrogen ion per molecule without any complicating further reactions. The $H_0$ acidity function was derived from ionisation equilibria of these probes (Hammett bases), with the bases behaving in the Brønsted-Lowry sense as uncharged bases,

$$B + H^+ \rightleftharpoons B \tag{2.2.1}$$

and is defined by the equation

$$H_0 = pK_{BH^+} + log\frac{[BH^+]}{[B]} \tag{2.2.2}$$

in which $pK_{BH^+}$ is the $pK_a$ of the conjugate acid of the probe base (referred to an ideal dilute solution in water) are the concentrations of the base in its protonated and unprotonated forms. Equation 2.2.2 is derived based on the assumption that the solvent is dissociating with regards to the base. The mathematical proof for the transformation from eqn. 2.2.1 to eqn. 2.2.2 can be found in the appendix. The "0" subscript of $H_0$ denotes the charges of the probe bases. Thus, for acid indicator whose colour change is determined by the reaction;[153]

$BH^+ + H^+ \rightleftharpoons BH^{2+}$

the acidity function $H_+$ is determined by the equations

$H_+ = pK_{BH^{2+}} - log\left(\frac{[BH^{2+}]}{[BH^+]}\right)$

Similarly, the acidity function H_ is defined by the extent of the indicator reactions;

$B^- + H^+ \rightleftharpoons BH$ ; $H_- = pK_{BH} - log\left(\frac{[BH]}{[B^-]}\right)$

The first application on the $H_0$ function was for the $H_2SO_4$ - $H_2O$ system using a series of nitroanilines as probe to measure the acidity of the mixture (Figure 1.3.4).[153] These nitroanilines are suitable as probes for measuring the acidity of very acidic solutions, because they are very weak bases. The $pK_{BH^+}$ of these nitroanilines range from 2.50 to -11 (where bases with conjugate acids with more negative $pK_a$ values are less basic, see section 1.2.1 - Brønsted-Lowry theory). These nitroanilines are weak bases due to the highly electron-withdrawing nitro group on the benzene ring, thus causing the lone pair on the $NH_2$ to be less basic.

All Hammett bases have at least one nitro group. Different combinations of other substituents produce bases with different $pK_{BH^+}$ values. Other ring substituents such as methyl groups increase the $pK_{BH^+}$ values of the bases while chloro-, bromo- or additional nitro groups decrease them.

The $pK_{BH^+}$ for probe that were used to established Hammett acidity functions were compiled by Paul and Long in 1957 (Table 2.2.1).[154] These data cover the whole acidity range from dilute acid to the superacid media. For the $H_0$ values up to -10, all indicators are a primary amine and therefore suitable to be used for the measurement of the Hammett $H_0$ function. For stronger acids, nitro-compound based indicators have been used, which may not be a satisfactory extension of the aniline indicator scale. However, Gillespie has shown that the most basic nitro-compound indicator, 4-nitrotoluene overlaps with the weakest indicator in the aniline series, 2,4,6-trinitroaniline ( $pK_{BH^+}$= -10.10).[155, 156] Overall, the acidity measurements using the nitro compounds are acceptable to give the best picture of the acidity of the various superacid systems.

**Table 2.2.1** – Selected $pK_{BH^+}$ values for extended Hammett Bases[154]

| Base | $pK_{BH^+}$ |
|---|---|
| 3-nitroaniline | 2.50 |
| 4-nitroaniline | 1.00 |
| 2-nitroaniline | -0.29 |
| 4-chloro-2-nitroaniline | -1.03 |
| 2,4-dichloro-6-nitroaniline | -3.24 |
| 2,6-dichloro-4-nitroaniline | -3.29 |
| 2,4-dinitroaniline | -4.28 |
| 2,6-dinitroaniline | -4.48 |
| 2-bromo-4,6-dinitroaniline | -8.22 |
| 4-nitrotoluene | -11.35 |

## 2.2.1 Determination of $H_0$ values

The determination of $H_0$ values can be divided into two separate calculations; the measurement with the chosen probe of $\frac{[BH^+]}{[B]}$ and the measurement of $pK_{BH^+}$.

#### 2.2.1.1 Step 1: Measurement of $\frac{[BH^+]}{[B]}$

The indicator or Hammett base has an acid (protonated form, $BH^+$) and a base (unprotonated form, B), where those two forms must have different spectral absorptions using UV-Vis spectroscopy. The Hammett bases must be weak enough to be partially protonated by strong acids, and UV-Vis spectroscopy must be easily able to detect them. The concentration of the base must be low enough to make sure that the Beer-Lambert law is relevant (eqn. 2.2.3):

$$A = \epsilon \cdot c \cdot l \tag{2.2.3}$$

where A is the absorbance, $\epsilon$ is the extinction coefficient of the chromophore ($mol^{-1}Lcm^{-1}$), c is its concentration and l is the pathlength of the cuvette used (cm). Following the Beer-Lambert law, the absorbance of a chromophore at any wavelength is directly proportional to its concentration as long as the concentration of the chromophore is lower than a certain threshold. Thus, any changes in absorbance are directly relevant to the change of concentrations. In the UV-Vis measurements, the spectrum of a UV active species will have the lambda max ($\lambda_{max}$) which will give the wavelength of the maximum value of the extinction coefficient and the absorbance (A) (Figure 2.2.1).

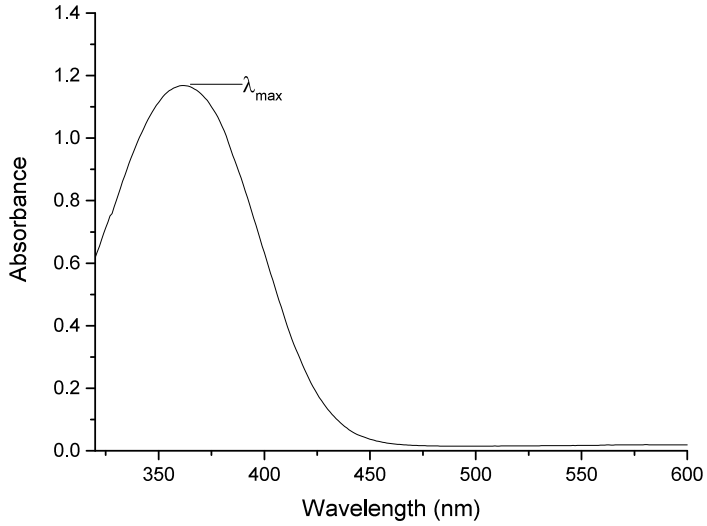



**Figure 2.2.1** – UV spectrum of 3-nitroaniline in DCM (example of UV spectrum with ($\lambda_{max}$)

The UV-Vis spectrum of a solution containing an acidic solution with a suitable Hammett base (when the base is partially protonated) will have two peaks in it. The peaks belong to the $BH^+$ and B of the Hammett base. An example of the UV-Vis spectrum for a partially protonated Hammett base in an acidic solution is shown in Figure 2.2.2. Most of the Hammet bases have the peak for $BH^+$ at the shorter wavelength than the peak for B. As the solution becomes more acidic, the peak for $BH^+$ becomes more intense than the peak for B. Thus, since the peak of B lies within the UV-Vis range, it is easier to observe the loss of B than the gain of $BH^+$ (where usually only part of the peak is present).

The ratio of $\frac{[BH^+]}{[B]}$ can be calculated after obtaining $\lambda_{max}$values from two reference solutions, where the base is completely protonated and unprotonated. In a situation where the same concentration of the probe base was added into three solutions, the ratio $\frac{[BH^+]}{[B]}$ of the unknown solution with absorbance A will be defined as:

$$\frac{[BH^+]}{[B]} = \frac{A_0 - A}{A - A_+} \tag{2.2.4}$$

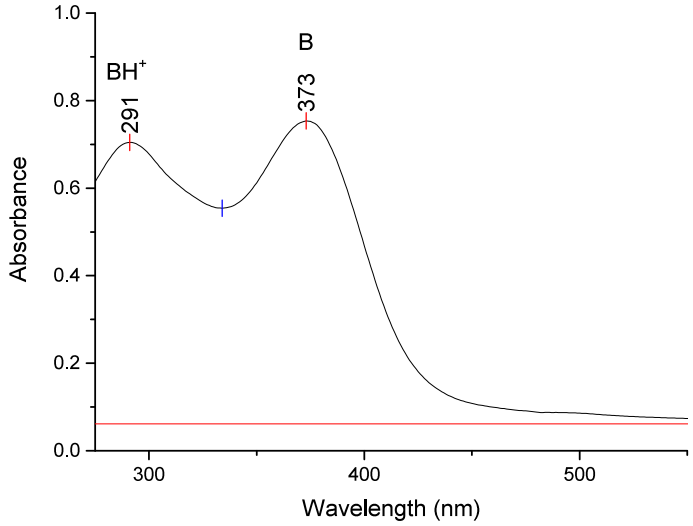



**Figure 2.2.2** – UV spectrum of 4-nitrotoluene in neat $H_2SO_4$

where $A_0$ is the absorbance of the unprotonated solution, $A_+$ is the absorbance of the completely protonated solution, and A is the absorbance of the unknown solution. However, sometimes it is impossible to measure the absorbance values for the same concentrations of bases in all of the solutions, because of the limitations in the maximum absorbance that can be measured by the machines. Therefore, it is better to use the effective $\epsilon$ values in place of absorbance and to have freedom in the concentration of base.

By rearranging the Beer-Lambert Law equation, the effective epsilon can be calculated by;

$$\epsilon = \frac{A}{c \cdot l} \tag{2.2.5}$$

$$\epsilon = \frac{A}{([B] + [BH^+]) \cdot l} \tag{2.2.6}$$

The effective epsilon shows the loss of B due to the conversion $BH^+$, so $\epsilon$ is calculated by dividing absorbance of B over both ([B] + [$BH^+$]). The ratio of $\frac{[BH^+]}{[B]}$ of an unknown solution with epsilon $\epsilon$ can be calculated by;

$$\frac{[BH^+]}{[B]} = \frac{\epsilon_0 - \epsilon}{\epsilon - \epsilon_+} \tag{2.2.7}$$

where A and $\epsilon$ are proportional, $\epsilon_0$ is the epsilon when the base is completely unprotonated and $\epsilon_+$ is the epsilon when the base is completely protonated. Hammett and Deyrup mentioned that there is a possibility of spectral shifting of the whole spectrum as the $\epsilon_0$ and $\epsilon_+$ are always measured in solutions of different compositions from the test solution.[153] Spectral shifts were found with certain indicators in sulphuric acid-water solutions as the concentration of the acid was changed. This is due to medium effects that are unrelated to acidity. In the paper, Hammett and Deyrup also reported on measuring the $\epsilon_0$ and $\epsilon_+$ in solutions that were as close in composition to the test solution to reduce the medium effect. The ideal reference solutions can be found by measuring the absorbance of several different acidities until the extinction coefficient is found. However, this method is exceptionally time-consuming even though it is the most accurate.

#### 2.2.1.2 Step 2: Measurement of $pK_{BH^+}$

The $pK_{BH^+}$ is the dissociation constant of the conjugate acid of the base in an ideal diluted aqueous solution. Once these constants are established, it is possible to use these constants again and again. The $pK_{BH^+}$ values used in this work are from the compilation of Hammett bases' $pK_{BH^+}$ values compiled by Paul and Long.[154] The $pK_{BH^+}$ can be defined as[154];

$$pK_{BH^+} = -log\frac{[BH^+]}{[B][H^+]} - log\frac{f_{BH^+}}{f_B f_{H^+}} \tag{2.2.8}$$

where $f$, the activity coefficient is relevant to the value unity for an infinitely dilute solution in water. As the concentration of the indicator is usually low,

$$log\frac{f_{BH^+}}{f_B f_{H^+}} = 0$$

and

$$pK_{BH^+} = \lim_{[A]\to 0}\left[log\left(\frac{[BH^+]}{[B]}\right) - log[H^+]\right] \tag{2.2.9}$$

where [A] is the molar concentration of strong acid, A in water. From the equation 2.2.9, the $pK_{BH^+}$ value can be obtained by plotting the $\left[log\left(\frac{[BH^+]}{[B]}\right) - log[H^+]\right]$

values against the concentration of strong acid present in the solution, followed by extrapolation to zero concentration of A.

Since A is a strong acid, A completely dissociates into $H^+$ and protonates B into [$BH^+$]. Therefore, the concentration of acid added is equal to:

$[A] = [H^+] + [BH^+]$

assuming that the indicator is introduced in its uncharged form. Therefore, the [ $H^+$] and $\left[log\left(\frac{[BH^+]}{[B]}\right) - log[H^+]\right]$ can be calculated once the ratio of $\frac{[BH^+]}{[B]}$ is known. Originally, Hammett used average values of $pK_{BH^+}$ available from literature where for example for 4-nitroaniline dye, the $pK_{BH^+}$ is 1.40.[157] Paul[158] and Braude[159] reported on measuring the $pK_{BH^+}$ values of 4-nitroaniline dye (one of the strongest Hammett base). HCl was chosen instead of sulphuric acid due to the complications arising from the second ionisation of $H_2SO_4$. The reports shows that the $\left[log\left(\frac{[BH^+]}{[B]}\right) - log[H^+]\right]$ varies linearly with the [HCl] concentration up to at least 2M concentration (Figure 2.2.3). In the Fig. 2.2.3 , the $pK_{BH^+}$ value for 4-nitroaniline obtained by Paul and Braude are 0.99 and 0.98, respectively after extrapolating the straight line obtained from plotting $\left[log\left(\frac{[BH^+]}{[B]}\right) - log[H^+]\right]$ against [HCl]. As the purpose of work by Paul and Braude is to revise the $pK_{BH^+}$ value for 4-nitroaniline, the agreed $pK_{BH^+}$ values for 4-nitroaniline used nowadays is 1.00.[160]

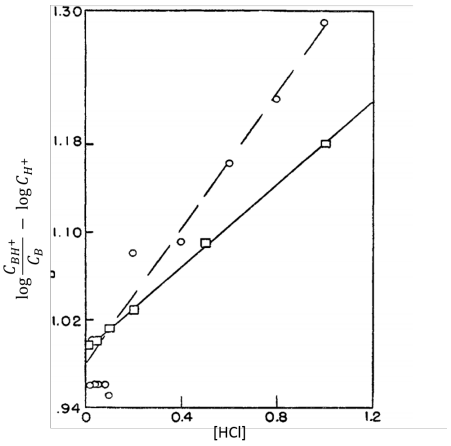



**Figure 2.2.3** – Plot for determination of $pK_{BH^+}$ of 4-nitroaniline in hydrochloric acid solutions. ○ Braude[159] and □ Paul[158]. Image taken from the paper by Paul and Long.[154]

The direct determination of $pK_{BH^+}$ for a weaker base is not practical using the above method (e.g. in dilute aqueous solutions).[153, 154] For a weaker base, the ratio of $\frac{[BH^+]}{[B]}$ becomes less miniscule compared to the stronger bases. Thus, it is impossible to calculate any accurate $pK_{BH^+}$ value using the physical measurements. A step-wise comparison method must be used by comparing two different indicator bases, (for example; B and C bases). Both of these bases are studied in the same solution where:

$$pK_{CH^+} - pK_{BH^+} = log\left(\frac{[CH^+])}{[C]}\right) - log\left(\frac{[BH^+)}{[B]}\right) - log\left(\frac{[f_C f_{BH^+})}{[f_{CH^+} f_B]}\right) \quad (2.2.10)$$

Hammett concluded that if the bases B and C are have similar structure, then it is reasonable to ignore the $(log\left(\frac{[f_C f_{BH^+})}{[f_{CH^+} f_B]}\right)$ ) terms.[153] The $pK_{BH^+}$ values can be determined by the relation:

$$pK_{CH^+} - pK_{BH^+} = log\left(\frac{[CH^+])}{[C]}\right) - log\left(\frac{[BH^+)}{[B]}\right) \quad (2.2.11)$$

provided that the ionisation constants values of the bases B and C are close enough so that both ratios can be measured with good precision in the same medium. By using the same procedure, it is possible to calculate the $pK_{DH^+} - pK_{CH^+}$ for an indicator D whose ionisation overlaps with C, and so on. Thus, the $pK_{BH^+}$ values for all probes can be established if any one of the probes is determined by a direct measurement in dilute aqueous solution. Hammett was able to establish the $pK_{BH^+}$ values of many nitroaniline bases using this step-wise method (Figure 2.2.4). In Figure 2.2.4, Hammett shows the log of the ionisation ratios of all the bases that he used, which cover the whole $H_2O$-$H_2SO_4$ mixture (from pure water to pure $H_2SO_4$). These findings support Hammett's hypothesis (eqn. 2.2.11) as most of the lines align parallel to each other in the graph. The degree of parallelism is acceptable except at the concentration of sulfuric acid from 60-80%, where the bases used gave off-trend results (bases 7-12). Hammett discussed that at the medium effect is significant in these regions or with increasing concentration of acid used. Thus, the molar activity coefficients and the transfer activity coefficients of the two adjacent bases became too different for the log e

$(log\left(\frac{[f_C f_{BH+})}{[f_{CH+} f_B]}\right)$ ) terms to be cancelled out.[153]

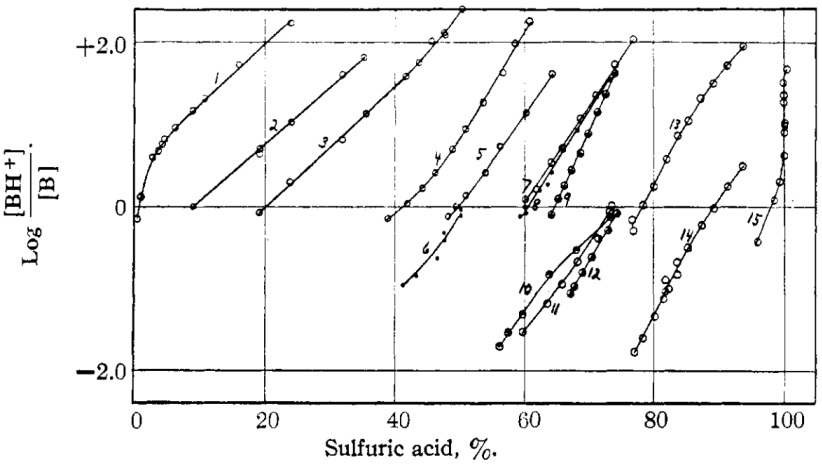



**Figure 2.2.4** – Logarithm of ionisation ratios of Hammett bases in sulphuric acid-water solutions. Dye: (1) 4-nitroaniline, (2) 2-nitroaniline, (3) 4-chloro-2-nitroaniline, (4) p-nitrodiphenylamine, (5) 2,4-dichloro-6-nitroaniline, (6) p-nitroazobenzene, (7) 2,6-dinitro-4-methylaniline. (8) 2,4-dinitroaniline, (9) *N,N*-dimethyl-2,4,6-trinitroaniline, (10) benzalacetophenone, (11) $\beta$-benzoylnaphthalene, (12) p-benzoylbiphenyl, (13) 6-bromo-2,4-dinitroaniline, (14) anthraquinone, (15) 2,4,6-trinitroaniline. Image taken from Hammett's paper.
[153]

The establishment of the Hammett acidity function, ($H_0$) by Hammett as an early foundation of a truly robust acidity scale has gained considerable attention by other researchers and offers an expansion in the study of the acidity measurements of different solutions. More $pK_{BH^+}$ values have been determined since then by different research groups.[161] Other research groups also measured the acidity at lower and higher temperature than the temperature used by Hammett in his acidity measurements (25 $^0$C).[160] Since it is acceptable to use the equation 2.2.11 for any solvent with high dielectric constants and water[153], the $H_0$ values of other acid systems were investigated using the$pK_{BH^+}$ values obtained from the sulphuric acid-water mixtures.[154] For example, Randles and Tedder reported on the $H_0$ measurements of trichloroacetic acid and trifluoroacetic acid in water.[162] Also, data for the acidity of phosphoric acid, perchloric acid and hydrochloric acid were also collected using this Hammett acidity measurement.[163] The $H_0$ values of acids in molecular solvents have also been reported, such as trifluoroacetic

acid[164, 165] and phosphoric acid[166] in dimethylformamide and methanesulfonic acid in 2-pyrrolidine[164]. The Hammett acidity function was further adapted and applied in measuring the acidity of strong acid and superacid catalysts.[167, 168] Both of these papers used the $^{13}C$ NMR spectroscopy measurements using a carbon base as an indicator to measure the $H_0$ values of the strong acid. Following these papers, Fărcaşiu and Ghenciu then developed a new method of measuring the acidity of acidic solutions using $^{13}C$ NMR Spectroscopy of unsaturated ketones as the base indicator.[148, 169]

## 2.3 Acidity functions from $^{13}C$ NMR Spectroscopy - The $^{13}C$ NMR Probe

Although the methods developed by Hammett have set a foundation in the measuring the acidity of solutions, the Hammett method requires an immense amount of work to measure the acidity of a solution. The Hammett acidity measurements also have several shortcomings which limit the application of the Hammett method:

1. A coloured or opaque solution is not suitable for UV-Vis spectroscopy. Many acid catalyst systems are dark-coloured and sometimes opaque.[168]

2. The method is extremely sensitive to water impurity. The preparation of the solution before the UV measurement is time-consuming and increases the exposure of the solution into the air over time. Thus, it is possible to get an inaccurate $H_0$ value of the measured solution.

3. Since there are a lot of bases available, it is difficult to choose a suitable indicator for a solution with an unknown acidity. Again, the process to determine a suitable indicator will be lengthy and requires lots of work and materials.

4. There is a chance of choosing a wrong indicator as it is possible for two different bases used for measuring a solution to give different $H_0$ values.[142, 143]

Fărcaşiu's research group has developed an alternative method overcome the shortcomings (point 1-4) of the use of UV-Vis spectroscopy in Hammett's method.[148]

The technique developed used $^{13}C$ NMR spectroscopy to generate the $H_0$ value of a measured solution. Instead of establishing another acidity function, the difference between the chemical shifts of the signals for the probe used ($\Delta\delta^0$) is correlated with the $H_0$ values for sulphuric acid solutions. Since the $H_0$ value is calculated using the Equation 2.2.2, the method was developed by finding both of the $\frac{[BH^+]}{[B]}$ and ($pK_a$) values of the indicator used.

## 2.3.1 Principle and development of the method

### 2.3.1.1 Determination of the $\Delta\delta^0$ value

The principle used in establishing the NMR spectrum to determine the acidity is; a single average chemical shift will show in the NMR spectrum when the two forms of a base (the protonated form and the free base) undergo a fast-exchange, which is faster than the time-scale of NMR spectroscopy. The acidity can then be determined by calculating their ratios where:

$$\frac{[BH^+]}{[B]} = \frac{(\delta_{av} - \delta_B)}{(\delta_{BH^+} - \delta_B)} \tag{2.3.1}$$

where $\delta_{av}$ is the average chemical shift of the base when it is partially protonated, $\delta_B$ is the chemical shift of the free base, and $\delta_{BH^+}$ is the chemical shift of the protonated base. The method was built on the well-established chemical shift method to determine the $H_0$. For example, $^1H$ NMR spectroscopy was used to measure the $H_0$ value of perfluorooctanesulfonic acid with the hydronation of diethyl ether[170], $^{19}F$ NMR (p-fluorobenzamide and p-fluoroacetophenone)[171], $^{13}C$ NMR for the measurement of the protonation of aliphatic ketones in sulfuric acid[172], $^{31}P$ and $^{17}O$ NMR for measuring the protonation of selected bases in strong acids (e.g. difluorophosphoric acid and nitric acid)[173], and $^{13}C$ NMR of acetone to measure the acidity of ionic liquids[174]. Fărcaşiu and Ghenciu suggested that the all these NMR-derived $H_0$ values mentioned above are questionable, because the chemical shift is influenced by other factors in addition to the extent of positive charge, especially of the magnetic properties of the acid as a solvent. To correct these effects, the chemical shift difference between the signals of two atoms (A and B) in the same molecule can be used instead of the chemical shift of a single nucleus

in the base molecule. The correction will work ideally if A has all the charge while B has none. The chemical shift difference between A and B will be proportional to the extent of charge obtained by the molecule as the solvent effect is exerted upon all atoms in the molecule, thus correcting the solvent effects[148].

Fărcaşiu and Ghenciu choose $^{13}$C NMR because the medium effects are insignificant in the $^{13}$C NMR compared to $^{1}$H NMR spectroscopy.[175] They used the well-established Hammett $H_2O$-$H_2SO_4$ system and worked on finding a suitable NMR acid indicator that works well with the system rather than establishing a new acidity function. In the early development of the method, the difference in the chemical shift was tested with aliphatic alcohols and conjugated alkenones as an indicator. During the protonation, most of the charge is localised at $C_\beta$ , while a minimal charge is present at $C_\alpha$. The difference between these chemical shifts of the two carbons ($\Delta\delta = \delta_{C_\alpha} - \delta_{C_\beta}$) was correlated with acidity.

$CH_3CH_2OH + AH \rightleftharpoons CH_3CH_2OH_2^+ + A^-$

with the formation of ethyl hydrogen sulfate;

$EtOH + H_2SO_4 \rightarrow EtHSO_4 + H_2O$

The initial study concluded that the formation of ethyl hydrogen sulfate in the solution did not change the overall acidity of the solution, but it did affect the precision of the chemical shifts, although the results could be used for acidity evaluations. The accuracy of the chemical shifts was influenced by the similar acidity of $H_2SO_4$ with $EtHSO_4$ (even though there are no accurate measurements).[176] Moreover, the difference in the basicity of $H_2O$ with EtOH was not far apart (the $pK_a$ for EtOH and water are 15.2 and 15.7 respectively).

The $^{13}$C NMR method was further developed using $\alpha,\beta$-unsaturated ketones as the probe. Mesityl oxide or 4-methylpent-3-en-2-one is a popular example used to study strong acids[177, 178] and superacids to determine the charge distribution in and structure of the conjugate acids[179, 180]. Thus, the work done in this thesis will use mesityl oxide as the probe, due to the extensive literature reported on this $\alpha,\beta$-unsaturated ketones. The proton is attached to the oxygen during the protonation (Figure 2.3.1).

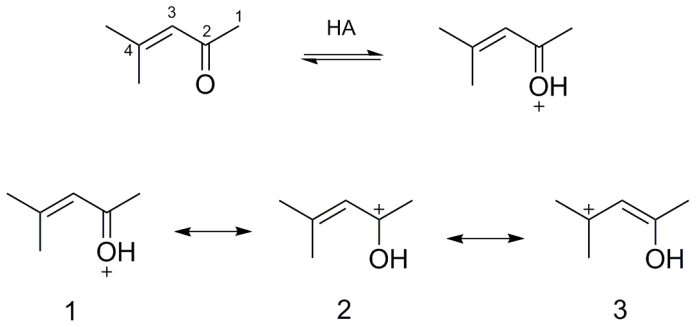



**Figure 2.3.1** – Conjugation mode of mesityl oxide

In a superacid, the signal for the C-4 carbon of mesityl oxide moved downfield by 50 ppm compared to the C-2 (12 ppm), and small upfield change in C-3 (3 ppm)[180]. The difference in the chemical shifts indicated that C-4 carried most of the positive charge compared to C-2 and left C-3 unchanged in charge. Hence, the most protonated form of mesityl oxide is best represented by the canonical form 3 (Figure 2.3.1). Fărcaşiu and Ghenciu decided that conjugated enones are suitable probes for acidity measurements using the $^{13}C$ NMR spectroscopy, because of their large changes in chemical shifts upon protonation and the type of charge distribution. The chemical shift difference $\Delta\delta$ can be used as an acidity dependent parameter corrected for medium effects. $\Delta\delta$ can be defined as:

$\Delta\delta = \delta_4 - \delta_3$

However, Fărcaşiu and Ghenciu mentioned in the paper that there is a shortcoming in their developed method. The $^{13}C$ NMR method needs higher concentrations of indicator compared to the Hammett method. The Hammett method needs higher concentrations of indicator compared to the Hammett's method. The Hammett's method requires only small amount (in millimolar concentration) while a higher amount of mesityl oxide is needed for it to be detectable in the $^{13}C$ NMR method (1% - 8 % w/w). The higher concentration of indicator will affect the acidity measured, which reduces the acidity of the solution. To solve this problem, the $\Delta\delta^0$ value is used instead of the $\Delta\delta$ value. The $\Delta\delta^0$ is obtained from the extrapolation of $\Delta\delta$ vs. mesityl oxide concentration . $\Delta\delta^0$ is a parameter the acidity at infinite dilution of mesityl oxide. Fărcaşiu and Ghenciu plotted $H_0$ values against concentration of 4-hexen-3-one (Figure 2.3.2) and obtained a linear correlation between these two parameters[169]. They mentioned that mesityl oxide

behaves the same manner as 4-hexen-3-one, so, it is possible to use the $\Delta\delta^0$ value to calculate the $H_0$ values (using the eqn. 2.2.2) in the $^{13}C$ NMR method.

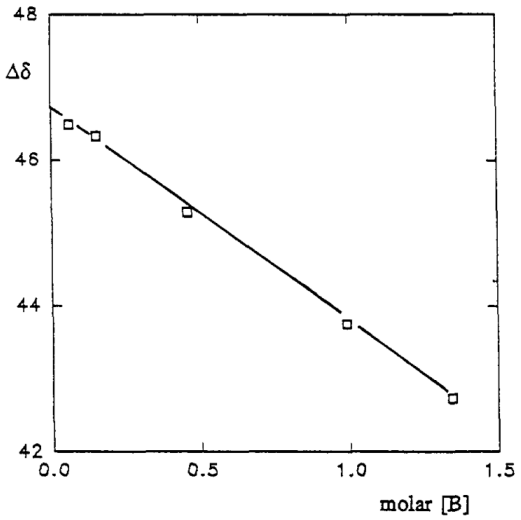
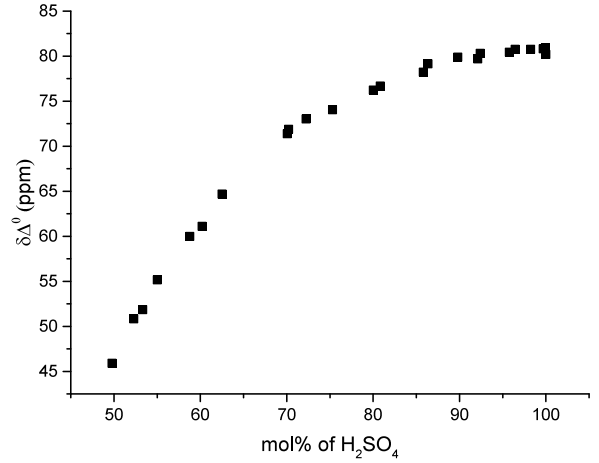
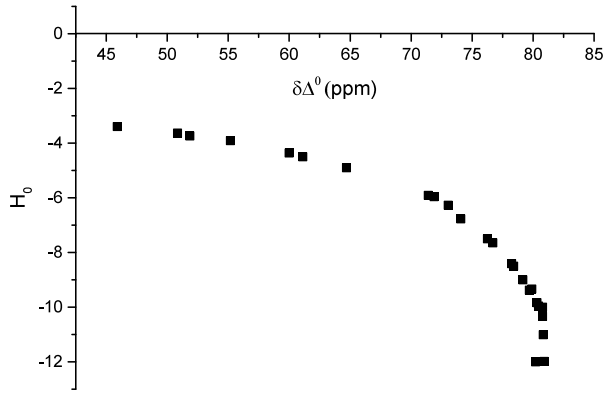



**Figure 2.3.2** – $\Delta\delta$ vs. concentration of 4-hexen-3-one in 75% $H_2SO_4$ where $\Delta\delta^0$= 46.7 ppm.[169]

As there are several acidity functions in reference,[181] Fărcaşiu and Ghenciu did not want to add furthermore another acidity function ($H_{\Delta\delta^0}$). Hence they decided to use the same $H_0$ function from the Hammett's method. Fărcaşiu and Ghenciu used the same water and sulphuric acid mixtures used in the Hammett's method to calculate the $\Delta\delta^0$ and the $H_0$ values for each mixture (Figure 2.3.3). The results show that the $H_0$ value increases as the concentration of $H_2SO_4$ are increased, which was the same as the trend in the Hammett's method results. However, no results were collected for less than 50 mol % of $H_2SO_4$ due to the insolubility of mesityl oxide in water. The data collected are thought to be interesting, as the single mesityl oxide probe can cover a broad range of $H_0$ values (-3.39 to 12.00). Thus, from the calibration curve obtained from sulphuric acid, it is possible to determine the acid strength of other acids by finding the $\Delta\delta^0$ for the mesityl oxide in the tested acids.




(a)




(b)

**Figure 2.3.3** – Plot of (a) mol % $H_2SO_4$ in $H_2O$-$H_2SO_4$ system vs. $\Delta\delta^0$ , and (b) $\Delta\delta^0$ vs. $H_0$ values.

### 2.3.1.2 Determination of the $pK_a$ of the mesityl oxide

The $pK_a$ of the mesityl oxide is calculated by plotting the slopes, $s$ against the $\Delta\delta^0$ values. The $s$ can be obtained by plotting $H_0$ values vs the concentration of mesityl oxide. As mentioned before, increasing the concentration of mesityl oxide will decrease the $\Delta\delta$ , and thus, reduce the overall acidity. This situation led to a

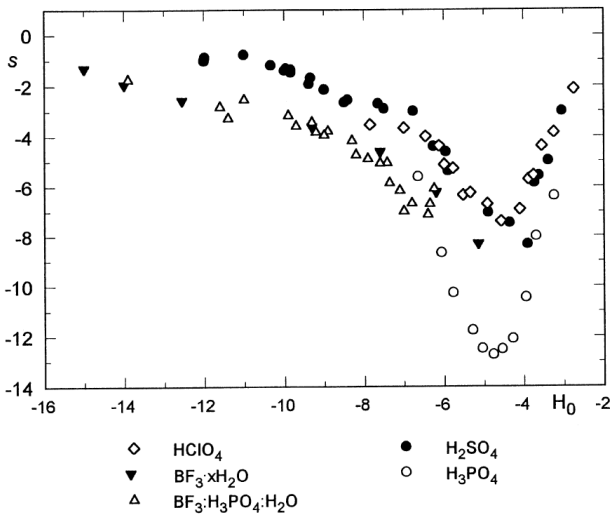



**Figure 2.3.4** – Plot of *s*, slopes of the linear correlations between $\Delta\delta$ vs. total concentration of mesityl oxide against $H_0$ values obtained using UV-Vis spectroscopy. Image taken from Fărcaşiu and Ghenciu's paper.[169]

query on how much is the $\Delta\delta$ affected by increasing the concentration of mesityl oxide. Fărcaşiu and Ghenciu discussed that *s* is small in a weak acid because hydrogen bonding is the only interaction that occurs between the indicator and the mixture/solvent. The interaction that occurs is not significant enough to affect the acidity of the solution. Conversely, in a strong acid, since the concentration of mesityl oxide is smaller than the acid in the solution, there is enough excess acid available to protonate the indicator fully. Thus, *s* will remain small in the normal range of the concentration measured. Fărcaşiu and Ghenciu predicted that the *s* is steepest at the acidity where the base is half converted to $BH^+$. To prove this prediction, they plotted the measured s of various aqueous acidic solutions against their $H_0$ values (Figure 2.3.4). Results from the graph proved Fărcaşiu and Ghenciu's prediction where the lowest value of *s* was spotted at the ends of the graph and the steepest $H_0$ values was at -4.4 $\pm$ 0.4 for all of the aqueous acidic solutions.

The $pK_a$ value of the mesityl oxide determined by Fărcaşiu and Ghenciu is equal to $(H_0)_{1/2}$ provided that unsaturated ketones be the true Hammett indicators. At half-protonation, the last term in the eqn. 2.3.2 is cancelled;

$$H_0 = pK_a - log\frac{[BH^+]}{[B]} \tag{2.3.2}$$

Thus,

$$(H_0)_{1/2} = pK_a \tag{2.3.3}$$

From the $pK_a$ value of the mesityl oxide obtained, the strongest acidity that can be measured by the mesityl oxide probe (solution that can protonate 99% mesityl oxide) should be $H_0 \approx$ -6.5 and the plot of $\Delta\delta^0$ vs. $H_0$ is expected to be flat by $H_0$ -7.5 (about 80% $H_2SO_4$). However, the curve steadily rises to 100% $H_2SO_4$($H_0$-12) and beyond. A fast, reversible protonation occurs where the cation can form a dication explains this situation (Figure 2.3.5). A second protonation proved to happen in other indicators studied in other superacid solutions[168]. Thus, mesityl oxide can be used as an indicator in a broader acidity range and in the region of acid strength where the second protonation occurs. Fărcaşiu and Ghenciu then used their $^{13}C$ Spectroscopy spectroscopy method to measure other acids, complexes and working catalysts. All these measurements can be found in the articles published.[148]

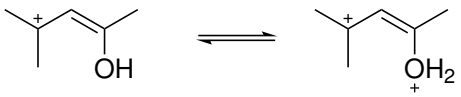



**Figure 2.3.5** – Second protonation of Mesityl oxide

Note: From this point onwards, the $^{13}C$ Spectroscopy method will be referred as the $^{13}C$ NMR Probe while the traditional Hammett acidity method will be referred as the UV-Vis Probe.

### 2.3.2 Applying the $^{13}C$ Probe into Brønsted acid-ionic liquid systems

A paper on measuring the acidity of ionic liquids using the $^{13}C$ NMR Probe by the Welton research group (Gräsvik and co-workers) was published in 2014.[147] The paper measured the acidity of [$C_4C_1$im][$HSO_4$ ] and [$HC_4$im][$HSO_4$ ] mixed with

$H_2SO_4$ at various concentrations. These ionic liquids were initially chosen to mimic as close as they can to the $H_2O$-$H_2SO_4$ system done by Fărcaşiu and Ghenciu. The $^{13}C$ NMR Probe was found to work well in both of the acid-ionic liquids systems, but with some modification in the calculation to obtain the $H_0$ values. In this method, the data points of the [$C_4C_1$im][$HSO_4$ ]-$H_2SO_4$ system is used as the calibration points to recreate Fărcaşiu and Ghenciu's method where they used the calibration curve form the $H_2O$-$H_2SO_4$ system to measure other acidic systems. The [$C_4C_1$im][$HSO_4$ ]-$H_2SO_4$ calibration curve was then evaluated using the $\Delta\delta^0$ values of the [$HC_4$im][$HSO_4$ ]-$H_2SO_4$ system. The $H_0$ value is calculated using the eqn. 2.3.2. Rearranging eqn. 2.3.2 gives:

$$\frac{[BH^+]}{[B]+[BH^+]} = \frac{(\delta_{av}-\delta_B)}{(\delta_{BH^+}-\delta_B)}$$

$$\frac{[BH^+]}{[B]} = \frac{(\delta_{av}-\delta_B)}{(\delta_{BH^+}-\delta_{av})} \tag{2.3.4}$$

where $\delta_{av}$ is the observed chemical shift when the indicator is partially protonated, and $\delta_B$ and $\delta_{BH^+}$ are the chemical shifts of the acid indicator when it is completely unprotonated and completely protonated. This equation applies to the $\Delta\delta^0$ values because it is applicable to any average chemical shift:

$$\frac{[BH^+]}{[B]]} = \frac{(\triangle\delta^0_{av}-\triangle\delta^0_B)}{(\triangle\delta^0_{BH^+}-\triangle\delta^0_{av})} \tag{2.3.5}$$

By incorporating eqn. 2.3.5 into eqn. 2.3.2, the $H_0$ value for the $^{13}C$ NMR Probe is equal to:

$$H_0 = pK_a - log\frac{(\triangle\delta^0_{av}-\triangle\delta^0_B)}{(\triangle\delta^0_{BH^+}-\triangle\delta^0_{av})} \tag{2.3.6}$$

The $\triangle\delta^0_B$ and $\triangle\delta^0_{BH^+}$ are an unknown parameter while the $pK_a$ value of the mesityl oxide is -4. Gräsvik failed to produce a good match in his attempts to fit a curve to the $H_0$ vs. $\Delta\delta^0$ values of [$C_4C_1$im][$HSO_4$]-$H_2SO_4$ using eqn. 2.3.6. Thus, Gräsvik used a normal smoothing function to connect the points and asymptotically fitted the limits of the mesityl oxide $^{13}C$ NMR shifts by extrapolating the

minimum $\Delta\delta$ and the $\Delta\delta$ maximum. An asymptotic behaviour was observed as the fully deprotonated and fully protonated states are approached. The ratio $\frac{[BH^+]}{[B]}$ was calculated by assuming a linear behaviour between the two extremes, as the NMR shift is associated to the relative amounts of protonated and deprotonated mesityl oxide. Thus, the $H_0$ value for the $^{13}C$ NMR Probe was calculated as:

$$H_0 = -4 - log\frac{(\triangle\delta^0 - \triangle\delta^0_{min})}{(\triangle\delta^0_{max} - \triangle\delta^0)}$$

$$H_0 = -4 - log\frac{(\triangle\delta^0 - 31.07)}{(80.91 - \triangle\delta^0)} \tag{2.3.7}$$

Figure 2.3.6 shows the comparison plot for the $[C_4C_1im][HSO_4]$-$H_2SO_4$ calibration points, $H_2O$-$H_2SO_4$ system Fărcaşiu and Ghenciu and new calibration points for $[C_4C_1im][HSO_4]$-$H_2SO_4$ calculated using the eqn. 2.3.7. However, both of the fits at very high or very low acidity are too steep and may arise due to the hydrogen bonding effects between the mesityl oxide and the multiple anions. The hydrogen bonding can reduce the relative activities of deprotonated and protonated mesityl oxide, which would misalign the concentration profile. Gräsvik then corrected the equation with separate values for the hydrogen bonding factor, s for each side of the function:

$$H_0 = -4 - s * log\frac{(\triangle\delta^0 - 31.07)}{(80.91 - \triangle\delta^0)} \tag{2.3.8}$$

where s = 2.32 for $H_0$ below -4 and s = 3.19 for $H_0$ below -4 (Figure 2.3.7). The results in Fig. 2.3.7 shows that the $^{13}C$ NMR Probe acidity range covers the range from to 1.93 to -11.3.

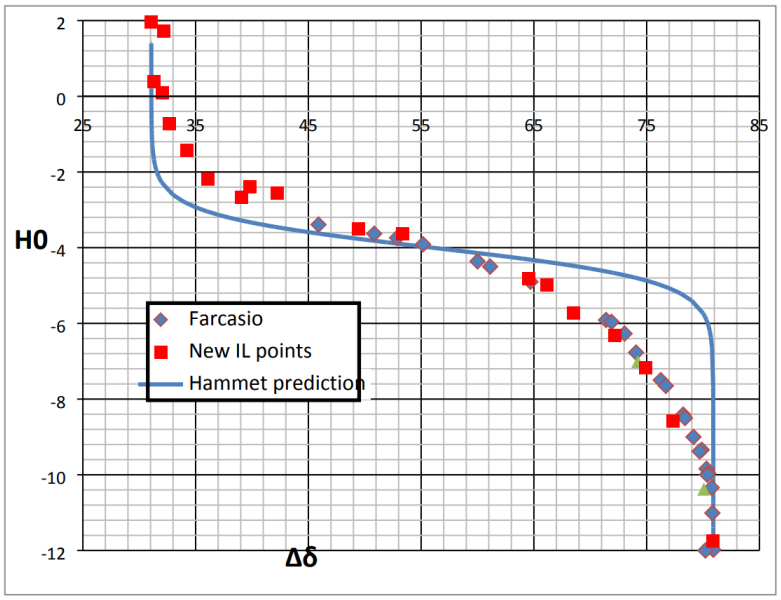



**Figure 2.3.6** – $\Delta\delta^0$ vs. $H_0$ for $[C_4C_1im][HSO_4]$-$H_2SO_4$ (new IL points), $H_2O$-$H_2SO_4$ system (Farcasio) and Hammett prediction of $[C_4C_1im][HSO_4]$-$H_2SO_4$using eqn. 2.3.7.[147]

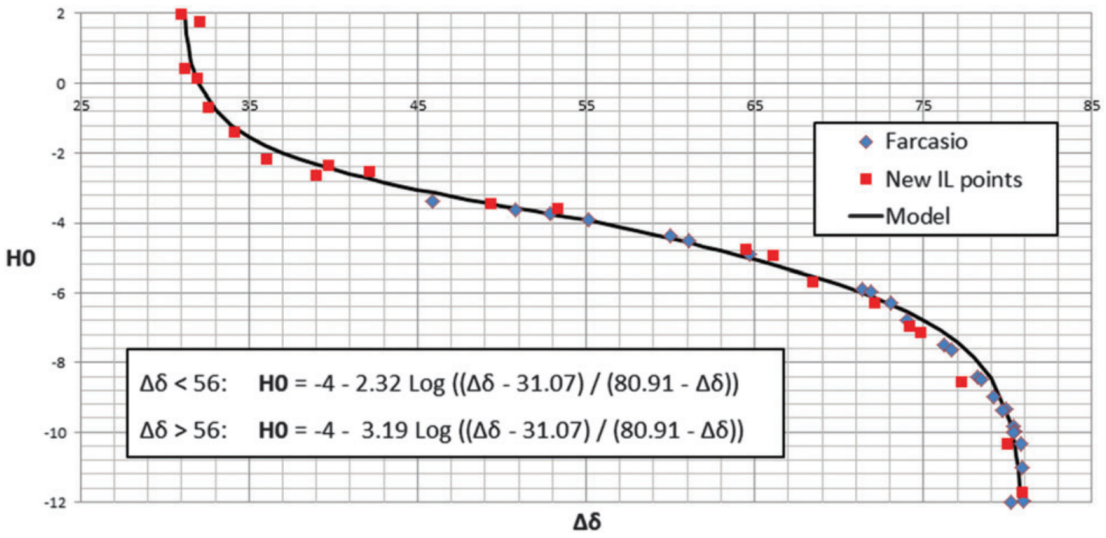



**Figure 2.3.7** – $\Delta\delta^0$ vs. $H_0$ for $[C_4C_1im][HSO_4]$-$H_2SO_4$, $[HC_4im][HSO_4]$-$H_2SO_4$ and $H_2O$-$H_2SO_4$ system.[147]

## 2.4 Results: The acidity measurements of Brønsted acids-ionic liquids system with the same conjugate anion using the $^{13}C$ NMR Probe

The success in the measurement of the acidity of the $[HSO_4]^-$ anion ionic liquids with $H_2SO_4$ using the $^{13}C$ NMR Probe shows the possibility of measuring other Brønsted acids and ionic liquids. Motivated by this possibility and the robustness of this single-step $^{13}C$ NMR Probe, the acidity of Brønsted acids-ionic liquids ($[C_4C_1im][NTf_2]$, $[C_4C_1im][OTf]$, $[C_4C_1im][Me_2PO_4]$ and $[C_2C_1im][OAc]$) were measured with different Brønsted acids (bis(trifluoromethanesulfonyl) imide, $H[NTf_2]$; triflic acid, H[OTf]; phosphoric acid, $H_3PO_4$ and acetic acid, H[OAc]). Solutions with increasing acidity were prepared by adding a Brønsted acid into an ionic liquid and their acidity measured. However, no data could be collected for the $[C_2C_1im][OAc]$-H[OAc] system as the acidity of the 100 % H[OAc] fell below the minimum detection limits of the $^{13}C$ NMR Probe. The acidity of four different Brønsted acid-ionic liquid systems with general formula $[C_4C_1im][A]$-HA (A = $NTf_2$, OTf and $Me_2PO_4$) were measured using the $^{13}C$ NMR Probe with mesityl oxide as an indicator. The data for $[C_4C_1im][HSO_4]$-$H_2SO_4$ system were recreated from the Gräsvik's paper[147] to expand the acidity measurements of the ionic liquids-sulphuric acid system (in the chapter 3). The main objective of this work is to investigate the acidity of the Brønsted acids-ionic liquid systems as a function of their composition by investigating both strong and weak acids. These ionic liquids were chosen as they are useful in industrial processes and by knowing their acidic properties, it can help to increase the effectiveness of these ionic liquids in the application of each ionic liquid. Also, the data collected will provide more understanding of the selection of ionic liquid system as homogeneous catalysts.

The acids chosen represent a broad acidity range. Strong sulfonic acids are commonly used in catalysis while weak acids are known to form strong anionic clusters.[150] Moreover, by measuring the acidity of strong acids, it is hoped to extend acidity range that can be obtained using the $^{13}C$ NMR Probe with mesityl oxide as indicator in the Brønsted acid-ionic liquids system. The highest $H_0$ values reported in the Brønsted acid-ionic liquids system calculated is = -11.93.[147]

Each system shares the same anion, and conjugate base of the acid and the same $[C_4C_1im]^+$ was used to provide a systematic investigation of the effect of the anion on the acidity of the Brønsted acids-ionic liquids system. It is worth to mention that during the data collection for this thesis, another research group has published a paper on measuring the acidity of ionic liquids with H[OTf] in 2016.[182] The paper proved that the $^{13}C$ NMR Probe is replicable by other researchers and this method worked with different ionic liquids which motivate me more on measuring the acidity of Brønsted acid-ionic liquid system.

### 2.4.1 The acidity measurements of $[C_4C_1im][NTf_2]$-$H[NTf_2]$ system

Solutions of the $[C_4C_1im][NTf_2]$-$H[NTf_2]$ system were prepared with varying the molar ratio of acid $\chi_{H[NTf_2]}$. To each of the different $\chi_{H[NTf_2]}$, solutions, mesityl oxide was added to make between three to five different concentrations from 1% to around 8% w/w (refer to the synthesis section for sample preparations). These samples were then transferred to separate NMR tubes with an external DMSO-$d^6$ standard in a glass capillary and sent for $^{13}C$ NMR spectrometry measurements. Figure 2.4.1 shows an example for the $^{13}C$ NMR spectra of $[C_4C_1im][NTf_2]$ + $\chi_{H[NTf_2]}$= 0.69 with the addition of mesityl oxide where the carbon peaks for the ionic liquids and the mesityl oxide were assigned. The mesityl oxide peaks are visible in the spectrum and make the acidity measurements of the $[C_4C_1im][NTf_2]$-$H[NTf_2]$ system possible.

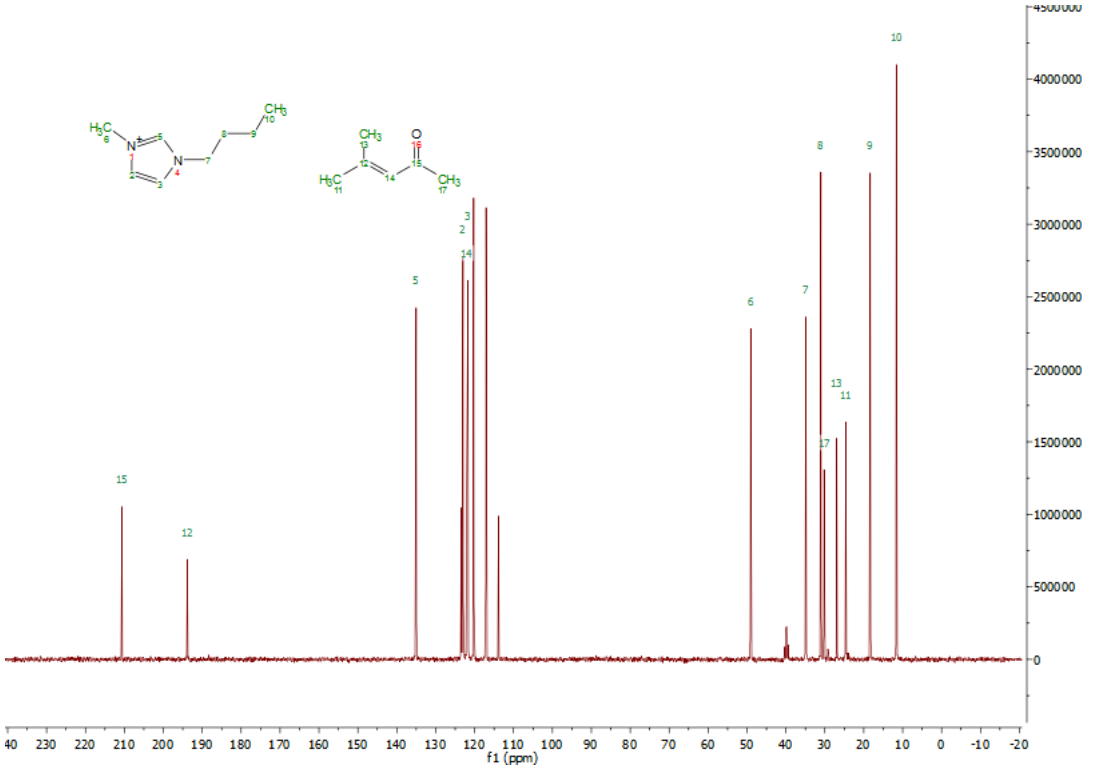



**Figure 2.4.1** – $^{13}C$ NMR spectrum of mesityl oxide in $[C_4C_1im][NTf_2]$ + 0.69 $\chi_{H[NTf_2]}$

In each of the $^{13}C$ NMR spectra obtained, the main focus would be on the chemical shift of the C3 and C4 of the mesityl oxide. These chemical shift values were used to calculate the $\Delta\delta$ for each of the mixtures with a different concentration of mesityl oxide, followed by the extrapolation to the y-axis to give the $\Delta\delta^0$. The $\Delta\delta^0$ value was then incorporated into equation 2.3.8 to calculate the $H_0$ value for each mixture. Table 2.4.1 listed some of the $\Delta\delta$ values obtained in the $[C_4C_1im][NTf_2]$-$H[NTf_2]$ system. By comparing the chemical shifts of C4 at lower molar ratio of $H[NTf_2]$ ( $\chi_{H[NTf_2]}$= 0.085), and at higher molar ratio of $\chi_{H[NTf_2]}$ the C4 moves downfield for about ≈40 ppm from the lower to the higher molar ratio of $H[NTf_2]$. On the other hand, small upfield changes were observed for the C3 of the mesityl oxide. Since the chemical shift of the mesityl oxide behaves the same for the $H_2O$-$H_2SO_4$[148] and the $[C_4C_1im][HSO_4]$-$H_2SO_4$[147] systems, it is safe to say that mesityl oxide works well as an indicator for the $[C_4C_1im][NTf_2]$-$H[NTf_2]$ system. A graph of $\Delta\delta$ against the concentration of the mesityl oxide added was

then plotted and extrapolated to the y-axis to obtain the $\Delta\delta^0$ (Figure 2.4.2). The $\Delta\delta^0$ is the intercept value of the plotted graph. The $\Delta\delta^0$ values obtained is the value that corresponds to zero concentration of mesityl oxide. All of the $\Delta\delta^0$ values obtained were used to calculate the $H_0$ values for each mixture in the system.

**Table 2.4.1 –** $\Delta\delta$ values for each different [mesityl oxide] for several $\chi_{H[NTf_2]}$ in the $[C_4C_1im][NTf_2]$-$H[NTf_2]$ system.

| $\chi_{H[NTf_2]}$ | [Mesityl oxide] (weight%) | C4 shift (ppm) | C3 shift (ppm) | $\Delta\delta$ (ppm) |
|---|---|---|---|---|
| 0.0085 | 4.996 | 155.21 | 123.40 | 31.81 |
| | 6.589 | 154.9 | 123.41 | 31.49 |
| | 9.134 | 154.63 | 123.43 | 31.2 |
| 0.1525 | 0.873 | 192.22 | 122.11 | 70.11 |
| | 2.593 | 190.27 | 122.18 | 68.09 |
| | 2.850 | 190.06 | 122.34 | 67.72 |
| | 4.375 | 187.59 | 122.35 | 65.24 |
| 0.399 | 0.691 | 194.14 | 121.99 | 72.15 |
| | 1.579 | 193.83 | 122.11 | 71.72 |
| | 2.047 | 193.61 | 122.17 | 71.44 |
| | 2.732 | 193.16 | 122.06 | 71.10 |
| | 3.258 | 192.93 | 122.06 | 70.87 |
| 0.514 | 2.368 | 194.48 | 121.99 | 72.49 |
| | 5.385 | 192.79 | 121.09 | 71.7 |
| | 8.011 | 192.52 | 122.16 | 70.36 |
| | 10.410 | 191.45 | 122.12 | 69.33 |
| 0.775 | 2.335 | 198.09 | 121.74 | 76.35 |
| | 5.715 | 195.54 | 121.95 | 73.59 |
| | 6.045 | 195.31 | 121.96 | 73.35 |

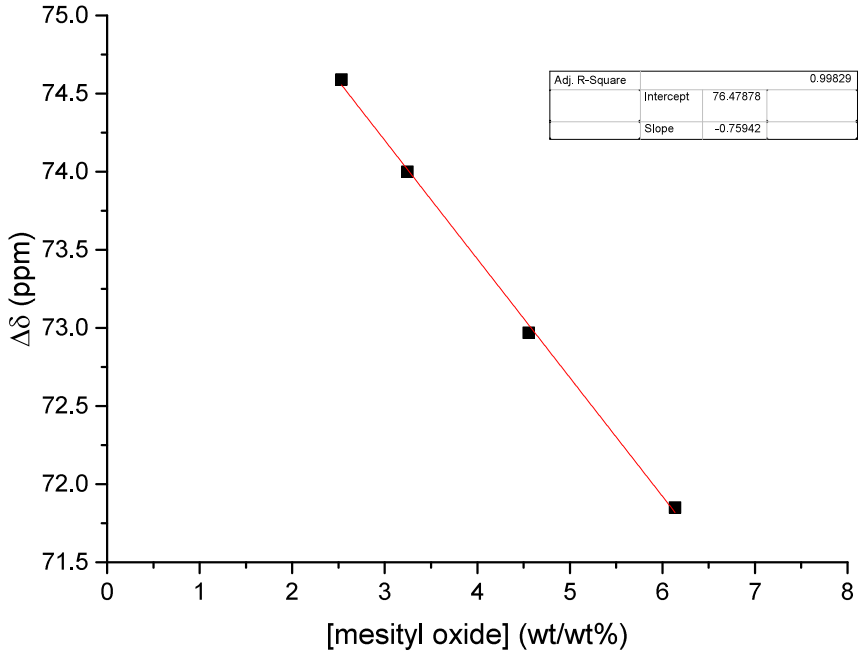



**Figure 2.4.2** – Determination of $\Delta\delta^0$ mesityl oxide in extrapolation $[C_4C_1im][NTf_2]$ + 0.67 $\chi_{H[NTf_2]}$

In the $[C_4C_1im][NTf_2]$-H$[NTf_2]$ system, homogeneous solutions were formed for up to $\chi_{H[NTf_2]} \leq 0.774$. The acid was not fully solubilised at higher concentrations of acid and formed a liquid-solid mixture. The $H_0$ value of neat $[C_4C_1im][NTf_2]$ is not available since mesityl oxide did not dissolve in the neat ionic liquid. This may be explained by the lower acidity of $[C_4C_1im][NTf_2]$ that falls below the minimum detection limit of the mesityl oxide as an indicator in the $^{13}$ NMR Probe. Mesityl oxide is completely dissolved in this system for $0.003 \leq \chi_{H[NTf_2]} \leq 0.774$. It is expected that the acidity will increase (decrease in $H_0$ values) as the $\chi_{H[NTf_2]}$ is increased, which was reported in other published literature.[150] The results from Figure 2.4.3 shows the compilation of $H_0$ values against the molar ratio of H$[NTf_2]$ where a sigmoid curve was observed in the graph.

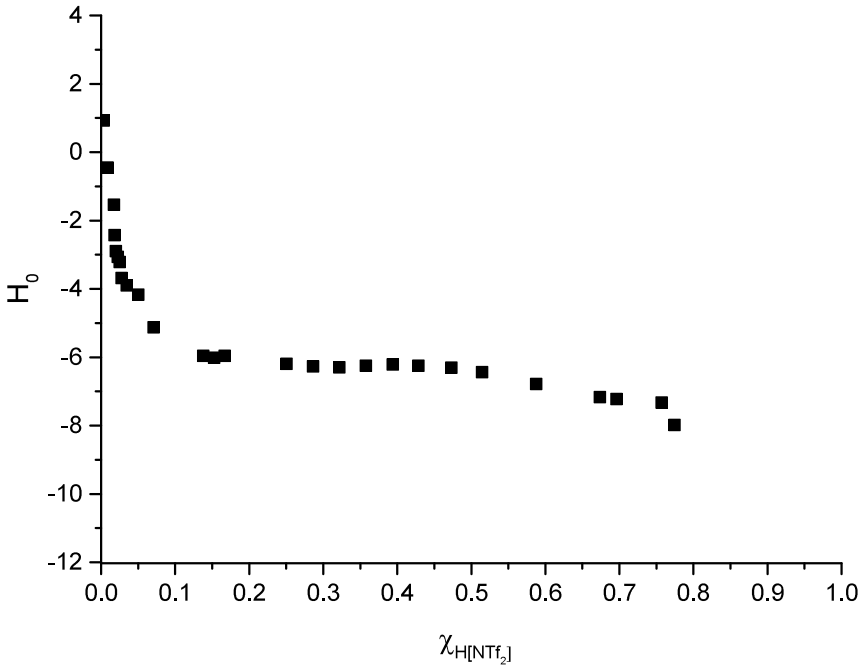



**Figure 2.4.3** – The $H_0$ values against the molar ratio $\chi_{H[NTf_2]}$ for the $[C_4C_1im][NTf_2]$-$H[NTf_2]$ system

At the lower $\chi_{H[NTf_2]} \leq 0.07$, the addition of small amount of acid increases the acidity, up to the $H_0$ value = -5.125. At these points, the $[C_4C_1im][NTf_2]$ ionic liquids dominate the molar composition of this mixture, and the ionic liquid has a very low acidity. Thus, the total acidity of the $[C_4C_1im][NTf_2]$-$H[NTf_2]$ may significantly be affected even with the small amount of acid added at these concentrations. For $0.138 \leq \chi_{H[NTf_2]} \leq 0.429$, the acidity increases with a small significant difference where $H_0$ values obtained were between -5.959 to -6.252. It can be assumed that $HNTf_2$ is dissolved in its molecular form and there are no $[NTf_2(HNTf_2)]^-$ clusters formed in this range. The assumption can be supported from the paper published by McCune *et al.* where a similar trend was observed in the $[C_4C_1im][NTf_2]$-$H[NTf_2]$ system (using the Gutmann Acceptor Number method)[150] and as reported by Stayanov *et al.* in their work on acid solutions in non-polar solvents[183]. With further increase in the $\chi_{H[NTf_2]} \geq 0.6$, the acidity increases with more acid added. At this point, as the $H[NTf_2]$ is a

strong acid and it dominates the mixture over the ionic liquids, and hence, the overall acidity is based on the strength of the acid itself. As more acid is added into the $[C_4C_1im][NTf_2]$-$H[NTf_2]$ system, the protonation ability of the acid is also increased which increases the acidity of the mixture.[184] The $HNTf_2$ is noted as one of the strongest gas-phase acids measured.[185] The $H_0$ value of pure $HNTf_2$ cannot be measured, because it exists in a solid form. However, $HNTf_2$ is only a few orders of magnitude weaker that triflic acid ($H_0$ = -14.10[170]) (when the $pK_a$ values are measured in acetic acid solution[186]). The highest $H_0$ value obtained in this system is $H_0$=-7.981 at $\chi_{H[NTf_2]}$= 0.774, whereas the pure triflic acid is about -7. As the $[C_4C_1im][NTf_2]$ has a weak acidity, it is possible that the presence of the ionic liquid levels down the total acidity of the mixture.

Mass spectrometry analysis of the $[C_4C_1im][NTf_2]$ mixtures with $H[NTf_2]$ was done using the electrospray mass spectrometry method (ES-MS). Jackson and Duckworth reported that ES-MS of undiluted RTILs is a more straightforward approach to obtain the mass spectrometric information of the RTILs and their composition without any remarkable loss in analytical performance.[187] The ES-MS method is also suitable for the $[C_4C_1im][NTf_2]$-$H[NTf_2]$ mixture and other Brønsted acids-ionic liquids mixtures most of which are hygroscopic, especially at a higher concentrations of acid mixed with the ionic liquid. The results are compiled in Table 2.4.2 and Table 2.4.3. Clusters of the cations and the anions from the ionic liquid and the acid were detected in the positive mass spectra, for example; $([C_4C_1im]^+ \cdot F)$. In the negative mass spectra, only clusters from the anion were detected. However, there are no $[NTf_2](H[NTf_2])^-$ clusters present may be due to the poor H-bond accepting ability of the $[NTf_2]^-$ ion. Also, the steric hindrance and the oxygen-oxygen and fluorine-fluorine repulsion make the formation of N-H $\cdots$ N bond difficult.[150] It is important to take note that since the technique used is electrospray, these fragments detected in the mass spectra cannot be said to be certainly present in the liquid state.

**Table 2.4.2 –** The positive mass spectra of $[C_4C_1im][NTf_2]$-H$[NTf_2]$ : Detected ion fragments and their relative abundances

| $\chi_{H[NTf_2]}$ | Ions |
|---|---|
| 0 | $[C_4C_1im]^+$ (100 %) |
| 0.012 | $[C_4C_1im]^+$ (100 %), $[HC_1im]^+$ (10 %), ($[C_4C_1im]^+$·F) (5 %) |
| 0.049 | $[C_4C_1im]^+$ (100 %), $[HC_1im]^+$ (10 %), ($[C_4C_1im]^+$·F) (5 %) |
| 0.093 | $[C_4C_1im]^+$ (100 %), $[HC_1im]^+$ (5 %), ($[C_4C_1im]^+$·F) (5 %) |
| 0.290 | $[C_4C_1im]^+$ (100 %), $[HC_1im]^+$ (15 %), ($[C_4C_1im]^+$·F) (10 %) |
| 0.487 | $[C_4C_1im]^+$ (100 %), $[C_3im]^+$ (25%), $[HC_1im]^+$ (25%), ($[C_4C_1im]^+$ ·F )$^+$ (20%) |
| 0.717 | $[C_4C_1im]^+$ (100%), $[HC_1im]^+$ (15%), $[C_3im]^+$ (5%), ($[C_4C_1im]^+$ ·F )$^+$ (5%) |
| 1 | $[CF_2S]^+$ (100%), $[CSNO]^+$ (65%), $[CF_3HNS]^+$ (65%), $[C_2F_3HNO_4S_2]^+$ (25%), $[C_3F_7H_2N_2O_6S_2]^+$ (5%) |

**Table 2.4.3 –** The negative mass spectra of $[C_4C_1im][NTf_2]$-H$[NTf_2]$ : Detected ion fragments and their relative abundances

| $\chi_{H[NTf_2]}$ | Ions |
|---|---|
| 0 | $[(CF_3SO_2)_2N]^-$ (100%) |
| 0.012 | $[(CF_3SO_2)_2N]^-$(100%), $[(CF_3SO_2)_2NH]^-$(10%), $[(CF_3SO_2)N]^-$(5%) |
| 0.049 | $[(CF_3SO_2)_2N]^-$(100%), $[(CF_3SO_2)_2NH]$ (15%), $[(CF_3SO_2)N]^-$(5%) |
| 0.093 | $[(CF_3SO_2)_2N]^-$(100%),$[(CF_3SO_2)_2NH]$ (20%), $[(CF_3SO_2)N]^-$(5%) |
| 0.290 | $[(CF_3SO_2)_2N]^-$(100%), $[(CF_3SO_2)_2NH]^-$ (20%), $[(CF_3SO_2)N]^-$(5%) |
| 0.487 | $[(CF_3SO_2)_2N]^-$(100%), $[(CF_3SO_2)_2NH]$ (15%), $[(CF_3SO_2)N]^-$(5%) |
| 0.717 | $[(CF_3SO_2)_2N]^-$100%), $[(CF_3SO_2)_2NH]$ (15%), $[(CF_3SO_2)N]^-$(5%) |
| 1 | $[(CF_3SO_2)_2N]^-$(100%), $[(CF_3SO_2)_2NH]^-$ (15%), $[(CF_3SO_2)N]^-$(5%) |

Overall, the $^{13}C$ NMR Probe works well with the with the $[C_4C_1im][NTf_2]$-H$[NTf_2]$ system for $0.003 \leq \chi_{H[NTf_2]} \leq 0.774$ with the highest $H_0$ value obtained at -7.981. Since the acidity of this system is still in the published range from the Gräsvik's paper[147], it is a question whether the $^{13}C$ NMR Probe will work for acidity higher than -12 or not. Further investigation was explored on measuring the acidity of another strong acid, triflic acid will be discussed in the subchapter of 2.4.2.

### 2.4.2 The acidity measurements of [$C_4C_1$im][OTf]-H[OTf] system

The acidity of solutions of triflic acid, H[OTf] added into the [$C_4C_1$im][OTf] ionic liquid were measured at a different molar ratios of the acid, $\chi_{H[OTf]}$ using the $^{13}C$ NMR Probe. As mentioned before, the $H_0$ value of pure H[OTf] recorded using the UV-Vis probe is -14.10, which is higher than pure sulphuric acid ($H_0$ = -11.8). The method used is the same as the acidity measurements of the [$C_4C_1$im][$NTf_2$]-H[$NTf_2$] system. Figure 2.4.4 shows the results of the acidity measurements of the [$C_4C_1$im][OTf]-H[OTf] system. From the graph, the $H_0$ values were obtained for $0.030 \leq \chi_{H[OTf]} \leq 0.093$ and $0.552 \leq \chi_{H[OTf]} \geq 0.905$. No data were collected for the molar ratio of H[OTf] in between 0.100 and 0.500, because the mesityl oxide did not fully dissolve in these mixtures. At lower concentration of acid added ($0.030 \leq \chi_{H[OTf]} \leq 0.093$), a gradual increase in the acidity is observed. The $H_0$ values obtained at these points are from 0.526 to -1.753. It is observed that with a small amount of acid added cause a rapid increase in the acidity values ($H_0$ values are decreased). As the H[OTf] acid is a very strong acid, a small addition of the acid into the ionic liquid significantly change the acidity values of the mixture. The $H_0$ values for $\chi_{H[OTf]} \leq 0.030$ cannot be calculated as the mesityl oxide was not fully dissolved in the mixtures. Two separate layers were observed after leaving the sample for a while. Afterwards, starting from the $\chi_{H[OTf]} = 0.552$, the acidity of the system continued to increase up to the $\chi_{H[OTf]} = 0.905$. The highest $H_0$ values obtained for this system is -11.269. For the $0.552 \leq \chi_{H[OTf]} \leq 0.905$ region, the structure of the liquid changes to ionic liquid dissolved in acid rather than acid dissolved in the ionic liquid (at a lower concentration of acid added).[150] Thus, the $H_0$ values obtained are from the protonation of the mesityl oxide by the acid. The acidity measurements were done up to $\chi_{H[OTf]} = 1$. However, for the neat H[OTf], the $\Delta\delta^0$ value calculated are 82.317 which is beyond the maximum detection limit ($\Delta\delta^0_{max} = 80.91$) of the mesityl oxide indicator. Thus, the $H_0$ value of the neat H[OTf] cannot be measured using the $^{13}C$ NMR Probe.

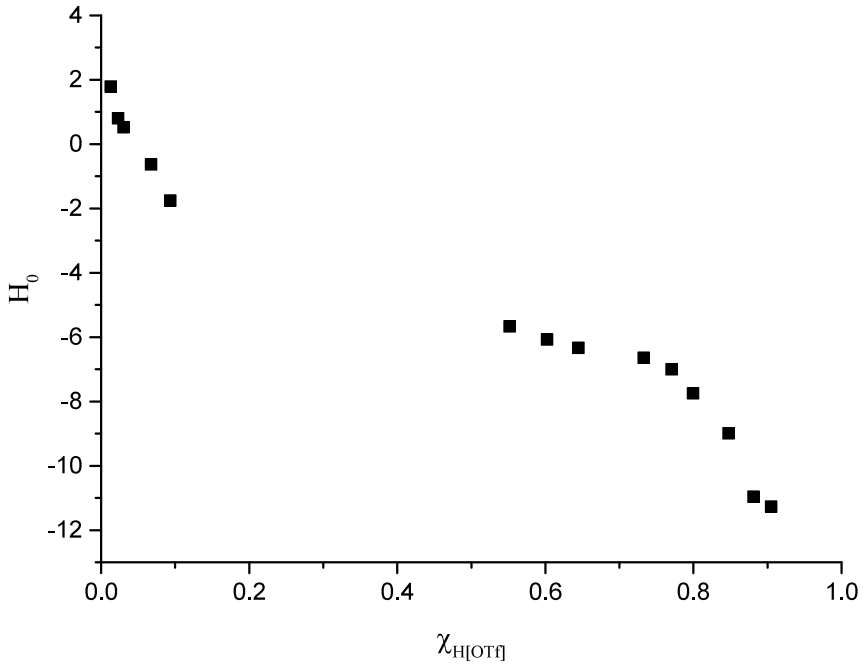



**Figure 2.4.4** – The $H_0$ values against the molar ratio $\chi_{H[OTf]}$ for the $[C_4C_1im][OTf]$-H[OTf] system

There were no data obtained from $0.100 \leq \chi_{H[OTf]} \leq 0.500$. Samples for these concentrations were actually prepared and sent for the $^{13}C$ NMR spectroscopy. However, in the NMR spectra collected for these mixtures, the peaks for mesityl oxide were too small for the $\Delta\delta$ of each mixture to be measured. Figure 2.4.5 to Figure 2.4.7 compares the $^{13}C$ NMR spectra for different $\chi_{H[OTf]}$ added into the ionic liquids. At the $\chi_{H[OTf]} = 0.0303$ (Figure 2.4.5) and 0.732 (2.4.7), all NMR peaks are clearly visible and all of the peaks can be easily assigned. Thus, the $\Delta\delta$ of these mixtures can be calculated and it is possible to calculate the $H_0$ values of this mixture. All of the peaks in the $^{13}C$ NMR spectra for $0.030 \leq \chi_{H[OTf]} \leq 0.093$ and $0.552 \leq \chi_{H[OTf]} \leq 0.905$ can be assigned and thus, the $H_0$ values can be calculated. Meanwhile, in the $\chi_{H[OTf]} = 0.100$ to $\chi_{H[OTf]} = 0.500$ range, the $\Delta\delta$ cannot be observed as the intensity of the mesityl oxide peaks were too low makes and it is impossible observe the chemical shift of C4 and C3.

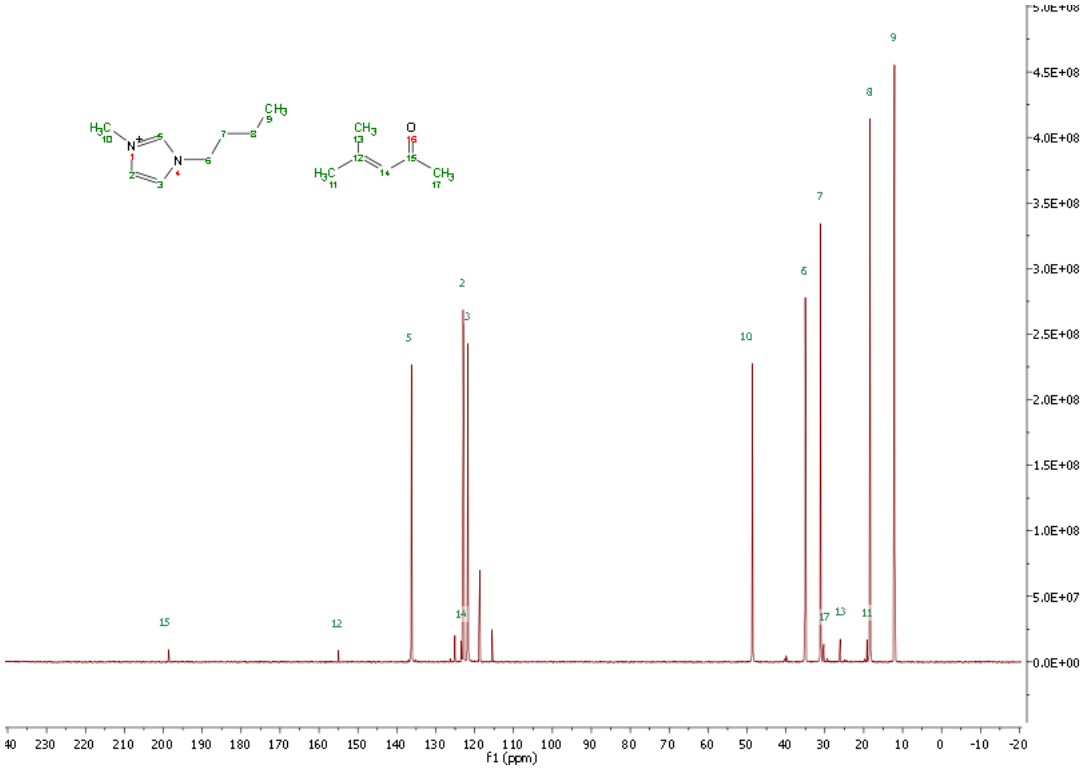



**Figure 2.4.5 –** $^{13}$C NMR spectrum for $[C_4C_1im][OTf] + \chi_{H[OTf]} = 0.0303 +$ mesityl oxide

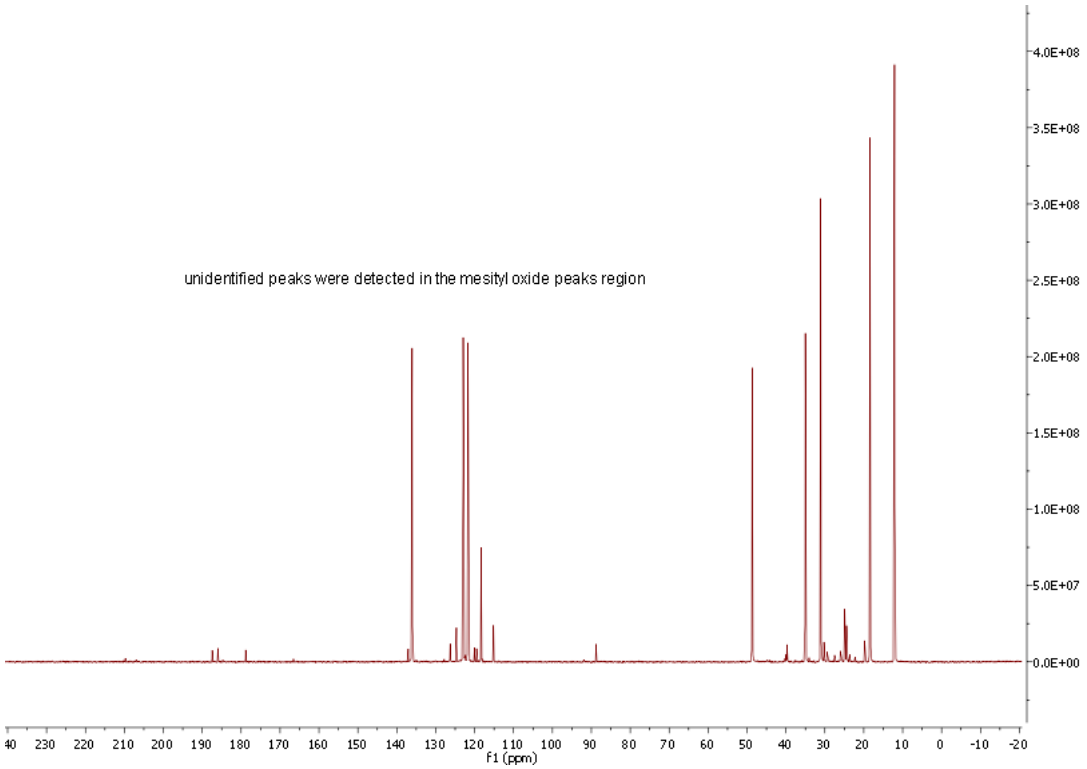



**Figure 2.4.6 –** $^{13}$C NMR spectrum for $[C_4C_1im][OTf] + \chi_{H[OTf]} = 0.300 +$ mesityl oxide

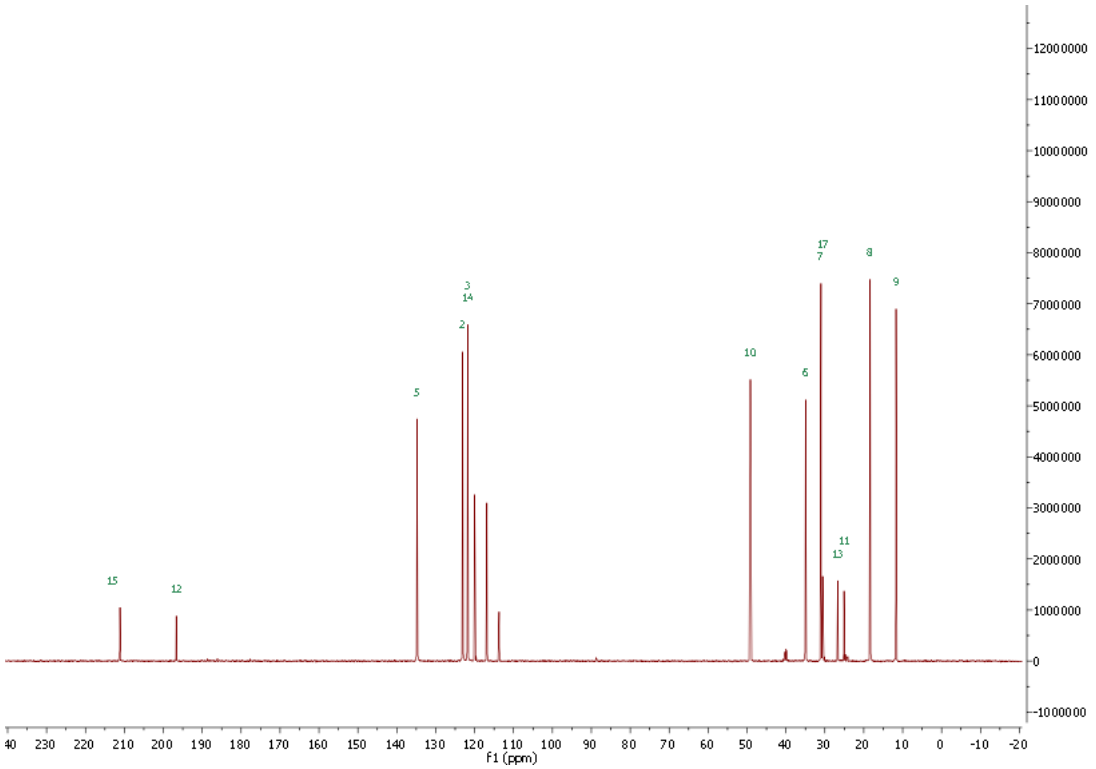



**Figure 2.4.7 –** $^{13}$C NMR spectrum for [$C_4C_1$im][OTf] + $\chi_{H[OTf]}$= 0.732 + mesityl oxide

Zhang *et al.* who measured the same [$C_4C_1$im][OTf]-H[OTf] system using the $^{13}$C NMR probe also only managed to measure the acidity of $0.500 \leq \chi_{H[OTf]} \geq 1.00$.[182] They also mentioned the difficulty in detecting the mesityl oxide probe in the $^{13}$C NMR spectra. Fărcaşiu and Ghenciu also reported on a similar problem in the $H_2O$-$H_2SO_4$ ssystem where they only managed to measure the $H_0$ values for $\chi_{H_2SO_4} \geq 0.523$.[169] However, Fărcaşiu and Ghenciu mentioned that the mesityl oxide was not dissolved in the mixture with $\chi_{H_2SO_4} < 0.523$. In these results, the mesityl oxide was completely dissolved in the mixture except $\chi_{H[OTf]} \leq 0.300$. Zhang *et al.* did not comment on solubility aspect / observation for the mesityl oxide in the [$C_4C_1$im][OTf]-H[OTf] mixture in the paper.[182]

Initially, it is assumed that the amount of mesityl oxide added was too low to be detected in this concentration. Additional experiments were done by increasing the amount of mesityl oxide in the mixture (10 - 18 wt%) for $\chi_{H[OTf]}$ from 0.007 to 0.600. It is normally expected that the acidity of the mixture will decrease as more

mesityl oxide is added in the mixture.[148] However, the aim of these measurements was to find out if the concentration of mesityl oxide added was not enough to be protonated by the strong acid, H[OTf]. Table 2.4.4 compiles the results for 0.042 $\leq \chi_{H[OTf]} \leq$ 0.190 with excess mesityl oxide added (10 - 18 wt%). By comparing the results with the 10-18 wt% of mesityl oxide added, the same trend was observed as with the results obtained with 1-8 wt% of mesityl oxide added (Figure 2.4.4) where the acidity increases as the $\chi_{H[OTf]}$ increases. However, as expected the $H_0$ values obtained from the 10 - 18 wt% mesityl oxide added is lower than the 1-8 wt% of mesityl oxide results. The mesityl oxide peaks were clearly observed in the $^{13}$C NMR spectra and make it possible to calculate the $H_0$ values. Also, the $H_0$ values for $\chi_{H[OTf]} \leq 0.030$ could not be calculated as the $\Delta\delta^0$ values obtained were lower than the minimum detection limit for the mesityl oxide probe. However, at 0.200$\leq \chi_{H[OTf]} \leq$ 0.600, it is difficult to observe and measure the $\Delta\delta$ of the mesityl oxide in this mixture.Thus, the initial assumption where the concentration of mesityl oxide is not enough to be protonated by the acid is invalid. It is assumed that the mesityl oxide decomposes at 0.200$\leq \chi_{H[OTf]} \leq$ 0.600.

There is a possibility that mesityl oxide completely reacted with the nucleophilic anion, $[OTf]^-$ explaining the disappearance of the mesityl oxide peak where mesityl oxide decomposes. The $[OTf]^-$ anion is a good nucleophile and it could completely react with the mesityl oxide to give 4-trifluoromethanesulfonate-4-methylpent-2-one (Fig. 2.4.8). Since both [$C_4C_1$im][OTf] and H[OTf] have the same anion, it is predicted that the anion of the ionic liquid itself reacted with the mesityl oxide instead of the anion from the acid. The assumption was made because the $H_0$ values can be started to be measured again from $\chi_{H[OTf]} \geq 0.552$ where the amount of acid is in excess over the amount of ionic liquid. Trang To reported on the decomposition of mesityl oxide in the [$C_4C_1$im][Cl] and HCl mixtures,[188] supporting the assumption that the $^{13}$C NMR method is not suitable when strong nucleophiles are present.

**Table 2.4.4** – $0.030 \leq \chi_{H[OTf]} \geq 0.093$

| $\chi_{H[OTf]}$ | $\Delta\delta^0$ | $H_0$ value |
|---|---|---|
| 0.007 | 30.705 | - |
| 0.010 | 30.725 | - |
| 0.021 | 30.922 | - |
| 0.031 | 31.038 | - |
| 0.042 | 31.670 | -0.44 |
| 0.055 | 31.752 | -0.31 |
| 00717 | 31.984 | -0.01 |
| 0.088 | 32.517 | -0.46 |
| 0.095 | 32.644 | -0.55 |
| 0.103 | 32.954 | -0.74 |
| 0.125 | 34.621 | -1.41 |
| 0.141 | 36.290 | -1.84 |
| 0.165 | 37.250 | -2.03 |
| 0.191 | 37.299 | -2.04 |

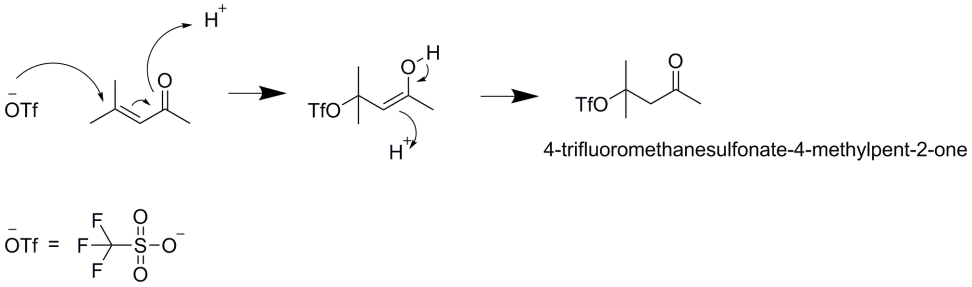



**Figure 2.4.8** – Decomposition of mesityl oxide in presence of [OTf]-

Mass spectrometry data of $[C_4C_1im][OTf]$-H[OTf] mixtures at different $\chi_{H[OTf]}$ were collected and presented in the Table 2.4.5 and Table 2.4.6. Clusters of the cations and the anions were detected in the negative mass spectra. In the negative mass spectra, $[CF_3SO_3]^-$ was observed, which possibly formed from the dissociation of the H[OTf] itself. There is no higher order cluster detected in either of the positive or negative mass spectra except for pure H[OTf]. $[CF_3SO_3]^-$ ion ion was detected in all the mixtures of $[C_4C_1im][OTf]$-H[OTf]. As the $[CF_3SO_3]^-$ ion was absence in the pure $[C_4C_1im][OTf]$ and H[OTf], the formation of $[CF_3SO_3]^-$ ion is thought to require both the $[C_4C_1im]^+$ cation and the presence of acid. Burba *et al.* reported that in a mixture of $[C_4C_1im][OTf]$-H[OTf] with lower concentrations of

acid, the cations from the ionic liquid take part in the stronger hydrogen-bonding interactions and the cation $\cdots$ $OTf^-$ is gradually replaced by the $H^+ \cdots$ $OTf^-$ as the triflic acid content is increased.[189] In the negative mass spectra, the intensity of the peak for the ion $[CF_3SO_3]^-$ is slightly increased at $\chi_{H[OTf]} = 0.289$ to 15% and decrease again to 10% at $\chi_{H[OTf]} = 0.495$. This can be explained by as the $\chi_{H[OTf]}$ increases, the hydrogen bonds between protons and triflate ions dominate the species and thus reducing the hydrogen bonds between the imidazolium cations and the triflate anions.

**Table 2.4.5 –** The positive mass spectra of $[C_4C_1im][OTf]$-H[OTf] : Detected ion fragments and their relative abundances

| $\chi_{H[OTf]}$ | Ions |
|---|---|
| 0 | $[C_4C_1im]^+$ (100 %) |
| 0.026 | $[C_4C_1im]^+$ (100 %), $[HC_1im]^+$ (5 %) |
| 0.102 | $[C_4C_1im]^+$ (100 %), $[HC_1im]^+$ (5 %) |
| 0.289 | $[C_4C_1im]^+$ (100 %), $[HC_1im]^+$ (5 %) |
| 0.495 | $[C_4C_1im]^+$ (100 %), $[HC_1im]^+$ (5 %) |
| 0.598 | $[C_4C_1im]^+$ (100 %), $[HC_1im]^+$ (5 %) |
| 0.852 | $[C_4C_1im]^+$ (100 %), $[HC_1im]^+$ (5 %) |
| 1 | $[CF_2S]^+$ (100%), $[CSO_2H]^+$ (75%), $[CF_2SO_2H]^+$ (35%), $[C_2F_6S_2O_4]^+$ (10%) |

**Table 2.4.6 –** The negative mass spectra of $[C_4C_1im][OTf]$-H[OTf] : Detected ion fragments and their relative abundances

| $\chi_{H[OTf]}$ | Ions |
|---|---|
| 0 | $[CF_3SO_3]^-$ (100%) |
| 0.026 | $[CF_3SO_3]^-$ (100%), $[SO_3]^-$ (20%), $[CF_3S]^-$ (10%), $[CF_3SO_3H]^-$ (10%) |
| 0.102 | $[CF_3SO_3]^-$ (100%), $[SO_3]^-$ (20%), $[CF_3S]^-$ (10%), $[CF_3SO_3H]^-$ (10%), $[CF_3S_2O_6H_2]^-$ (5%) |
| 0.289 | $[CF_3SO_3]^-$ (100%), $[SO_3]^-$ (25%), $[CF_3S]^-$ (15%), $[CF_3SO_3H]^-$ (15%), $[CF_3S_2O_6H_2]^-$ (5%) |
| 0.495 | $[CF_3SO_3]^-$ (100%), $[SO_3]^-$ (25%), $[CF_3S]^-$ (10%), $[CF_3SO_3H]^-$ (10%), $[CF_3S_2O_6H_2]^-$ (5%) |
| 0.598 | $[CF_3SO_3]^-$ (100%), $[SO_3]^-$ (25%), $[CF_3S]^-$ (10%), $[CF_3SO_3H]^-$ (10%) |
| 0.852 | $[CF_3SO_3]^-$ (100%), $[SO_3]^-$ (25%), $[CF_3S]^-$ (10%), $[CF_3SO_3H]^-$ (10%) |
| 1 | $[CF_3SO_3]^-$ (100%), $[SO_3]^-$ (25%), $[CF_3SO]^-$ (10%) |

The acidity of the $[C_4C_1im][OTf]$-H[OTf] mixtures are possible to be measured using the $^{13}C$ NMR probe at $0.030 \leq \chi_{H[OTf]} \leq 0.093$ and $0.552 \leq \chi_{H[OTf]} \leq 0.905$. In the next part, the acidity of a weak acid, $H_3PO_4$ dissolved in a $[C_4C_1im][Me_2PO_4]$ ionic liquid will be measured in order to collect more data on at less acidic acid than H[OTf] and $H[NTf_2]$.

### 2.4.3 The acidity measurements of $[C_4C_1im][Me_2PO_4]$-$H_3PO_4$ system

The next Brønsted acid-ionic liquid system measured was the $[C_4C_1im][Me_2PO_4]$-$H_3PO_4$ system. In this system, phosphoric acid, ($H_3PO_4$) replaced the conjugate acid of the ionic liquid anion, dimethyl phosphate $[C_2H_7O_4P]^-$. Phosphoric acid is cheaper and easily available compared to dimethyl phosphate. To date, the cost for 100 mg dimethyl phosphate is £40.40 which is not cost-effective compared to £87.20 for 100 g of phosphoric acid. It is possible to synthesise the dimethyl phosphate in the laboratory but further purification and more isolation steps are required in these methods because other compounds are also produced in the

reaction.[190, 191] This study aims to investigate whether the $^{13}C$ NMR probe is suitable for measuring the acidity of a weak acid. The $pK_a$ value for phosphoric acid is equal to 2.16[192], which widens the range of acidity to be measured in this study. The same preparation method was used to prepare the $[C_4C_1im][Me_2PO_4]$-$H_3PO_4$ mixtures.

Figure 2.4.9 shows the results for the $H_0$ values against different $\chi_{H_3PO_4}$ in the $[C_4C_1im][Me_2PO_4]$-$H_3PO_4$ mixtures. For this system, the $H_0$ values are obtained from the $0.609 \leq \chi_{H_3PO_4} \leq 0.952$ with the highest $H_0$ value = -5.141 at $\chi_{H_3PO_4} = 0.952$. The mesityl oxide was not fully dissolved in the mixtures with $\chi_{H_3PO_4}$ less than 0.550. As $[C_4C_1im][Me_2PO_4]$ is a viscous ionic liquid, it is almost impossible to mix the mesityl oxide with the $[C_4C_1im][Me_2PO_4]$-$H_3PO_4$ mixture at the lower concentration of acid in the room temperature. The mixtures are less viscous as the acid concentration is increased, allowing proper mixing between the mesityl oxide and the $[C_4C_1im][Me_2PO_4]$-$H_3PO_4$ mixtures. There is no $H_0$ value calculated for neat $H_3PO_4$ as it exists in solid form. The acid was observed to be not fully solubilised in the ionic liquids at $\chi_{H_3PO_4} \geq 0.970$. As expected, the $H_0$ values decrease with increasing acid concentration.

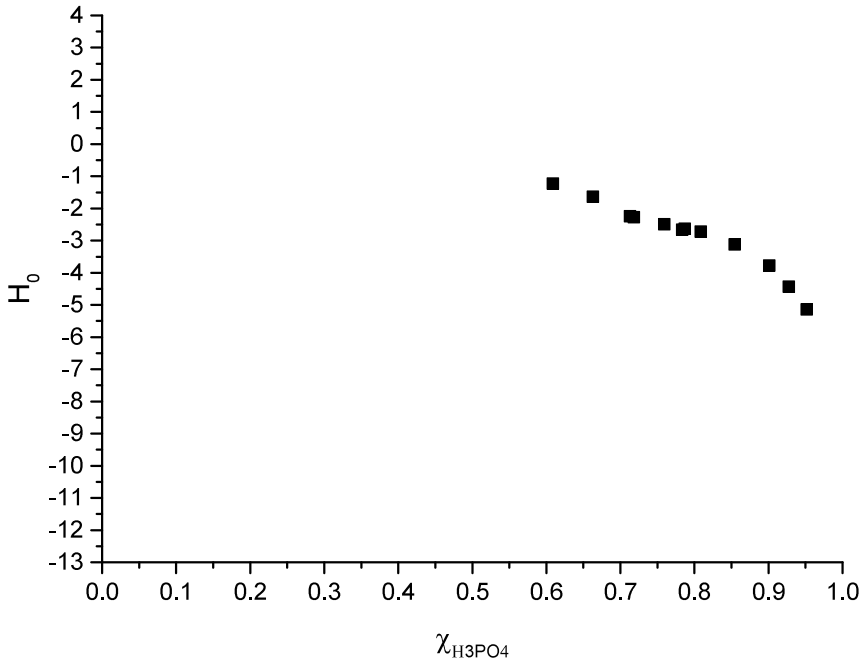



**Figure 2.4.9** – $H_0$ values vs. $\chi_{H_3PO_4}$ in the $[C_4C_1im][Me_2PO_4]$-$H_3PO_4$ mixtures

From the graph, a gradual increase in acidity was observed as the acid concentration increases. At lower concentration of acid added, the $H_3PO_4$ is diluted with the $[C_4C_1im][Me_2PO_4]$ ionic liquid, thus explaining the lower $H_0$ values obtained. The same trend was reported by Fadeeva *et al.* on the $H_0$ values of phosphoric acid solutions in N,N-dimethylformamide[166] using the UV-Vis probe where the acidity of the mixtures increased as the concentration of phosphoric acid in the mixture is increased. Phosphoric acid in its pure state in both crystalline structures forms dimers linked in polymeric chains.[193] Thus, the pure phosphoric acid molecules are bound into dimers which form polymer-like chains.[166] These polymer-like chains cause the pure phosphoric acid to be the most acidic and have highest protonation ability. Although there is no $H_0$ value recorded for pure phosphoric acid, in my study the highest $H_0$ value obtained at $\chi_{H_3PO_4}$ = -5.141. It is possible that dimers are formed in this mixture from the interaction of the anion from the ionic liquid and the acid and because there is more acid present in the system compared to the ionic liquid (also see mass spectrometry below). At lower concentration of acid

added, the ionic liquid ions were incorporated into the acid structure and thus lowers their proton donating ability. The proton donating ability was reduced due to the hydrogen bonding that is formed between the acid and the molecules of the ionic liquids. Thus, the acidity of the mixture is lowered as the proton donating ability is decreased.[166]

Mass spectrometry data were recorded on few samples with different ratio of molar concentration of phosphoric acid (Table 2.4.7 and Table 2.4.8 ). The mass spectra data for $\chi_{H_3PO_4} \leq 0.600$ were collected as well for comparison purpose even though it is not possible to measure the acidity of theses mixtures using the $^{13}$C NMR probe. In the positive mass spectra, clusters of the cations and anions were detected (for example $([HC_1im][H_2PO_4])^+$ and $([C_4C_1im][H_2PO_4]_2)^+$ in the mixtures of $[C_4C_1im][Me_2PO_4]$-$H_3PO_4$. On the other hand, clusters of $H_3PO_4$ and $[H_2PO_4]^-$ of up to $[H_{11}P_4O_{16}]^-$ from the phosphoric acid were observed in the negative spectra. No higher order clusters were seen in the mixtures with $\chi_{H_3PO_4}$ less than 0.48. These higher order cluster ions were present in the mixture with $\chi_{H_3PO_4}$ 0.578 and in the pure phosphoric acid. The negative mass spectra results support the proposed formation of dimers at higher concentration of acid mentioned above. The mass spectrometry results suggested that once the ratio of the concentration of acid added exceeds the concentration of ionic liquids, the higher order clusters ions were formed (for example, the ratio of IL:acid, 1:1.344, at $\chi_{H_3PO_4} = 0.578$). The higher order clusters between the $H_3PO_4$ and $[H_2PO_4]^-$ anions from the acid, is described as follows;

$H_3PO_4 + [H_2PO_4]^- \rightleftharpoons [H_5P_2O_8]^-$ or $[H_2PO_4(\ H_3PO_4)]^-$

$H_3PO_4 + [H_5P_2O_8]^- \rightleftharpoons [H_8P_3O_{12}]^-$ or $[H_2PO_4(\ H_3PO_4)_2]^-$

$H_3PO_4 + [H_8P_3O_{12}]^- \rightleftharpoons [H_8P_3O_{12}]^-$ or $[H_2PO_4(\ H_3PO_4)_3]^-$

The acidity measurements of the $[C_4C_1im][Me_2PO_4]$-$H_3PO_4$ system is possible using the $^{13}$C NMR probe with $\chi_{H_3PO_4}$ range from $0.609 \leq \chi_{H_3PO_4} \leq 0.952$. The mass spectra results obtained help to understand the reason behinds the increase in the acidity as the concentration of the acid is increased. Therefore, $^{13}$C NMR probe can be used to predict the acidity of weak acid but with limited acidity range.

**Table 2.4.7** – The positive mass spectra of $[C_4C_1im][Me_2PO_4]$-$H_3PO_4$ system : Detected ion fragments and their relative abundances

| $\chi_{H_3PO_4}$ | Ions |
|---|---|
| 0 | $[C_4C_1im]^+$ (100%) |
| 0.303 | $[C_4C_1im]^+$ (100%), $[HC_1im]^+$ (5%) |
| 0.482 | $[C_4C_1im]^+$ (100%), $[HC_1im]^+$ (5%) |
| 0.578 | $[C_4C_1im]^+$ (100%), $[HC_1im]^+$ (5%) |
| 0.755 | $[C_4C_1im]^+$ (100%), $[HC_1im]^+$ (5%) |
| 0.962 | $[C_4C_1im]^+$ (100%), $([HC_1im][H_2PO_4])^+$ (85%), $[HC_1im]^+$ (50%), $([C_4C_1im][H_2PO_4]_2)^+$ (30%) |
| 1 | $[H_3O_3P]^+$(100%), $[H_8O_7P_2]^+$(35%), $[H_{14}O_{16}P_4]^+$(5%) |

**Table 2.4.8** – The negative mass spectra of $[C_4C_1im][Me_2PO_4]$-$H_3PO_4$ system : Detected ion fragments and their relative abundances

| $\chi_{H_3PO_4}$ | Ions |
|---|---|
| 0 | $[Me_2PO_4]^-$ (100%),$[PO_3]^-$ (40%), $[PO_2]^-$ (10%) |
| 0.303 | $[Me_2PO_4]^-$ (100%), $[PO_3]^-$ (40%), $[PO_2]^-$ (15%) |
| 0.482 | $[Me_2PO_4]^-$ (100%), $[PO_3]^-$ (45%), $[PO_2]^-$ (15%) |
| 0.578 | $[Me_2PO_4]^-$ 100%), $[PO_3]^-$ (45%), $[PO_2]^-$ (15%), $[H_5P_2O_8]^-$ (10%) |
| 0.755 | $[Me_2PO_4]^-$ (100%), $[PO_3]^-$ (50%), $[PO_2]^-$ (15%), $[H_5P_2O_8]^-$ (20%) |
| 0.962 | $[H_8P_3O_{12}]^-$ (100%), $[H_5P_2O_8]^-$ (95%), $[H_{11}P_4O_{16}]^-$ (50%), $[H_2PO_4]^-$ (45%), $[PO_3]^-$ (40%), $[Me_2PO_4]^-$ (20%), $[PO_2]^-$ (5%) |
| 1 | $[PO_3]^-$ (100%), $[H_2PO_4]^-$ (60%), $[H_5P_2O_8]^-$ (35%), $[H_8P_3O_{12}]^-$ (25%), $[HPO_3]^-$ (20%), $[H_{11}P_4O_{16}]^-$ (10%) |

### 2.4.4 Discussion and Conclusions for $^{13}$C NMR Probe

Prior work has documented the acidity measurements of Brønsted acids-ionic liquids systems; $[C_4C_1im][NTf_2]$-H$[NTf_2]$ system and $[C_4C_1im][OTf]$-H[OTf] system using the UV-Vis[58] probe and $^{13}$C NMR probe[182] respectively. However, the studies of the acidity of $[C_4C_1im][NTf_2]$-H$[NTf_2]$ system reported was measured at low concentrations of H$[NTf_2]$ (maximum 0.337 M) with $H_0$ value = -5.05. Several indicators and trials were done to obtain the $H_0$ values. Gräsvik *et al.* reported on measuring the acidity of $[HSO_4]^-$ based ionic liquids with sulphuric acid using the $^{13}$C NMR probe.[147] The publications reported a single-step method of measuring the acidity of Brønsted acids-ionic liquids mixtures using one indicator that is capable of measuring acidity over a wide range of concentrations of acid. This method was applied to the $[HSO_4]^-$ but only $[HSO_4]^-$ based ionic liquids were used using this method.

In this study, the measurements of Hammett acidity function ($H_0$) of $[C_4C_1im][NTf_2]$-H$[NTf_2]$, $[C_4C_1im][OTf]$-H[OTf] and $[C_4C_1im][Me_2PO_4]$-$H_3PO_4$ were done using the $^{13}$C NMR probe. The $H_0$ values obtained are varies for each system. The acidity of $[C_4C_1im][NTf_2]$-H$[NTf_2]$ system was succesfully measured using this probe. With this probe, the range of $H_0$ values obtained are from 1 to -7, which shows an improvement from the previous literature which managed to calculate the $H_0$ values from -1 to -9. The acidities of both of the $[C_4C_1im][OTf]$-H[OTf] and $[C_4C_1im][Me_2PO_4]$-$H_3PO_4$ systems can also be measured using the using the $^{13}$C NMR probe. The highest acidity obtained in the $[C_4C_1im][OTf]$-H[OTf] system is -11.26 at $\chi_{H[OTf]} = 0.9$. Further acidity measurements were not possible as the $\Delta\delta^0$ obtained were over the maximum detection limit of the $^{13}$C NMR probe. The acidity of the $[C_4C_1im][Me_2PO_4]$-$H_3PO_4$ due to the insolubility of mesityl oxide at lower concentration of acid added. Mass spectra data were obtained for each system for further understanding of the acidity for each system.

The $H_0$ values obtained using the $^{13}$C NMR probe provided early insight on the scale of acidity for the Brønsted acids-ionic liquids mixtures and possibly other non-aqueous mixtures. In addition, this method only requires one indicator that capable on measuring from low to high $H_0$ values (0.938 to -11.81). The one step method shows an advantage over the long and arduous UV-Vis probe specifically

when measuring the acidity of [$C_4C_1$im][$NTf_2$]-H[$NTf_2$] system.[58] The results from this study proved that the $^{13}$C NMR probe is suitable for measuring other ionic liquids besides [$HSO_4$]$^-$ anion based ionic liquids as the method and calculation used in this study is based on the development and the calibration using the ionic liquids [$HSO_4$]$^-$ anion. Moreover, the extension to lower acidity range was also obtained, expanding the previously reported acidity range. The results achieved in this study verified that the $^{13}$C NMR probe is suitable for wide range of acidity from weak acids to superacids.

Unfortunately, some limitations are worth noting. The mesityl oxide did not dissolve at certain molar ratios of acid added especially at lower concentration of acid. Also, the mesityl oxide reacted with some of the mixture, causing the $\Delta\delta$ of the mesityl oxide to not be calculated. Further studies are suggested to find out the interaction between the mesityl oxide and the mixture.

## 2.5 The acidity measurements using the UV-Vis Probe

The acidity measurements of the Brønsted acids-ionic liquids systems were repeated using the UV-Vis probe. As mentioned in the Chapter 1, the UV-Vis probe is not a straightforward method and requires lots of trials for a successful measurements. The main difficulty in this method is choosing the right Hammett probe for each measurement as there are a lot of Hammett bases available with different $pK_{BH^+}$ values. The base could be either too strong or too weak for a particular solution. Usually the right base will have a $pK_{BH^+}$ value close to the $H_0$ value of the measured solution. An appropriate Hammett base or indicator (the one which exhibits the right $pK_{BH^+}$) and concentration of the Hammett base to provide an optimal absorbance are required in the Hammett acidity measurements. Generally, several dyes are required to complete full acidity measurements of one ionic liquid-acid system. In addition, the UV-Vis probe is very sensitive to any impurities as the Hammett probe used is in a very small concentration compared to the $^{13}$C NMR pobe. In this subchapter, the acidity of three different systems, [$C_4C_1$im][$NTf_2$]-H[$NTf_2$], [$C_4C_1$im][OTf]-H[OTf] and [$C_4C_1$im][$Me_2PO_4$]-

$H_3PO_4$ will be measured again using the UV-Vis probe. The aim of these experiments is to validate the results obtained from the $^{13}C$ NMR probe measured in the previous subchapter. Also, it is also to prove that by using the $H_0$ values for each mixtures from the $^{13}C$ NMR probe helps me to make an educated guess in choosing the right Hammett probe when measuring the acidity of ionic liquids-Brønsted acids mixtures using the UV-Vis probe. Moreover, it is expected that a lot of time and materials can be saved by choosing the right dye if the approximate $H_0$ value of the mixture is known in advance.

## 2.5.1 Experimental procedures

All sample preparations and measurements were done at room temperature, under inert $N_2$ atmosphere. UV spectra were recorded using a Perkin Elmer Lambda 25 spectrometer. Samples preparations can be found in the synthesis chapter.

### 2.5.1.1 Measurement of $\epsilon_0$ in non-acidic reference solution

The non-acidic solvent used for the Hammett bases is dichloromethane (DCM). Six data points of absorbance at $\lambda_{max}$ against concentration were collected for each of the Hammett bases used. The $\epsilon_0$ value (extinction coefficient)for each Hammett base is a gradient obtained from a plot of absorbance against concentration of the dye diluted in DCM (according to the Beer-Lambert Law).

### 2.5.1.2 Measurement of $\epsilon$ in Brønsted acid-ionic liquids mixtures

Six data points of absorbance at $\lambda_{max}$ against concentration were collected for each of the Hammett bases used. The $\epsilon$ value (the effective $\epsilon$ of the base) for each Hammett base is a gradient obtained from a plot of absorbance against concentration of the mixture. $H_0$ was calculated using eqn. 2.2.2 using the $\epsilon$ obtained.

## 2.5.2 Measurement of $\epsilon_0$ of Hammett bases in dichloromethane

Dichloromethane (DCM) was chosen because it offer advantages for Hammett acidity measurement due to its ability to dissolve all Hammett bases, the amount of water impurity is very low and it is not viscous and it is easy to handle. To

determine the $\epsilon_0$value, the concentrations of the solutions must be easily detectable by UV spectroscopy. According to the Beer-Lambert law, absorption will remain linear to the concentration as long as the concentration of the chromophore is lower than a certain threshold. Thus, any change of concentration is directly reflected in the change of absorbance. We need to assume that the extinction coefficient will remain the same for the unprotonated peak across different solutions. Six different concentrations of Hammett bases solutions in DCM were measured using the UV-Vis spectrometer. The absorbance obtained were plotted against the concentration of base used. Plot of absorbance against Hammett bases used in this study can be found in the Synthesis chapter. The slope of each graph was the calculated $\epsilon_0$ value of the probe. The slope of each graph was is the calculated$\epsilon_0$ value of the probe. Table 2.5.1 compiles the $\epsilon_0$ and the $pK_{BH^+}$ values for each probe. The $pK_{BH^+}$ values were obtained from the literature.[154]

**Table 2.5.1** – Extinction coefficients for Hammett bases in DCM

| Base | $pK_{BH^+}$ | $\epsilon_0$ | Standard error* | Error (%) |
|---|---|---|---|---|
| 3-nitroaniline | 2.47 | 347.03 | 9.45 | 0.02 |
| 4-nitroaniline | 1.00 | 10465.96 | 459.46 | 0.04 |
| 2-nitroaniline | -0.26 | 3855.46 | 173.89 | 0.03 |
| 4-chloro-2-nitroaniline | -0.97 | 4162.62 | 245.89 | 0.05 |
| 2,4-dichloro-6-nitroaniline | -3.01 | 5606.56 | 92.25 | 0.03 |
| 2,6-dichloro-4-nitroaniline | -3.27 | 13119.91 | 165.54 | 0.03 |
| 2,4-dinitroaniline | -4.27 | 11669.06 | 249.36 | 0.018 |
| 2,6-dinitroaniline | -5.37 | 1405.50 | 55.85 | 0.03 |
| 2-bromo-4,6-dinitroaniline | -6.46 | 2455.27 | 194.27 | 0.07 |
| 4-nitrotoluene | -11.35 | 2550.89 | 82.714 | 0.02 |

* Standard errors were obtained using regression analysis. The standard error referred to the errors of the gradient of the best-fit line of the plot of absorbance against the concentration of probe.

### 2.5.3 The acidity measurements of $[C_4C_1im][NTf_2]$-H$[NTf_2]$ system

The acidity measurements of $[C_4C_1im][NTf_2]$-H$[NTf_2]$ system were measured using the UV-Vis probe (Figure 2.5.1). The $H_0$ value for the neat $[C_4C_1im][NTf_2]$ is 1.99

using the 4-nitroaniline as UV-Vis probe. Previously, the $H_0$ value of the neat $[C_4C_1im][NTf_2]$ could not be calculated using the $^{13}C$ NMR probe due to the insolubility of mesityl oxide in the neat ionic liquid. The UV-Vis probe chosen to measure each mixture was decided based on the $H_0$ value obtained from the $^{13}C$ NMR probe. For example, at $\chi_{H[NTf_2]} = 0.322$, the $H_0$ value obtained from the $^{13}C$ NMR probe is -6.296. In the UV-Vis probe, the right base will have $pK_{BH^+}$ value close to the $H_0$ value of the measured solution. In the Table 2.5.1, 2-bromo-4,6-dinitroaniline has a $pK_{BH^+}$ value of -6.46. Thus, the 2-bromo-4,6-dinitroaniline was selected to measure the mixture at $\chi_{H[NTf_2]} = 0.306$. The $H_0$ value of mixture at $\chi_{H[NTf_2]} = 0.306$ calculated was -6.448. In this study, each of the mixtures are freshly prepared prior to the measurements (for both UV-Vis probe and $^{13}C$ NMR probe), hence the difference in $\chi_{H[NTf_2]}$ in each set of probe measurements.

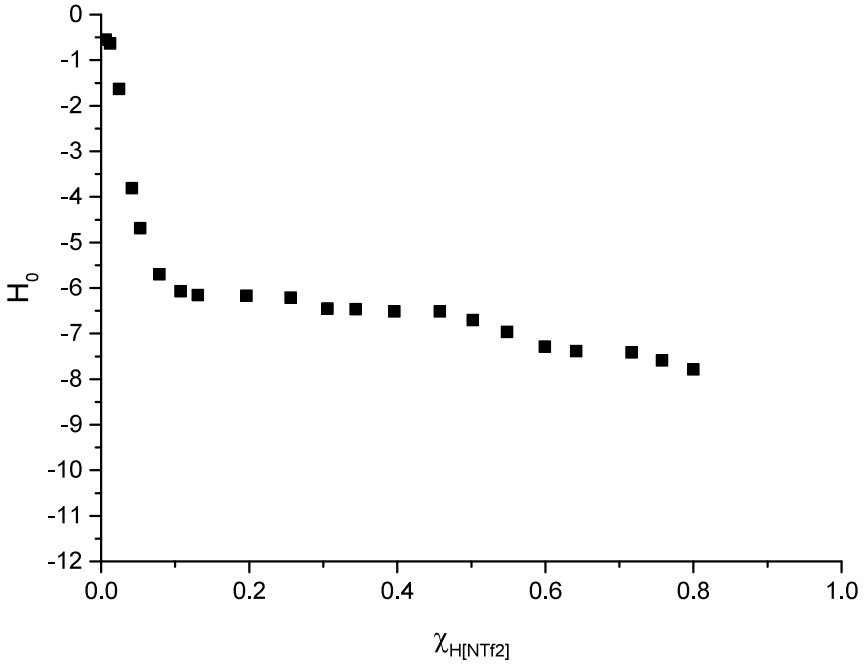



**Figure 2.5.1** – The $H_0$ values against the molar ratio $\chi_{H[NTf_2]}$ for the $[C_4C_1im][NTf_2]$-$H[NTf_2]$ system

**Table 2.5.2 –** List of dye used

| $\chi_{H[NTf_2]}$ | $H_0$ | Dye |
|---|---|---|
| 0 | 1.99 | 4-nitroaniline |
| 0.006 | -0.550 | 4-chloro-2-nitroaniline |
| 0.012 | -0.630 | |
| 0.024 | -1.628 | |
| 0.042 | -3.810 | 2,4-dichloro-6-nitroaniline |
| 0.053 | -4.685 | 2,6-dinitroaniline |
| 0.079 | -5.700 | |
| 0.107 | -6.067 | |
| 0.130 | -6.156 | |
| 0.196 | -6.171 | |
| 0.256 | -6.208 | |
| 0.306 | -6.448 | |
| 0.344 | -6.460 | 2-bromo-4,6-dinitroaniline |
| 0.396 | -6.510 | |
| 0.458 | -6.512 | |
| 0.502 | -6.703 | |
| 0.548 | -6.965 | |
| 0.599 | -7.282 | |
| 0.642 | -7.384 | |
| 0.716 | -7.409 | |
| 0.757 | -7.589 | |
| 0.800 | -7.784 | |

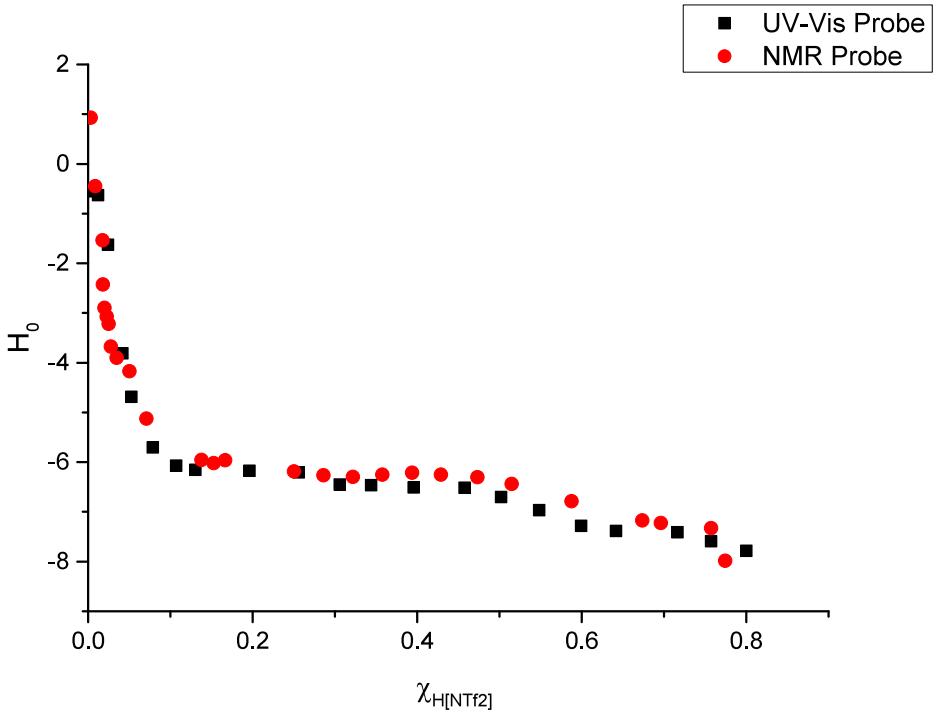



**Figure 2.5.2** – The $H_0$ values against the molar ratio $\chi_{H[NTf_2]}$ for the $[C_4C_1im][NTf_2]$-$H[NTf_2]$ system using the $^{13}C$ NMR Probe and UV-Vis Probe

Table 2.5.2 lists the dye used for each $[C_4C_1im][NTf_2]$-$H[NTf_2]$ mixtures at different $\chi_{H[NTf_2]}$ . In this system, four different Hammett probe were used to measure the acidity of $[C_4C_1im][NTf_2]$-$H[NTf_2]$ mixtures of $0 \leq \chi_{H[NTf_2]} \leq 0.79$. The results of the UV-Vis probe were then compared with the results obtained from the $^{13}C$ NMR Probe (Fig. 2.5.2). The results show both of the probes have good agreement with each other. There are differences in $H_0$ values observed starting from $\chi_{H[NTf_2]} > 0.05$, however the differences are small and did not deviate too much from each other. The results from the UV-Vis probe are usually less acidic than the NMR probe. As the Hammett probes used in the measurements are very sensitive to moisture and the $H[NTf_2]$ itself is very hygroscopic, it is possible that moisture from contact with air during the UV-Vis measurements has affected these results. It is worth to mention that all of the samples were prepared and transferred under nitrogen, however the UV-Vis measurements were done at ambient conditions

**Table 2.5.3 –** Calculation of the $H_0$ values for various concentrations of $H[NTf_2]$ in $[C_4C_1im][NTf_2]$[58]

| $\chi_{H[NTf_2]}$ | $H_0$ | Dye |
|---|---|---|
| 0 | - | 2,4-dinitroaniline |
| 0.012 | -3.35 | |
| 0.029 | -4.00 | |
| 0.062 | -4.35 | |
| 0.010 | -4.55 | |
| 0.130 | -4.70 | |
| 0.209 | -4.90 | |
| 0.337 | -5.05 | |

Data comparison with literature[58] were done with the acidity results with the results in this study. Thomazeau and co-workers measured the acidity of $[C_4C_1im][NTf_2]$-$H[NTf_2]$ mixtures using the UV-Vis probes. The results from the literature were compiled in Table 2.5.3. The author reported that initial measurements were done using 4-nitroaniline as a Hammett probe. However, the probe was found out to be fully protonated by the $H[NTf_2]$ where the acidity level is too high for the probe. 2.4-dinitroaniline was then used to measure the acidity of the mixtures prepared. They were able to collect the $H_0$ values of the prepared mixtures. Figure 2.5.3 compares the acidity of $[C_4C_1im][NTf_2]$-$H[NTf_2]$ mixtures obtained in this study and from Thomazeau *et al.* In my results, two different dyes with lower $pK_{BH^+}$ than 2,4-dinitroaniline were used (4-chloro-2-nitroaniline and 2,4-dichloro-6-nitroaniline) to measure the acidity at similar $\chi_{H[NTf_2]}$ with the report[58]. All of the probe were able to measured the mixtures, but my probe gave different $H_0$ values than 2,4-dinitroaniline. These results show that care is required to select the probe to be used to measure a mixture with a particular acidity. Overall, the results from the $^{13}C$ NMR Probe helps in selecting the right probe for the UV-Vis measurement. Moreover, lots of time is saved as finding the right dye can be skipped.

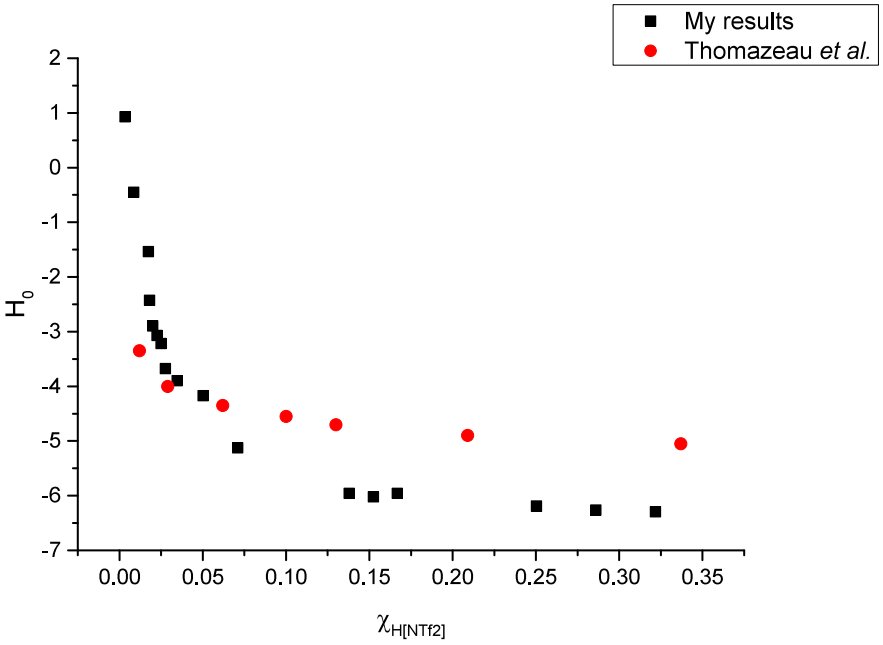



**Figure 2.5.3** – Comparison of data from Thomazeau *et al.*[58] and my results for $[C_4C_1im][NTf_2]$-$H[NTf_2]$ mixtures using the UV-Vis probe

### 2.5.4 The acidity measurements of [$C_4C_1$im][OTf]-H[OTf] system

The mixtures of the [$C_4C_1$im][OTf]-H[OTf] system were prepared and their acidity were measured using the UV-Vis probe. The results were compiled in the Figure 2.5.4. The acidity of the [$C_4C_1$im][OTf]-H[OTf] system was successfully measured for $\chi_{H[OTf]}$ between 0 to 1. Seven different probes were used for a complete set of measurements of the [$C_4C_1$im][OTf]-H[OTf] system (Table 2.5.4). Previously, in the $^{13}$C NMR Probe, there was a gap at $0.100 \leq \chi_{H[OTf]} \leq 0.500$ where mesityl oxide decomposes, and consequently the $H_0$ values could not be obtained. At this gap, the probe chosen was based on the $H_0$ range from -2 to -5. There are six different probes (2-nitroaniline, 4-chloro-2-nitroaniline, 2,4-dichloro-6-nitroaniline, 2,6-dichloro-4-nitroaniline, 2,4-dinitroaniline, 2,6-dinitroaniline) that have the $pK_{BH^+}$ from -2 to -5. At this step, several trials and error measurements were done to get the right dye.

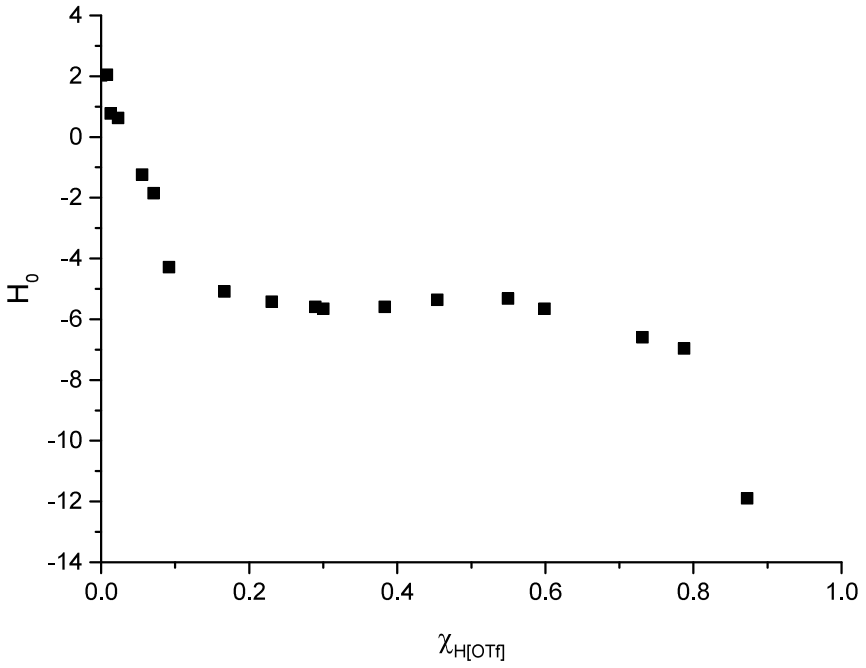



**Figure 2.5.4** – The $H_0$ values against the molar ratio $\chi_{H[OTf]}$ for the $[C_4C_1im][OTf]$-H[OTf] system

**Table 2.5.4** – List of dye used

| $\chi_{H[OTf]}$ | $H_0$ | Dye |
|---|---|---|
| 0 | 2.029 | 4-nitroaniline |
| 0.013 | 0.776 | |
| 0.023 | 0.631 | |
| 0.055 | -1.236 | 2-nitroaniline |
| 0.071 | -1.849 | 4-chloro-2-nitroaniline |
| 0.092 | -4.282 | 2,4-dinitroaniline |
| 0.166 | -5.084 | 2,6-dinitroaniline |
| 0.231 | -5.317 | |
| 0.289 | -5.353 | |
| 0.300 | -5.42 | |
| 0.383 | -5.453 | |
| 0.454 | -5.59 | |
| 0.550 | -5.587 | |
| 0.599 | -5.593 | |
| 0.645 | -5.649 | |
| 0.674 | -5.651 | |
| 0.731 | -6.595 | 2-bromo-4,6-dinitroaniline |
| 0.787 | -6.962 | |
| 0.836 | -7.542 | |
| 0.872 | -11.894 | 4-nitrotoluene |
| 0.892 | -12.482 | |
| 0.937 | -13.253 | |
| 0.969 | -13.579 | |
| 1 | -14.031 | |

The results from both of the UV-Vis probe and the $^{13}$C NMR Probe were compared in the Figure 2.5.5. Results from the graph show that the acidity obtained from both of the probes has a similar acidity except at χH[OTf] $>$ 0.77. During the measurements of $\chi_{H[OTf]}>$ 0.77, three probes were used; 2-bromo-4,6-dinitroaniline, 3-methyl-2,4,6-trinitroaniline and 4-nitrotoulene with $pK_{BH^+}$ = -6.46, -8.22 and -11.35 respectively. The results from the $^{13}$C NMR probe at $\chi_{H[OTf]}$= 0.823 has the $H_0$ = -7.65, hence 2-bromo-4,6-dinitroaniline probe were used at this concentration and at higher concentration. However, at 0.872 $\leq \chi_{H[OTf]} \leq$ 0.892, the 2-bromo-4,6-dinitroaniline was fully protonated by the mixture. Further trials were done by measuring the acidity of these mixtures using

the 3-methyl-2,4,6-trinitroaniline probe. Again, the probe is fully protonated and no $H_0$ values can be calculated. The results shows that 4-nitrotoluene is the most suitable probe to measure these mixtures. As the $H_0$ values of the neat H[OTf] is in agreement with the reference value, -14.10[170] it is safe to decide that the $H_0$ values obtained using the UV-Vis probe are more accurate than the $^{13}C$ NMR Probe.

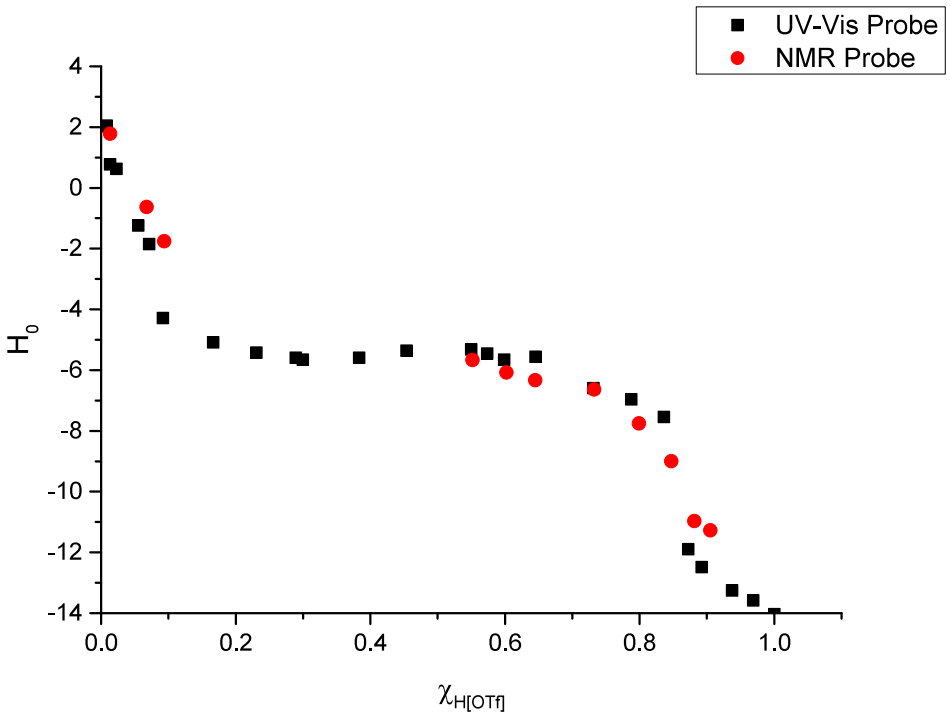



**Figure 2.5.5** – The $H_0$ values against the molar ratio $\chi_{H[NTf_2]}$ for the $[C_4C_1im][OTf]$-H[OTf] system using the $^{13}C$ NMR Probe and UV-Vis Probe

## 2.5.5 The acidity measurements of $[C_4C_1im][Me_2PO_4]$-$H_3PO_4$ system

The acidity measurements of the $[C_4C_1im][Me_2PO_4]$-$H_3PO_4$ system were measured using the UV-Vis probe. The $^{13}C$ NMR probe only managed to measure the acidity of this system at $\chi_{H_3PO_4}$ higher than 0.6 due to the insolubility of the probe in the mixture. In this system the acidity of the mixtures were measured

in reverse concentration ($\chi_{H_3PO_4}$ 1 to 0) due to the incomplete data from the $^{13}$C NMR probe and to avoid random guessing in choosing the right dye at lower $\chi_{H_3PO_4}$. The acidity of the $[C_4C_1im][Me_2PO_4]$-$H_3PO_4$ mixtures were successfully measured (Figure 2.5.6). As expected, the acidity increases as more acid added in the mixtures. Unfortunately there is no data for neat $[C_4C_1im][Me_2PO_4]$ as it cannot be measured using the most basic probe available (3-nitroaniline). It is assumed that the $H_0$ value of neat $[C_4C_1im][Me_2PO_4]$ would be greater than 3.543. In this system, five different probes were used to obtained a complete measurements (Table 2.5.5). Data comparison of both $^{13}$C NMR probe and UV-Vis probe were compiled in the Figure 2.5.7). At $0.645 \leq \chi_{H_3PO_4} \leq 0.811$, the results from both of the probes did not agrees very well. However, as mentioned in the $[C_4C_1im][OTf]$-H[OTf] system, it is decided that the $H_0$ values from the UV-Vis probe is far more accurate than the $^{13}$C NMR probe.

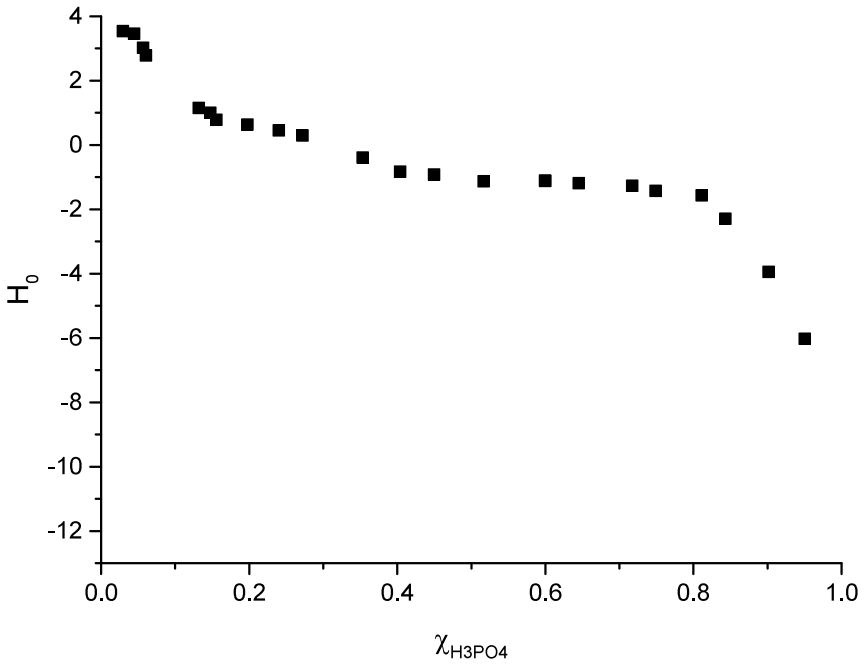



**Figure 2.5.6** – The $H_0$ values against the molar ratio $\chi_{H_3PO_4}$ for the $[C_4C_1im][Me_2PO_4]$-$H_3PO_4$ system

**Table 2.5.5 –** List of dye used

| $\chi_{H_3PO_4}$ | $H_0$ | Dye |
|---|---|---|
| 0.029 | 3.543 | 3-nitroaniline |
| 0.044 | 3.462 | |
| 0.057 | 3.027 | |
| 0.061 | 2.784 | |
| 0.132 | 1.150 | 4-nitroaniline |
| 0.147 | 1.004 | |
| 0.155 | 0.787 | |
| 0.197 | 0.635 | |
| 0.240 | 0.454 | |
| 0.272 | 0.297 | |
| 0.353 | -0.202 | |
| 0.404 | -0.829 | 2-nitroaniline |
| 0.450 | -0.915 | |
| 0.516 | -1.103 | |
| 0.600 | -1.130 | |
| 0.645 | -1.185 | |
| 0.717 | -1.264 | 4-chloro-2-nitroaniline |
| 0.749 | -1.426 | |
| 0.811 | -1.560 | |
| 0.843 | -2.290 | 2,6-dichloro-4-nitroaniline |
| 0.902 | -3.938 | |
| 0.950 | -6.028 | |

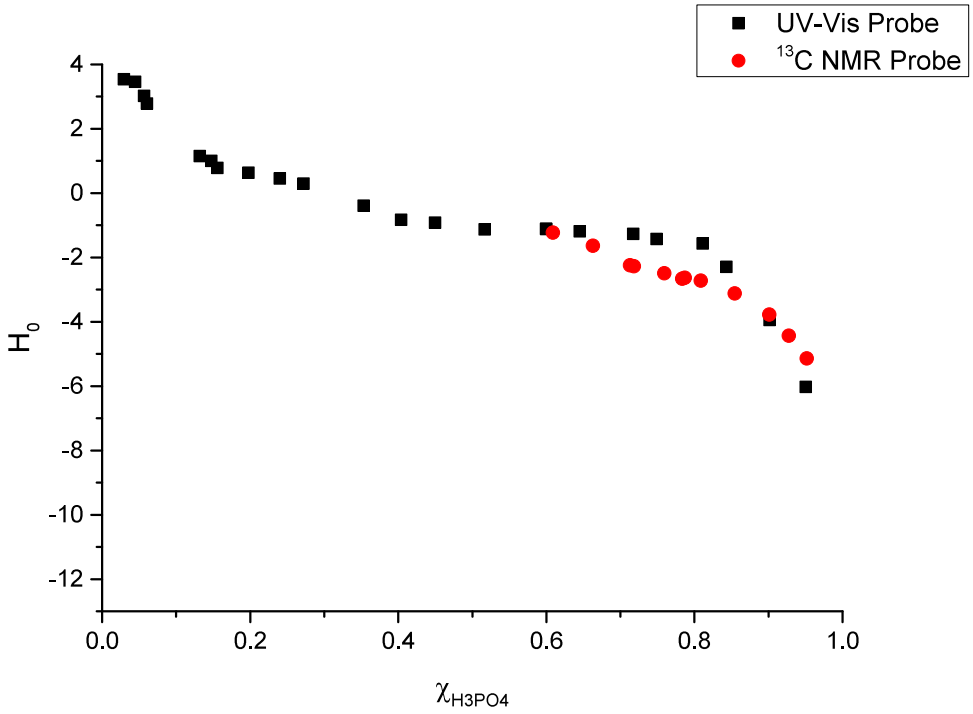



**Figure 2.5.7** – The $H_0$ values against the molar ratio $\chi_{H_3PO_4}$ for the $[C_4C_1im][C_4C_1im][Me_2PO_4]$-$H_3PO_4$ system using the $^{13}C$ NMR Probe and UV-Vis Probe

## 2.5.6 Discussion

The measurements of $H_0$ values of three different ionic liquids-Brønsted acids were done using the $^{13}C$ NMR Probe and UV-Vis Probe. The acidity of $[C_4C_1im][NTf_2]$-$H[NTf_2]$ mixtures were significantly affected with a small amount of acid added up to $\chi_{HNTf_2} = 0.1$. The $H_0$ values then remain constant or buffered at $0.138 \leq \chi_{H[OTf]} \leq 0.5$, suggesting that there is no formation of higher order clusters of $H[NTf_2]$. The $H[NTf_2]$ is dissolved in its molecular form and the same buffering trend has been observed in the same IL-acid system[150] and $H[NTf_2]$ in non-polar solvents.[183] Measurements of Gutmann Acceptor Numbers of the closely related ionic liquid-Brønsted acid mixture, $[C_2C_1im][NTf_2]$-$H[NTf_2]$ also support this conclusion.[150, 183] McCune *et al.* has noted that this buffering arises because the protonation of the IL anion yields the same acid $H[NTf_2]$. Thus, the acidity of the overall system is determined by the acidity of the $H[NTf_2]$ only.

In the [$C_4C_1$im][OTf]-H[OTf] system, addition of a small amount of acid causes an increase of the acidity of the mixture. A buffered or unchanging acidity was observed at $0.2 \leq \chi_{H[OTf]} \leq 0.65$. The buffering has been explained due to the formation of [OTf(HOTf)]$^-$ speciation.[150] Although there was no [OTf(HOTf)]$^-$ detected in the mass spectrometry results, the speciation has been detected in the [$C_2C_1$im][OTf]-H[OTf] mixture using Raman spectra.[189] The acid speciation formed that caused the buffering occurs due to the equation 2.5.1;

$$[A(HA)_x]^- + HA \rightleftharpoons [A(HA)_{x+1}]; \tag{2.5.1}$$

where A = [OTf]$^-$ and x = 0.2 to 0.65. Equation 2.5.1 explains the dynamic equilibria of the buffering trend where the equilibrium is strongly shifted to the right.[150] Further increases in acidity which deviated from the buffering may due to the presence of the pure acid.

In the [$C_4C_1$im][$Me_2PO_4$]-$H_3PO_4$ system, several steps of increase in the acidity were observed as $\chi_{H_3PO_4}$ is increased. The steps may be due to the polyprotic properties of the $H_3PO_4$ added. $H_3PO_4$ has more than one ionisable $H^+$ atom in its molecule. Thus, protons are lost in separate steps with one proton loss at each stage explaining the stepwise trend in the graph. $H_3PO_4$ and its higher order clusters were formed from the reactions of the acid when mixed with the [$C_4C_1$im][$Me_2PO_4$] ionic liquid. When more higher order clusters were present compared to the ionic liquid ions, the total acidity of the mixture increaes as more acid is added into the ionic liquids. The formation of higher order clusters of $H_3PO_4$ was confirmed with mass spectrometry results.

The acidity measurements of ionic liquids-Brønsted acids mixtures using the UV-Vis probe is well-known as an extremely arduous and time consuming method. Lots of trial and error is involved to obtain an acidity of a mixture. These difficulties are the reason why there are few data available for neat ionic liquids and ionic liquid-strong acid mixtures. A series of papers published by researchers from the Institut Francais du Petrole, France and Universite de Liege, Belgium from 2003 to 2009 report on the measurements of the acidity scale of Brønsted acids - ionic liquids systems.[58, 142, 143, 144] The researchers point out that the Hammett probe played an important role in measuring the acidity as two probes can give different

acidities for one mixture. In this study, the step of choosing the right probe was skipped as the $H_0$ values obtained from the the $^{13}C$ NMR probe has helped to make an intelligent selection of the right probe. The chosen probe is based on the $H_0$ values of each mixture where a probe with $pK_{BH^+}$ near to the $H_0$ of the solution will give the most reliable results. The acidity of $[C_4C_1im][NTf_2]$-H$[NTf_2]$, $[C_4C_1im][OTf]$-H[OTf] and $[C_4C_1im][Me_2PO_4]$-$H_3PO_4$ systems were successfully measured using the UV-Vis probe. Each of the systems requires five to seven probes to measure the $\chi_{acid}$ from 0 to 1.

The acidity measurements of the $[C_4C_1im][NTf_2]$-H$[NTf_2]$ system were easily done and did not require lots of trial and error as results from the $^{13}C$ NMR probe helped a lot in choosing the right dye. However, several trial and error were required in measuring the other two systems because of the incomplete results from the $^{13}C$ NMR probe. The comparison of published data[58] in the $[C_4C_1im][NTf_2]$-H$[NTf_2]$ system was also done with my results. In regards of this comparison, the data from this work are more reliable than the published work. In this work, the selection of probe was supported by the results from the $^{13}C$ NMR probe while in the published report, the author chose the indicator based on trial and error. The results for both probe in the $[C_4C_1im][NTf_2]$-H$[NTf_2]$ system agreed well with each other.

On the other hand, for $[C_4C_1im][OTf]$-H[OTf] and $[C_4C_1im][Me_2PO_4]$-$H_3PO_4$ there were noticeable differences in some of the data produced. The $H_0$ results calculated from the UV-Vis probe are expected to be more accurate than the $^{13}C$ NMR probe because of the big difference in the amount of concentration of probe added in each method. In the UV-Vis probe, the concentration of probe added into each of the Brønsted acid-ionic liquid mixture is very small amount, for example, 0.000311 M of 4-nitroaniline was added into the 2 mL of Brønsted acid-ionic liquid mixture. On the other hand, in the $^{13}C$ NMR probe, the concentration of mesityl oxide added is varied from 0.2446 to 1.278 M (1- 8 wt/wt%) in 0.5 mL of Brønsted acid-ionic liquid mixture. Even though the $H_0$ values from the $^{13}C$ NMR probe were calculated using the $\Delta\delta^0$ value obtained at infinite dilution of the indicator, the amount of probe added in the $^{13}C$ NMR probe are larger than the UV-Vis probe. The concentration of the $^{13}C$ NMR probe is high enough that it can contribute to the overall acidity of the system, so making it less acidic. The

results from the UV-Vis probe shows that the probe are able to measure a wide range of acidity where $H_0$ values can be calculated from 3.5 to -14.08. This is due to there being lots of Hammett probes that available compared to the single $^{13}C$ NMR probe.

## 2.6 Conclusions

The Hammett acidity measurements of three different systems were succesfully measured using both of the $^{13}C$ NMR probe and UV-Vis probe. In the $^{13}C$ NMR probe, the $H_0$ prediction was found out to be suitable for measuring the acidity of the whole $[C_4C_1im][NTf_2]$-H$[NTf_2]$ system. In contrast with $[C_4C_1im][OTf]$-H[OTf] and $[C_4C_1im][Me_2PO_4]$-$H_3PO_4$ systems, full measurements could not be achieved due to the decomposition of mesityl oxide and/or insolubility of the mesityl oxide in the mixtures. An extension of the acidity scale at lower $H_0$ was obtained to 4 compared to the reported literature ($H_0$ = -1). The single probe used in the $^{13}C$ NMR method saved a lot of time compared to the UV-Vis probe. In this chapter, the results from the $^{13}C$ NMR probe were used as a reference value in choosing the right indicator for the UV-Vis probe. The acidity measurements of the three systems were repeated using the UV-Vis probe. The purpose of these experiments was to validate the results obtained from the $^{13}C$ NMR probe. Also, the repeated measurements was also done to solve the long-time problem in the UV-Vis method of choosing a right probe.

Successful measurements for all of the systems were demonstrated using the UV-Vis probe. In these measurements a wide acidity scale was demonstrated using five to seven probes. With the estimation of $H_0$ values from the $^{13}C$ NMR probe, a suitable probe was chosen and used to measure each mixture. Disagreements of data were found, however the data from the UV-Vis probe are more accurate than from the $^{13}C$ NMR probe. It is important to mention that the $^{13}C$ NMR probe can be used to calculate the acidity of the mixtures qualitatively while UV-Vis probe gave a more accurate and reliable results. Nevertheless, thanks to the data from the $^{13}C$ NMR probe, it has saved a lot of time and less experiments were required in measuring the acidity of the Brønsted acid-ionic liquids mixtures in the UV-Vis probe.

# Chapter 3

# Acidity Measurements of Brønsted acids in ionic liquids with different conjugate bases

## 3.1 Aims and Objectives

The study of the acidity measurements of Brønsted acid-ionic liquids mixtures were further continued in this chapter. Previously, the acidity of Brønsted acid-ionic liquids systems were successfully done using the $^{13}C$ NMR probe and the UV-Vis probe. The Brønsted acids used had the same anion as the ionic liquids themselves. In these systems, equilibrium exists between the anion of the ionic liquid and the acid. Since the anion of the ionic liquids is the conjugate base of the acid, both of the left and right hand sides of the equilibrium are identical. Thus, the ionic liquids will possess no buffering ability. As more acid is added into the ionic liquids, the acid will either form higher order clusters with the anion of the ionic liquids or stay intact together. This explains the correlations between the concentrations of acids and the $H_0$ values.

In this chapter, the acidity of Brønsted acids-ionic liquids systems were done with different conjugate acids or anionic species. Each of these ionic liquids: $[C_4C_1im][NTf_2]$, $[C_4C_1im][OTf]$, $[C_4C_1im][HSO_4]$ and $[C_4C_1im][Me_2PO_4]$ will be mixed with Brønsted acids with different conjugate bases ($H[NTf_2]$, $H[OTf]$, $H_2SO_4$

and $H_3PO_4$) which will produce 11 different systems. There were no data collected for $[C_4C_1im][NTf_2]$-$H_3PO_4$ as the acid was not dissolved in the ionic liquid at all. The $^{13}C$ NMR probe was selected as a probe to measure the acidity of these systems as $^{13}C$ NMR spectroscopy has successfully managed to give good $H_0$ values of the acidity of the Brønsted acids-ionic liquids mixtures. Also, since the $^{13}C$ NMR probe method is a single step method, lots of time will be saved compared to the UV-Vis probe. It is expected that the $^{13}C$ NMR probe would not be able to measure the complete systems ($\chi_{acid}$ from 0 to 1) based on the results from the previous chapter. Any gap obtained will be filled with data measured using the UV-Vis probe in order to get complete data for each system.

Literature on measuring the acidity of Brønsted acids-ionic liquids systems was found in several papers.[58, 142, 143, 182] All of the papers used $^{13}C$ NMR probe except the paper published by Zhang *et al.*,[182] where the author used the $^{13}C$ NMR probe. The author reported on measuring the acidity of $[C_4C_1im][HSO_4]$ and $[C_4C_1im]$[TFA] with H[OTf]. Since the paper was published during the data collection time, the data collected for the $[C_4C_1im][HSO_4]$-H[OTf] system will still be presented in this thesis.

The aim of this study is to investigate how far the ionic liquids can affect the acid strength as each ionic liquid and acid mixture has a very different acid strength. Also, this study is expected to expand the application of the $^{13}C$ NMR probe in measuring the acidity of Brønsted acids-ionic liquids systems.

## 3.2 Acidity measurements of $[C_4C_1im][NTf_2]$ with different acids

The $[C_4C_1im][NTf_2]$ ionic liquid was mixed with three different acids, H[OTf], $H_2SO_4$ and $H_3PO_4$. Only $H_3PO_4$ did not dissolve at all in the $[C_4C_1im][NTf_2]$. The acidities of both of the $[C_4C_1im][NTf_2]$-H[OTf] and $[C_4C_1im][NTf_2]$-$H_2SO_4$ systems were measured using the $^{13}C$ NMR probe. Sample preparations were done using the standard procedure for the $^{13}C$ NMR probe.

### 3.2.1 [$C_4C_1$im][$NTf_2$]-H[OTf] system

Figure 3.2.1 shows the $H_0$ values plotted against the $\chi_{H[OTf]}$. A anticipated, the acidity increases as more is acid added into the ionic liquid. At lower concentrations of acid added, $\chi_{H[OTf]} < 0.08$, a gradual linear in decrease of $H_0$ values was observed. Since [$C_4C_1$im][$NTf_2$] has low acidity ( $H_0 = 1.99$), the acidity increased rapidly as more $\chi_{H[OTf]}$ was added into the ionic liquid. A noticeable increase in acidity can be observed at $\chi_{H[OTf]} = 0.079$ and 0.0912 where the $H_0$ values for each of the mixtures are -2.819 and -5.753 respectively. Between $\chi_{H[NTf_2]} = 0.0912$ and 0.755, the $H_0$ values remained buffered or increases with only a slight difference. Afterwards, the acidity increrases up to $\chi_{H[OTf]} = 0.914$. Further increase in the $\chi_{H[NTf_2]}$ could not be measured as the $\Delta\delta^0$ exceeds the maximum detection limit of the $^{13}$C NMR probe.

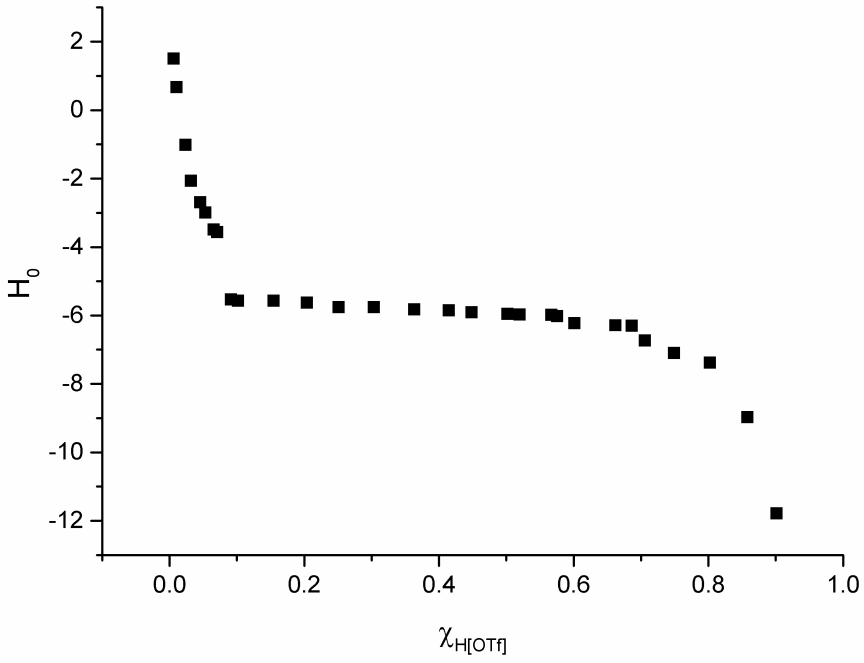



**Figure 3.2.1** – The $H_0$ values against the $\chi_{H[OTf]}$ for the [$C_4C_1$im][$NTf_2$]-H[OTf] system

Mass spectrometry data were recorded for the [$C_4C_1$im][$NTf_2$]-H[OTf] mixtures

with different $\chi_{H[OTf]}$. In the positive mass spectra, clusters of the cations and the anions was detected, notably $([C_4C_1im]\cdot F)^+$ clusters. The fragmentations are the same as found in the $[C_4C_1im][NTf_2]$-H$[NTf_2]$ systems. There were no higher order of H[OTf] containing clusters detected even at higher $\chi_{H[OTf]} = 0.904$. In the negative mass spectra, the $[(CF_3SO_2)N]^-$ ion fragments were found to be present at highest intensity (Table 3.2.1). The $[(CF_3SO_2)N]^-$ion from the ionic liquid were found to be the highest abundance even at the highest $\chi_{H[OTf]}$ added. The abundance of $[CF_3SO_3]^-$ ion from the H[OTf] was increased up 15% for $\chi_{H[OTf]} > 0.690$. There were no higher order clusters detected in these systems.

**Table 3.2.1 –** The negative mass spectra of $[C_4C_1im][NTf_2]$-H[OTf] : Detected ion fragments and their relative abundance

| $\chi_{H[OTf]}$ | Ions |
|---|---|
| | $[(CF_3SO_2)_2N]^-$ (100%) |
| 0.03 | $[(CF_3SO_2)_2N]^-$ (100%), $[(CF_3SO_2)_2NH]^-$ (10%), $[CF_3SO_3]^-$ (5%), $[NSO_2]^-$ (5%) |
| 0.065 | $[(CF_3SO_2)_2N]^-$ (100%),$[(CF_3SO_2)_2NH]^-$ (10%), $[CF_3SO_3]^-$ (10%), $[NSO_2]^-$ (5%) |
| 0.445 | $[(CF_3SO_2)_2N]^-$ (100%), $[(CF_3SO_2)_2NH]^-$ (10%), $[CF_3SO_3]^-$ (10%), $[NSO_2]^-$ (5%) |
| 0.695 | $[(CF_3SO_2)_2N]^-$ (100%), $[(CF_3SO_2)_2NH]^-$ (10%), $[CF_3SO_3]^-$ (15%), $[NSO_2]^-$ (5%) |
| 0.854 | $[(CF_3SO_2)_2N]^-$ (100%), $[(CF_3SO_2)_2NH]^-$ (10%), $[CF_3SO_3]^-$ (15%), $[NSO_2]^-$ (5%) |
| 1 | $[CF_3SO_3]^-$ (100 %), $[CF_3SO_3H]^-$(15%), $[SO_3H]$ (5%) |

### 3.2.2 $[C_4C_1im][NTf_2]$-$H_2SO_4$ system

The acidity of the $[C_4C_1im][NTf_2]$-$H_2SO_4$ system was measured and the data were presented in Figure 3.2.2. The acid did not dissolve in the ionic liquid at $\chi_{H_2SO_4} > 0.700$. For $0.09 \leq \chi_{H_2SO_4} \leq 0.263$, the acidity of the mixture increases gradually as more acid is added into the ionic liquid. Upon further increase in the $\chi_{H_2SO_4}$ up to 0.700, the increase in the acidity is not noticeable. The results were not as seen in the $[C_4C_1im][HSO_4]$-$H_2SO_4$ system, where the acidity increases linearly with increasing molar ratio of acid added. The highest $H_0$ values obtained is -6.41

at $\chi_{H_2SO_4} = 0.0673$. As the $H_0$ value of neat $H_2SO_4$ is -11.98, it is expected that the acidity of the $[C_4C_1im][HSO_4]$-$H_2SO_4$ at $\chi_{H[OTf]} = 0.673$ will be higher than -6.41. The levelling effect was observed in this mixture. Since the $[C_4C_1im][NTf_2]$ ionic liquids has weak acidity properties, it levels down the acidity of the $H_2SO_4$ in the mixtures of $[C_4C_1im][NTf_2]$-$H_2SO_4$ system. The results explain the absence of higher order cluster of $H_2SO_4$ in the mass spectrometry results. Clusters of the cations and the anions, $([C_4C_1im]\cdot F)^+$ was detected in the positive mass spectra in the mixtures of this system. In the negative mass spectra, ions from the ionic liquids; $[(CF_3SO_2)N]^-$, $[(CF_3SO_2)_2NH]^-$ and $[(CF_3SO_2)_2N]^-$ were found in the highest abundance up to $\chi_{H[OTf]} = 0.700$. Most of the relative abundance of $[HSO_4]^-$ ion was less than 10%.

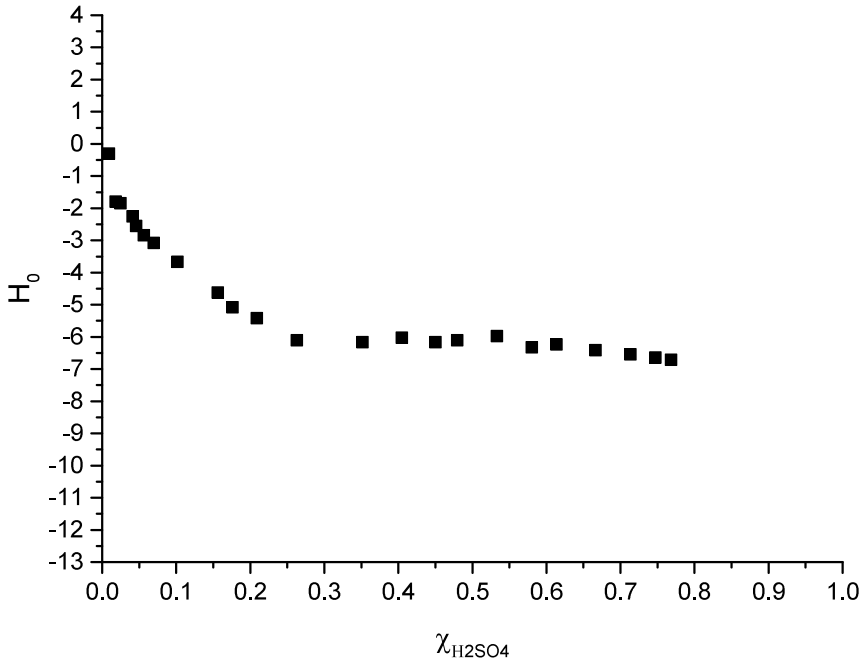



**Figure 3.2.2** – The $H_0$ values against the $\chi_{H_2SO_4}$ for the $[C_4C_1im][NTf_2]$-$H_2SO_4$ system

The acidity results for $[C_4C_1im][NTf_2]$ with three different acids; $H[NTf_2]$, H[OTf] and $H_2SO_4$ were compiled in Figure 3.2.3 to understand the effect of the

acidity of each acid when mixed with the ionic liquid. At lower $\chi_{acid}$, the acidity increases until $\chi_{acid} < 0.200$. As all of the three acids used in the measurements are extremely acidic, it is expected that the acidity of the mixtures increases as more acid added into the ionic liquid. With further increase in the molar ratio of acid up to 0.500, the acidity remains constant which diminishes the difference in acidity at lower concentration. This suggest that there are no cluster formed in this range, and the acids are dissolved in its molecular forms.[150] The acidities for H[OTf] and $H_2SO_4$ added in to $[C_4C_1im][NTf_2]$ remain constant up to $\chi_{acid} = 0.650$ while in the $[C_4C_1im][NTf_2]$-H$[NTf_2]$, the acidity of the mixtures increases with increasing molar ratio of the acid. In the $[C_4C_1im][NTf_2]$-H$[NTf_2]$ system, the left and right side of the equilibrium are identical, thus the ionic liquid did not have any buffering ability that will affect the acidity of the mixtures. In contrast, in the ionic liquid mixture containing different conjugate acid, the acidity of the mixture was levelled down by the ionic liquid. In the $[C_4C_1im][NTf_2]$-H[OTf] system, at $> 0.68$, the acidity increases gradually again. At this point, the structures of the mixture changes from acid dissolved in ionic liquid to ionic liquid dissolved in acid.

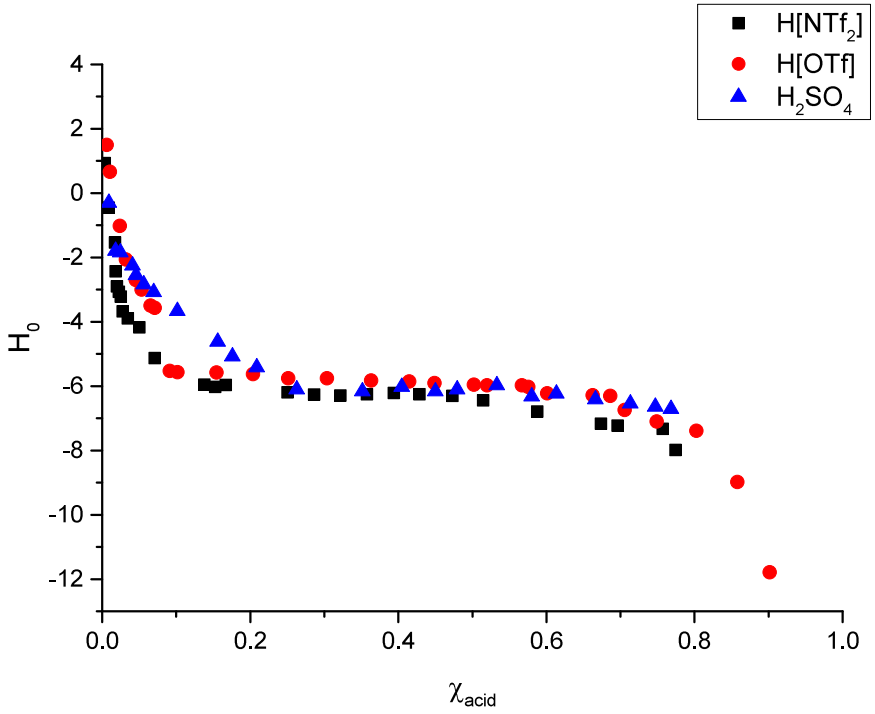



**Figure 3.2.3** – The $H_0$ values against the $\chi_{acid}$ mixed with [$C_4C_1$im][$NTf_2$]

## 3.3 Acidity measurements of [$C_4C_1$im][OTf] with different acids

### 3.3.1 [$C_4C_1$im][OTf]-H[$NTf_2$] system]

The results for the acidity measurements of [$C_4C_1$im][OTf]-H[$NTf_2$] systems are shown in Figure 3.3.1. The results show that the acidity increases as the $\chi_{H[NTf_2]}$ increased. However, for $0.80 \leq \chi_{H[NTf_2]} \leq 1.00$ and because the mesityl oxide did not dissolve completey in the mixtures. In the $^{13}$C NMR spectra for $0.0751 \leq \chi_{H[NTf_2]} \leq 0.186$, there were no data collected because in the $^{13}$C NMR spectra, there are no mesityl oxide peaks detected or if any is detected, the concentration would be too small. To fill in the gap in this system, the acidity of the mixtures were measured using the UV-Vis probe (Figure 3.3.2).

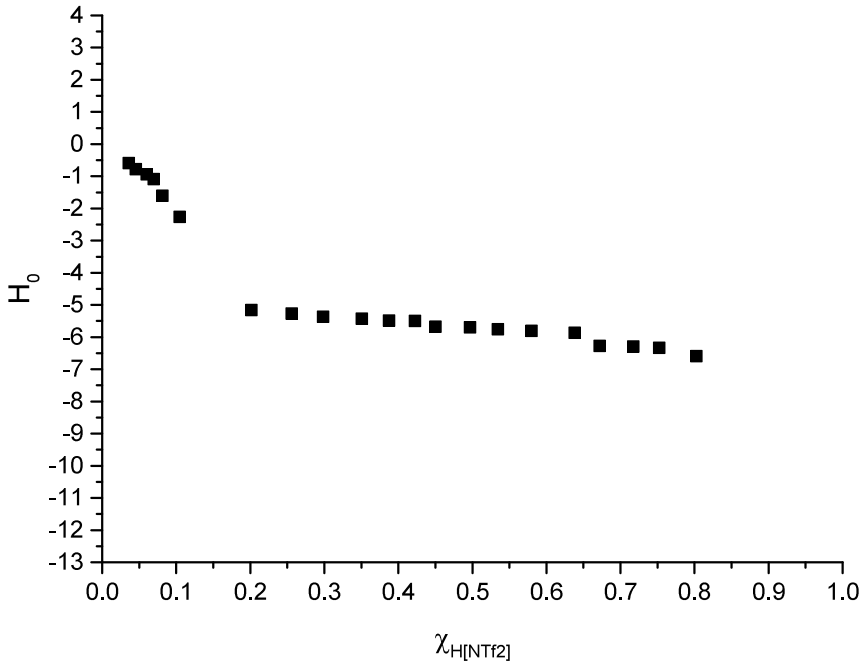



**Figure 3.3.1** – The $H_0$ values against the $\chi_{H[NTf_2]}$ for the $[C_4C_1im][OTf]$-$H[NTf_2]$ system

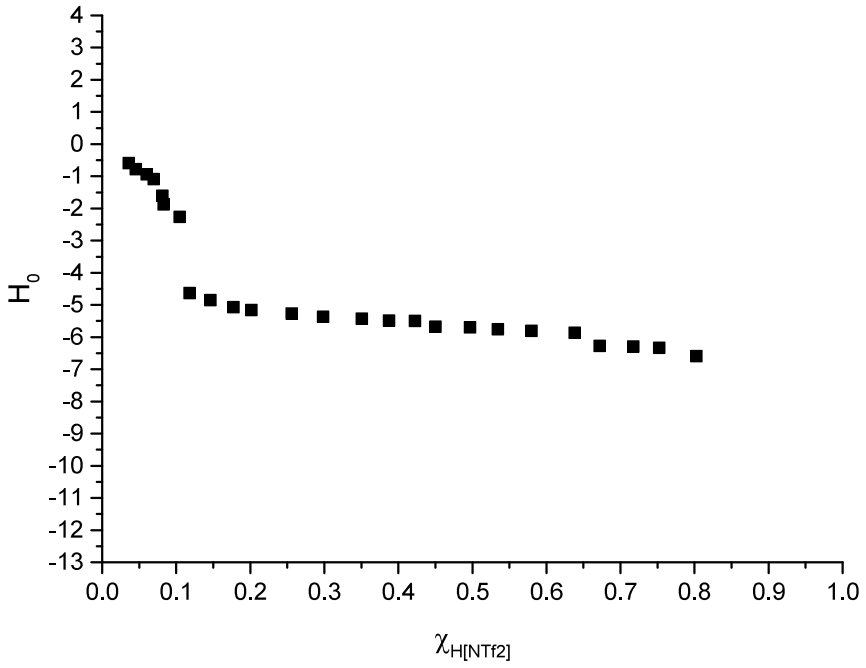



**Figure 3.3.2** – The $H_0$ values against the $\chi_{H[NTf_2]}$ for the [$C_4C_1$im][OTf]-H[$NTf_2$] system (results combined from the $^{13}C$ NMR probe and UV-Vis probe)

The results show that the acidity of the mixture increases gradually as more acid is added into the ionic liquid until $\chi_{H[NTf_2]}$ up to 0.200. There is a huge difference in the $H_0$ values between $\chi_{H[NTf_2]}$ = 0.082 and 0.102, where the values = -1.873 and -4.85. Initially, 4-chloro-2-nitroaniline was used as probe in both of the mixtures. However, at $\chi_{H[NTf_2]}$ = 0.102, the probe was fully protonated by the mixture, and no $H_0$ value can be calculated. The mixture was then measured using the 2,4-dichloro-6-nitroaniline which has $pK_{BH^+}$ = -3.01, but it is full protonated as well. The 2,6-dichloro-4-nitroaniline probe was the used to replace the previous probe and the probe was found to be suitable to measure the acidity of this mixture. It is safe to say that the $H_0$ value for the $\chi_{H[NTf_2]}$ = 0.102 is correct since several trials were done using three different probe. Further increase in the $\chi_{H[NTf_2]}$ increased the acidity but not at any significant amount. The highest $H_0$ value obtained is -6.58 at $\chi_{H[NTf_2]}$ = - 0.826. At this point, the acidity measured is based on the acidity of the acid instead of the ionic liquids.

Mass spectrometry results were collected for this system. In the positive mass spectra, clusters from the cations and the anions were detected *i.e* $([C_4C_1im]\cdot F)^+$. The fragmentations are the similar to those found in the $[C_4C_1im][NTf_2]$-$H[NTf_2]$ systems. There were no higher order of $H[NTf_2]$ containing clusters detected even at higher $\chi_{H[NTf_2]} = 0.826$. The absence of higher order clusters in any of the $H[NTf_2]$ solutions is because the $[NTf_2]^-$ anion is a poor H-bond acceptor and thus, $H[NTf_2]$ only existed in its molecular form or undergoes dissociation.[150] The dissociation of the $H[NTf_2]$ into $H^+$ and the $[NTf_2]^-$ can be supported in the negative mass spectra results (Table 3.3.1). In this system, the $[(CF_3SO_2)N]^-$ ion was observed with highest abundance in each mixture up to highest $\chi_{H[NTf_2]}$.

**Table 3.3.1** – The negative mass spectra of $[C_4C_1im][OTf]$-$H[NTf_2]$ : Detected ion fragments and their relative abundance

| $\chi_{H[NTf_2]}$ | Ions |
|---|---|
| 0 | $[CF_3SO_3]^-$ (100 %) |
| 0.010 | $[(CF_3SO_2)_2N]^-$(100%), $[(CF_3SO_2)_2NH]^-$(20%), $[CF_3SO_3]^-$ (30 %), $[CF_3SO_3H]^-$ (5 %), $[SO_2N]^-$ (5 %) |
| 0.051 | $[(CF_3SO_2)_2N]^-$(100%), $[(CF_3SO_2)_2NH]^-$(10%), $[CF_3SO_3]^-$ (5 %), $[CF_3SO_3H]^-$ (5 %), $[SO_2N]^-$ (5 %) |
| 0.132 | $[(CF_3SO_2)_2N]^-$(100%), $[(CF_3SO_2)_2NH]^-$(20%), $[CF_3SO_3]^-$ (10 %), $[CF_3SO_3H]^-$ (5 %), $[SO_2N]^-$ (5 %) |
| 0.186 | $[(CF_3SO_2)_2N]^-$(100%), $[(CF_3SO_2)_2NH]^-$(20%), $[CF_3SO_3]^-$ (80 %), $[CF_3SO_3H]^-$ (15 %), $[SO_3]^-$ (20 %) |
| 0.425 | $[(CF_3SO_2)_2N]^-$(100%), $[(CF_3SO_2)_2NH]^-$(20%), $[CF_3SO_3]^-$ (90 %), $[CF_3SO_3H]^-$ (10 %), $[SO_3]^-$ (10 %) |
| 0.534 | $[(CF_3SO_2)_2N]^-$(100%), $[(CF_3SO_2)_2NH]^-$(20%), $[CF_3SO_3]^-$ (50 %), $[CF_3SO_3H]^-$ (10 %), $[SO_3]^-$ (10 %) |
| 1 | $[(CF_3SO_2)_2N]^-$(100%), $[(CF_3SO_2)NH]^-$ (15%), $[(CF_3SO_2)N]^-$(5%) |

### 3.3.2 $[C_4C_1im][OTf]$-$H_2SO_4$ system

The acidity measurements of the $[C_4C_1im][OTf]$-$H_2SO_4$ system were carried out and the results can be found in Figure 3.3.3. In this system, the $H_0$ values were collected at $\chi_{H_2SO_4}$ from 0.028 to 0.960. At $\chi_{H_2SO_4} < 0.028$. the mesityl oxide was not dissolved in these mixtures. In the $\chi_{H_2SO_4}$ range between 0.028 to 0.960,

there is a gap where the $H_0$ values cannot be calculated using the $^{13}C$ NMR probe . The $H_0$ of this system cannot be measured at $0.248 \leq \chi_{H_2SO_4} \leq 0.459$. The peaks of mesityl oxide was not available or appeared in a very small peaks. At these concentrations, the acidities of the mixtures were collected using the UV-Vis probe (Figure 3.3.4).

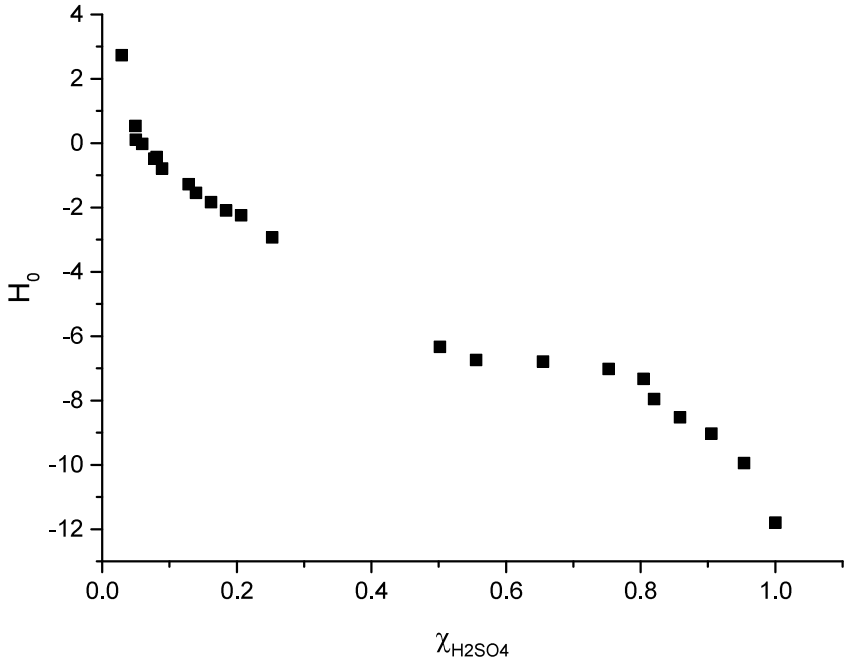



**Figure 3.3.3** – The $H_0$ values against the $\chi_{H_2SO_4}$ for the $[C_4C_1im][OTf]$-$H_2SO_4$ system

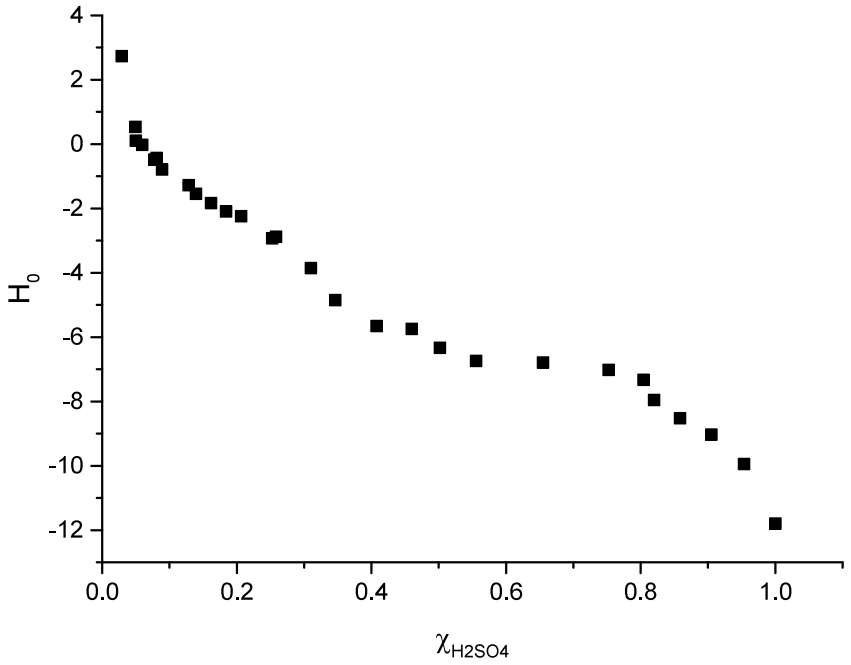



**Figure 3.3.4** – The $H_0$ values against the $\chi_{H_2SO_4}$ for the $[C_4C_1im][OTf]$-$H_2SO_4$ system (results combined from the $^{13}C$ NMR probe and UV-Vis probe)

Results from Figure 3.3.4 shows that the acidity increases as more acid is added into the ionic liquids. A linear increase in the acidity was observed from $0.028 \leq \chi_{H_2SO_4} \leq 0.530$. At $0.530 \leq \chi_{H_2SO_4} \leq 0.750$, the acidity remains constant and further addition of acid increases the acidity again. At $0.750 \leq \chi_{H_2SO_4} \leq 0.960$, the acidity measured in the mixture is the acidity of ionic liquid dissoved in the acid.

In the positive mass spectra of mass spectrometry results, no higher order clusters of sulphuric acid were detected. Clusters of the cations and the anions were detected in the positive mass spectra, $([C_4C_1im]\cdot F)^+$. Negative mass spectra of the $[C_4C_1im][OTf]$-$H_2SO_4$ system are compiled in the Table 3.3.2. In the negative mass spectra, higher order of sulphuric acid clusters were found in the $\chi_{H_2SO_4} > 0.600$. The $[H_3S_2O_8]^-$ can be suggested to formed from a small cluster when a proton is solvated by two anions $([HSO_4]_2H)^-$.

**Table 3.3.2 –** The negative mass spectra of [$C_4C_1$im][OTf]-$H_2SO_4$ : Detected ion fragments and their relative abundance

| $\chi_{H_2SO_4}$ | Ions |
|---|---|
| 0 | $[CF_3SO_3]^-$ (100 %) |
| 0.029 | $[CF_3SO_3]^-$ (100 %), $[CF_3SO_3H]^-$ (10 %) |
| 0.253 | $[CF_3SO_3]^-$ (100 %), $[CF_3SO_3H]^-$ (15 %), $[SO_3]^-$ (20%), $[CF_3SO_3{\cdot}CF_3SO_2]^-$ (15%) |
| 0.303 | $[CF_3SO_3]^-$ (100 %), $[CF_3SO_3H]^-$ (15 %), $[SO_3]^-$ (20%), $[CF_3SO_3{\cdot}CF_3SO_2]^-$ (15%) |
| 0.463 | $[CF_3SO_3]^-$ (100 %), $[CF_3SO_3H]^-$ (40 %), $[SO_3]^-$ (20%), $[CF_3SO_3{\cdot}CF_3SO_2]^-$ (20%), $[HSO_4]^-$ (40%), $[H_3S_2O_8]^-$ (10%) |
| 0.633 | $[CF_3SO_3]^-$ (100 %), $[CF_3SO_3H]^-$ (15 %), $[SO_3]^-$ (30%), $[CF_3SO_3{\cdot}CF_3SO_2]^-$ (20%), $[HSO_4]^-$ (80%), $[H_2SO_4]^-$ (30%), $[H_3S_2O_8]^-$ (10%) |
| 0.85 | $[CF_3SO_3]^-$ (100 %), $[CF_3SO_3H]^-$ (15 %), $[SO_3]^-$ (30%), $[CF_3SO_3{\cdot}CF_3SO_2]^-$ (20%), $[HSO_4]^-$ (80%), $[H_2SO_4]^-$ (30%), $[H_3S_2O_8]^-$ (10%) |

### 3.3.3 [$C_4C_1$im][OTf]-$H_3PO_4$ system

Acidity measurements were then continued with the [$C_4C_1$im][OTf]-$H_3PO_4$ system. In this system, the whole system was successfully measured using the $^{13}C$ NMR probe. There were no data collected at $\chi_{H_3PO_4} < 0.086$ as mesityl oxide did not dissolve in the mixtures. Results from Figure 3.3.5 show that at $\chi_{H_3PO_4} < 0.123$, the acidity increases gradually. The $H_0$ value of the neat [$C_4C_1$im][OTf] = 1.93. However, with the addition of $\chi_{H_3PO_4} = 0.086$, the acidity of the mixture lowered down to $H_0$ = -3.03. Further increase in $\chi_{H_3PO_4}$ up to 0.889 shows a gradual increase in the acidity. For $\chi_{H_3PO_4} > 0.889$, the acid was not fully solubilised in the ionic liquid.

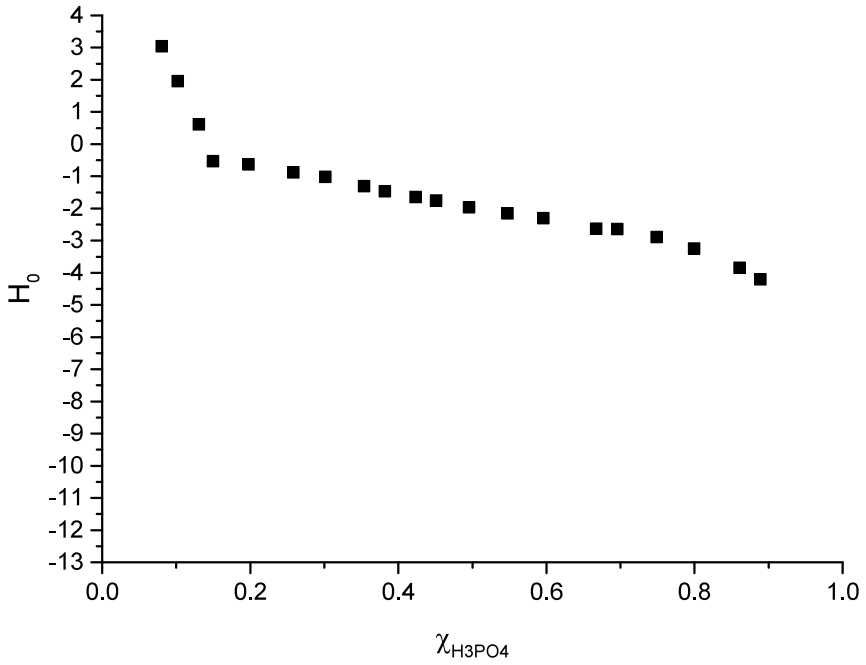



**Figure 3.3.5** – The $H_0$ values against the $\chi_{H_3PO_4}$ for the $[C_4C_1im][OTf]$-$H_3PO_4$ system

Mass spectrometry data recorded show that in the positive mass spectra, clusters of the cations and the anions was detected, $([C_4C_1im]\cdot F)^+$. There were no higher order clusters from the phosphoric acid detected in the mass spectra. In the negative mass spectra, higher order clusters of $H_3PO_4$ were found starting from $\chi_{H_3PO_4}$ 0.579 to $\chi_{H_3PO_4} = 0.889$ (Table 3.3.3). The higher order cluster detected are $[H_6P_2O_8]^-$ and $[H_3P_2O_{12}]^-$ that probably formed from the self-ionisation of the $H_3PO_4$ itself.

**Table 3.3.3 –** The negative mass spectra of [[$C_4C_1$im][OTf]-$H_3PO_4$ : Detected ion fragments and their relative abundance

| $\chi_{H_3PO_4}$ | Ions |
|---|---|
| 0 | $[CF_3SO_3]^-$ (100 %) |
| 0.009 | $[CF_3SO_3]^-$ (100 %), $[CF_3SO_3H]^-$ (20 %), $[SO_3H]^-$ (20%), $[H_3PO_4]^-$ (15%) |
| 0.299 | $[CF_3SO_3]^-$ (100 %), $[CF_3SO_3H]^-$ (20 %), $[SO_3H]^-$ (20%), $[H_3PO_4]^-$ (10%) |
| 0.579 | $[CF_3SO_3]^-$ (100 %), $[CF_3SO_3H]^-$ (20 %), $[SO_3H]^-$ (30%), $[H_3PO_4]^-$ (20%), $[H_6P_2O_8]^-$ (20%) and $[H_3P_2O_{12}]^-$ (10%) |
| 0.823 | $[CF_3SO_3]^-$ (100 %), $[CF_3SO_3H]^-$ (20 %), $[SO_3H]^-$ (40%), $[H_3PO_4]^-$ (20%), $[H_6P_2O_8]^-$ (30%) and $[H_3P_2O_{12}]^-$ (10%) |

## 3.4 The acidity measurements of [$C_4C_1$im][$HSO_4$] with different acids

### 3.4.1 [$C_4C_1$im][$HSO_4$]-H[$NTf_2$] system

The results for the acidity measurements of [$C_4C_1$im][$HSO_4$]-H[$NTf_2$] system are presented in the Figure 1.11. At $\chi_{H[NTf_2]} > 0.812$, the acid was not fully dissolved in the ionic liquid. The acidity of the [$C_4C_1$im][$HSO_4$]-H[$NTf_2$] mixtures increased as the $\chi_{H[NTf_2]}$ was increased. The highest $H_0$ value obtained is -6.933 at $\chi_{H[NTf_2]} > 0.400$; the mixture is changing from acid dissolved in ionic liquid to ionic liquid dissolved in the acid. The mixtures were further characterised using mass spectrometry (Table 3.4.1 and Table 3.4.2). In both the positive and negative mass spectram clusters of the cations and the anions was detected (for example; $[(CF_3SO_2)_2NH]^-$). Higher order clusters of $H_2SO_4$ were found in both positive and negative mass spectra (for example, ($[H_3S_2O_8]^-$ and $[H_9S_4O_{16}]^-$ ). In both of the the positive and negative mass spectra, higher order clusters were detected at $\chi_{H[NTf_2]} \geq 0.613$.

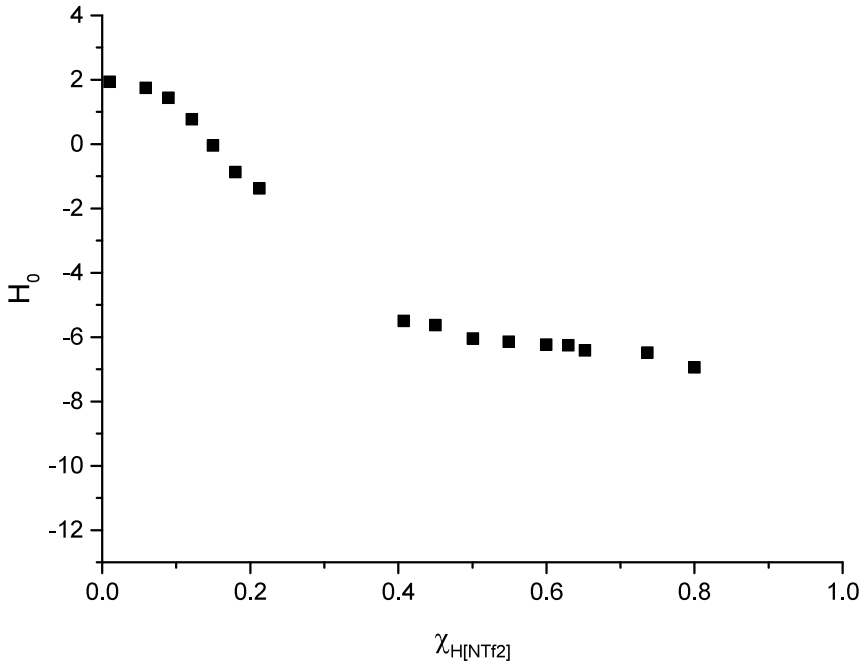



**Figure 3.4.1** – The $H_0$ values against the $\chi_{H[NTf_2]}$ for the $[C_4C_1im][HSO_4]$-$H[NTf_2]$ system

**Table 3.4.1** – The positive mass spectra of $[C_4C_1im][HSO_4]$-$H[NTf_2]$ : Detected ion fragments and their relative abundances

| $\chi_{H[NTf_2]}$ | Ions |
|---|---|
| 0 | $[C_4C_1im]^+$ (100 %) |
| 0.059 | $[C_4C_1im]^+$ (100 %), $[HC_1im]^+$ (20 %), $([C_4C_1im]^+ \cdot F)$ (5 %), $[SO_2NH]^+$ (10%) |
| 0.121 | $[C_4C_1im]^+$ (100 %), $[HC_1im]^+$ (20 %), $([C_4C_1im]^+ \cdot F)$ (10 %), $[SO_2NH]^-$ (10%) |
| 0.613 | $[C_4C_1im]^+$ (100 %), $[HC_1im]^+$ (40 %), $([C_4C_1im]^+ \cdot F)$ (15 %), $[SO_2NH]^+$ (20%) , $[H_7S_4O_{16}]^-$ (5%) |
| 0.79 | $[C_4C_1im]^+$ (100 %), $[HC_1im]^+$ (40 %), $([C_4C_1im]^+ \cdot F)$ (10 %), $[SO_2NH]^+$ (20%) , $[H_7S_4O_{16}]^-$ (5%) |

There is no data collected at $\chi_{H[NTf_2]}$ from 0.250 to 0.350. Homogenous mixtures could not be achieved in this region. After adding the acid into the ionic

**Table 3.4.2 –** The negative mass spectra of [$C_4C_1$im][$HSO_4$]-H[$NTf_2$] : Detected ion fragments and their relative abundance

| $\chi_{H[NTf_2]}$ | Ions |
|---|---|
| 0 | $[HSO_4]^-$ (100 %) |
| 0.059 | $[(CF_3SO_2)_2N]^-$(100%), $[(CF_3SO_2)_2NH]^-$(15%), $[HSO_4]^-$ (5 %) |
| 0.121 | $[(CF_3SO_2)_2N]^-$(100%), $[(CF_3SO_2)_2NH]^-$(10%), $[HSO_4]^-$ (15 %), $[H_3S_2O_8]^-$ (5%) |
| 0.613 | $[(CF_3SO_2)_2N]^-$(100%), $[(CF_3SO_2)_2NH]^-$(20%), $[HSO_4]^-$ (5 %), $[H_9S_4O_{16}]^-$ (5%) |
| 0.79 | $[(CF_3SO_2)_2N]^-$(100%), $[(CF_3SO_2)_2NH]^-$(10%), $[HSO_4]^-$ (5 %), $[H_3S_2O_8]^-$ (5%), $[H_9S_4O_{16}]^-$ (5%) |

**Table 3.4.3 –** The negative mass spectra of [$C_4C_1$im][$HSO_4$]-H[$NTf_2$] : Detected ion fragments and their relative abundances

| $\chi_{H[NTf_2]}$ | $[(CF_3SO_2)_2N]^-$ | $[(CF_3SO_2)_2NH]^-$ | $[HSO_4]^-$ | $[(HSO_4)\cdot H]^-$ |
|---|---|---|---|---|
| 0.25 top layer | 100 % | 15 % | 10 % | 5 % |
| 0.25 bottom layer | 100 % | 15 % | 5 % | - |
| 0.35 top layer | 100 % | 15 % | 15 % | 5 % |
| 0.35 bottom layer | 100 % | 15 % | 5 % | - |

liquid, the solutions became cloudy and separated into two layers after settling down. Further investigations were done by sending the samples to mass spectrometry analysis (Table 3.4.3). The positive mass spectra did not show any difference in the ion fragmentations for each layer. The negative mass spectra also shows the same abundance of each layer except for the $[HSO_4]^-$ ion and $[(HSO_4)\cdot H]^-$ ion. The top layer for both of the mixtures has more $[HSO_4]^-$ ion than the bottom layer. On the other hand, there are no $[(HSO_4)\cdot H]^-$ ion present in the either of bottom layers. $[(HSO_4)\cdot H]^-$ is the neutral acid $H_2SO_4$ that might formed from the proton exchange between the acid and the ionic liquid anion. Care is needed in this assignment, because identification of the $[HSO_4]^-$ in an ES spectrum does not prove that the species was present in the liquid phase.

### 3.4.2 $[C_4C_1im][HSO_4]$-H[OTf] system

The acidity measurements of $[C_4C_1im][HSO_4]$-H[OTf] system were done using the $^{13}C$ NMR probe. In this system, the acidity from $0.032 \leq \chi_{H[OTf]} \leq 0.901$ were successfully measured using the the $^{13}C$ NMR probe. At $\chi_{H[OTf]} < 0.032$, the mesityl oxide was not dissolved while at $\chi_{H[OTf]} > 0.901$, the value of the $\Delta\delta^0$ exceeds the maximum detection limit. Results in Figure 3.4.2 show that the acidity increases as more acid is added into the ionic liquids for the whole concentration range. This is similar to the behaviour seen for $[C_4C_1im][HSO_4]$-$H_2SO_4$ (see below).[114]

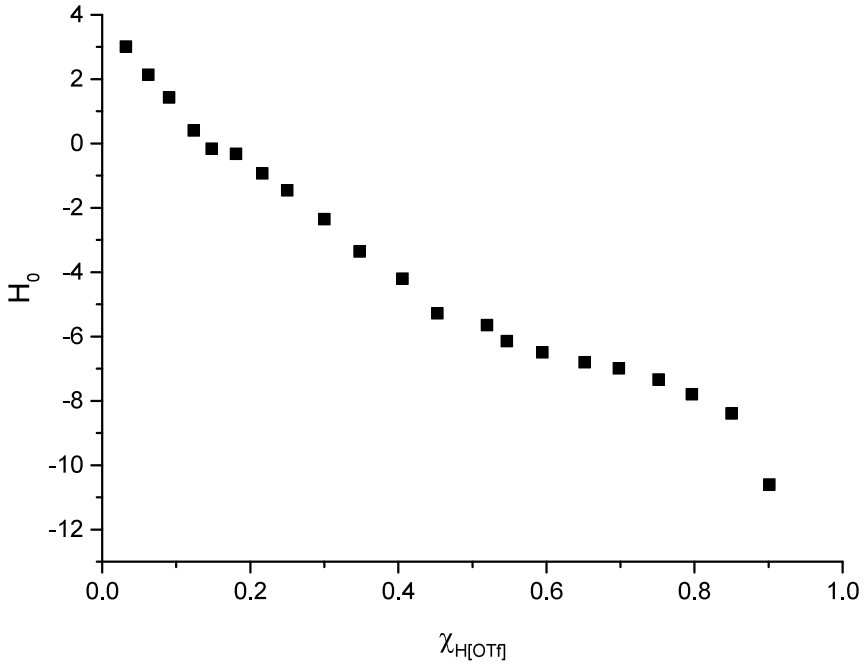



**Figure 3.4.2** – The $H_0$ values against the $\chi_{H[OTf]}$ for the $[C_4C_1im][HSO_4]$-H[OTf] system

The mixtures were further characterized using the mass spectrometry. In the positive mass spectra, ($[C_4C_1im]^+$) clusters was mainly found for all of the mixtures at $\chi_{H[OTf]} = 0.219$, 0.595, 0.76 and 0.95. In the negative mass spectra, $[HSO_4]^-$ anion were the most abundant ion found in each of previously mentioned $\chi_{H[OTf]}$.

Also, higher order of clusters were found in the $\chi_{H[OTf]} = 0.219$, 0.595, 0.76 and 0.95. The clusters obtained are $[H_5S_2O_8]^-$ and $[H_9S_4O_{16}]^-$.

### 3.4.3 [$C_4C_1$im][$HSO_4$]-$H_3PO_4$ system

The acidities of the [$C_4C_1$im][$HSO_4$]-$H_3PO_4$ system were measured using the $^{13}C$ NMR probe and is compiled in Figure 3.4.3. In this system, the acidity of the mixtures increases as the $\chi_{H_3PO_4}$ is increased. However, the mesityl oxide did not dissolve in $\chi_{H_3PO_4} < 0.370$ and no data were able to be produced using the $^{13}C$ NMR probe. There is no data collected at $\chi_{H_3PO_4} > 0.91$ as well as the acid was not fully solubilised in the ionic liquid.

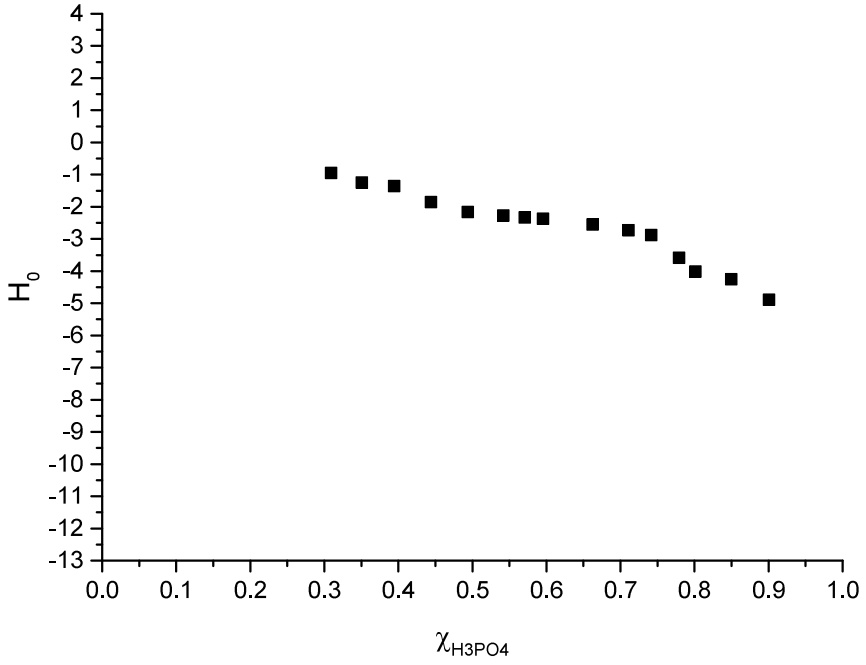



**Figure 3.4.3** – The $H_0$ values against the $\chi_{H_3PO_4}$ for the [$C_4C_1$im][$HSO_4$]-$H_3PO_4$ system

In order to get a complete data for the [$C_4C_1$im][$HSO_4$]-$H_3PO_4$ system, the acidity of mixtures at $\chi_{H_3PO_4} < 0.370$ were measured using the UV-Vis probe

(Figure 3.4.4). The additional plots matched well with the data previously obtained using the $^{13}C$ NMR probe. The measurements were done from $\chi_{H_3PO_4}$ = 0.370 to 0.016. There are three different Hammett probes used in order to obtain the $H_0$ values of these mixtures (Table 3.4.4).

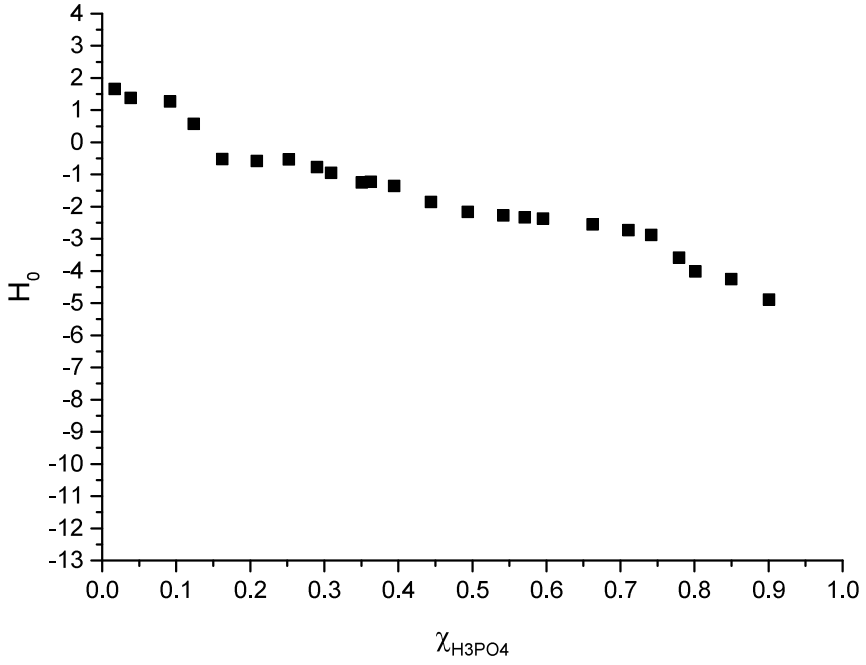



**Figure 3.4.4** – The $H_0$ values against the $\chi_{H_3PO_4}$ for the $[C_4C_1im][HSO_4]$-$H_3PO_4$ system

**Table 3.4.4 –** The $H_0$ values and Hammett probe used in the UV-Vis measurements of [$C_4C_1$im][$HSO_4$]-$H_3PO_4$ system at $\chi_{H_3PO_4} < 0.370$

| $\chi_{H_3PO_4}$ | $H_0$ | Hammett probe |
|---|---|---|
| 0.017 | 1.662 | 3-nitroaniline |
| 0.038 | 1.382 | |
| 0.123 | 0.572 | |
| 0.162 | -0.514 | 4-nitroaniline |
| 0.208 | -0.575 | |
| 0.252 | -0.534 | |
| 0.290 | -0.767 | 2-nitroaniline |
| 0.362 | -1.227 | |

Mass spectrometry data were recorded on a few samples with different ratio of molar concentration of phosphoric acid (Table 3.4.5 and Table 3.4.6). In the positive mass spectra, clusters of the cations and anions were detected. The cluster of $[(C_4C_1im)\ (H_2PO_4)_2)]^+$ was found only at $\chi_{H_2SO_4} = 0.06$. The cluster is formed from the cation from the ionic liquid and anion of the acid added. On the other hand, clusters of $H_3PO_4$ and $[H_2PO_4]^-$ of up to $[H_{11}P_4O_{16}]^-$ from the phosphoric acid were observed in the negative spectra. The higher order clusters of phosphoric acid were found in all of the mass spectra samples measured. In addition the cluster form the anion of the ionic liquid, $[HSO_4]^-$ was also detected. However, there is no ion interaction between the acid and ionic liquid found in the negative mass spectra.

**Table 3.4.5** – The positive mass spectra of [$C_4C_1$im][$HSO_4$]-$H_3PO_4$ system : Detected ion fragments and their relative abundances

| $\chi_{H_3PO_4}$ | Ions |
|---|---|
| 0 | $[C_4C_1im]^+$ (100%) |
| 0.06 | $[C_4C_1im]^+$ (100%), $[(C_4C_1im)\ (H_2PO_4)_2)]^+$ (20%) |
| 0.09 | $[C_4C_1im]^+$ (100%), $[(C_4C_1im)\ (H_2PO_4)_2)]^+$ (30%) |
| 0.25 | $[C_4C_1im]^+$ (100%), $[(C_4C_1im)\ (H_2PO_4)_2)]^+$ (10%) |
| 0.45 | $[C_4C_1im]^+$ (100%), $[(C_4C_1im)\ (H_2PO_4)_2)]^+$ (5 %) |
| 0.60 | $[C_4C_1im]^+$ (100%), $[(C_4C_1im)\ (H_2PO_4)_2)]^+$ (5 %) |
| 0.80 | $[C_4C_1im]^+$ (100%), $[(C_4C_1im)\ (H_2PO_4)_2)]^+$ (5 %) |

**Table 3.4.6 –** The negative mass spectra of $[C_4C_1im][HSO_4]$-$H_3PO_4$ system : Detected ion fragments and their relative abundances

| $\chi_{H_3PO_4}$ | Ions |
|---|---|
| 0 | $[HSO_4]^-$ (100 %) |
| 0.06 | $[H_2PO4]^+$ (100%), $[HSO_4]^-$ (40 %), $[HPO_3]^-$ (40 %), $[H_5P_2O_8]^-$ (5%) |
| 0.09 | $[H_2PO4]^+$ (100%), $[HSO_4]^-$ (50 %), $[HPO_3]^-$ (60 %), $[H_5P_2O_8]^-$ (5%) |
| 0.25 | $[H_2PO4]^+$ (100%), $[HSO_4]^-$ (40 %), $[HPO_3]^-$ (60 %), $[H_5P_2O_8]^-$ (20%) |
| 0.45 | $[H_2PO4]^+$ (100%), $[HSO_4]^-$ (40 %), $[HPO_3]^-$ (50 %), $[H_5P_2O_8]^-$ (40%) |
| 0.60 | $[H_2PO4]^+$ (100%), $[HSO_4]^-$ (40 %), $[HPO_3]^-$ (50 %), $[H_5P_2O_8]^-$ (40%) |
| 0.80 | $[H_2PO4]^+$ (100%), $[HSO_4]^-$ (30 %), $[HPO_3]^-$ (60 %), $[H_5P_2O_8]^-$ (5%), $[H_8P_3O_{12}]^-$ (20%) |

The results for each acid mixed with $[C_4C_1im][HSO_4]$ were combined in Figure 3.4.5. The acidities were successfully measured with the combinations of $H_0$ values from $^{13}C$ NMR probe and the UV-Vis probe. At $\chi_{acid} < 0.03$, the acidity of the mixture depends on the acid added into the ionic liquids. Above this $\chi_{acid}$ the solutions of $H_3PO_4$ are less acidic than the solution of all of the other acids, which have approximately the same acidity values. This suggests that $H_3PO_4$ is a weak acid in this ionic liquid, whereas the $H_2SO_4$, H[OTf] and $H[NTf_2]$ are all strong acids in this ionic liquids and proton transfer from the acid to the ionic liquid anion leads to the same acidic species, and therefore acidic strength, for all of their solutions. Even when there is a greater amount of acid than ionic liquid, this appears to remain true. This suggests that the sulphuric acid based clusters, such as are $[H_5S_2O_8]^-$ and $[H_9S_4O_{16}]^-$, are preferred to the H[OTf] and $H[NTf_2]$ free acids. This is confirmed by the mass spectrometry results.

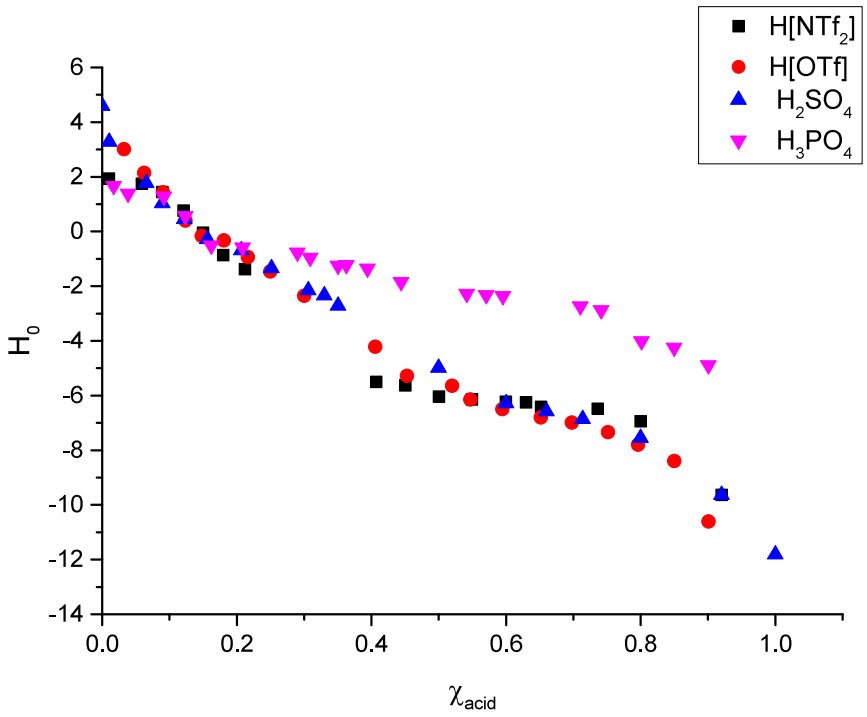



**Figure 3.4.5** – The $H_0$ values against the $\chi_{acid}$ with [$C_4C_1$im][$HSO_4$]

## 3.5 Acidity measurements of [$C_4C_1$im][$Me_2PO_4$] with different acids

The [$C_4C_1$im][$Me_2PO_4$] ionic liquid was mixed with three different acids; H[$NTf_2$], H[OTf] and $H_2SO_4$. The acidity of these three systems were measured using the $^{13}$C NMR probe. Since the [$C_4C_1$im][$Me_2PO_4$] has a very low acidity, it is expected that each of the systems will require the acidity measurements using the UV-Vis probe as well.

### 3.5.1 [$C_4C_1$im][$Me_2PO_4$]-H[$NTf_2$] system

Figure 3.5.1 shows the $H_0$ values plotted against the $\chi_{H[NTf_2]}$. The acidity values could only be measured from $\chi_{H[NTf_2]} \geq 0.509$. Initially a rapid increase in acidity

can be seen until $\chi_{H[NTf_2]}$ 0.603. Afterwards, the acidity increases gradually as the $\chi_{H[NTf_2]}$ increases. At $\chi_{H[NTf_2]} > 0.86$, the acid was not dissolved and stayed in the solid form.

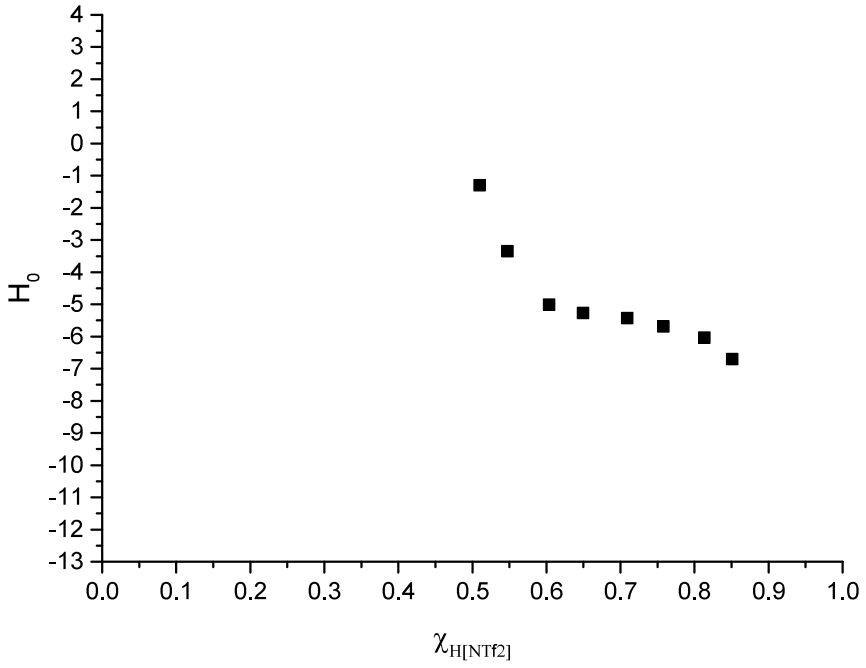



**Figure 3.5.1** – The $H_0$ values against the molar ratio $\chi_{H[NTf_2]}$ for the $[C_4C_1im][Me_2PO_4]$-$H[NTf_2]$ system

Additional measurements were done using the UV-Vis probe to obtain the full acidity scale (Figure 3.5.2). The acidity of mixtures measured are between $\chi_{H[NTf_2]} = 0.01$ to 0.46. Three dyes were used; 3-nitroaniline, 4-nitroaniline and 2-nitroaniline to get the $H_0$ values of these mixtures.

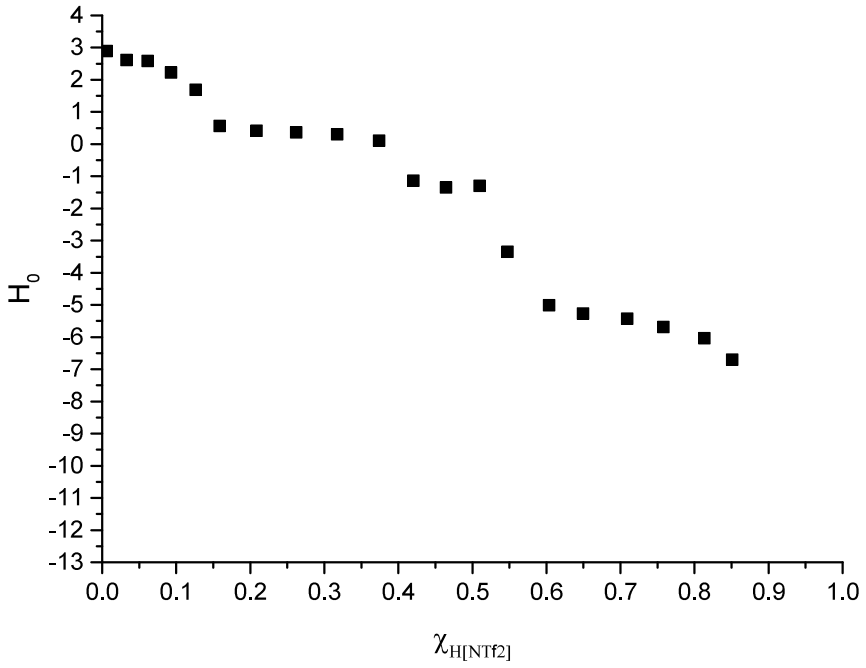



**Figure 3.5.2** – The $H_0$ values against the molar ratio $\chi_{H[NTf_2]}$ for the [$C_4C_1$im][$Me_2PO_4$]-H[$NTf_2$] system

The mixtures from the [$C_4C_1$im][$Me_2PO_4$]-H[$NTf_2$] system were sent for mass spectrometry for data analysis. In the positive mass spectra, only the clusters from the cation were detected with $[C_4C_1im]^+$ existing in high abundance in all spectra. The negative mass spectrometry results for the [$C_4C_1$im][$Me_2PO_4$]-H[$NTf_2$] system can be found in Table 3.5.1. Clusters of cations and anions were detected *i.e.* $[(CF_3SO_2)_2NH]^-$ in each of the samples measured. There are no higher order clusters in any of the H[$NTf_2$] because $[NTf_2]^-$ anion is a poor H-bond acceptor. Thus, H[$NTf_2$] only existed in its molecular form or undergoes dissociation.[150]

**Table 3.5.1 –** The negative mass spectra of $[C_4C_1im][Me_2PO_4]$-$H[NTf_2]$ system: Detected ion fragments and their relative abundances

| $\chi_{H[NTf_2]}$ | Ions |
|---|---|
| 0 | $[Me_2PO_4]$ (100%) |
| 0.102 | $[(CF_3SO_2)_2N]^-$ (100%), $[(CF_3SO_2)_2NH]^-$ (20%), $[Me_2PO_4]^-$ (20%) , $[(CF_3SO_2N]^-$ (5%) |
| 0.454 | $[(CF_3SO_2)_2N]^-$ (100%), $[(CF_3SO_2)_2NH]^-$ (20%), $[Me_2PO_4]^-$ (5%) , $[(CF_3SO_2N]^-$ (5%) |
| 0.613 | $[(CF_3SO_2)_2N]^-$ (100%), $[(CF_3SO_2)_2NH]^-$ (15%), $[Me_2PO_4]^-$ (5%) , $[(CF_3SO_2N]^-$ (5%) |
| 0.864 | $[(CF_3SO_2)_2NH]^{-\ -}$ (100%), $[(CF_3SO_2)_2NH]^-$ (20%), $[Me_2PO_4]^-$ (5%) , $[(CF_3SO_2N]^-$ (5%) |

### 3.5.2 $[C_4C_1im][Me_2PO_4]$-H[OTf] system

The acidity measurements of the $[C_4C_1im][Me_2PO_4]$-H[OTf] system were done and the results can be found in Figure 3.5.3. In this system, the $H_0$ values were collected at $\chi_{H[OTf]} \geq 0.500$. At $\chi_{H[OTf]} < 0.500$, the mesityl oxide was not fully dissolved in these mixtures, explaining the absence of data points at these regions. The acidity of the mixtures increases as the $\chi_{H[OTf]}$ was increased. From $\chi_{H[OTf]} = 0.50$ to -5.140, the acidity increases sharply with the addition of the H[OTf]. At this stage, the $[C_4C_1im][Me_2PO_4]$ ionic liquid has a very weak acidity and the molar ratio of H[OTf] is higher than the ionic liquids. Thus, the ionic liquids is dissolved in the acid causing a rapid change in the $H_0$ value. At $\chi_{H[OTf]} >$ -5.140, the acidity increases gradually until $\chi_{H[OTf]} = 0.949$ with highest $H_0$ = -9.498. The solution at $\chi_{H[OTf]} > 0.960$ solidifies preventing measurements of these mixtures.

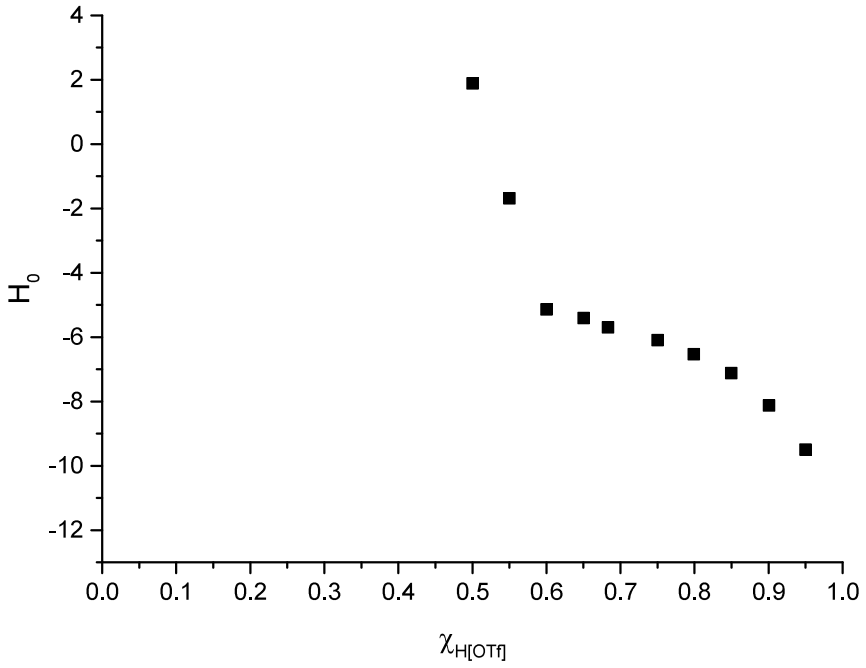



**Figure 3.5.3** – The $H_0$ values against the $\chi_{H[OTf]}$ for the [$C_4C_1$im][$Me_2PO_4$]-H[OTf] system

The data collection were completed using the UV-Vis probe for $\chi_{H[OTf]} < 0.500$. The results were compiled in the Figure 3.5.4. In these mixtures, 3-nitroaniline is the only probe used to measure all of the mixtures. The $H_0$ values obtained from the UV-Vis probe fits well with the results from the $^{13}$C NMR probe.

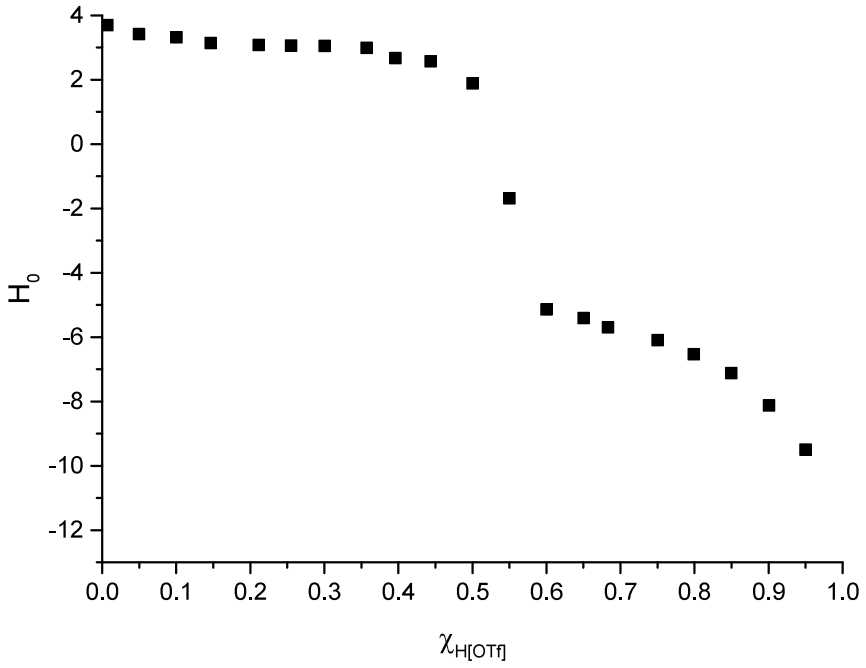



**Figure 3.5.4** – The $H_0$ values against the $\chi_{H[OTf]}$ for the $[C_4C_1im][Me_2PO_4]$-H[OTf] system

The mass spectrometry results were collected for this system. In the positive mass spectra, only ions from the cations were observed with $[C_4C_1im]^+$ ion as the most abundant ion in all spectra. Results for negative mass spectra can be found in Table 3.5.2. There were no higher order H[OTf] containing clusters detected. Pure ion of H[OTf] can be detected even at low concentration of $\chi_{H[OTf]}$. $[CF_3SO_3]^-$ or $[OTf]^-$ anion is the most abundant ion observed in the mass spectra followed by the $[Me_2PO_4]^-$anion. There is no evidence of any ion-pairing interaction happening between these two anions. Thus, the $H_0$ values obtained is based on the acidity of the anion itself.

**Table 3.5.2 –** The negative mass spectra of [$C_4C_1$im][$Me_2PO_4$]-H[OTf] system: Detected ion fragments and their relative abundances

| $\chi_{H[OTf]}$ | Ions |
|---|---|
| 0 | [$Me_2PO_4$] $^-$(100%) |
| 0.044 | [$CF_3SO_3$]$^-$ (100%), [$Me_2PO_4$]$^-$ (60%), [$SO_3$]$^-$ (40%), [$CF_3SO_3H$]$^-$ (15%), [$CF_3S$]$^-$ (10%) |
| 0.55 | [$CF_3SO_3$]$^-$ (100%), [$Me_2PO_4$]$^-$ (60%), [$SO_3$]$^-$ (30%), [$CF_3SO_3H$]$^-$ (20%), [$CF_3S$]$^-$ (10%) |
| 0.65 | [$CF_3SO_3$]$^-$ (100%), [$Me_2PO_4$]$^-$ (40%), [$SO_3$]$^-$ (30%), [$CF_3SO_3H$]$^-$ (20%), [$CF_3S$]$^-$ (10%) |
| 0.900 | [$CF_3SO_3$]$^-$ (100%), [$Me_2PO_4$]$^-$ (60%), [$SO_3H$]$^-$ (30%), [$CF_3SO_3H$]$^-$ (20%), [$CF_3S$]$^-$ (10%) |

### 3.5.3 [$C_4C_1$im][$Me_2PO_4$]-$H_2SO_4$ system

The acidity measurements of the [$C_4C_1$im][$Me_2PO_4$]-$H_2SO_4$ system were done and the results can be found in the Figure 3.5.5. Again, the full data scale cannot be measured using the $^{13}$C NMR probe due to the insolubility of the mesityl oxide in the mixture with $\chi_{H_2SO_4} < 0.500$. At $0.500 \leq \chi_{H_2SO_4} \leq 0.766$, an increase in the acidity values was observed. Afterwards, the acidity increases until $\chi_{H_2SO_4} = 1$.

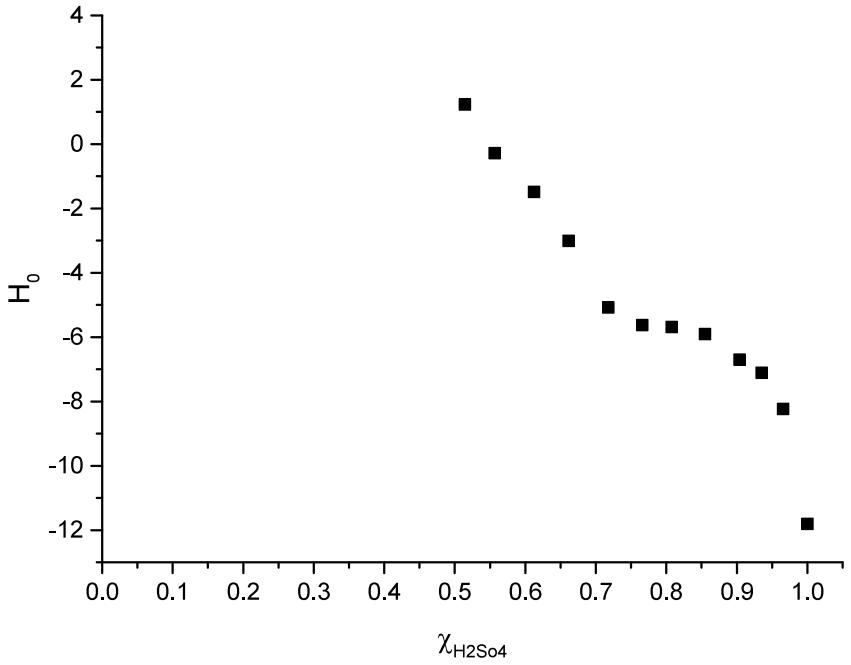



**Figure 3.5.5** – The $H_0$ values against the $\chi_{H_2SO_4}$ for the $[C_4C_1im][Me_2PO_4]$-$H_2SO_4$ system

The acidity of the $[C_4C_1im][Me_2PO_4]$-$H_2SO_4$ mixtures with $\chi_{H_2SO_4} < 0.500$ were measured using the UV-Vis probe. The results were combined with the $^{13}C$ NMR probe and the data fits well with the $^{13}C$ NMR probe results. In the UV-Vis measurements, one probe is used, which is 3-nitroaniline.

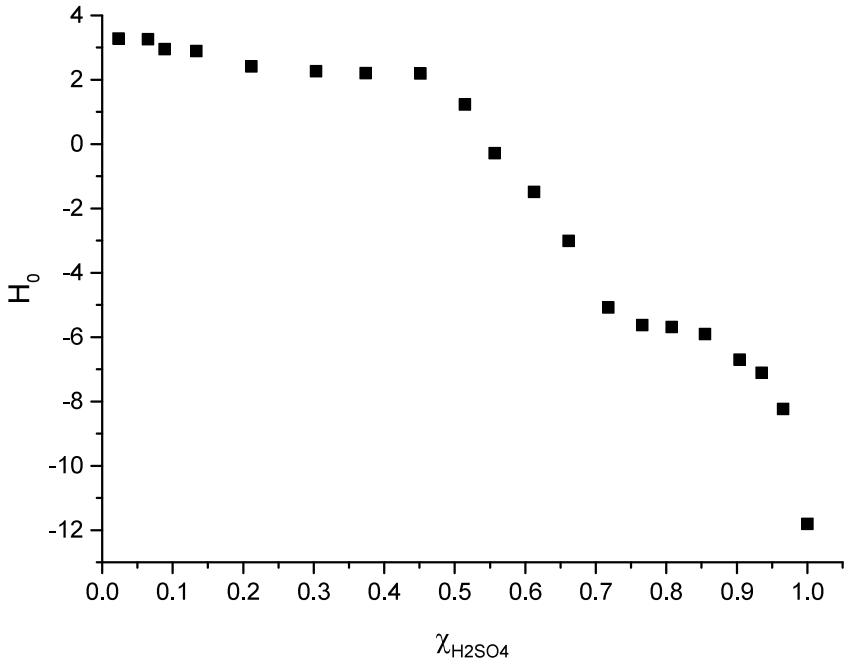



**Figure 3.5.6** – The $H_0$ values against the $\chi_{H_2SO_4}$ for the $[C_4C_1im][Me_2PO_4]$-$H_2SO_4$ system

Mass spectrometry data were collected for $[C_4C_1im][Me_2PO_4]$-$H_2SO_4$ mixtures for further analysis. In the positive mass spectra, ions from the cations was observed, where $[C_4C_1im]^+$ ions was the most abundant ions in each spectrum. Results for negative mass spectra can be found in the Table 3.5.3. Higher order clusters of $[HSO_4]^-$ and $H_3PO_4$ were found in the negative spectra at $\chi_{H_2SO_4} \geq 0.65$.

**Table 3.5.3 –** The negative mass spectra of $[C_4C_1im][Me_2PO_4]$-$H_2SO_4$ system: Detected ion fragments and their relative abundances

| $\chi_{H_2SO_4}$ | Ions |
|---|---|
| 0 | $[Me_2PO_4]^-$ (100%) |
| 0.06 | $[Me_2PO_4]^-$ (100%), $[HSO_4]^-$ (60 %), $[SO_3]^-$ (20 %) |
| 0.12 | $[Me_2PO_4]^-$ (100%), $[HSO_4]^-$ (30 %), $[SO_3]^-$ (15 %) |
| 0.25 | $[Me_2PO_4]^-$ (100%), $[HSO_4]^-$ (45 %), $[SO_3]^-$ (20 %) |
| 0.45 | $[Me_2PO_4]^-$ (100%), $[HSO_4]^-$ (50 %), $[SO_3]^-$ (20 %) |
| 0.65 | $[HSO_4]^-$ (100 %), $[H_3S_2O_8]^-$ (30 %), $[H_7P_2O_8]^-$ (5 %), $[H_8P_3O_8]^-$ (5 %), $[H_{11}P_4O_{16}]^-$ (5 %), $[Me_2PO_4]^-$ (65%), $[H_3SO_4]^-$ (20 %), $[SO_3]^-$ (40 %) |

To understand the effect of the acidity of each acid when mixed with the ionic liquid, the acidity results for $[C_4C_1im][Me_2PO_4]$ with four different acids; $H[NTf_2]$, H[OTf], $H_2SO_4$ and $H_3PO_4$ were compared in Figure 3.5.7. The behaviour of the acids in this ionic liquid is very complex. At lower $\chi_{acid}$ , $H[NTf_2]$ and $H_3PO_4$ gives solutions of a similar acidity until $\chi_{acid}$ up to 0.500, while H[OTf] and $H_2SO_4$ give less acidic solutions (but similar to each other). This is followed by a range of rapid increase in the acidity of the solutions for $H[NTf_2]$, H[OTf] and $H_2SO_4$, when further acid is added, whereas the strength of the solutions of $[C_4C_1im][Me_2PO_4]$-$H_3PO_4$ do not change so greatly. Hence at higher concentrations of acid, the solutions of $H[NTf_2]$, H[OTf] and $H_2SO_4$ are all much stronger than the $[C_4C_1im][Me_2PO_4]$-$H_3PO_4$ system. This change appears to be associated with the changeover from the mixtures being acid dissolved in ionic liquid to ionic liquids dissolved in acid.

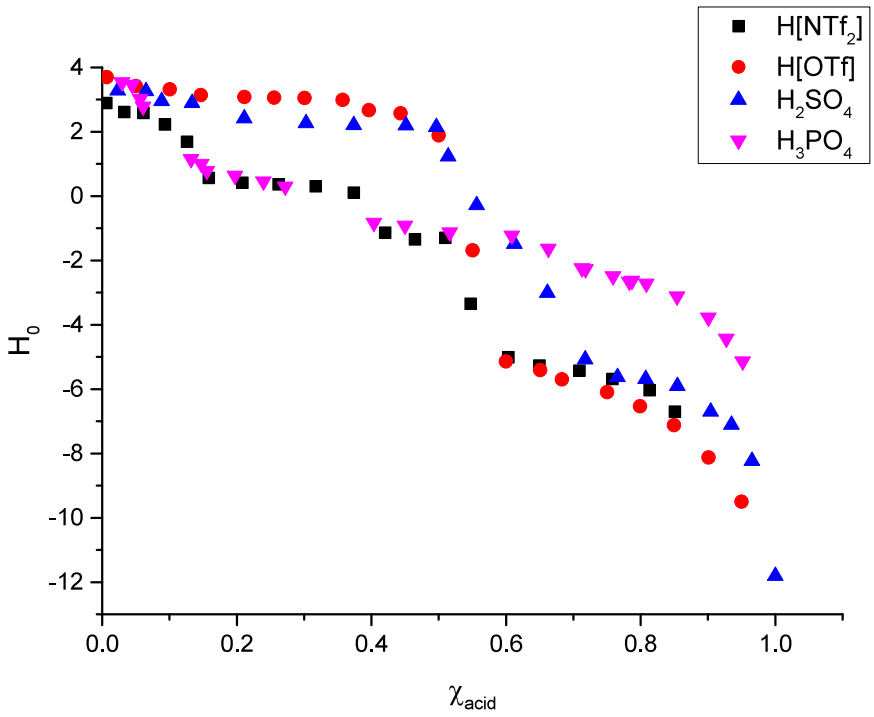



**Figure 3.5.7** – The $H_0$ values against the $\chi_{acid}$ mixed with [$C_4C_1$im][$Me_2PO_4$]

## 3.6 Discussion

### 3.6.1 Ionic liquids with different Brønsted acids

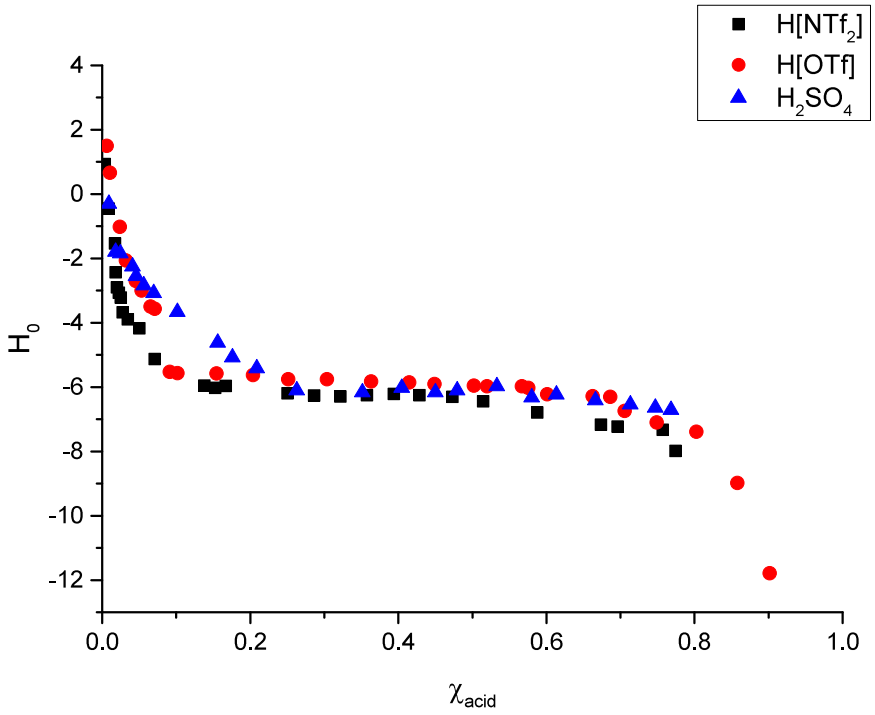



**Figure 3.6.1** – The $H_0$ values against the $\chi_{acid}$ mixed with $[C_4C_1im][NTf_2]$

The acidity of four different ionic liquids; $[C_4C_1im][NTf_2]$, $[C_4C_1im][OTf]$, $[C_4C_1im][HSO_4]$ and $[C_4C_1im][Me_2PO_4]$ were successfully measured with different acids using the $^{13}C$ NMR probe with some of the data measured using the UV-Vis probe. The acidity results for $[C_4C_1im][NTf_2]$ with three different acids; $H[NTf_2]$, H[OTf] and $H_2SO_4$ were compiled in Figure 3.6.1 to understand the effect of the acidity of each acid when mixed with the ionic liquid. At lower $\chi_{acid}$, ($0.2 > \chi_{acid}$ ), it does appear that $H_2SO_4$ gives slightly weaker solutions, suggesting that relatively weakly acidic $H_2SO_4$ derived species are present. At lower $\chi_{acid}$, the acidity increases until $\chi_{acid}$ $< 0.200$. There are differences in the $H_0$ values between the three acids where $H[NTf_2] > H[OTf] > H_2SO_4$. As all of the three acids used in the measurements are extremely acidic, it is expected that the acidity of the mixtures increases as

more acid is added into the ionic liquid. With further increase in the molar ratio of acid up to 0.500, the acidity remains constant which diminishes the difference in acidity for the different added acids. This suggests that the most acidic species in these solutions are the same and is determined by the ionic liquid. At these acid concentrations, it is assumed there are no clusters formed in this range, and the acids are dissolved in their molecular forms.[150] Another possible suggestion is that at $0.200 \leq \chi_{acid} \leq 0.500$, the acidity of these mixtures were buffered because all of these three strong acids react with the ionic liquid's anion $[NTf_2]^-$ to generate $H[NTf_2]$. The $H[NTf_2]$ that is produced or resulting from the levelling effect of the solvent is the strongest acid in the mixture and dominates the acidity value of the mixtures at these acid concentrations.[143] The acidities for H[OTf] and $H_2SO_4$ added in to $[C_4C_1im][NTf_2]$ remain constant up to $\chi_{acid} = 0.650$ while in the $[C_4C_1im][NTf_2]$-$H[NTf_2]$, the acidity of the mixtures increases with increasing molar ratio of the acid. In the $[C_4C_1im][NTf_2]$-$H[NTf_2]$ system, the left and right side of the equilibrium are identical, thus the ionic liquid did not have any buffering ability that will affect the acidity of the mixtures. In contrast, in the ionic liquid mixture containing different acids, the acidity of the mixture was levelled down by the ionic liquid. At $0.68 \leq \chi_{acid} \leq 0.78$, $H[NTf_2]$ is the strongest acid followed by H[OTf] and $H_2SO_4$. In the $[C_4C_1im][NTf_2]$-H[OTf] system, at $\chi_{acid} \geq 0.68$, the acidity increases gradually again. At this point, the structures of the mixture changes from acid dissolved in ionic liquid to ionic liquid dissolved in acid.

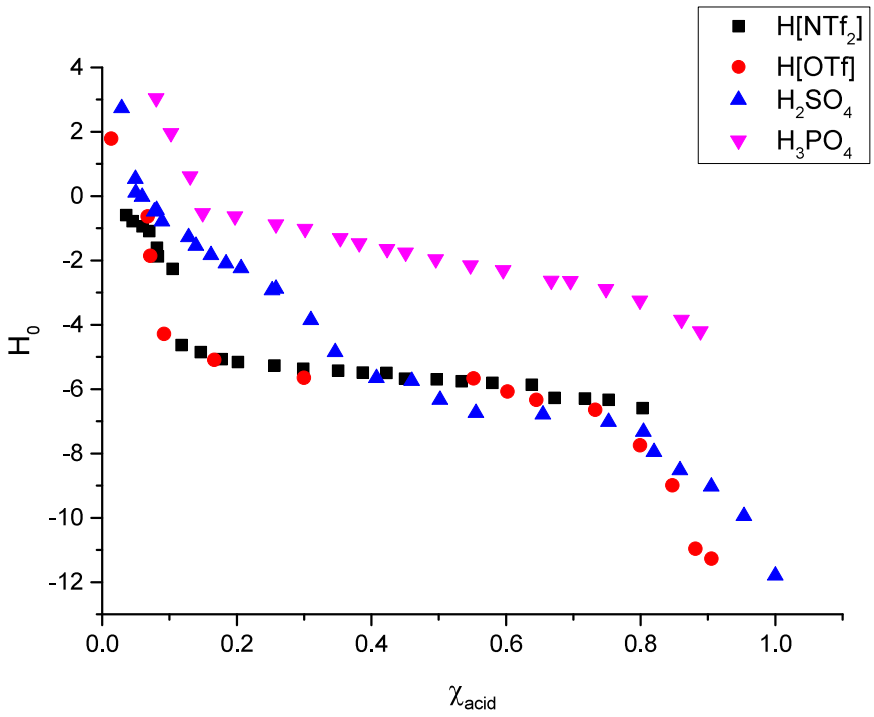



**Figure 3.6.2 –** The $H_0$ values against the $\chi_{acid}$ mixed with $[C_4C_1im][OTf]$

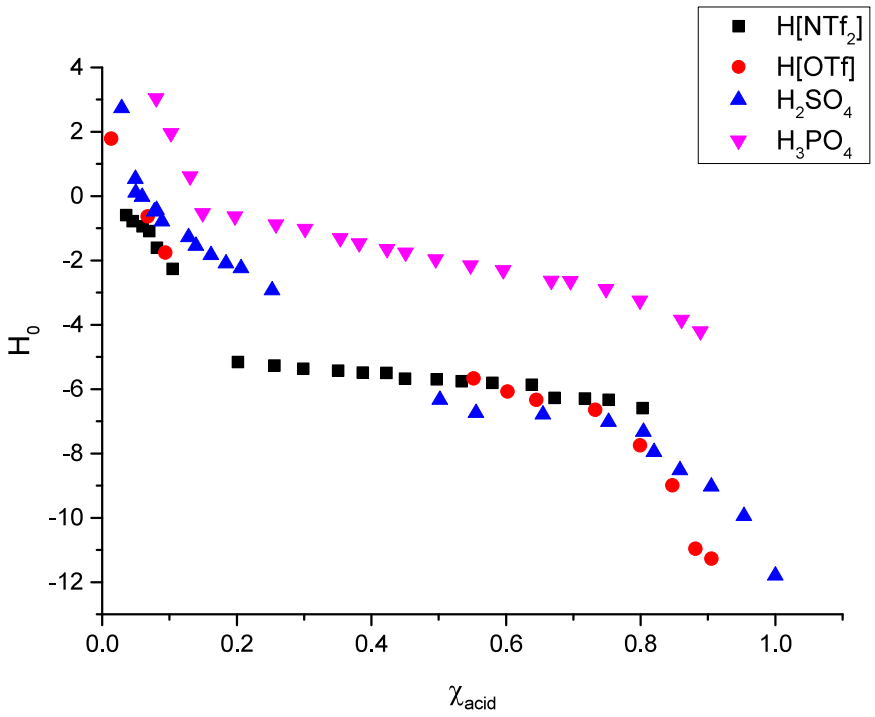



**Figure 3.6.3** – The $H_0$ values against the $\chi_{acid}$ mixed with $[C_4C_1im][OTf]$ ($^{13}C$ NMR Probe results)

The results for each Brønsted acid mixed with $[C_4C_1im][OTf]$ are compiled in Figure 3.6.2. The acidities were successfully measured with the combination of $^{13}C$ NMR probe with the help of UV-Vis probe. All of the mixtures behave differently depending on the acid added into the ionic liquids. $H_3PO_4$ gives weaker acid solutions at all concentrations, with this difference being greatest at higher concentrations of acid. This is due to $H_3PO_4$ being a weaker acid than H[OTf] and so the strongest acidic species in the system is $H_3PO_4$ or its clusters. $H_2SO_4$ gives weaker acid solutions than $H[NTf_2]$ and H[OTf] at $\chi_{acid} < 0.4$. This suggests that it forms a relatively weak acid species, maybe through hydrogen bonding to the ionic liquid. However, we see no evidence for what this is in the mass spectra. $H[NTf_2]$ and H[OTf] give very similar acidities at all concentrations, showing that these two acids have very similar acid species in the $[C_4C_1im][OTf]$-Brønsted acids mixtures. The similar acid species that affect the acidity of the mixture can be assumed to be due to the formation of H[OTf] that is generated when the acids react with the

$[OTf]^-$ anion. H[OTf] is the strongest acid in the mixture and dominates the total acidity of the mixtures. Overall, the acidity behaviour of $[C_4C_1im][OTf]$-Brønsted acids systems depends on the acid mixed with it.

Further analysis using the $^{13}C$ NMR probe were done as it was noticed that the acidity of $[C_4C_1im][OTf]$-Brønsted acids cannot be measured at certain acid concentrations. Results from Figure 3.6.3 show that the acidity of $[C_4C_1im][OTf]$-Brønsted acids mixtures were not able to be detected at $H_0$ varied approximately from -3 to -5 and it happened for all acids except $H_3PO_4$. Previously, it was assumed that the decomposition of the mesityl oxide is based on the interaction of the nucleophile from the $[OTf]^-$ anion of the ionic liquid. Since in this results, it shows that the decomposition occurs at specific acidity values in the $[C_4C_1im][OTf]$ ionic liquid with H[OTf], $H[NTf_2]$ and $H_2SO_4$, it confirms that the nucleophilic reaction occured selectively at specific acidity.

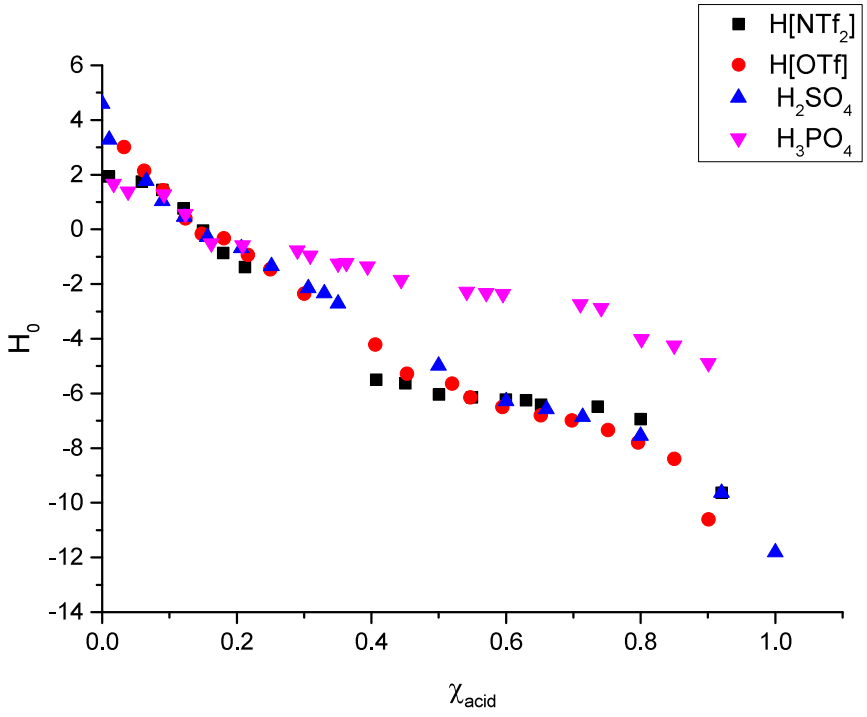



**Figure 3.6.4** – The $H_0$ values against the $\chi_{acid}$ with $[C_4C_1im][HSO_4]$

The results for each acid mixed with $[C_4C_1im][HSO_4]$ were combined in Figure 3.6.4. The acidities were successfully measured with the combinations of $H_0$ values from $^{13}C$ NMR probe and the UV-Vis probe. At $\chi_{acid} < 0.03$, the acidity of the mixture depends on the acid added into the ionic liquids. At $0.03 \leq \chi_{acid} \leq 0.2$, the acidity of all acids in the $[C_4C_1im][HSO_4]$ are similar which might be due to the same acidic species being present in the mixture. At $\chi_{acid} \geq 0.3$, the solutions of $H_3PO_4$ are less acidic than the solution of all of the other acids, which have approximately the same acidity values. This suggests that $H_3PO_4$ is a weak acid in this ionic liquid, whereas the $H_2SO_4$, H[OTf] and $H[NTf_2]$ are all strong acids in this ionic liquid and proton transfer from the acid to the ionic liquid anion leads to the same acidic species, and therefore acidic strength, for all of their solutions. Even when there is a greater amount of acid than ionic liquid, this appears to remain true. $H_2SO_4$ and its higher order clusters were formed from the reactions of all strong acids when mixed with the $[C_4C_1im][HSO_4]$ ionic liquid. This suggests that the sulphuric acid based clusters, such as are $[H_5S_2O_8]^-$ and $[H_9S_4O_{16}]^-$, are preferred to the H[OTf] and $H[NTf_2]$ free acids. This is confirmed by the mass spectrometry results. In the $[C_4C_1im][HSO_4]$-$H_3PO_4$ ($\chi_{acid} \geq 0.03$), $H_3PO_4$ is a weaker acid than $H_2SO_4$ causing the total acidity of the mixtures to depend on the acid species of $H_3PO_4$. The higher order clusters of $H_3PO_4$ were present and detected using mass spectrometry.

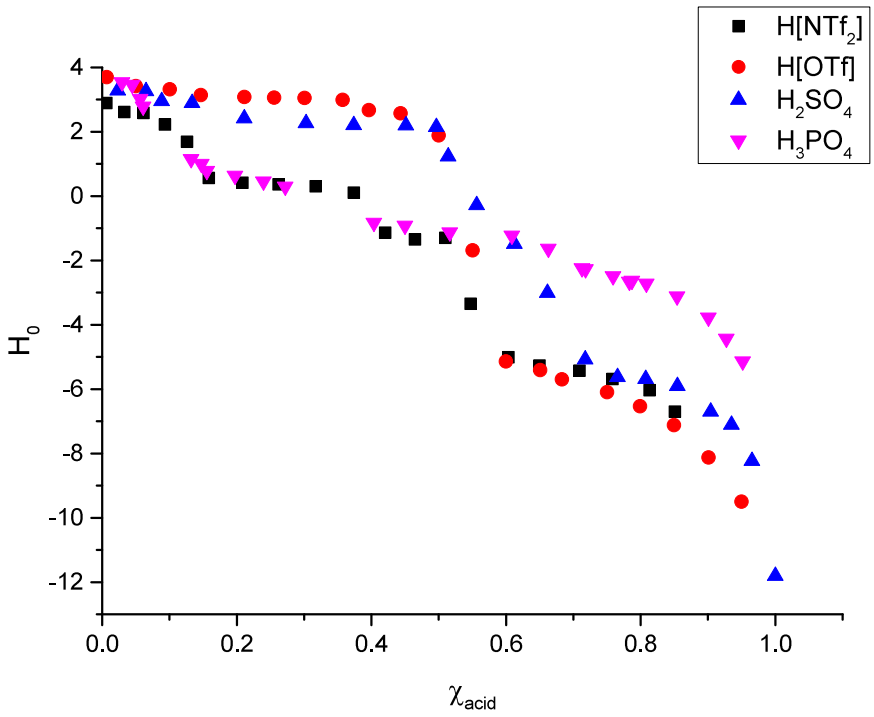



**Figure 3.6.5** – The $H_0$ values against the $\chi_{acid}$ mixed with $[C_4C_1im][Me_2PO_4]$

Finally for $[C_4C_1im][Me_2PO_4]$, H[OTf] and $H_2SO_4$ give less acidic mixtures than $H[NTf_2]$ and $H_3PO_4$ at $\chi_{acid} \geq 0.5$, but all of $H[NTf_2]$, H[OTf] and $H_2SO_4$ are give more acidic mixtures than $H_3PO_4$ at higher concentrations (Figure 3.6.5). The behaviour of the acids in this ionic liquid is very complex. At lower $\chi_{acid}$ , $H[NTf_2]$ and $H_3PO_4$ gives solutions of a similar acidity until $\chi_{acid}$ up to 0.500, while H[OTf] and $H_2SO_4$ give less acidic solutions (but similar to each other). This is followed by a range of rapid increase in the acidity of the solutions for $H[NTf_2]$, H[OTf] and $H_2SO_4$, when further acid is added, whereas the strength of the solutions of $[C_4C_1im][Me_2PO_4]$-$H_3PO_4$ do not change so greatly. Hence at higher concentrations of acid, the solutions of $H[NTf_2]$ , H[OTf] and $H_2SO_4$ are all much stronger than the $[C_4C_1im][Me_2PO_4]$-$H_3PO_4$ system. This change appears to be associated with the changeover from the mixtures being acid dissolved in ionic liquid to ionic liquids dissolved in acid.

### 3.6.2 Brønsted acids behaviour in different ionic liquids

With the same data, it is also interesting to observe the behaviour of Brønsted acids in different ionic liquids and to ask how each of ionic liquid affects the acidity of different acids. By using all of the results measured, plot of $H_0$ against the $\chi_{acid}$ for each ionic liquid in a graph were presented below.

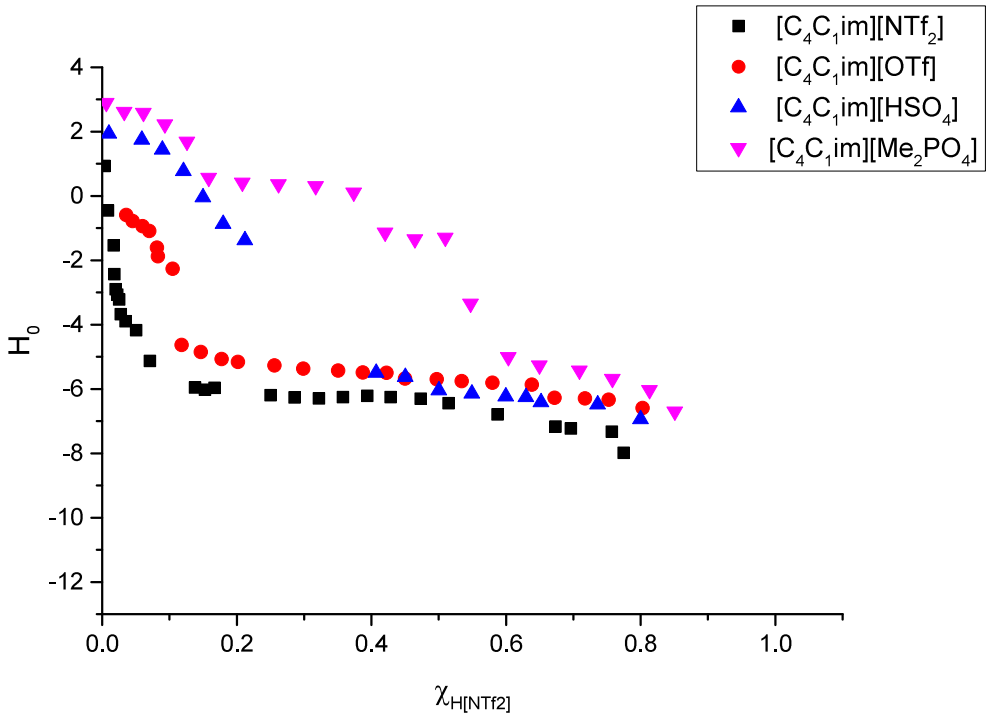



**Figure 3.6.6** – The $H_0$ values against the $\chi_{H[NTf_2]}$ for the H[$NTf_2$]-ionic liquids system

H[$NTf_2$] is a strong acid and addition of any of the ionic liquids used, reduces the acidity of the solution. The more ionic liquid added, the greater the reduction in the acidity of the solution. At all concentrations, the acidity of the solution is [$C_4C_1$im][$NTf_2$] > [$C_4C_1$im][OTf] > [$C_4C_1$im][$HSO_4$] > [$C_4C_1$im][$Me_2PO_4$]. For $\chi_{H[NTf_2]} > 0.6$, while there are small differences, all of the ionic liquids have similar acidity. At this point, the ionic liquids are not basic enough to greatly affect the strength of the acid. However, it can be seen that each ionic liquid has a different effect at lower concentrations. For [$C_4C_1$im][$Me_2PO_4$], there is a dramatic reduc-

tion in the acidity at $\chi_{H[NTf_2]} < 0.6$, for $[C_4C_1im][HSO_4]$ this occurs at $\chi_{H[NTf_2]} < 0.4$, for $[C_4C_1im][OTf]$ this occurs at $\chi_{H[NTf_2]} < 0.1$ and for $[C_4C_1im][NTf_2]$ it only occurs at very low concentrations. Below each of these concentrations, the ionic liquid begins to play a significat role in determining the acidity of the solution, the concentration at which this happens infers the basicity of the ionic liquid anions: $[Me_2PO_4]^- > [HSO_4]^- > [OTf]^- > [NTf_2]^-$.

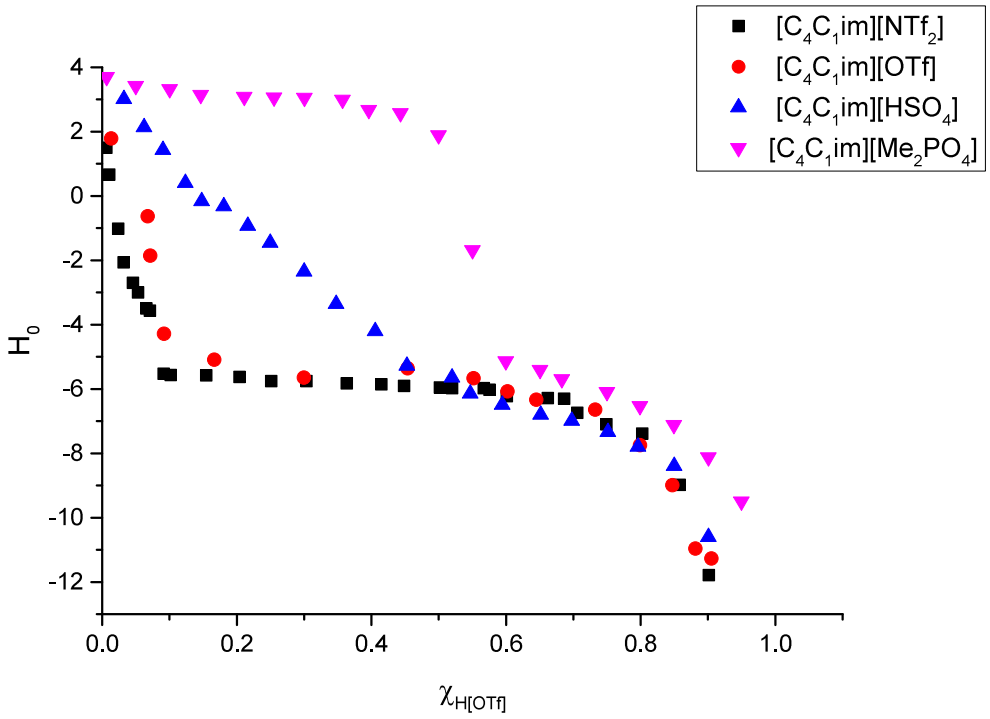



**Figure 3.6.7** – The $H_0$ values against the $\chi_{H_2SO_4}$ for the H[OTf]-ionic liquids system

For H[OTf] the behaviour is very similar to $H[NTf_2]$. One change between the two acid systems is that there is now less difference in the acidities of the $[C_4C_1im][NTf_2]$ and $[C_4C_1im][OTf]$ solutions. This suggests that $[OTf]^-$ is more basic than $[NTf_2]^-$ and that $H[NTf_2]$ is protonating $[OTf]^-$. For $[C_4C_1im][HSO_4]$, it can be seen that the acidity begins to reduce at $\chi_{H[OTf]} < 0.5$, indicating the involvement of both ionic liquid and acid derived species in controlling the acidity of the solution. $[C_4C_1im][Me_2PO_4]$ has very low and hardly changing acidity at concentrations $\chi_{H[OTf]} < 0.5$. This suggests that only ionic liquid derived species

are involved in controlling the acidity of these solutions and that $[C_4C_1im][Me_2PO_4]$ is a acidity levelling solvent at these concentrations.

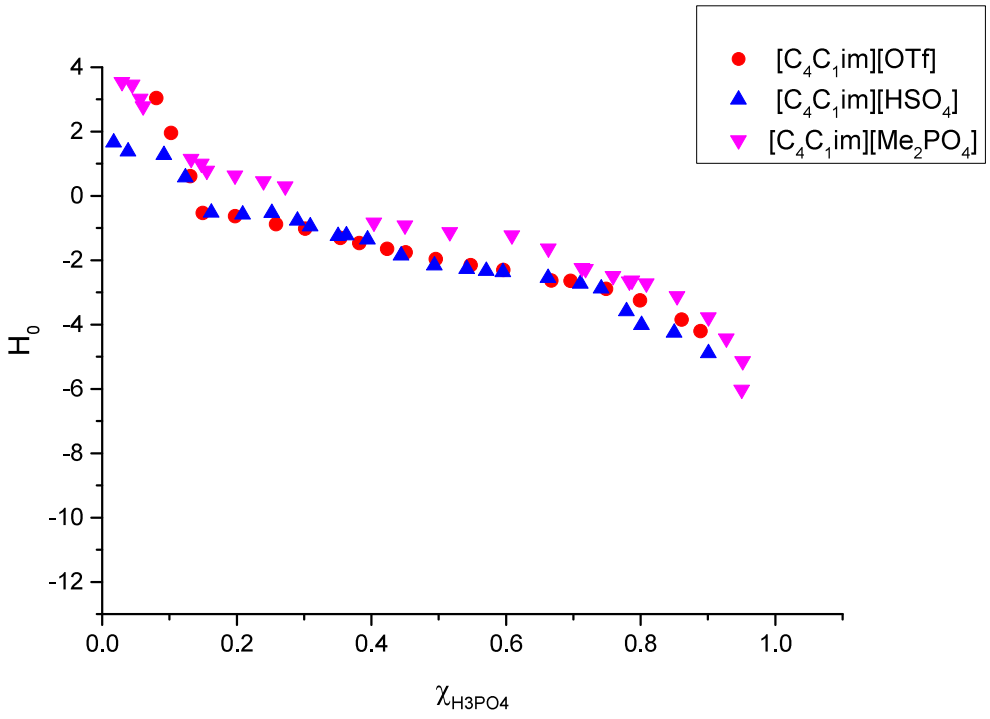



**Figure 3.6.8** – The $H_0$ values against the $\chi_{H_2SO_4}$ for the $H_2SO_4$-ionic liquids system

For $H_2SO_4$ it can be seen that at $\chi_{H[OTf]} < 0.5$, the acidity of ionic liquids are different from each other with the order of the acidities of the ionic liquid solutions being $[C_4C_1im][NTf_2] > [C_4C_1im][OTf] > [C_4C_1im][HSO_4] > [C_4C_1im][Me_2PO_4]$. While this is the same qualitative trend as seen for H[$NTf_2$] and H[OTf] it can be seen that the differences for $H_2SO_4$ are greater. This arises because $H_2SO_4$ is a weaker acid in these ionic liquids and does not fully dominate the acidities of the solutions until it is in much greater concentration. Starting from the $\chi_{H[OTf]} > 0.5$, all of the ionic liquid solutions have similar acidic properties with the exception of the $[C_4C_1im][Me_2PO_4]$, which remains a weak acid at all concentrations.

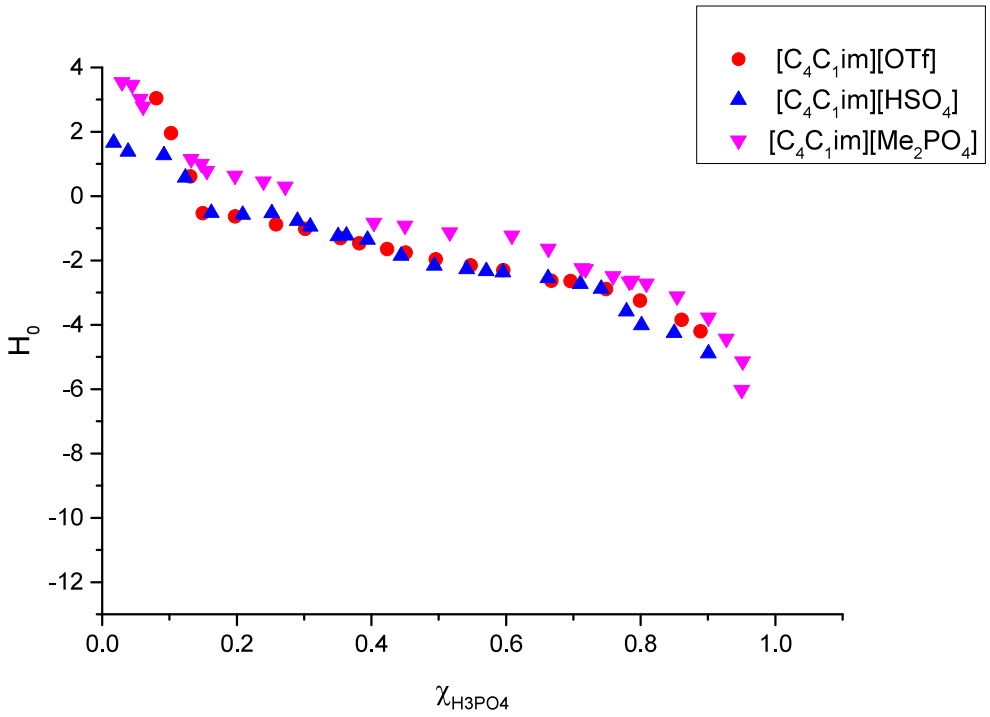



**Figure 3.6.9** – The $H_0$ values against the $\chi_{H_3PO_4}$ for the ionic liquids-$H_3PO_4$ system

Finally, it can be seen that the acidities of all of the ionic liquids-$H_3PO_4$ systems are markedly lower than the others at all concentrations. It can also be seen that while the solutions in $[C_4C_1im][OTf]$ and $[C_4C_1im][HSO_4]$ have slightly higher acidities than the solutions in $[C_4C_1im][Me_2PO_4]$, the differences are much smaller than had been seen for the other acids. This arises because $H_3PO_4$ is a weak acid in all of the ionic liquids used and the acidities of its solutions are controlled by $H_3PO_4$ derived species alone.

## 3.7 Conclusion

Successful measurements of the Hammett acidity function ($H_0$) were demonstrated for ionic liquids-Brønsted acids using the $^{13}C$ NMR Probe. Additional measurements using the UV-Vis probe were done to get a full acidity measurements for each system that cannot be measured using the $^{13}C$ NMR Probe. It is important

to recall that the $H_0$ values obtained from the $^{13}C$ NMR Probe is less precise than the UV-Vis probe results. If the more precise $H_0$ values is needed, the acidity measurements using the UV-Vis probe should be done.

It can be seen that the acidity of ionic liquids-acids solutions is complex. It depends upon the concentration of the acid, particularly whether the system is a solution of the acid in a greater amount of ionic liquid, or a solution of the ionic liquid in a greater amount of acid. The acidity of the solution also depends upon the difference in the acidity of the added acid and the conjugate acid of the anion of the ionic liquid.

# Chapter 4

# Acidity Measurements of Brønsted acid in ionic liquids with different cations

## 4.1 Acidity measurements of [$HC_4$im][$HSO_4$] with different acids

In the previous chapter, the acidity measurements of Brønsted acids in ionic liquids were done using the same 1-butyl-3-methylimidazolium cation or $[C_4C_1im]^+$ for easy comparison of the data obtained. With the results obtained, it is thought to be interesting to measure and compare the acidity of ionic liquids with same anion with Brønsted acids. In this work, [$HC_4$im][$HSO_4$] ionic liquid was chosen to measure its acidity with three different Brønsted acids; H[$NTf_2$], H[OTf] and $H_3PO_4$. The [$HC_4$im][$HSO_4$]-$H_2SO_4$ system will not be measured and discussed here as it has been properly discussed by Trang To.[188] The [$HC_4$im][$HSO_4$] ionic liquid chosen in this study has been used in many processes, especially in biomass processes.[14] Furthermore, this ionic liquid is easily prepared using the acid base reaction and the starting materials are very cheap. As [$HC_4$im][$HSO_4$] is a very hygroscopic ionic liquid, it is important to make to make sure that the water content of this ionic liquid is less than 100 ppm prior measuring. The acidity of [$HC_4$im][$HSO_4$]-Brønsted acids will be measured using the $^{13}C$ NMR probe.

### 4.1.1 [$HC_4im$][$HSO_4$]-H[$NTf_2$] system

The acidity measurements of the [$HC_4im$][$HSO_4$]-H[$NTf_2$] system were successfully measured using the $^{13}C$ NMR probe. The results are presented in the Figure 4.1.1. At $\chi_{H[NTf_2]} \leq 0.31$, the acidity increases as more acid added into the ionic liquid up to H0 = -5.666. The [$HC_4im$][$HSO_4$] has a very low acidity, thus even a small amount of strong acid added is able to affect the total acidity of the mixture. At higher concentrations, the acidity increases with only a small difference where the $H_0$ values obtained between -5.66 to -6.111. At $\chi_{H[NTf_2]} \geq 0.760$, the acid did not fully dissolve in the ionic liquids and no $H_0$ values were collected from this point onwards. It can be assumed that $HNTf_2$ is dissolved in its molecular form and there are no $[NTf_2(HNTf_2)]^-$ clusters formed in this range.

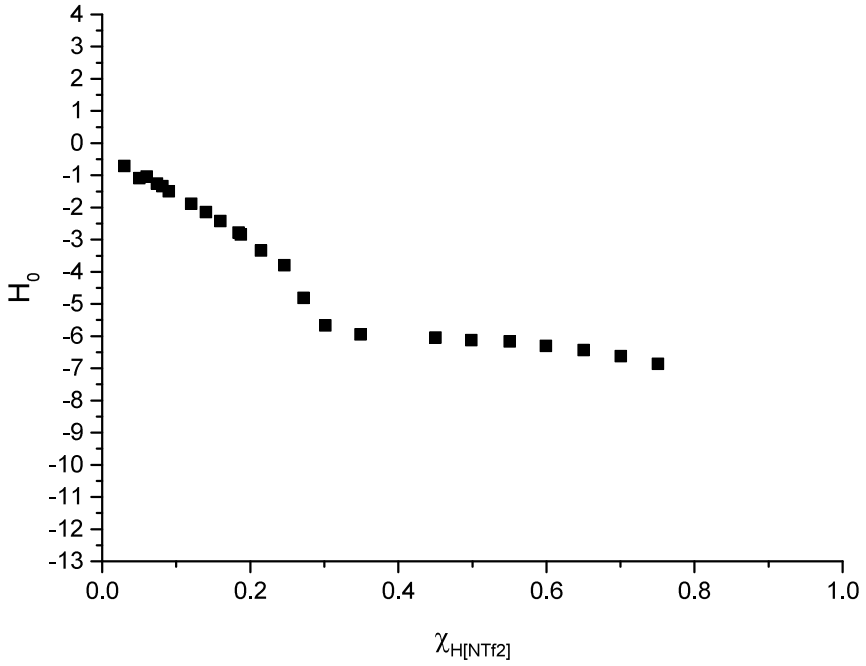



**Figure 4.1.1** – The $H_0$ values against the molar ratio $\chi_{H[NTf_2]}$ for the [$HC_4im$][$HSO_4$]-H[$NTf_2$] system

Mass spectrometry analysis data were collected for the [$HC_4im$][$HSO_4$]-H[$NTf_2$] mixtures and the positive mass spectra were compiled in Table 4.1.1. In the posi-

tive mass spectra, clusters of cation and anion were found, *i.e* $[(HC_4im)(SO_2CF_3N)]^+$. In addition, higher order clusters of $H_2SO_4$ were found in each of the mass spectra measured for examples $[H_7S_3O_{12}]^+$ and $[H_9S_4O_{16}]^+$ .

**Table 4.1.1** – The positive mass spectra of $[HC_4im][HSO_4]$-$H[NTf_2]$ system: Detected ion fragments and their relative abundances

| $\chi_{H[NTf_2]}$ | Ions |
|---|---|
| 0 | $[HC_4im]^+$ (100 %) |
| 0.03 | $[HC_4im]^+$ (100 %), $[HC_1im]^+$ (25 %), $[(SO_2NH]^+$ (15%), $[(HC_4im)(SO_2CF_3N)]^+$ (15%), $[H_7S_4O_{16}]^-$ (5 %) |
| 0.11 | $[HC_4im]^+$ (100 %), $[HC_1im]^+$ (15 %), $[(HC_4im)_2(HSO_4)]^+$ (20%), $[H_9S_4O_{16}]^+$ (5 %), $[HC_1im]^+$ (5 %) |
| 0.44 | $[HC_4im]^+$ (100 %), $[HC_1im]^+$ (25 %), $[(HC_4im)(SO_2CF_3N)]^+$ (5%), $[H_7S_3O_{12}]^+$ (5 %) |
| 0.66 | $[HC_4im]^+$ (100 %), $[HC_1im]^+$ (5 %), $[(HC_4im)(SO_2CF_3N)]^+$ (5%), $[H_7S_3O_{12}]^+$ (10 %) |
| 0.75 | $[HC_4im]^+$ (100 %), $[HC_1im]^+$ (10 %), $[(HC_4im)(SO_2CF_3N)]^+$ (10%), |

### 4.1.2 [$HC_4$im][$HSO_4$]-H[OTf] system

The acidity measurements of the $[HC_4im][HSO_4]$-H[OTf] system were measured using the $^{13}C$ NMR Probe. A curve was obtained in the Figure 4.1.2. At $\chi_{H[OTf]} \leq 0.35$, the acidity increases as more acid is added into the ionic liquid. Then, between $0.400 \leq \chi_{H[OTf]} \leq 0.690$, the acidity increases with small difference. The $H_0$ values obtained are between -6.25 to -6.7. The acidity change increases again as more acid is added into the ionic liquid up to $\chi_{H[OTf]} = 0.900$. After that, the solutions did not mix well and separated into two layers at $\chi_{H[OTf]} = 0.900$ to 0.986.

The mass spectrometry data were collected for this system (Table 4.1.2 and Table 4.1.3). In the positive mass spectra, clusters of cations and anions were found *i.e* $[(HC_4im)_2(HSO_4)]^+$ and $[(HC_4im)_2(CF_3SO_3)]^+$. Also, in both of the positive and negative mass spectra, higher order clusters of $H_2SO_4$ were found, *i.e.* $[H_7S_4O_{16}]^+$ and $[H_7S_3O_{12}]^-$ .

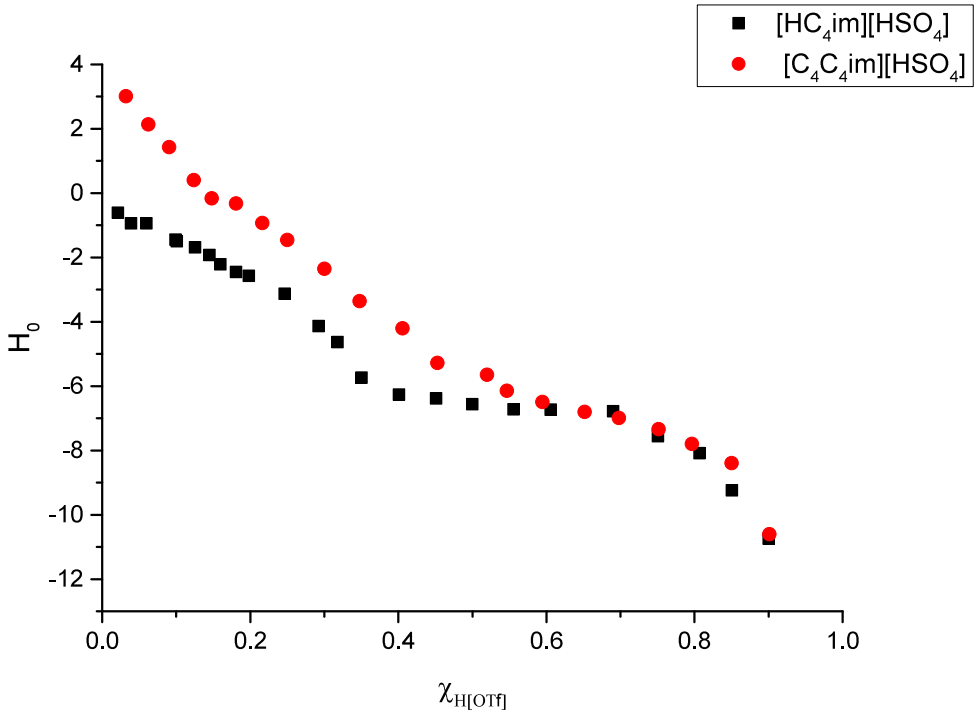



**Figure 4.1.2** – The $H_0$ values against the molar ratio $\chi_{H_2SO_4}$ for the $[HC_4im][HSO_4]$-H[OTf] system

**Table 4.1.2** – The positive mass spectra of $[HC_4im][HSO_4]$-H[OTf] system: Detected ion fragments and their relative abundances

| $\chi_{H[OTf]}$ | Ions |
|---|---|
| 0 | $[HC_4im]^+$ (100 %) |
| 0.021 | $[HC_4im]^+$ (100 %), $[NSCF_3]^+$ (15%), $[(HC_4im)_2(HSO_4)]^+$ (50 %), $(HC_4im)_2(OTf)]^+$ (50 %) |
| 0.24 | $[HC_4im]^+$ (100 %), $[NSCF_3]^+$ (15%), $[(HC_4im)_2(HSO_4)]^+$ (50 %), $[(HC_4im)_2(OTf)]^+$ (80 %) |
| 0.6 | $[HC_4im]^+$ (100 %), $[NSCF_3]^+$ (15%), $[(HC_4im)_2(CF_3SO_3)]^+$ (5 %), $[H_7S_4O_{16}]^+$ (5 %) |
| 0.9 | $[HC_4im]^+$ (100 %), $[(HC_4im)_2(CF_3SO_3)]^+$ (5 %), $[H_7S_4O_{16}]^+$ (5 %) |

**Table 4.1.3 –** The negative mass spectra of [$HC_4$im][$HSO_4$]-H[OTf] system: Detected ion fragments and their relative abundances

| $\chi_{H[OTf]}$ | Ions |
|---|---|
| 0 | $[HSO_4]^-$ (100%) |
| 0.021 | $[OTf]^-$ (100%), $[HSO_4]^-$ (50%), $[HOTf]^-$ (20%), $[H_3S_2O_8]^-$ (50%), $[H_5S_3O_{12}]^-$ (5%) |
| 0.24 | $[OTf]^-$ (100%), $[HSO_4]^-$ (90%), $[HOTf]^-$ (10%), $[H_3S_2O_8]^-$ (20%), $[H_5S_3O_{12}]^-$ (5%) |
| 0.6 | $[OTf]^-$ (100%), $[HSO_4]^-$ (60%), $[HOTf]^-$ (20%), $[H_3S_2O_8]^-$ (20%), $[H_5S_3O_{12}]^-$ (5%) |
| 0.9 | $[OTf]^-$ (100%), $[HSO_4]^-$ (50%), $[HOTf]^-$ (20%), $[H_3S_2O_8]^-$ (20%), $[H_5P_3O_{12}]^-$ (5%) |

### 4.1.3 [$HC_4$im][$HSO_4$]-$H_3PO_4$ system

The final system measured in this Chapter is the [$HC_4$im][$HSO_4$]-$H_3PO_4$ system. The whole acid range system was successfully measured using the $^{13}$C NMR Probe. Figure 4.1.3 shows that the acidity of the mixtures increases as more acid is added into the system. The highest $H_0$ values obtained in this system is -5.36 at $\chi_{H_3PO_4}$ = 0.900. The mixture is no longer homogeneous after at $\chi_{H_3PO_4} = 0.900$.

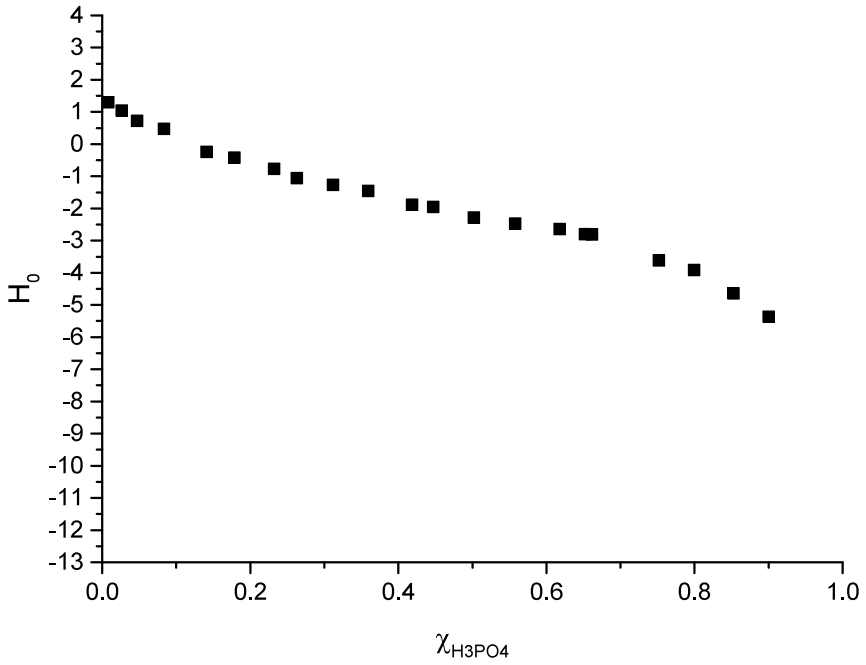



**Figure 4.1.3** – The $H_0$ values against the molar ratio $\chi_{H_3PO_4}$ for the $[HC_4im][HSO_4]$-$H_3PO_4$ system

The mass spectrometry results were compiled in Table 4.1.4 and Table 4.1.5. In the positive mass spectra, clusters of cations and anions were detected *i.e.* $[(HC_4im)_2(HSO_4)]^+$ . Higher order clusters of $H_2SO_4$ were observed in the positive and negative mass spectra. Interestingly, higher order cluster of $H_3PO_4$ was also detected in the negative mass spectra ($[H_8P_3O_8]^-$).

**Table 4.1.4 –** The positive mass spectra of $[HC_4im][HSO_4]$-$H_3PO_4$ system: Detected ion fragments and their relative abundances

| $\chi_{H_3PO_4}$ | Ions |
|---|---|
| 0 | $[HC_4im]^+$ (100 %) |
| 0.04 | $[HC_4im]^+$ (100 %), $[(HC_4im)_2(HSO_4)]^+$ (5 %), $[H_7S_4O_{16}]^+$ (5 %) |
| 0.14 | $HC_4im]^+$ (100 %), $[(HC_4im)_2(HSO_4)]^+$ (5 %), $[H_7S_4O_{16}]^+$ (5 %) |
| 0.26 | $HC_4im]^+$ (100 %), $[(HC_4im)_2(HSO_4)]^+$ (20 %), $[H_7S_4O_{16}]^+$ (5 %) |
| 0.44 | $HC_4im]^+$ (100 %), $[(HC_4im)_2(HSO_4)]^+$ (50 %), $[H_7S_4O_{16}]^+$ (5 %) |
| 0.66 | $HC_4im]^+$ (100 %), $[(HC_4im)_2(HSO_4)]^+$ (5 %), $[H_7S_4O_{16}]^+$ (5 %) |
| 0.85 | $HC_4im]^+$ (100 %), $[(HC_4im)_2(HSO_4)]^+$ (50 %), $[H_7S_4O_{16}]^+$ (5 %) |
| 1 | $[H_2PO_4]^-$ (100 %) |

**Table 4.1.5** – The negative mass spectra of $[HC_4im][HSO_4]$-$H_3PO_4$ system: Detected ion fragments and their relative abundances

| $\chi_{H_3PO_4}$ | Ions |
|---|---|
| 0 | $[HSO_4]^-$ (100%) |
| 0.04 | $[H_2PO_4]^-$ (100 %), $[HPO_3]^-$ (50%), $[H_2SO_4]^-$ (50 %), $[H_3S_2O_8]^-$ (90%), $[H_8P_3O_8]^-$ (20%) |
| 0.14 | $[H_2PO_4]^-$ (100 %), $[HPO_3]^-$ (60%), $[H_2SO_4]^-$ (40 %), $[H_3S_2O_8]^-$ (70%), $[H_8P_3O_8]^-$ (10%) |
| 0.26 | $[H_2PO_4]^-$ (90 %), $[HPO_3]^-$ (60%), $[H_2SO_4]^-$ (40 %), $[H_3S_2O_8]^-$ (100%), $[H_8P_3O_8]^-$ (20%) |
| 0.44 | $[H_2PO_4]^-$ (90 %), $[HPO_3]^-$ (60%), $[H_2SO_4]^-$ (50 %), $[H_3S_2O_8]^-$ (60%), $[H_8P_3O_8]^-$ (5%) |
| 0.66 | $[H_2PO_4]^-$ (80 %), $[HPO_3]^-$ (60%), $[H_2PO_4]^-$ (30 %), $[H_3S_2O_8]^-$ (60%), $[H_8P_3O_8]^-$ (60%) |
| 0.85 | $[H_2PO_4]^-$ (100 %), $[HPO_3]^-$ (50%), $[H_2PO_4]^-$ (40 %), $[H_3S_2O_8]^-$ (40%), $[H_8P_3O_8]^-$ (5%) |
| 1 | $[H_2PO_4]^-$ (100 %) |

## 4.2 Discussions and conclusions

The acidity of $[HC_4im][HSO_4]$ with different acids were successfully measured using the $^{13}C$ NMR Probe. Interestingly, all of the mixtures work well with this probe. This makes the $[HC_4im][HSO_4]$ more attractive in addition to it being cheap and

easily prepared. Based on the results, the acidity of the $[HC_4im][HSO_4]$-Brønsted acids depends on the type of acids used in a similar way to the $[C_4C_1im][HSO_4]$-Brønsted acids. In order to understand the effect of the cation of the ionic liquid on the acidity, graphs were plotted for both of $[HC_4im][HSO_4]$ and $[C_4C_1im][HSO_4]$ with each of the acids respectively (Figure 4.2.1 to Figure 4.2.3).

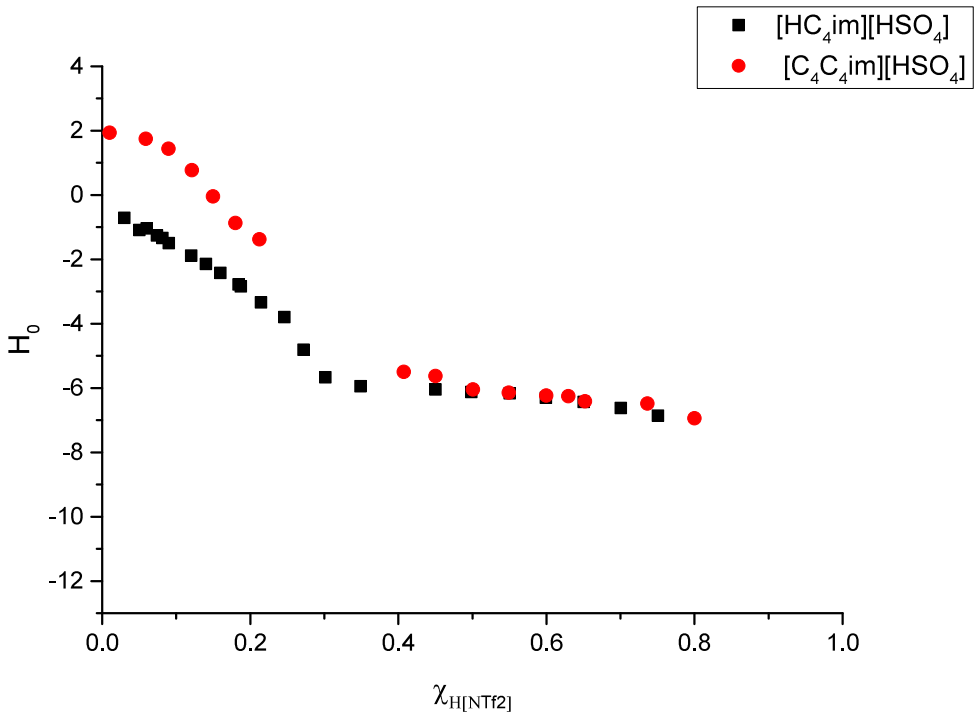



**Figure 4.2.1** – The comparison for $H[NTf_2]$ mixed with $[HSO_4]^-$ based ILs

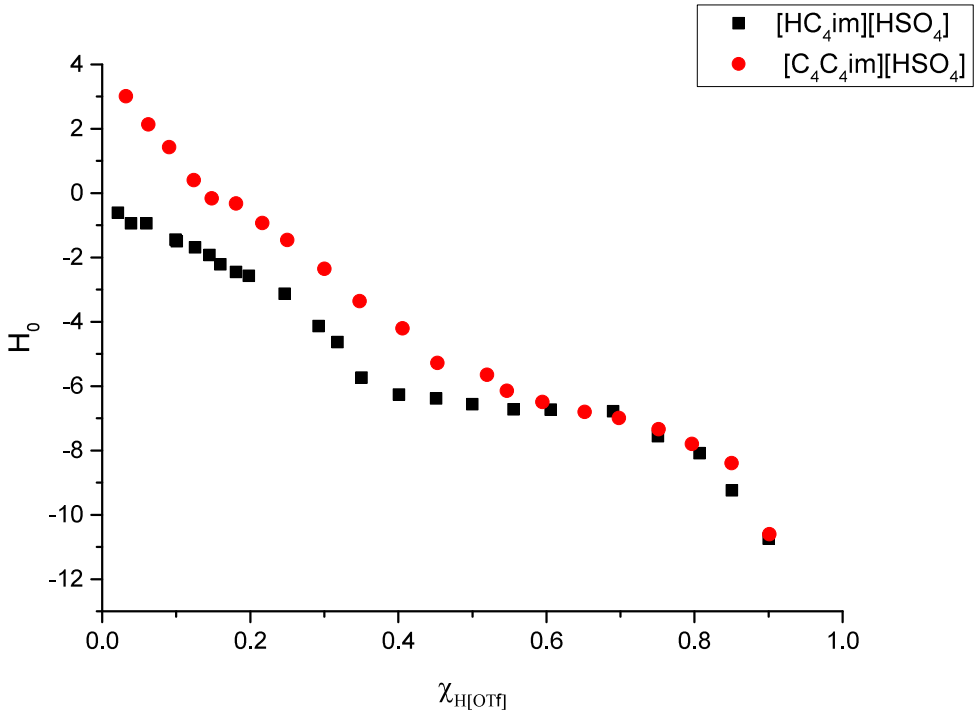



**Figure 4.2.2** – The comparison for H[OTf] mixed with $[HSO_4]^-$ based ILs

Figure 4.2.1 shows the comparison of both ionic liquids with H[NTf]. At $\chi_{H[NTf_2]} < 0.4$, there are differences in the acidity values. In this acid, the mixtures with $[HC_4im][HSO_4]$ are more acidic than $[C_4C_1im][HSO_4]$. Further increases in the amount of acid added eliminate the acidity difference between the ionic liquids. In Figure 4.2.2, a similar trend was also observed where there are differences in the acidities of solutions of the ionic liquids at lower concentration of H[OTf]. Both of the ionic liquids start to have similar $H_0$ values from $\chi_{H[OTf]} \geq 0.6$. The NH-proton on the imidazolium ring of $[HC_4im]^+$ cations is capable of forming hydrogen bonds with $[HSO_4]^-$ and acids, and even transferring to these, but not $[C_4C_1im]^+$. This explains why there are differences in the acidity of the two ionic liquids with the same acid at lower concentration of acid added. However, as more acid is added into the ionic liquids the effect of the NH-proton becomes insignificant, as the ionic liquid is dissolved in an excess of the acid and more available protons come directly from the acid.

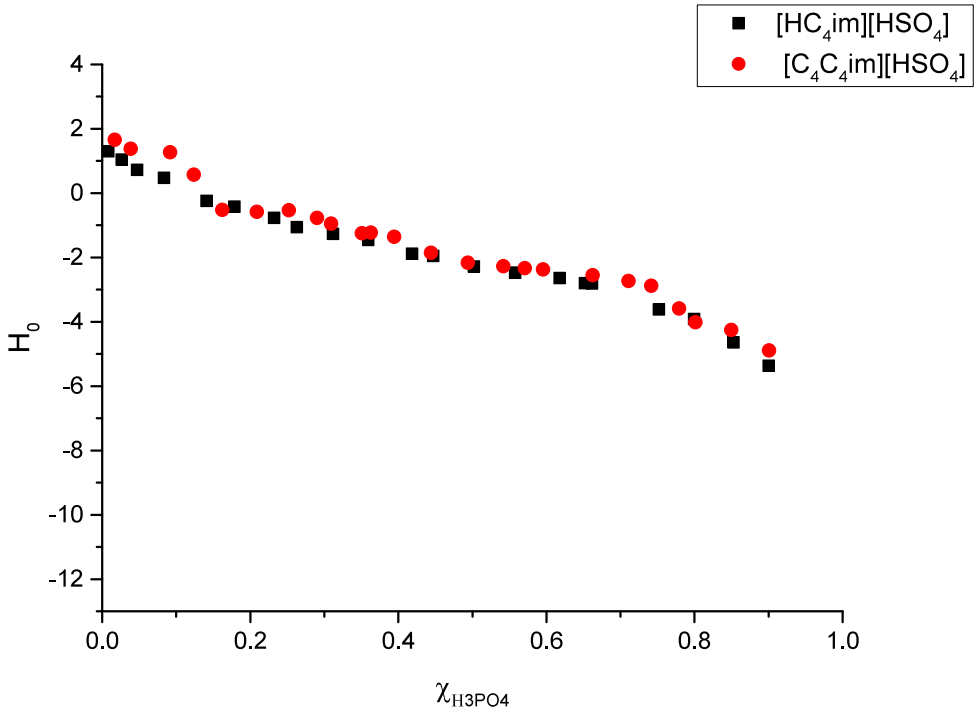



**Figure 4.2.3** – The comparison for $H_3PO_4$ mixed with $[HSO_4]^-$ based ILs

In contrast, for the $H_3PO_4$ mixed with $[HSO_4]^-$ based ILs there were no differences in the acidity (Figure 4.2.3). As $H_3PO_4$ is a weak acid, the acidic NH-proton in the imidazolium ring was levelled down to the acidity of the $H_3PO_4$ derived species. The NH-proton on the imidazolium ring of $[HC_4im]^+$ cation does not have any effect or role in the ionic liquid-$H_3PO_4$ mixture compared to $H[NTf_2]$ and H[OTf]. If the NH-proton is in principal considered as an acidic proton, the acidity of the proton is lower than the acidity of $H_3PO_4$ added. Thus, the similar acidity obtained in both of the ionic liquids mixtures proved that the NH-proton on the imidazolium ring of $[HC_4im]^+$ has no influence.[143]

Finally, $[HC_4im][HSO_4]$-Brønsted acids were successfully measured using the $^{13}C$ NMR probe without any additional help from the UV-Vis probe. For highly acidic acids, it can be concluded that there is an effect in the acidity of cation of the ionic liquids at certain concentration of acid which shows that the acidity of ionic liquids does not only depend on the anion of the ionic liquid. However as more

acid is mixed with the ionic liquids, the difference in the acidity was eliminated making the acidity of the mixture depends more on the acid than the ionic liquids. There is no effect of different cation when the ionic liquid is mixed with the weak acid.

# Chapter 5

# Synthesis and Experimental

## 5.1 General Laboratory Procedures

All reactions involving an inert atmosphere were conducted under standard Schlenk techniques using dry nitrogen. All of the starting materials were dried overnight with drying agent and distilled prior using except silver nitrate that was used as received. NMR Spectra were recorded on 'Bruker Avance-400' ($^{1}$H, 400 MHz; $^{13}$C $\{^{1}$H$\}$, 100 MHz) NMR spectrometers. $^{1}$H and $^{13}$C chemical shifts ($\delta$) are reported downfield of tetramethylsilane, ($Si(CH_3)_4$), in units of ppm (referenced against the DMSO-$d^6$ residual peak). ES-MS mass spectra were obtained with a 'Waters LCT Premier' mass spectrometer. Water content were checked using a 'Mettler Toledo (V20)' Karl Fisher Titrator. Where 'vacuo' is used for drying, the pressure achieved was between 0.1 and 0.01 mbar.

## 5.2 Synthesis of Ionic Liquids

### 5.2.1 1-Butyl-3-methylimidazolium chloride

Freshly distilled 1-chlorobutane (194.32 g, 2.1 mol) was added slowly (dropwise) to a mixture of freshly distilled 1-methylimidazole (164.18 g, 2.0 mol) and ethyl acetate (100 ml) at room temperature. The temperature used was 50 °C and was increased up to 60 °C once a biphasic temperature had formed and was stirred

for a further one week. The colorless biphasic mixture was placed in a freezer overnight and a white precipitate was formed. The solvent was removed via Schlenk techniques, and the remaining crystals were washed with ethyl acetate and then recrystallized in acetonitrile. The solid obtained was dried in vacuo after removing the remaining solvent to yield 1-butyl-3-methylimidazolium chloride (95.5%) as a white crystalline solid. The water content was maintained at less than 100 ppm of $H_2O$.

$^1$H NMR (400 MHz, DMSO-d$^6$): 9.16 (1H, s, NC**H**N), 7.79 (1H, s, NC**H**CHN), 7.72 (1H, s, NCHC**H**N), 4.17 (2H, t, $^3J_{HH}$ = 7.41 Hz, NC**H**$_2$CH$_2$CH$_2$CH$_3$), 3.86 (3H, s, NC**H**$_3$), 1.77 (2H, quintet, $^3J_{HH}$ = 7.20 Hz, NCH$_2$C**H**$_2$CH$_2$CH$_3$), 1.26 (2H, sextet, $^3J_{HH}$ = 7.20 Hz, NCH$_2$CH$_2$C**H**$_2$CH$_3$), 0.91 (3H, t, $^3J$ = 8.0 Hz, NCH$_2$CH$_2$CH$_2$C**H**$_3$).

$^{13}$C NMR (101 MHz, DMSO-d$^6$): 136.52 (s, N**C**HN), 123.60 (s, N**C**HCHN), and 122.25 (s, NCH**C**HN), 48.46 (s, N**C**H$_2$(CH$_2$)$_2$CH$_3$), 36.71 (s, N**C**H$_3$), 31.32 (s, NCH$_2$CH$_2$**C**H$_2$CH$_3$), 18.75 (s, N(CH$_2$)$_3$**C**H$_3$).

m/z (ES-MS$^+$): 139 (100%) [C$_4$C$_1$im]$^+$

m/z (ES-MS$^-$): 35 (100%) [$^{35}$Cl]$^-$, 37 (30%) [$^{37}$Cl]$^-$

Reference:[194]

### 5.2.2 1-Butyl-3-methylimidazolium trifluoromethanesulfonate

Lithium trifluoromethanesulfonate (26.79 g, 0.17 mol) was added into a mixture of 1-butyl-3-methylimidazolium chloride (30.23 g, 0.17 mol) and dichlomomethane (160 mL) and the slurry were stirred vigorously for 3 days at RT. The residual salt was washed with dichloromethane (3 x 20 mL) and the combined organic were transferred into liquid-liquid extractor (water/DCM) to extract the product. The aqueous phase was tested with $AgNO_3$(aq) (0.1M) and the extraction was stopped after the aqueous phase showed no trace of chloride salts. The solvent was then removed in vacuo for overnight giving a colorless viscous liquid of 1-butyl-3-methylimidazolium trifluoromethanesulfonate (88.9 %). The water content was maintained at less than 20 ppm of $H_2O$.

$^1$H NMR (400 MHz, DMSO-d$^6$): 9.11 (1H, s, NC**H**N), 7.77 (1H, s, NC**H**CHN), 7.71 (1H, s, NCHC**H**N), 4.17 (2H, t, $^3J_{HH}$ = 7.19 Hz, NC**H**$_2$CH$_2$CH$_2$CH$_3$), 3.85 (3H, s,

$NC\mathbf{H}_3$), 1.77 (2H, quintet, $^3J_{HH}$ = 8.0 Hz, $NCH_2C\mathbf{H}_2CH_2CH_3$), 1.26 (2H, sextet, $^3J_{HH}$ = 8.0 Hz, $NCH_2CH_2C\mathbf{H}_2CH_3$), 0.91 (3H, t, $^3J$ = 8.0 Hz, $NCH_2CH_2CH_2C\mathbf{H}_3$). $^{13}$C NMR (100 MHz, DMSO-d$^6$): 136.49 (s, N**C**HN), 123.62 (s, N**C**HCHN), 122.27 (s, NCH**C**HN), 118.5 (q, $^3J_{13C\text{-}19F}$ = 270.8 Hz, $N(SO_3CF_3)$), 48.50 (s, N $\mathbf{C}H_2(CH_2)_2$-$CH_3$), 35.74 (s, $N\mathbf{C}H_3$), 31.33 (s, $NCH_2\mathbf{C}H_2CH_2CH_3$), 18.77 (s, $N(CH_2)_2\mathbf{C}H_2CH_3$), 13.25 (s, $N(CH_2)_3\mathbf{C}H_3$).
m/z (ES-MS$^+$): 139 (100%) $[C_4C_1im]^+$
m/z (ES-MS$^-$): 149 (100%) $[CF_3SO_3]^-$

References:[194]

### 5.2.3 1-Butyl-3-methylimidazolium bis(trifluoromethylsulfonyl)imide

Lithium bis(trifluoromethylsulfonyl)imide (32.87 g, 0.11 mol) was added into a mixture of 1-butyl-3-methylimidazolium chloride (20.02 g, 0.11 mol) and dichloromethane (160 mL) and the slurry was stirred vigorously for 3 days at RT. The mixture was washed repeatedly with water (10 x 100 mL) until no chloride traces remained in the washings (tested with $AgNO_3$(aq) (0.1M)). The solvent was then removed in vacuo for overnight giving a colorless viscous liquid of 1-butyl-3-methylimidazolium bis(trifluoromethylsulfonyl)imide (87.2 %). The water content was maintained at less than 10 ppm of $H_2O$.
$^1$H NMR (400 MHz, DMSO-d$^6$): 9.11 (1H, s, NC**H**N), 7.77 (1H, s, NC**H**CHN), 7.71 (1H, s, NCHC**H**N), 4.17 (2H, t, $^3J_{HH}$ = 7.34 Hz, $NC\mathbf{H}_2CH_2CH_2CH_3$), 3.35 (3H, s, $NC\mathbf{H}_3$), 1.77 (2H, quintet, $^3J_{HH}$ = 8.0 Hz, $NCH_2C\mathbf{H}_2CH_2CH_3$), 1.28 (2H, sextet, $^3J_{HH}$ = 8.0 Hz, $NCH_2CH_2C\mathbf{H}_2CH_3$), 0.91 (3H, t, $^3J$ = 8.0 Hz, $NCH_2CH_2CH_2C\mathbf{H}_3$). $^{13}$C NMR (101 MHz, DMSO-d$^6$): 134.93 (s, N**C**HN), 122.38 (s, N**C**HCHN), 121.15 (s, NCH**C**HN), 118.77 (q, $^3J_{13C\text{-}19F}$ 321.8 Hz, $[N(SO_2\mathbf{C}F_3)_2]$), 48.36 (N $\mathbf{C}H_2(CH_2)_2CH_3$), 34.45 (s, $N\mathbf{C}H_3$), 30.51 (s, $NCH_2\mathbf{C}H_2CH_2CH_3$), 17.86 (s, $N(CH_2)_2\mathbf{C}H_2CH_3$), 11.36 (s, $N(CH_2)_3\mathbf{C}H_3$).
m/z (ES-MS$^+$): 139 (100%) $[C_4C_1im]^+$
m/z (ES-MS$^-$): 280 (100%) $[NTF_2]^-$

References:[194]

### 5.2.4 1-Butylimidazolium hydrogen sulphate

Concentrated sulphuric acid (97 %) was titrated with water to reach a concentration between 60 wt% to 70 wt%. The exact weight of both the acid and water added were recorded to calculate the exact concentration of the diluted sulphuric acid. Diluted sulphuric acid (37.2 g, 0.30 mol) was added dropwise into a cooled 1-butylimidazole (37.81 g, 0.30 mol) in an ice bath. The mixture was stirred overnight and was purified using ISOLUTE C18(EC) column after diluting the viscous ionic liquid with water. The column was washed with denatured alcohol (IMS) prior using and after each cycle of purification to remove any impurities adsorbed in the column. The remaining water was removed using rotary evaporator and dried in vacuo overnight to give a yellow viscous liquid of 1-butylimidazolium hydrogensulfate. The water content was maintained at less than 100 ppm of $H_2O$.
$^1$H NMR (400 MHz, DMSO-d$^6$): 9.10 (s, 1H, NC**H**N), 7.79 (s, 1H, NC**H**CHN), 7.68 (s, 1H, NCHC**H**N), 4.2 (t, 2H, $^3J$ = 7.38 Hz, NC**H**$_2$CH$_2$CH$_2$CH$_3$), 1.79 (m, 2H, NCH$_2$C**H**$_2$CH$_2$CH$_3$), 1.25 (m, 2H, NCH$_2$CH$_2$C**H**$_2$CH$_3$), 0.95 (t, 3H, $^3J$ = 8.0 Hz, N(CH$_2$)$_3$C**H**$_3$).
$^{13}$C NMR (100 MHz, DMSO-d$^6$): 135.81 (s, N**C**HN), 122.36 (s, N**C**HCHN), 120.77 (s, NCH**C**HN), 48.57 (s, N**C**H$_2$CH$_2$CH$_2$CH$_3$), 31.96 (s, NCH$_2$**C**H$_2$CH$_2$CH$_3$), 19.25 (s, NCH$_2$CH$_2$**C**H$_2$CH$_3$), 13.74 (s, N-(CH$_2$)$_3$**C**H$_3$).
m/z (ES-MS$^+$): 126 (100%) [C4im]$^+$
m/z (ES-MS$^-$): 97 (100%) [HSO$_4$]$^-$
Reference:[147]

### 5.2.5 1-Butyl-3-methylimidazolium methyl sulphate

A solution of dimethyl sulfate (0.143 mL, 1.09mol) was added dropwise into a solution of 1-butylimidazole (diluted in toluene) (135.35 g, 1.09 mol) with stirring. The reaction mixture was stirred for another hour at room temperature followed by the removal of upper layer toluene using Schlenk techniques. The bottom layer was washed three times with 100 ml of toluene. The washed product was dried overnight at 65 °C under vacuo. The water content was maintained at less than 100 ppm of $H_2O$.
$^1$H NMR (400 MHz, DMSO-d$^6$): 9.12 (1H, s, NC**H**N), 7.78 (1H, s, NC**H**CHN), 7.71

(1H, s, NCHC**H**N), 4.16 (2H, t, $^3J_{HH} = 7.38$ Hz, NC**H**$_2$CH$_2$CH$_2$CH$_3$), 3.84 (3H, s, NC**H**$_3$), 3.31 (3H, s, C**H**$_3$OS) 1.77 (2H, quintet, $^3J_{HH} = 8.0$ Hz, NCH$_2$C**H**$_2$CH$_2$CH$_3$), 1.25 (2H, sextet, $^3J_{HH} = 8.0$ Hz, NCH$_2$CH$_2$C**H**$_2$CH$_3$), 0.91 (3H, t, $^3J = 8.0$ Hz, NCH$_2$CH$_2$CH$_2$C**H**$_3$).
$^{13}$C NMR (100 MHz, DMSO-d$^6$): 137.13 (s, N**C**HN), 123.83 (N**C**H), 122.48 (N**C**H), 48.69 (s, N**C**H$_2$CH$_2$CH$_2$CH$_3$), 35.94 (N**C**H$_3$), 31.84 (N-CH$_2$**C**H$_2$CH$_2$CH$_3$), 18.97 (N(CH$_2$)$_2$**C**H$_2$CH$_3$) and 13.47 (N(CH$_2$)$_3$CH$_3$).
m/z (ES-MS$^+$): 139 (100%) [C$_4$C$_1$im]$^+$
m/z (ES-MS$^-$): 110 (100%) [MeSO$_4$]$^-$
Reference:[147]

### 5.2.6 1-Butyl-3-methylimidazolium hydrogen sulphate

1-butyl-3-methylimidazolium methyl sulphate was diluted in 20 mL of deionised water in a three-necked round bottom flask. The flask was placed on a heating block at 215 °C. The temperature of the mixtured was monitored and must kept between 170 to 180 °C for 4 hours. The solution was stirred in an opened round bottom flask to facilitate the removal of boiling methanol from the solution. The reaction mixture was dried overnight under vacuo at 65 °C with vigorous stirring. The water content was maintained at less than 100 ppm of H$_2$O.
$^1$H NMR (400 MHz, DMSO-d$^6$): 9.11 (1H, s, NC**H**N), 7.77 (1H, s, NC**H**CHN), 7.71 (1H, s, NCHC**H**N), 4.17 (2H, t, $^3J_{HH} = 7.34$ Hz, NC**H**$_2$CH$_2$CH$_2$CH$_3$), 3.35 (3H, s, NC**H**$_3$), 1.77 (2H, quintet, $^3J_{HH} = 7.8$ Hz, NCH$_2$C**H**$_2$CH$_2$CH$_3$), 1.28 (2H, sextet, $^3J_{HH} = 8.0$ Hz, NCH$_2$CH$_2$C**H**$_2$CH$_3$), 0.91 (3H, t, $^3J = 8.0$ Hz, NCH$_2$CH$_2$CH$_2$C**H**$_3$).
$^{13}$C NMR (100 MHz, DMSO-d$^6$): 136.52 (s, N**C**HN), 123.60 (s, N**C**HCHN), 122.25 (s, NCH**C**HN), 48.46 (s, N**C**H$_2$(CH$_2$)$_2$CH$_3$), 36.71 (s, N**C**H$_3$), 31.32 (s, N-CH$_2$CH$_2$**C**H$_2$CH$_3$), 18.75 (s, N(CH$_2$)$_3$**C**H$_3$).
m/z (ES-MS$^+$): 139 (100%) [C$_4$C$_1$im]$^+$
m/z (ES-MS$^-$): 97 (100%) [HSO$_4$]$^-$
Reference:[147]

### 5.2.7 1-Butyl-3-methylimidazolium dimethyl phosphate

1-butylimidazole (90g, 0.725 mol) was diluted in 100 ml of toluene. Trimethylphosphate (101.09g, 0.725 mol) was added dropwise into a solution of 1-butylimidazole (diluted in toluene) (135.35 g, 1.09 mol) with stirring. The resulting mixture was stirred at 80 °C for 22 h. The mixture was cooled, then washed with toluene two times, the liquid was separated and was dried overnight under vacuo at 65 °C. The water content was maintained at less than 200 ppm of $H_2O$.
$^1$H NMR (400 MHz, DMSO-d$^6$): 9.16 (1H, s,NC**H**N), 7.75 (1H, s, NC**H**CHN) 7.82 (1H, s, NCHC**H**N), 4.27 (2H, t, $^3J$ = 8.0 Hz, 7.41 Hz, NC**H**$_2$CH$_2$CH$_2$CH$_3$), 3.78 (3H, t, $^3J_{HH}$ = 7.8 Hz, P-O-C**H**$_3$), 3.79 (t, P-O-C**H**$_3$) 3.76 (3H, t, $^3J_{HH}$ = 8.0 Hz, NC**H**$_3$), 1.76 (2H, m, NCH$_2$C**H**$_2$CH$_3$), 1.36 (2H, m, N CH$_2$CH$_2$C**H**$_2$CH$_3$), 0.90 (3H, t, $^3J_{HH}$ = 8.0 Hz, NCH$_2$CH$_2$CH$_2$C**H**$_3$).
$^{13}$C NMR (100 MHz, DMSO-d$^6$): 137.02 (s, N**C**HN), 123.0 (s, N**C**HCHN), 122.25 (s, NCH**C**HN), 54.3 (s, O=POCH$_3$), 54.3 (s, O=POCH$_3$) 48.46 (s, N**C**H$_2$(CH$_2$)$_2$CH$_3$), 36.71 (s, N**C**H$_3$), 31.32 (s, N-CH$_2$CH$_2$**C**H$_2$CH$_3$), 18.75 (s, N(CH$_2$)$_3$**C**H$_3$).
m/z (ES-MS$^+$): 139 (100%) [C$_4$C$_1$im]$^+$
m/z (ES-MS$^-$): 125 (100%) [Me$_2$PO$_4$]$^-$
Reference:[195]

## 5.3 Acidity Measurements of Brønsted Acids-Ionic Liquids

### 5.3.1 $^{13}$C NMR Probe[147]

Mesityl oxide from Sigma Aldrich were distilled before use. Each ionic liquid system was added to four vials and the vials were weighed to give the exact mass of ionic liquid. The correct amount of calculated mesityl oxide from 1% to 8% w/w of the ionic liquid were added into the vials. All of the measurements and transferring samples were done inside the glove box to maintain the inert conditions. The vials were then sealed and stirred to ensure thorough mixing. The homogenous mixtures were transferred to NMR tubes along with sealed capillary tube filled with DMSO-d$^6$ as external locks. $^{13}$C NMR was run using a Bruker NMR spectrometer.

## 5.3.2 UV-Vis probe[147]

### 5.3.2.1 Obtaining extinction coefficients, $\epsilon_0$ of Hammett probe

A stock solution of suitable dye was prepared in DCM using a volumetric flask. The stock solutions were diluted with DCM for ten different concentrations. UV spectra were recorded using a Perkin Elmer Lambda 25 spectrometer. Figure 5.3.1 to Figure 5.3.10 shows a plot of absorbance against Hammett bases. The slope of the plot is the $\epsilon_0$ of the Hammett probe.

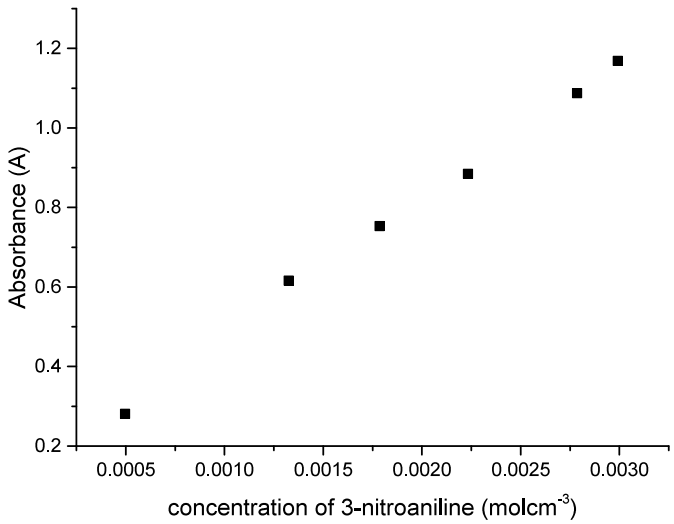



**Figure 5.3.1** – Plot of absorbance against concentration of 3-nitroaniline in DCM

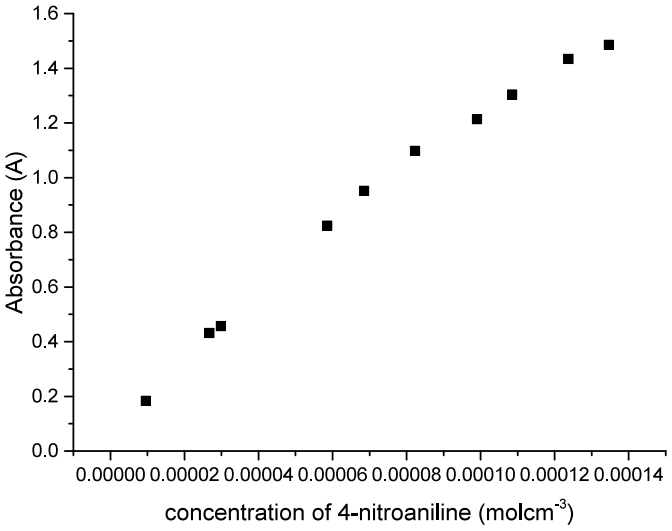



**Figure 5.3.2** – Plot of absorbance against concentration of 4-nitroaniline in DCM

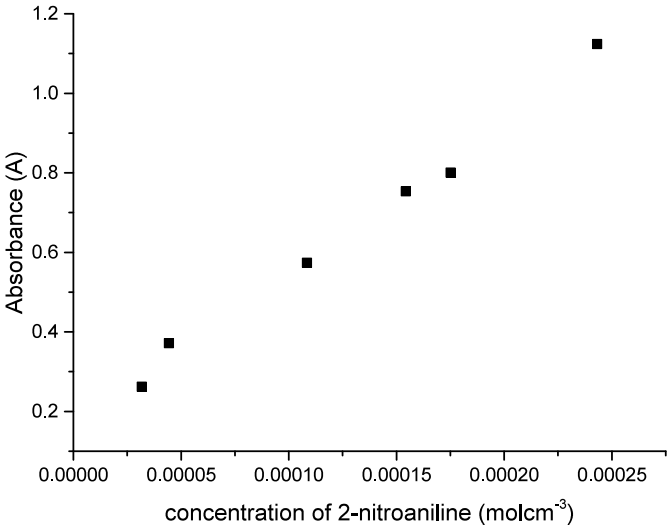



**Figure 5.3.3 –** Plot of absorbance against concentration of 2-nitroaniline in DCM

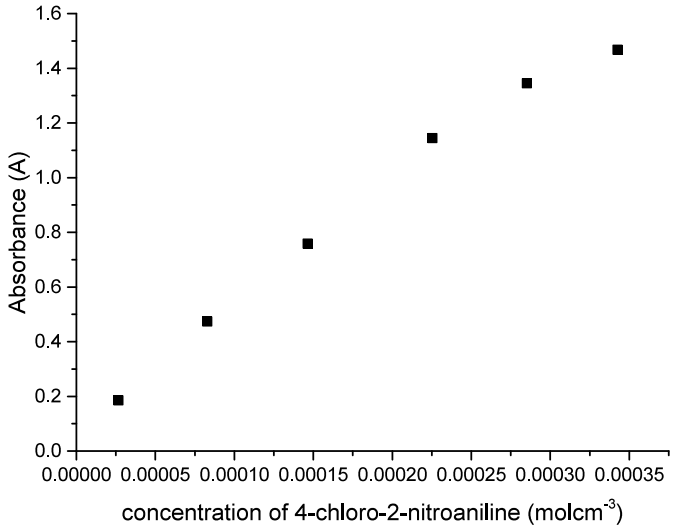



**Figure 5.3.4** – Plot of absorbance against concentration of 4-chloro-2-nitroaniline in DCM

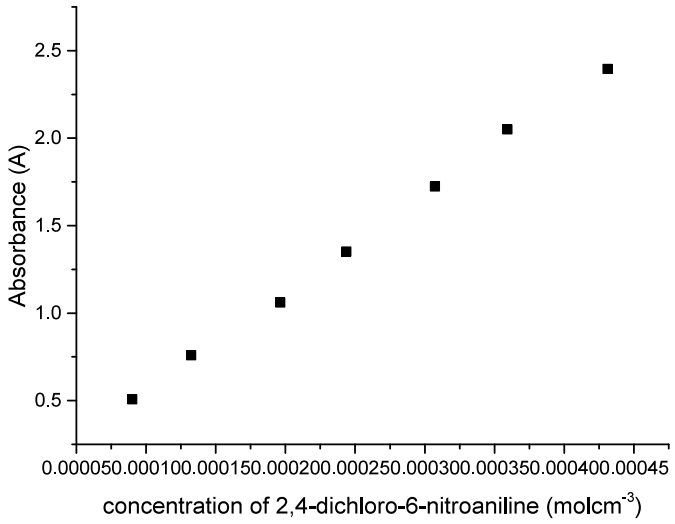



**Figure 5.3.5** – Plot of absorbance against concentration of 2,4-dichloro-6-nitroaniline in DCM

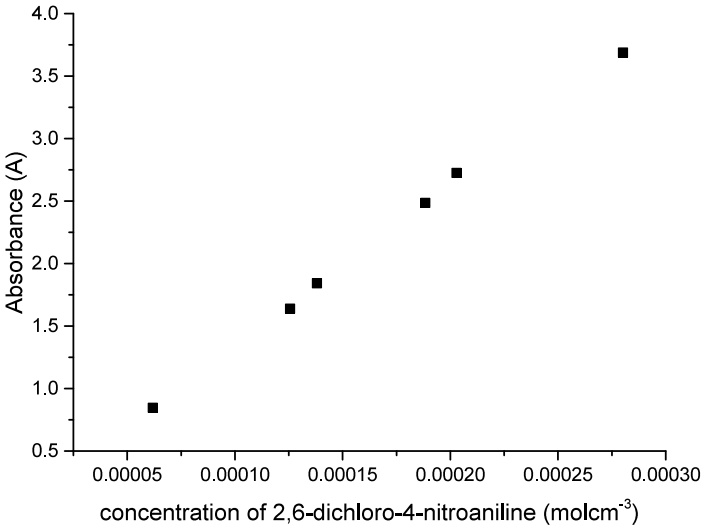



**Figure 5.3.6** – Plot of absorbance against concentration of 2,6-dichloro-4-nitroaniline in DCM

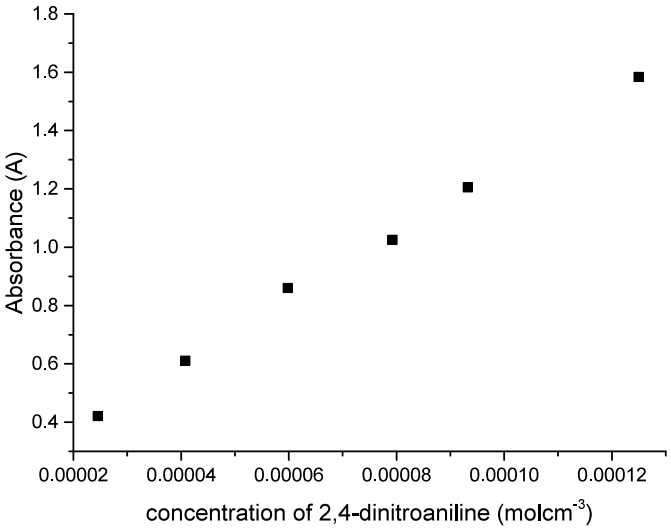



**Figure 5.3.7** – Plot of absorbance against concentration of 2,4-dinitroaniline in DCM

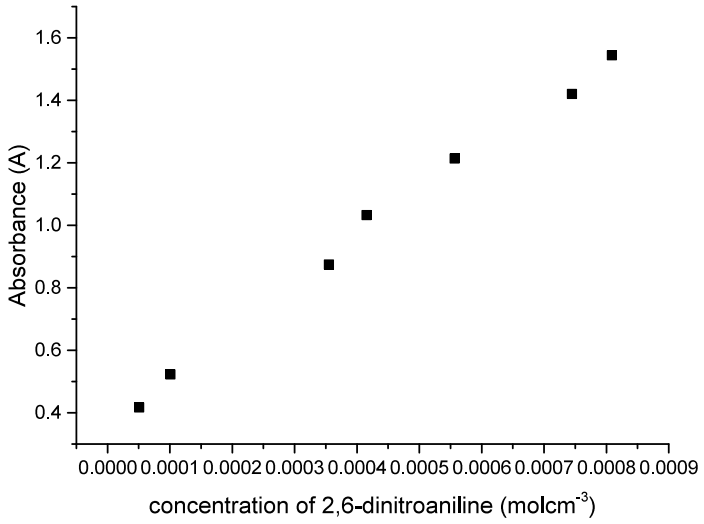



**Figure 5.3.8** – Plot of absorbance against concentration of 2,6-dinitroaniline in DCM

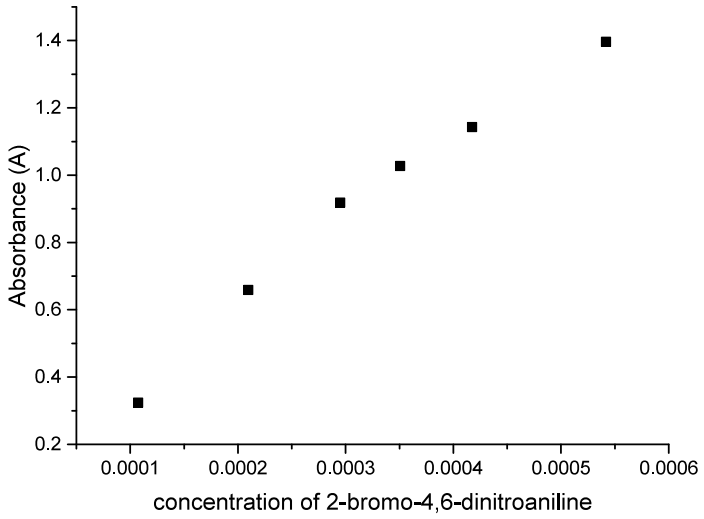



**Figure 5.3.9** – Plot of absorbance against concentration of 2-bromo-4,6-dinitroaniline in DCM

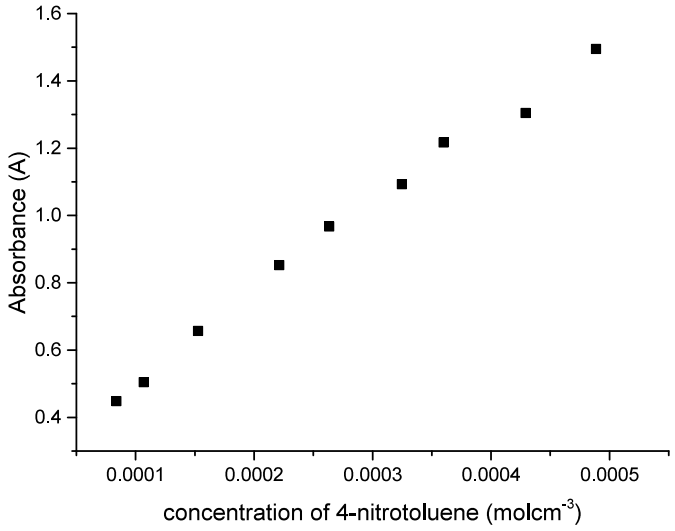



**Figure 5.3.10** – Plot of absorbance against concentration of 4-nitrotoluene in DCM

#### 5.3.2.2 Preparation of solutions of Hammett dye mixtures of ionic liquids with their related Brønsted acids

5 mL of dye stock solution was added into capped glass vial, and the solvent was removed in vacuo. Pure ionic liquid was added into the glass vial. The mixture was stirred or sonicated to obtain a homogeneous stock solution. The stock solution (1.9 ml to 1 ml) was added to ten pre-weighed vials and pure IL (1.9 mL to 1.0 mL) was then added on top. The vials were weighed after each addition. Absorbance of each vials were recorded using UV spectrometer at 250 to 600 nm.

# Chapter 6

# Overall Conclusions and Outlook

## 6.1 Conclusions

The ultimate aim of this work is to measure the acidity of Brønsted acids-ionic liquids mixture. Understanding the effects of ionic liquids on acidity and proton transfer helps to understand what happens between acids, ionic liquids, acidic ionic liquids and their acidity.

1. The acidity measurements of Brønsted acids-ionic liquids systems were done using the $^{13}C$ NMR probe and the UV-Vis probe. Successful measurements for all of the systems were demonstrated using the UV-Vis probe. A suitable UV-Vis probe probe was chosen and used to measure each mixture with the estimation of $H_0$ values from the $^{13}C$ NMR probe. It is concluded that the $^{13}C$ NMR probe can be used to calculate the acidity of the mixtures approximately while the UV-Vis probe gave a more precise results. The $H_0$ prediction using the $^{13}C$ NMR Probe is suitable for measuring the acidity of the whole $[C_4C_1im][NTf_2]$-H$[NTf_2]$ system but with limitations on the $[C_4C_1im][OTf]$-H[OTf] and $[C_4C_1im][Me_2PO_4]$-$H_3PO_4$ systems, due to the decomposition of mesityl oxide and/or insolubility of the mesityl oxide in the mixtures. In depth investigation should be done in future work to find out what decomposition reaction of the mesityl oxide is occurring to give the limitation of the $^{13}C$ NMR probe in the $[C_4C_1im][OTf]$-H[OTf].

2. The Hammett acidity function ($H_0$) were successfully measured for the Brøn-

sted acids-ionic liquids systems with different acids using the $^{13}$C NMR probe. More measurements were done using the UV-Vis probe to get full acidity measurements for each system that cannot be measured using the $^{13}$C NMR probe. The acidity of Brønsted acids-ionic liquids systems is complex and depends on the concentration of the acid. Further characterisation of the Brønsted acids-ionic liquids is suggested to explore and to understand the complex Brønsted acids-ionic liquids systems.

3. The effect on acidity of the cation of the ionic liquid was succesfully measured. In the mixture of highly acidic Brønsted acids-ionic liquids, a clear effect can be observed in ionic liquids with different cations. In contrast, with a weaker acid, changing the cation of the ionic liquid did not bring any effect on the acidity level. The acidity measurements of more weak acid should be investigated to confirm the effect of acid strength in different cation of ionic liquids.

# Bibliography


[1] Janz, G. J. *Molten Salts Handbook*; Haase, R., Ed.; Academic Press, New York-London, 1967.

[2] Welton, T. *Chemical Reviews* **1999**, *99*, 2071–2084.

[3] Hallett, J. P.; Welton, T. *Chemical Reviews* **2011**, *111*, 3508–3576.

[4] Wasserscheid, P.; Welton, T. In *Ionic Liquids in Synthesis*; Wiley-VCH Verlag GmbH & Co. KGaA, Weinheim, 2003.

[5] Holbrey, J. D.; Seddon, K. R. *Clean Technologies and Environmental Policy* **1999**, *1*, 223–236.

[6] Wasserscheid, P.; Keim, W. *Angewandte Chemie International Edition* **2000**, *39*, 3772–3789.

[7] Safa, M.; Chamaani, A.; Chawla, N.; El-Zahab, B. *Electrochimica Acta* **2016**, *213*, 587–593.

[8] Eftekhari, A.; Liu, Y.; Chen, P. *Journal of Power Sources* **2016**, *334*, 221–239.

[9] Meksi, N.; Moussa, A. *Journal of Cleaner Production* **2017**, *161*, 105–126.

[10] Berton, P.; Bica, K.; Rogers, R. D. *Fluid Phase Equilibria* **2017**, *450*, 51–56.

[11] Rahmatinejad, J.; Khoddami, A.; Abdolmaleki, A.; Izadan, H. *Carbohydrate Polymers* **2017**, *157*, 468–475.

[12] Mumford, K. A.; Mirza, N. R.; Stevens, G. W. *Energy Procedia* **2017**, *114*, 2671–2674.

[13] Cardiano, P.; Gómez-Laserna, O.; Mineo, P. G.; Furia, E.; Triolo, C.; Patanè, S.; Schiavo, S. L. *Journal of Molecular Liquids* **2017**, *241*, 222–230.

[14] Brandt, A.; Ray, M. J.; To, T. Q.; Leak, D. J.; Murphy, R. J.; Welton, T. *Green Chemistry* **2011**, *13*, 2489–2499.

[15] Brandt, A.; Grasvik, J.; Hallett, J. P.; Welton, T. *Green Chemistry* **2013**, *15*, 550–583.

[16] George, A.; Brandt, A.; Tran, K.; Zahari, S. M. S. N. S.; Klein-Marcuschamer, D.; Sun, N.; Sathitsuksanoh, N.; Shi, J.; Stavila, V.; Parthasarathi, R.; Singh, S.; Holmes, B. M.; Welton, T.; Simmons, B. A.; Hallett, J. P. *Green Chemistry* **2015**, *17*, 1728–1734.

[17] Walden, P. *Bulletin de l'Academie Imperiale des Sciences de St.-Petersbourg. VI serie* **1914**, *8*, 405–422.

[18] Plechkova, N. V.; Seddon, K. R. *Chemical Society Reviews* **2008**, *37*, 123–150.

[19] Hurley, F. H.; Wier, T. P. *Journal of The Electrochemical Society* **1951**, *98*, 207–212.

[20] Hurley, F. H.; Wier, T. P. *Journal of The Electrochemical Society* **1951**, *98*, 203–206.

[21] Chum, H. L.; Koch, V. R.; Miller, L. L.; Osteryoung, R. A. *Journal of the American Chemical Society* **1975**, *97*, 3264–3265.

[22] Wilkes, J. S.; Levisky, J. A.; Wilson, R. A.; Hussey, C. L. *Inorganic Chemistry* **1982**, *21*, 1263–1264.

[23] Wilkes, J. S.; Zaworotko, M. J. *Journal of the Chemical Society, Chemical Communications* **1992**, 965–967.

[24] Fuller, J.; Carlin, R. T.; Long, H. C. D.; Haworth, D. *Journal of the Chemical Society, Chemical Communications* **1994**, *0*, 299–300.

[25] Bonhôte, P.; Dias, A.-P.; Papageorgiou, N.; Kalyanasundaram, K.; Gratzel, M. *Inorganic Chemistry* **1996**, *35*, 1168–1178.

[26] Cravotto, G.; Gaudino, E. C.; Boffa, L.; Lévêque, J.-M.; Estager, J.; Bonrath, W. *Molecules* **2008**, *13*, 149–156.

[27] Boon, J. A.; Levisky, J. A.; Pflug, J. L.; Wilkes, J. S. *The Journal of Organic Chemistry* **1986**, *51*, 480–483.

[28] Zhang, H.; Xu, F.; Zhou, X.; Zhang, G.; Wang, C. *Green Chemistry* **2007**, *9*, 1208–1211.

[29] Angelini, G.; Maria, P. D.; Chiappe, C.; Fontana, A.; Gasbarri, C.; Siani, G. *The Journal of Organic Chemistry* **2009**, *74*, 6572–6576.

[30] Wasserscheid, P.; van Hal, R.; Bosmann, A. *Green Chemistry* **2002**, *4*, 400–404.

[31] Ebner, G.; Schiehser, S.; Potthast, A.; Rosenau, T. *Tetrahedron Letters* **2008**, *49*, 7322–7324.

[32] Amarasekara, A. S. *Chemical Reviews* **2016**, *116*, 6133–6183.

[33] Lassègues, J. C.; Grondin, J.; Holomb, R.; Johansson, P. *Journal of Raman Spectroscopy* **2007**, *38*, 551–558.

[34] Huang, J.; Hollenkamp, A. F. *The Journal of Physical Chemistry C* **2010**, *114*, 21840–21847.

[35] Marsh, K.; Boxall, J.; Lichtenthaler, R. *Fluid Phase Equilibria* **2004**, *219*, 93–98.

[36] Seddon, K. R. *Journal of Chemical Technology & Biotechnology* **1997**, *68*, 351–356.

[37] Hart, W. E. S.; Harper, J. B.; Aldous, L. *Green Chemistry* **2015**, *17*, 214–218.

[38] Haynes, W. M. *CRC Handbook of Chemistry and Physics, 94th Edition*; CRC Press, New York, 2013.

[39] Sugden, S.; Wilkins, H. *Journal of the Chemical Society (Resumed)* **1929**, *0*, 1291–1298.

[40] Olivier-Bourbigou, H. *Aqueous-Phase Organometallic Catalysis: Concepts and Applications*; Wiley-VCH Verlag GmbH & Co. KGaA, Weinheim, 1998.

[41] Fox, D. M.; Awad, W. H.; Gilman, J. W.; Maupin, P. H.; Long, H. C. D.; Trulove, P. C. *Green Chemistry* **2003**, *5*, 724–727.

[42] Welton, T. *Coordination Chemistry Reviews* **2004**, *248*, 2459–2477.

[43] Simley, J.; *Honeywell UOP Introduces Ionic Liquids Alkylation Technology*; Press release; 2016; Date : 23. `https://www.uop.com/?press_release=honeywell-uop-introduces-ionic-liquids`.

[44] Freemantle, M. *BASF'S SMART IONIC LIQUID Process scavenges acid on a large scale without producing solids*; Chemical and Engineering News (American Chemical Society (ACS)), 2003; Vol. 81.

[45] Seddon, K. R. *Nature Materials* **2003**, *2*, 363–365.

[46] Rogers, R. D. *Science* **2003**, *302*, 792–793.

[47] Matthias Maase, K. H., Klemens Massonne; Noe, R.; *Ionic liquids in the chemical synthesis of pharmaceuticals*; 2003.

[48] Baker, J.; *ECN Innovation Awards 2004 - the winners!*; Eur. Chem. News; 2004; pp. 18-19.

[49] Burrell, A. K.; Sesto, R. E. D.; Baker, S. N.; McCleskey, T. M.; Baker, G. A. *Green Chemistry* **2007**, *9*, 449.

[50] Waterkamp, D. A.; Heiland, M.; Schluter, M.; Sauvageau, J. C.; Beyersdorff, T.; Thoming, J. *Green Chemistry* **2007**, *9*, 1084–1090.

[51] Khadilkar, B. M.; Rebeiro, G. L. *Organic Process Research & Development* **2002**, *6*, 826–828.

[52] Lévêque, J.-M.; Estager, J.; Draye, M.; Cravotto, G.; Boffa, L.; Bonrath, W. *Monatshefte fur Chemie - Chemical Monthly* **2007**, *138*, 1103–1113.

[53] Holbrey, J. D.; Reichert, W. M.; Swatloski, R. P.; Broker, G. A.; Pitner, W. R.; Seddon, K. R.; Rogers, R. D. *Green Chemistry* **2002**, *4*, 407–413.

[54] Bradaric, C. J.; Downard, A.; Kennedy, C.; Robertson, A. J.; Zhou, Y. *Green Chemistry* **2002**, *5*, 143–152.

[55] Gao, J.; Liu, J.; Liu, W.; Li, B.; Xin, Y.; Yin, Y.; Gu, J.; Zou, Z. *International Journal of Hydrogen Energy* **2012**, *37*, 13167–13177.

[56] Seddon, K. R.; Stark, A.; Torres, M.-J. *Pure and Applied Chemistry* **2000**, *72*, 2275–2287.

[57] Earle, M. J.; Gordon, C. M.; Plechkova, N. V.; Seddon, K. R.; Welton, T. *Analytical Chemistry* **2007**, *79*, 758–764.

[58] Thomazeau, C.; Olivier-Bourbigou, H.; Magna, L.; Luts, S.; Gilbert, B. *Journal of the American Chemical Society* **2003**, *125*, 5264–5265.

[59] Gericke, M.; Fardim, P.; Heinze, T. *Molecules* **2012**, *17*, 7458–7502.

[60] Stark, A.; Behrend, P.; Braun, O.; Muller, A.; Ranke, J.; Ondruschka, B.; Jastorff, B. *Green Chemistry* **2008**, *10*, 1152–1161.

[61] Muldoon, M. J.; McLean, A. J.; Gordon, C. M.; Dunkin, I. R. *Chemical Communications* **2001**, 2364–2365.

[62] Armarego, W. L.; Chai, C. *Purification of Laboratory Chemicals 7th Edition*; Butterworth-Heinemann, Massachusetts, 2012.

[63] Holbrey, J. D.; Rogers, R. D.; Shukla, S. S.; Wilfred, C. D. *Green Chem.* **2010**, *12*, 407–413.

[64] Mori S., U. M., Ida K.; *Process for producing quarternary salts*; 1990.

[65] Fukumoto, K.; Yoshizawa, M.; Ohno, H. *Journal of the American Chemical Society* **2005**, *127*, 2398–2399.

[66] Olah, G.; Prakash, G.; Sommer, J. *Superacids*; Wiley, New Jersey, 1985.

[67] Arrhenius, S. *Zeitschrift fur Physikalische Chemie* **1887**, *1U*.

[68] Finston, H.; Rychtman, A. *A New View of Current Acid-Base Theories*; Wiley, New Jersey, 1982.

[69] Bronsted, J. N. *Recueil des Travaux Chimiques des Pays-Bas* **1923**, *42*, 718–728.

[70] Lowry, T. M. *Journal of the Society of Chemical Industry* **1923**, *42*, 43–47.

[71] Bronsted, J. N. *Zeitschrift fur Physikalische Chemie* **1934**, *169A*.

[72] Audrieth, L. F.; Moeller, T. *Journal of Chemical Education* **1943**, *20*, 219–222.

[73] Lewis, G. N. *Valence and the structure of atoms and molecules*; The Chemical Catalog Company, inc., New York, 1923.

[74] Davis, M. M.; Schuhmann, P. J. *Journal of Research of the National Bureau of Standards* **1947**, *39*, 221.

[75] Hantzsch, A. *Berichte der Bunsengesellschaft fur physikalische Chemie* **1924**, *30*, 194–214.

[76] Hantzsch, A.; Voigt, W. *Berichte der deutschen chemischen Gesellschaft (A and B Series)* **1929**, *62*, 975–984.

[77] Kolthoff, M.; J., P. *Journal of the American Pharmaceutical Association (Scientific ed.)* **1960**, *49*, 181.

[78] Wilson, A. *pH Meters*; Kogan Page, London, 1970.

[79] Henderson, L. J. *American Physiological Society* **1908**, *22*, 427–448.

[80] Hasselbalch, K. A. *Biochemische Zeitschrift* **1917**, *78*, 112–114.

[81] Vanysek, P. *The Electrochemical Society INTERFACE* **2004.**

[82] Johnson, K. E.; Pagni, R. M.; Bartmess, J. *Monatshefte fÃŒr Chemie - Chemical Monthly* **2007**, *138*, 1077–1101.

[83] Weissermel, K.; Arpe, H.-J. *Industrial Organic Chemistry*; Wiley-VCH Verlag GmbH, Weinheim, 1997.

[84] Reichardt, C.; Welton, T. *Solvents and Solvent Effects in Organic Chemistry, 4th, Updated and Enlarged Edition*; Wiley-VCH Verlag GmbH, Weinheim, 2011.

[85] Clark, J. H.; Macquarrie, D. *Handbook of Green Chemistry and Technology*; Blackwell Science Ltd, Oxford, 2002.

[86] Panossian, Z.; de Almeida, N. L.; de Sousa, R. M. F.; de Souza Pimenta, G.; Marques, L. B. S. *Corrosion Science* **2012**, *58*, 1–11.

[87] Margolese, D.; Melero, J. A.; Christiansen, S. C.; Chmelka, B. F.; Stucky, G. D. *Chemistry of Materials* **2000**, *12*, 2448–2459.

[88] Melero, J. A.; van Grieken, R.; Morales, G. *Chemical Reviews* **2006**, *106*, 3790–3812.

[89] Dacquin, J. P.; Lee, A. F.; Pirez, C.; Wilson, K. *Chemical Communications* **2012**, *48*, 212–214.

[90] Karimi, B.; Zareyee, D. *Organic Letters* **2008**, *10*, 3989–3992.

[91] Wilkes, J. S.; Wasserscheid, P.; Welton, T. In *Ionic Liquids in Synthesis*; Wiley-VCH Verlag GmbH & Co. KGaA, Weinheim; pp 1–6.

[92] Greaves, T. L.; Drummond, C. J. *Chemical Reviews* **2008**, *108*, 206–237.

[93] MacFarlane, D. R.; Pringle, J. M.; Johansson, K. M.; Forsyth, S. A.; Forsyth, M. *Chemical Communications* **2006**, 1905–1917.

[94] Masahiro Yoshizawa, W. X.; Angell, C. A. *Journal of American Chemical Society* **2003**, 15411–15419.

[95] Matsuoka, H.; Nakamoto, H.; Susan, M. A. B. H.; Watanabe, M. *Electrochimica Acta* **2005**, *50*, 4015–4021.

[96] Noda, A.; Susan, M. A. B. H.; Kudo, K.; Mitsushima, S.; Hayamizu, K.; Watanabe, M. *The Journal of Physical Chemistry B* **2003**, *107*, 4024–4033.

[97] Nuthakki, B.; Greaves, T. L.; Krodkiewska, I.; Weerawardena, A.; Burgar, M. I.; Mulder, R. J.; Drummond, C. J. *Australian Journal of Chemistry* **2007**, *60*, 21–2.

[98] Bao, X. *National Science Review* **2015**, *2*, 137–137.

[99] Sheldon, R. *Chemical Communications* **2001**, 2399–2407.

[100] Muzart, J. *Advanced Synthesis & Catalysis* **2006**, *348*, 275–295.

[101] Taheri, A.; Lai, B.; Cheng, C.; Gu, Y. *Green Chemistry* **2015**, *17*, 812–816.

[102] Elavarasan, P.; Kondamudi, K.; Upadhyayula, S. *Chemical Engineering Journal* **2011**, *166*, 340–347.

[103] Cui, P.; Zhao, G.; Ren, H.; Huang, J.; Zhang, S. *Catalysis Today* **2013**, *200*, 30–35.

[104] Xu, Z.; Wan, H.; Miao, J.; Han, M.; Yang, C.; Guan, G. *Journal of Molecular Catalysis A: Chemical* **2010**, *332*, 152–157.

[105] Zhang, C.; Pan, X.-Y.; Yu, M.-J.; Jin, L.; Wu, G. *Chemical Engineering Journal* **2012**, *209*, 464–468.

[106] Ullah, Z.; Bustam, M. A.; Man, Z. *Renewable Energy* **2015**, *77*, 521–526.

[107] Olkiewicz, M.; Plechkova, N. V.; Earle, M. J.; Fabregat, A.; Stuber, F.; Fortuny, A.; Font, J.; Bengoa, C. *Applied Catalysis B: Environmental* **2016**, *181*, 738–746.

[108] Stocker, M. *Angewandte Chemie International Edition* **2008**, *47*, 9200–9211.

[109] Muhammad, N.; Omar, W. N.; Man, Z.; Bustam, M. A.; Rafiq, S.; Uemura, Y. *Industrial & Engineering Chemistry Research* **2012**, *51*, 2280–2289.

[110] Centi, G.; Lanzafame, P.; Perathoner, S. *Catalysis Today* **2011**, *167*, 14–30.

[111] Cox, B. J.; Ekerdt, J. G. *Bioresource Technology* **2013**, *134*, 59–65.

[112] Brandt, A.; Hallett, J. P.; Leak, D. J.; Murphy, R. J.; Welton, T. *Green Chemistry* **2010**, *12*, 672–679.

[113] Xu, J.-K.; Chen, J.-H.; Sun, R.-C. *Bioresource Technology* **2015**, *193*, 119–127.

[114] Grasvik, J.; Winestrand, S.; Normark, M.; Jonsson, L. J.; Mikkola, J.-P. *BMC Biotechnology* **2014**, *14*, 34.

[115] Malihan, L. B.; Nisola, G. M.; Mittal, N.; Seo, J. G.; Chung, W.-J. *Renewable Energy* **2014**, *66*, 596–604.

[116] Mood, S. H.; Golfeshan, A. H.; Tabatabaei, M.; Abbasalizadeh, S.; Ardjmand, M.; Jouzani, G. S. *Preparative Biochemistry and Biotechnology* **2014**, *44*, 451–463.

[117] Brandt-Talbot, A.; Gschwend, F. J. V.; Fennell, P. S.; Lammens, T. M.; Tan, B.; Weale, J.; Hallett, J. P. *Green Chemistry* **2017**, *19*, 3078–3102.

[118] Amarasekara, A. S.; Razzaq, A. *Carbohydrate Research* **2014**, *386*, 86–91.

[119] Ding, Z.-D.; Shi, J.-C.; Xiao, J.-J.; Gu, W.-X.; Zheng, C.-G.; Wang, H.-J. *Carbohydrate Polymers* **2012**, *90*, 792–798.

[120] Alam, M. I.; De, S.; Dutta, S.; Saha, B. *RSC Advances* **2012**, *2*, 6890.

[121] Eminov, S.; Wilton-Ely, J. D. E. T.; Hallett, J. P. *ACS Sustainable Chemistry & Engineering* **2014**, *2*, 978–981.

[122] Díaz, M.; Ortiz, A.; Ortiz, I. *Journal of Membrane Science* **2014**, *469*, 379–396.

[123] Yasuda, T.; Watanabe, M. *MRS Bulletin* **2013**, *38*, 560–566.

[124] Chen, B.-K.; Wong, J.-M.; Wu, T.-Y.; Chen, L.-C.; Shih, I.-C. *Polymers* **2014**, *6*, 2720–2736.

[125] Chen, B.-K.; Wu, T.-Y.; Kuo, C.-W.; Peng, Y.-C.; Shih, I.-C.; Hao, L.; Sun, I.-W. *International Journal of Hydrogen Energy* **2013**, *38*, 11321–11330.

[126] Pundir, S. S.; Mishra, K.; Rai, D. K.; AIP Conferece Proceedings; p 1266.

[127] Ye, Y.-S.; Rick, J.; Hwang, B.-J. *Polymers* **2012**, *4*, 913–963.

[128] Chen, L.; Mullen, G. E.; Le Roch, M.; Cassity, C. G.; Gouault, N.; Fadamiro, H. Y.; Barletta, R. E.; O'Brien, R. A.; Sykora, R. E.; Stenson, A. C.; West, K. N.; Horne, H. E.; Hendrich, J. M.; Xiang, K. R.; Davis, J. H. *Angewandte Chemie International Edition* **2014**, *53*, 11762–11765.

[129] Dupont, J.; de Souza, R. F.; Suarez, P. A. Z. *Chemical Reviews* **2002**, *102*, 3667–3692.

[130] Smith, G. P.; Dworkin, A. S.; Pagni, R. M.; Zingg, S. P. *Journal of the American Chemical Society* **1989**, *111*, 525–530.

[131] Olivier-Bourbigou, H.; Magna, L. *Journal of Molecular Catalysis A: Chemical* **2002**, *182-183*, 419–437.

[132] Qiao, C.-Z.; Zhang, Y.-F.; Zhang, J.-C.; Li, C.-Y. *Applied Catalysis A: General* **2004**, *276*, 61–66.

[133] Cole, A. C.; Jensen, J. L.; Ntai, I.; Tran, K. L. T.; Weaver, K. J.; Forbes, D. C.; Davis, J. H. *Journal of the American Chemical Society* **2002**, *124*, 5962–5963.

[134] Wasserscheid, P.; Sesing, M.; Korth, W. *Green Chemistry* **2002**, *4*, 134–138.

[135] Ross, J.; Xiao, J. *Green Chemistry* **2002**, *4*, 129–133.

[136] Tang, S.; Scurto, A. M.; Subramaniam, B. *Journal of Catalysis* **2009**, *268*, 243–250.

[137] Anouti, M.; Caillon-Caravanier, M.; Floch, C. L.; Lemordant, D. *The Journal of Physical Chemistry B* **2008**, *112*, 9406–9411.

[138] Shen, Y.; Kennedy, D. F.; Greaves, T. L.; Weerawardena, A.; Mulder, R. J.; Kirby, N.; Song, G.; Drummond, C. J. *Physical Chemistry Chemical Physics* **2012**, *14*, 7981.

[139] Afkhami, A.; Khajavi, F.; Khanmohammadi, H. *Analytica Chimica Acta* **2009**, *634*, 180–185.

[140] Adam, C.; Bravo, M. V.; Mancini, P. M. *Tetrahedron Letters* **2014**, *55*, 148–150.

[141] Chiappe, C.; Pieraccini, D. *The Journal of Physical Chemistry A* **2006**, *110*, 4937–4941.

[142] Robert, T.; Olivier-Bourbigou, H.; Magna, L.; Gilbert, B.; ECS Transactions; pp 71–82.

[143] Robert, T.; Magna, L.; Olivier-Bourbigou, H.; Gilbert, B. *Journal of The Electrochemical Society* **2009**, *156*, F115.

[144] Malherbe, C.; Robert, T.; Magna, L.; Olivier-Bourbigou, H.; Gilbert, B.; ECS Transactions; pp 3–16.

[145] Xing, H.; Wang, T.; Zhou, Z.; Dai, Y. *Journal of Molecular Catalysis A: Chemical* **2007**, *264*, 53–59.

[146] Shukla, S. K.; Kumar, A. *Chemical Physics Letters* **2013**, *566*, 12–16.

[147] Grasvik, J.; Hallett, J. P.; To, T. Q.; Welton, T. *Chemical Communications* **2014**, *50*, 7258–7261.

[148] Fărcaşiu, D.; Ghenciu, A. *Progress in Nuclear Magnetic Resonance Spectroscopy* **1996**, *29*, 129–168.

[149] Srinivasan, K.; Siddiqui, S.; Potewar, T.; Lahoti, R. *Synthesis* **2006**, *17*, 2849–2854.

[150] McCune, J. A.; He, P.; Petkovic, M.; Coleman, F.; Estager, J.; Holbrey, J. D.; Seddon, K. R.; Swadźba-Kwaśny, M. *Physical Chemistry Chemical Physics* **2014**, *16*, 23233–23243.

[151] Porras, S. P.; Kenndler, E. *Journal of Chromatography A* **2004**, *1037*, 455–465.

[152] Mussini, P. R.; Mussini, T.; Rondinini, S. *Pure and Applied Chemistry* **1997**, *69*, 1007–1014.

[153] Hammett, L. P.; Deyrup, A. J. *Journal of the American Chemical Society* **1932**, *54*, 2721–2739.

[154] Paul, M. A.; Long, F. A. *Chemical Reviews* **1957**, *57*, 1–45.

[155] Gillespie, R.; Peel, T. In *Advances in Physical Organic Chemistry*; Elsevier, 1971; pp 1–24.

[156] Gillespie, R. J.; Peel, T. E. *Journal of the American Chemical Society* **1973**, *95*, 5173–5178.

[157] Hammett, L. P.; Deyrup, A. J. *Journal of the American Chemical Society* **1932**, *54*, 4239–4247.

[158] Paul, M. A. *Journal of American Chemical Society* **1954**, *76*, 3236–3239.

[159] Braude, E. A. *Journal of the Chemical Society (Resumed)* **1948**, 1971–1975.

[160] Tickle, P.; Briggs, A. G.; Wilson, J. M. *Journal of the Chemical Society B: Physical Organic* **1970**, *0*, 65–70.

[161] Jorgenson, M. J.; Hartter, D. R. *Journal of the American Chemical Society* **1963**, *85*, 878–883.

[162] Randles, J. E. B.; Tedder, J. M. *Journal of the Chemical Society (Resumed)* **1955**, *0*, 1218–1223.

[163] Kuivila, H. G. *The Journal of Physical Chemistry* **1955**, *59*, 1028–1030.

[164] Kislina, I. S.; Sysoeva, S. G.; Librovich, N. B. *Kinetics and Catalysis* **2005**, *46*, 37–42.

[165] Kislina, I. S.; Librovich, N. B.; Sysoeva, S. G. *Russian Journal of Physical Chemistry A* **2009**, *83*, 1111–1116.

[166] Fadeeva, Y. A.; Nikolaeva, A. V.; Safonova, L. P. *Journal of Molecular Liquids* **2014**, *193*, 1–5.

[167] Farcasiu, D.; Fisk, S. L.; Melchior, M. T.; Rose, K. D. *The Journal of Organic Chemistry* **1982**, *47*, 453–457.

[168] Farcasiu, D.; Marino, G.; Miller, G.; Kastrup, R. V. *Journal of the American Chemical Society* **1989**, *111*, 7210–7213.

[169] Farcasiu, D.; Ghenciu, A. *Journal of the American Chemical Society* **1993**, *115*, 10901–10908.

[170] Grondin J., C. A., Sagnes P. *Bulletin de la Societe Chimique de France* **1976**, 1779.

[171] Taft, R. W.; Levins, P. L. *Analytical Chemistry* **1962**, *34*, 436–437.

[172] McClelland, R. A.; Reynolds, W. F. *Canadian Journal of Chemistry* **1976**, *54*, 718–725.

[173] Hibbert, R. C.; Logan, N. *Journal of the Chemical Society, Dalton Transactions* **1985**, 865.

[174] Angueira, E.; White, M. *Journal of Molecular Catalysis A: Chemical* **2007**, *277*, 164–170.

[175] Arnett, E. M.; Scorrano, G. In *Advances in Physical Organic Chemistry*; Elsevier, 1976; pp 83–153.

[176] Farcasiu, D.; Ghenciu, A. *The Journal of Organic Chemistry* **1991**, *56*, 6050–6052.

[177] Greig, C. C.; Johnson, C. D. *Journal of the American Chemical Society* **1968**, *90*, 6453–6457.

[178] Arnett, E. M.; Quirk, R. P.; Larsen, J. W. *Journal of the American Chemical Society* **1970**, *92*, 3977–3984.

[179] Brouwer, D. *Tetrahedron Letters* **1969**, 453.

[180] Olah, G. A.; Halpern, Y.; Mo, Y. K.; Liang, G. *Journal of the American Chemical Society* **1972**, *94*, 3554–3561.

[181] Cox, R. A.; Yates, K. *Canadian Journal of Chemistry* **1983**, *61*, 2225–2243.

[182] Zhang, S.; Zhang, T.; Tang, S. *Journal of Chemical & Engineering Data* **2016**, *61*, 2088–2097.

[183] Stoyanov, E. S.; Kim, K.-C.; Reed, C. A. *The Journal of Physical Chemistry A* **2004**, *108*, 9310–9315.

[184] Farcasiu, D.; Hâncu, D. *Journal of the Chemical Society, Faraday Transactions* **1997**, *93*, 2161–2165.

[185] Koppel, I. A.; Taft, R. W.; Anvia, F.; Zhu, S.-Z.; Hu, L.-Q.; Sung, K.-S.; DesMarteau, D. D.; Yagupolskii, L. M.; Yagupolskii, Y. L. *Journal of the American Chemical Society* **1994**, *116*, 3047–3057.

[186] Foropoulos, J.; DesMarteau, D. D. *Inorganic Chemistry* **1984**, *23*, 3720–3723.

[187] Jackson, G. P.; Duckworth, D. C. *Chemical Communications* **2004**, 522–523.

[188] To, T. Q.; Ph.D. thesis; Imperial College London; 2013.

[189] Burba, C. M.; Rocher, N. M.; Frech, R. *The Journal of Physical Chemistry B* **2009**, *113*, 11453–11458.

[190] Bradaric, C. J.; Zhou, Y.; *Phosphonium salts and methods of their preparation*; 2004.

[191] Davidson, R. M.; Kenyon, G. L. *The Journal of Organic Chemistry* **1980**, *45*, 2698–2703.

[192] Averill, B. A.; Eldredge, P. *General Chemistry: Principles, Patterns, and Applications*; Saylor Foundation, Washington DC, 2011.

[193] Tromp, R. H.; Spieser, S. H.; Neilson, G. W. *The Journal of Chemical Physics* **1999**, *110*, 2145–2150.

[194] Crowhurst, L.; Ph.D. thesis; University of London; 2006.

[195] Matthews, R. P.; Villar-Garcia, I. J.; Weber, C. C.; Griffith, J.; Cameron, F.; Hallett, J. P.; Hunt, P. A.; Welton, T. *Physical Chemistry Chemical Physics* **2016**, *18*, 8608–8624.

# Appendix A

# Appendix

## A.1 Maths : From equation 16 to equation 17 (Chapter 2)

The proton transfer equilibrium in the acid solution between the solvated proton and an electro-neutral weak base B (as the probe) can be written as follows:

$$B + AH_2^+ \rightleftharpoons BH^+ + AH \quad (16)$$

Since the proton is solvated ($AH_2^+$) and that AH is the solvent, the equilibrium can be written as;

$$B + H^+ \rightleftharpoons BH^+ (17)$$

The corresponding thermodynamic equilibrium constant is $K_{BH^+}$, which is defined as;

$$K_{BH^+} = \frac{\alpha_H \cdot \alpha_B}{\alpha_{BH^+}} = \frac{\alpha_H \cdot C_B}{C_{BH^+}} \cdot \frac{f_B}{f_{BH^+}} \quad (18)$$

where $\alpha$ is the activity, C the concentration and $f$ the activity coefficient. From this equation, it follows that;

$$\frac{C_{BH+}}{C_B} = \frac{1}{K_{BH+}} \bullet \alpha_{H+} \bullet \frac{f_B}{f_{BH+}} \quad (19)$$

As the first ratio stands for the degree of protonation, Hammett and Deyrupp defined the acidity function, $H_0$ by:

$$H_0 = \text{-log } \alpha_{H^+} \bullet \frac{f_B}{f_{BH+}} = \text{-log } K_{BH^+} + \log \frac{C_B}{C_{BH+}} (19)$$

where it can be written for further discussion in the more usual form:

$$H_0 = pK_{BH^+} \text{ - log } \frac{[BH+]}{[B]} \quad (20)$$

in which $pK_{BH^+}$ is the $pK_a$ of the conjugate acid of the probe base (referred to ideal dilute solution in water), and [BH+] and [B] are the concentration of base in its protonated and unprotonated forms. The "0" subscript of $H_0$ denotes the charges of the probe bases.

## A.2 Data for the acidity measurements of $[C_4C_1im][HSO_4]$-$H_2SO_4$ system

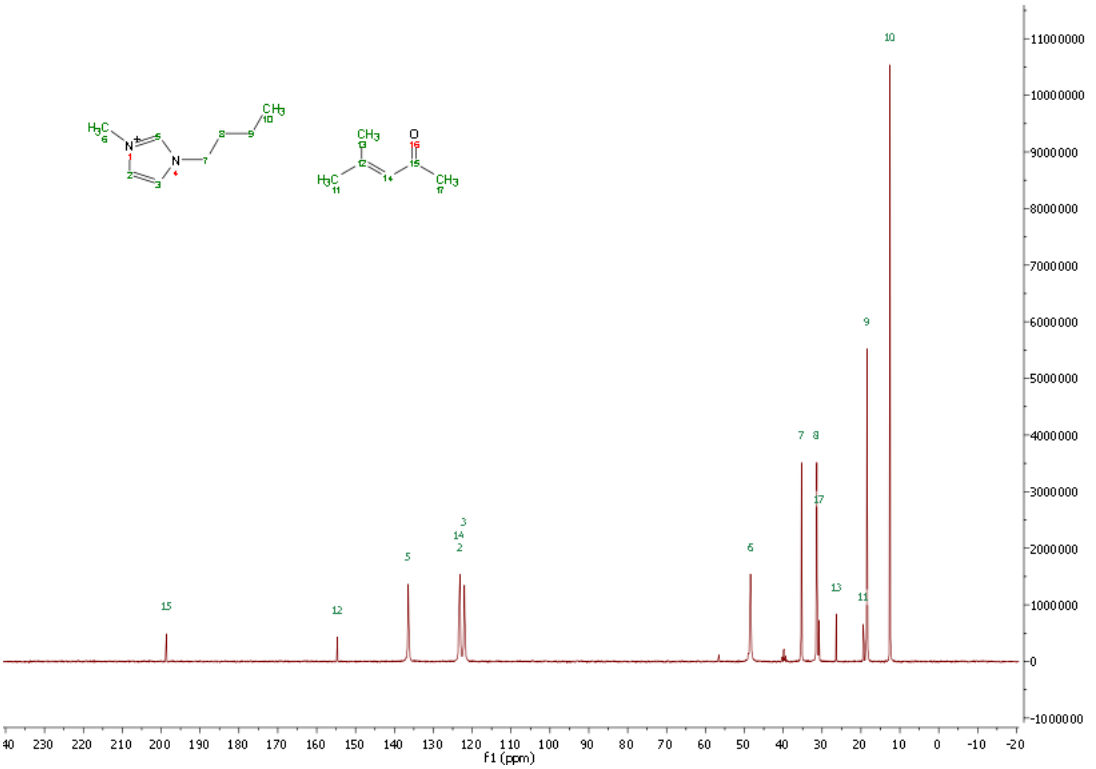



**Figure A.2.1** – $^{13}$C NMR spectra of mesityl oxide in [$C_4C_1$im][$HSO_4$] + 0.066 $\chi_{H_2SO_4}$

The results for the [$C_4C_1$im][$HSO_4$]-$H_2SO_4$ system were shown in the Figure A.2.2.

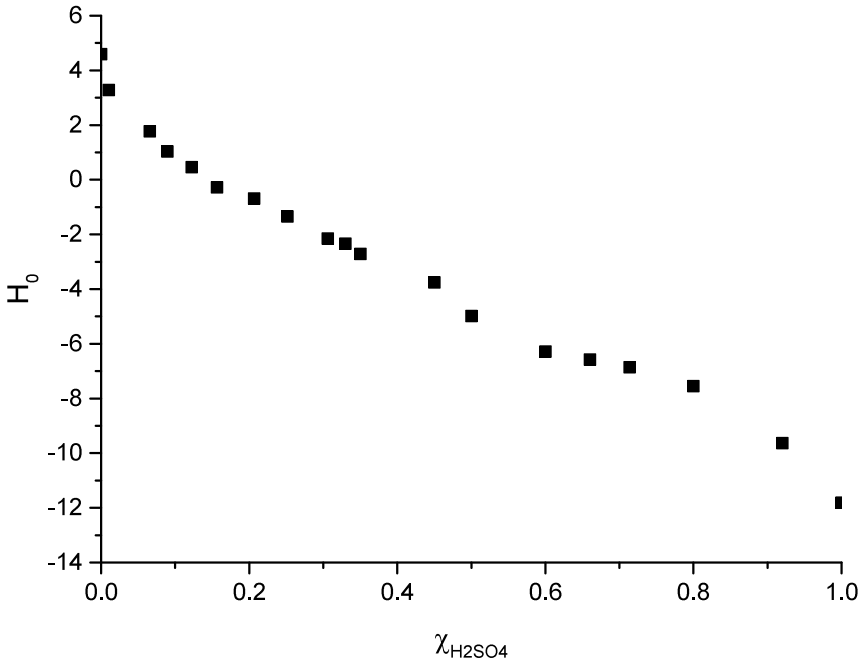



**Figure A.2.2** – $H_0$ values vs. $\chi_{H_2SO_4}$ in the $[C_4C_1im][HSO_4]$-$H_2SO_4$ mixture